



UNIVERSITÀ DEGLI STUDI DI PAVIA
DOTTORATO IN SCIENZE CHIMICHE E
FARMACEUTICHE
XXX CICLO

Coordinatore: Chiar.mo Prof. Mauro Freccero

***Membrane Vesicles secreted by
Mesenchymal Stem Cells for Drug Delivery
in Musculoskeletal Regeneration***

Tutor

Chiar.ma Prof.ssa Maria Luisa Torre

Tesi di Dottorato

Dott.ssa Barbara Crivelli

Co-tutor

Dott.ssa Theodora Chlapanidas

Dott.ssa Laura de Girolamo

a.a. 2016- 2017

Preface

In pharmaceuticals, nano carriers have emerged as suitable platforms for drug delivery and targeting. They are employed to improve the Active Principle Ingredient (API) technological features obtaining a sustained release, reducing cytotoxic events and avoiding off-target disseminations. This last feature is related to the “magic bullet theory” which is partially related to the nanoparticle ability to passively target tumoral or inflamed tissues due to the Enhanced Permeation Effect (EPR). Nano drug delivery systems are easily taken up by cells due to their small size, however this feature could lead to their quick clearance from the bloodstream. A lot of materials of different origin have been investigated even if the preferred and promising ones are those retaining a synthetic and metal nature. Among natural based polymers, silk fibroin (SF) shows an excellent combination of mechanical and biological features, hard to find simultaneously in other natural or synthetic materials. Despite silk evokes the idea of silkiness, it represents one of the most robust biomaterials reachable in nature, retaining a toughness higher than Kevlar (a para-aramid synthetic fiber employed for the production of bulletproof vests), a high tensile and breaking strength, great extensibility, thermo-stability and remarkable stiffness and ductility. Additionally, SF undergoes a biodegradation pathway directly influenced by the complexity and the architecture of the considered scaffold or carrier, leading to the release of natural and non-inflammatory by-products. For these reasons, SF is a suitable biomaterial for the development of a plethora of tissue engineering scaffolds and drug delivery systems. Also silk sericin (SS) has gained attention as a natural polymer due to its intrinsic activities, already employed in pharmaceutical and cosmetic fields. Both silk proteins can be actually considered as bioactive natural carriers, since they show not only optimal features typical of inert excipients, but also remarkable intrinsic biological activities. In fact, SF has an anti-inflammatory property, exploitable for the treatment of several diseases, while SS presents antioxidant, anti-tyrosine, anti-aging, anti-elastase and anti-bacterial features. Despite all of these eclectic features, working with a natural polymer, and in particular with SF, is quite complex especially in terms of standardization of the entire process from SF solubilization to nanoparticle creation. For this reason, scientists are always looking for innovative smart nano-platforms: they should be physiological, showing high stability once reaching the bloodstream, non immunogenic, non toxic and, finally, they should be able to interact exclusively with the targeted tissues or cells, without disseminating throughout the whole body, in which they have to release APIs in a controlled and sustained manner to achieve the desired therapeutic effect. Biological carriers, such as mesenchymal stem cells (MSCs), have been proposed as smart drug delivery systems due to

their high biocompatibility and bloodstream stability in physiological conditions. Recent discoveries proposed that the main biological effectors of MSC biological activities are their own secreted extracellular vesicles (EVs). This is due with their inner cargo which mimics their parent cell content. Concerning EVs secreted by MSCs, they can be considered as unique tools in the control of tissue regeneration by displaying long-term tissue reprogramming, immunomodulatory, regenerative and homing potential. Nowadays, EVs have been proposed as drug delivery system: they actually show liposome-like features, with higher stability in the bloodstream, slower clearance, innate tropism, low immunogenicity and the ability to deliver therapeutic agents of various sizes. Just think that they are physiologically enriched in lipids, proteins, and genetic material, since one of their function is to shuttle information or discard products between cells. Based on this, EV cargo could be tuned by using the genetic manipulation approach, promoting the expression of a specific set of proteins or finally, the cellular internalization of exogenous drugs or nanosystems could be engaged, thus achieving the secretion of EV enriched in the exogenous nanosystems or drugs. This last approach paved the way to the design and development of a novel class of “next generation drug delivery systems” based on coupling nanotechnology with nanobiology. This idea deals with the fusion of a classical technological approach, based on bio-inspired nanoparticles, with the more innovative EV application as physiological nanosystems, paving the way to cell-free therapies.

Outline

Introduction	6
Paper 1 Silk nanoparticles: from inert supports to bioactive natural carriers for drug delivery, Crivelli B. <i>et al</i> , 2018 <i>Soft Matter</i> , doi: 10.1039/c7sm01631j.	7
Paper 2 Mesenchymal stem/stromal cell extracellular vesicles: From active principle to next generation drug delivery systems, Crivelli B. <i>et al</i> , 2017 <i>Journal of Controlled Release</i> , 262:104-117	36
Aim	89
Results	91
First Action Results	93
Paper 3 Silk fibroin nanoparticles reduced cytotoxicity and showed anti-inflammatory efficacy in IL-1 β stimulated human chondrocytes, Crivelli B <i>et al</i> , submitted to <i>Colloids and Surfaces B: Biointerfaces</i>	106
Paper 4 Stem cell-extracellular vesicles as drug delivery systems: New frontiers for silk/curcumin nanoparticles, Perteghella S. <i>et al</i> , 2017 <i>International Journal of Pharmaceutics</i> , 520(1-2):86-97	131
Conclusions	161
Future Outlooks	164
Appendix – Paper 5 <i>In Vitro</i> Effectiveness of Microspheres Based on Silk Sericin and <i>Chlorella vulgaris</i> or <i>Arthrospira platensis</i> for Wound Healing Applications Bari E <i>et al</i> , 2017 <i>Materials</i> , 10(9).....	166

Introduction

The introduction of this PhD thesis includes two main topics, deeply reviewed in *Paper 1* and *Paper 2*, both concerning the nanomedicine field from two different point of view. In *Paper 1* a nanotechnological approach is shown, based on the application of both silk fibroin and silk sericin nano drug delivery systems for the treatment of several pathologies. Conversely, *Paper 2* retains a more biological footprint, providing an incisive overview on the different applications of the extracellular vesicles secreted by mesenchymal stem/stromal cells. As reported in the title of my thesis, this membranous systems can be employed as drug delivery systems for a plethora of actives of different nature but, as deeply reported in literature, they can be used as *per se* due to their ability to mirror their parent cells properties.

Paper 1



Soft Matter

REVIEW

[View Article Online](#)
[View Journal](#)

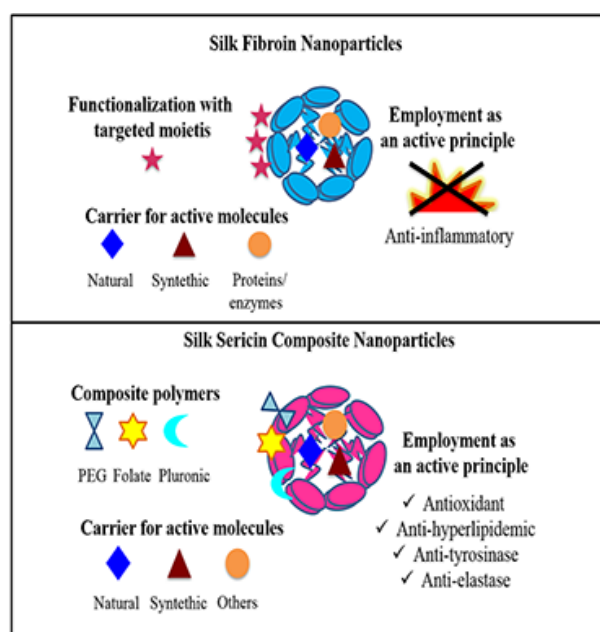


Silk nanoparticles: from inert supports to bioactive natural carriers for drug delivery

Cite this: DOI: 10.1039/c7sm01631j

Barbara Crivelli,^a Sara Perteghella,^{ib *ab} Elia Bari,^{id a} Milena Sorrenti,^{id a} Giuseppe Tripodo,^{id a} Theodora Chlapanidas^a and Maria Luisa Torre^{id ab}

Graphical abstract



Abstract

Silk proteins have been studied and employed for the production of drug delivery (nano)systems. They show excellent biocompatibility, controllable biodegradability and non-immunogenicity and, if needed, their properties can be modulated by blending with other polymers. Silk fibroin (SF), that forms the inner core of silk, is a (bio)material officially recognized by Food and Drug Administration for human applications. Conversely, the potential of silk sericin (SS), that forms the external shell of silk, could be still considered under evaluation. Based on our knowledge, nanoparticles based on silk sericin “alone” cannot be produced, due to its physicochemical instability influenced by extreme pH, high water solubility and temperature; for these reasons, it almost always needs to be combined with other polymers for the development of drug delivery systems. In this review, we focused on silk proteins as bioactive natural carriers, since they show not only optimal features as inert excipients, but also remarkable intrinsic biological activities. SF has anti-inflammatory properties, while SS presents antioxidant, anti-tyrosine, anti-aging, anti-elastase and anti-bacterial features. Here, we give an overview on SF or SS silk-based nanosystems, with particular attention on the production techniques.

Keywords: silk fibroin, silk sericin, nanomedicine, drug delivery, silk biological activity.

1. Introduction

Nanotechnology is moving quickly to become a part of our There still is much to learn about the nanotechnological world despite great progresses have been done within the past few years. The encapsulation of drugs into nanocarriers ameliorates their bioavailability and solubility profile, avoiding their biodegradation and instability.

The major challenge of drug delivery systems (DDS) is to deliver the drug to the targeted location at the right time and at the right dose ¹. Today, nano-drug delivery systems (NDDS), namely nanoparticles or nanospheres, both synthetic and natural-based, have been developed to overcome the major limitations related to conventional DDS; for example, exploiting their enhanced permeation and retention effect, nanosystems are able to passively reach cancer tissues, avoiding their dissemination to healthy tissues. NDDS are employed to improve both free Active Principle Ingredient (API) technological features, increasing their cargo loading, controlling drug fate, avoiding off-target dissemination, thus obtaining a controlled release and limiting cytotoxic effects mainly due to free drug presence and correlated side effects ^{2,3}. NDDS

are easily taken up by cells due to their small size; however, this feature leads to their quick clearance from the bloodstream.

Generally, NDDS “smartness” is related to their tunable sensitivity in responding to different stimuli such as variations in temperature, pH, magnetic field, light, and salt concentrations⁴⁻⁶. For example, introducing poloxamers as well as chitosan usually leads to temperature responsive systems.⁷ On the other side, the functionalization with polyacrylamides makes the polymer actively responsive to pH and temperature stimuli⁸. Unfortunately, these smart systems also suffer from several limitations including decreased mechanical strength, potential cytotoxicity (as for polyacrylamides) drug instability, chance of drug leakage or delay in payload release⁹.

Biological carriers, such as mesenchymal stem cells (MSCs), have been proposed as innovative smart nano-platforms due to their innate biocompatibility and stability in physiological conditions¹⁰. In particular, their secreted membranous vesicular systems (i.e. extracellular vesicles (EVs)) could be exploited, in combination with natural based nanoparticles (in this case silk fibroin nanoparticles), as nanobiological DDS, via a “carrier-in-carrier” approach¹¹⁻¹³.

Natural polymers have been investigated for the production of NDDS¹⁴⁻¹⁶: in particular, those characterized by a proteic structure have been widely employed due to their excellent biocompatibility, biodegradability, self-organization skills, large scale production and easy of functionalization, due to their amino acid groups¹⁷. Among them, silk occupies a key position in DDS production, due to its mechanical, physico-chemical and biological features: being produced by a wide variety of insects and spiders¹⁸.

This review paper highlights the development of nanosystems from silk proteins and in particular, it describes the structure and properties of SF or SS silk proteins, the production technique employed for silk-based nanoparticle production and their use as DDS.

2. Silk structure

Silk is natural fiber produced in the glands of arthropods including silkworms, scorpions, bees, mites and spiders (*Nephila clavipes*), with similarities and differences in both structure and properties¹⁹. In particular, *Bombyx mori* silkworm silk (*Bombycidae* family), also named mulberry silk, is the most renowned, characterized and employed silk; on the other hand, *Saturniidae* (*Antheraea mylitta*) produces non-mulberry silk. Otherwise, spider silk is not commonly employed due to the lack of commercially established supply chains, as occurs for sericulture, due to the smaller yield and wilder nature of spiders compared to silkworms²⁰.

B. mori silk cocoons are constituted by two proteins, namely SF and SS, closely linked but different in terms of structure and properties (Figure 1). Generally, the percentage of SF is about 65-85%, while SS ranges from 15% to 35%^{21 22 23}. Moreover, a non-sericin like component made of wax, pigments, sugars, mineral-salts and other impurities is also presents²¹.

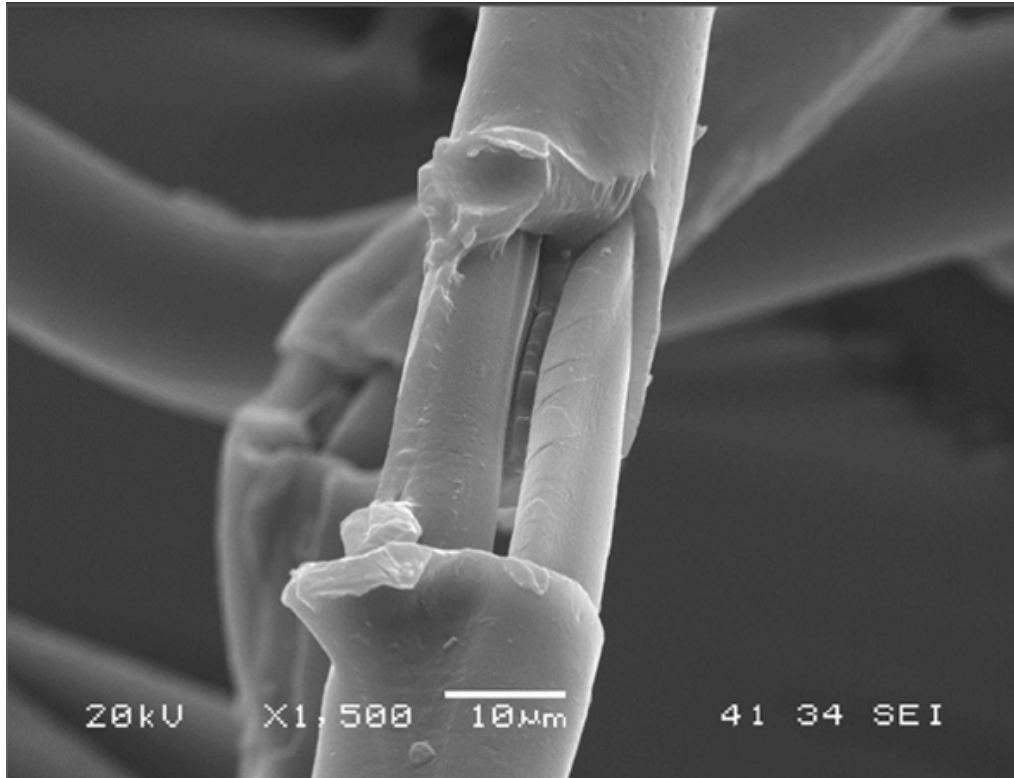


Figure 1. Scanning Electron Microscopy image of silk fiber.

The fibroin fibrous core is composed of a heavy (about 350 kDa) and a light (about 25 kDa) chain, linked together by both a single disulfide bond and a 25 kDa glycoprotein, entirely covered by a sericin glue-like structure, holding them together. The light chain is constituted by no-repeated sequences; contrastingly, the heavy chain is enriched in glycine (Gly) (46%), alanine (Ala) (29%), serine (Ser) (12%) and tyrosine (Tyr) (5%) creating typical highly-repeated sequences of hexapeptides (Gly-Ala-Gly-Ala-Gly-Ser) or dipeptides (Gly-Ala/Ser/Tyr), directly related to the secondary structure^{22 24}. Moreover, charged amino acids are present in fewer quantities, such as lysine, arginine, glutamate and aspartate^{25 26 27}.

SS has a globular structure and is enriched in aspartic acid (16%) and Ser (37%), polar amino acids²⁸ able to limit the shear stress during the SF spinning formation process. In nature, the SS coating is important for the silkworm's survival by protecting the larva from atmospheric hazards²⁹. Unfortunately, the simultaneous presence of SF and SS dramatically decreases the

biocompatibility of this biomaterial, thus limiting silk applications in its native form. For this reason, a degumming process is required to remove the SS coating from SF core, then the obtained degummed SF and SS solution are processed for the development of different DDS (Figure 2)²². Since SS is a water-soluble protein, it is easily removed by using boiling water or by exploiting alkaline and neutral proteases³⁰. Notably, the addition of detergents could alter the SS structure, molecular weight and functionalities²⁵. The degumming of cocoons in autoclave represents an effective strategy for obtaining an aqueous sericin solution, thus reusable for other purposes, but it is unable to remove all sericin, resulting in an impure SF. In fact, SS is constituted by three layers, characterized by different degrees of solubility due to their different amino acid composition (described in-depth below)²¹.

B. mori silk cocoons are constituted by two proteins, namely SF and SS, closely linked but different in terms of structure and properties (Figure 2). Generally, the percentage of SF is about 65-85%, while SS ranges from 15% to 35%^{21 22 23}. Moreover, a non-sericin like component made of wax, pigments, sugars, mineral-salts and other impurities is also presents²¹.

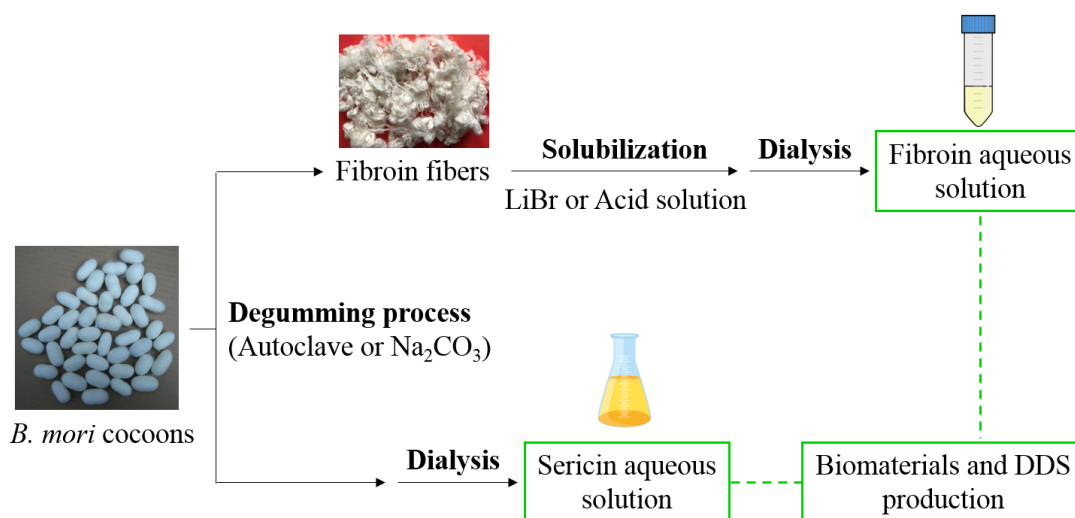


Figure 2. Processing of silk to obtain fibroin and sericin solution for biomaterials ad drug delivery system (DDS) production.

It is crucial to underline that SF molecular weight (MW) varies in relation to the degumming process time and procedure. Generally, a MW of about 100 kDa is obtained after a degumming with Na_2CO_3 for 30 minutes³¹. Moreover, the extraction time of SF strongly influences the

nanoparticle creation, since it directly regulates the degradation of silk chains and amorphous regions³².

Once obtained degummed fibers, regenerated SF is prepared by solubilizing it into chaotropic salts: the most common procedure is based on the use of highly concentrated lithium bromide solutions (LiBr), but other salts such as calcium chloride (CaCl₂) or lithium thiocyanate (LiSCN) are employed^{33 34 35}. Recently, Zheng and colleagues (2016) demonstrated that Ajisawa's reagent, a ternary mixture composed of CaCl₂, ethanol and water, is less expensive than LiBr, although it leads to SF aggregation during the subsequent dialysis steps, employed to remove solvent and salt³⁶.

Silk fibroin has been exploited for centuries due to its remarkable properties and today represents a suitable biomaterial for creating a spectrum of biomedical tools, starting from tissue engineering scaffolds to DDS^{37 38, 39}. In particular, nanoparticles could act as reservoir systems, achieving a sustained and controlled drug release with both high loadings and encapsulation efficiency^{40 41}. Today also silk sericin captured the attention of the scientific community for the development of a plethora of DDS and scaffolds²¹. For these reasons, several scientific research groups started working on silk-based nanosystems looking for new promising perspectives and therapeutic applications.

3. Silk fibroin

Since Galen's time, SF found its first application as a surgical suture material⁴². Overtime, SF has been employed in textile, cosmetic and biomedical fields and more recently as an innovative material in electric, optical and food industries²².

3.1 Silk fibroin structure

Considering its secondary structure, SF exists in three different structural models named Silk I, Silk II and Silk III. The first is mainly composed of α -helix domains, mixed with random coil and β -turn structures, and represents a metastable and water-soluble conformation. Conversely, Silk II is characterized by an antiparallel β -sheets/crystal molecular model, thus showing a higher stability and both water and solvent insolubility^{43 44}. Finally, Silk III structure prevails at the water/air interface⁴⁵.

Native SF exists in Silk II conformation, while regenerated SF is generally in Silk I. The secondary structure can be tuned by different processes: the treatment with alcohols, including ethanol and methanol, the application of physical shear, the exposure to water annealing

process, electromagnetic fields or autoclaving lead to SF conformational transition in its secondary structure, characterized by a dominant Silk II structure^{22 46 47 48}. For example, the water annealing process is a physical aqueous-based approach able to promote the SF conformational transition to β -sheets, avoiding the use of organic solvents : for this reason, it could be listed as a green method with suitable application for food coatings⁴⁹.

The peculiar self-assembly behavior of SF, from a molecular level to a hierarchical structure, is commonly exploited for creating micro-nanospheres, micro-nanoparticles and micro-nanofilaments, even if the mechanism has been not completely understood⁵⁰: hydrophilic polymers cause the phase separation, while water miscible solvents (such as methanol, ethanol and acetone) induce SF precipitation. This process, leading to nano-fibrils and micro-nanoparticle production, is influenced by changing molecular mobility, charge, hydrophilic interactions and concentrations⁵¹. For example, Bai and colleagues demonstrated that SF nano-fibrils have been developed by regulating the self-assembly mechanism during repeated drying-dissolving process steps⁵².

The presence of abundant carboxyl and amino groups in the side chains allows for suitable bio-functionalization, thus improving SF properties such as cellular adhesion and specific targeting²⁴. Surface modifications influence both cellular behavior and biological activity; for example, the presence of the arginine-glycine-aspartic acid (RGD) sequence facilitates cell adhesion and proliferation by an integrin binding mechanism⁵³. Moreover, the presence of tyrosine residues allows MSC adhesion, proliferation and differentiation⁵⁴.

3.2 Silk fibroin physico-chemical properties

SF retains an excellent combination of mechanical and biological features hard to find simultaneously in other natural or synthetic materials, which are strictly influenced by its secondary structure^{55,56}. Although silk evokes the idea of softness, it represents one of the most robust biomaterials in nature, retaining a toughness higher than Kevlar (para-aramid synthetic fiber employed for bulletproof vest production), a high tensile and breaking strength and elongation, stiffness and ductility. SF obtained from *B. mori* retains both the highest tensile strength and modulus when compared to other silkworm family silks⁵⁷. All of these mechanical features made SF one of the most employed polymer for the production of load bearing scaffolds in bone tissue regeneration⁵⁸.

SF shows great stability even when processed at extreme temperatures (higher than 250°C) without affecting its stability and structure⁵⁹. Exploiting this feature, SF was employed for the

development of rhodamine B-loaded microneedles by thermal drawing; the subsequent treatment with methanol influenced either SF microneedle mechanical strength and drug release⁶⁰. Additionally, it shows good permeability to oxygen and water vapor, thus paving the way to its innovative application for food coating^{49, 61}

All of these unique features made SF a biomaterial officially recognized by Food and Drug Administration (FDA) for the development of a plethora of nanotechnological tools⁶².

3.3 Silk fibroin biological properties

Despite its xenogeneic origin, SF is universally recognized as a biocompatible material, retaining a tolerability comparable to that observed for synthetic materials (PLA, PGA and PLGA) and other natural polymers such as chitosan. Inflammatory responses and immune-events, such as hypersensitivity reactions, are mainly linked to the presence of SS residues that still cover the SF after the degumming process⁶³. Surprisingly, recent suggestions showed that SF possess an intrinsic anti-inflammatory therapeutic potential as already observed in a mice edema model⁶⁴ and in the treatment of inflammatory bowel disease⁶⁵, even if its mechanism has not been explained. SF anti-inflammatory activity could substitute traditional anti-inflammatory therapies based on NSAIDs, COX-2 and PGE-2 inhibitors, glucocorticoids, which can even worsen the pathological condition. The biodegradation products of SF allowed to reduce the inflammatory conditions as reported in a mice edema model by suppressing the secretion of inflammatory markers including COX-2, IL-6, IL-1 β and TNF- α . A synergic effect was observed when employing SF and the superoxide dismutase enzyme⁶⁴. Disagreeing results were observed by Cui et al., where SF microparticles, obtained by grinding, up-regulated the production of IL-6, IL-1 β and TNF- α , resulting in an increasing of the inflammatory condition⁶⁶.

A synergic activity, accompanied with a boost of its anti-inflammatory activity, was observed in SF nanoparticles encapsulating resveratrol. The reduction of the expression of several mediators of inflammatory pathway, including chemokines, cytokines and adhesion molecules have been shown⁶⁵. The advantages to employ SF nanoparticles are that they can be easily targeted, thus adhering better to inflamed tissues compared to traditional drugs, increasing the therapeutic effect and limiting side effects and safety issues. Its intrinsic anti-inflammatory activity, makes SF an effective active ingredient, as actually occurs for other natural-based compounds such as chitosan, and no longer be regarded as a “simple” excipient employed for scaffold or drug delivery vehicle production.^{67, 68}

Concerning the biodegradation, the US Pharmacopeia (USP) lists SF as a non-biodegradable material, since it preserves more than 50% of its tensile strength after 60 days of implantation *in vivo*, yet this statement disputes what is reported in the literature by several authors^{69 70}. This different behavior depends on the type of SF (native or regenerated status), type of system (e.g. porous or not) and implantation site. 3D scaffolds, based on regenerated SF, completely biodegrade within one year via host immune system activity⁷¹. Since SF is a protein, it undergoes a proteolysis pathway lead by the host immune system reaction and also by the protease enzymes at the implantation site, which are responsible for the amino acid chain leakage. The implantation site, the animal model and the type of protease influence the SF biodegradation mechanism and rate. For example, protease XIV induces higher mass reduction of SF scaffolds than α -chymotrypsin⁷². In addition, the inflammation raised by the SF scaffold itself promotes its degradation. Moreover, the SF conformation strictly influences the degradation rate: high β -sheet content increases scaffold permanence at the implantation site. Nevertheless, even if SF undergoes a biodegradation pathway, it does not show issues related to the release of acidic by-products as occurs when employing synthetic polymers, such as poly lactic acid (PLA), poly glycolic acid (PGA) and their co-polymer poly lactic-co-glycolic acid (PLGA)⁷³.


Notably, in relation to all the described features, SF scaffolds can be sterilized in autoclave, a procedure not possible for other protein-based biomaterials including collagen without affecting their morphology and properties.^{74 75} Conversely, organic solvents such as ethylene oxide or γ -irradiations could produce conformational changes⁷⁶.

Native SF fibers and regenerated SF solutions have already been processed with different approaches to obtain several systems, including films⁷⁷, sponges⁴⁶, microparticles⁷⁸, non-woven mats⁷⁹, hydrogels⁸⁰, tubes⁸¹ and nanoparticles⁸².

4. SF nanoparticles

Nanoparticles are obtained from regenerated SF using a broad variety of methods, exploiting silk self-assembly behavior ruled by hydrophilic and hydrophobic chain interactions⁴³ (Figure 3). Notably, comparison studies of SF nanoparticles obtained by using mulberry and non-mulberry silks showed no significant differences in terms of particle size, geometry, surface charge and cellular uptake⁴⁰. When employing a natural protein-based material characterized by a high molecular weight, it is really hard to control and standardize the production process and thus to obtain nanosystems with a mean diameter lower than 100 nm⁸².

A broad spectrum of techniques could be used to develop SF nanosystems including those requiring specific instruments such as the milling technique, the electrospray and the supercritical fluid technology, those based on solvent or microemulsion formation and finally those considered as “niche” techniques such as the microcapillary dot method ⁸².



Encapsulated Active	Silk Fibroin - PTX	Silk Fibroin - DOX	Silk Fibroin - Cisplatin	Silk Fibroin - Curcumin
Production Technique	Desolvation (ethanol)	Salting out (potassium phosphate 1,25 M)	Electrospraying	Microdot capillary
Size	130 nm	130 nm	59-75 nm	100 nm
Therapeutic Effect	Superior anti-tumor activity than free PTX	Magnetic tumor targeting	Induced lung cell apoptosis	Efficacy against breast cancer
Reference	P. Wu et al., 2013	Tian, Jiang, Chen, Shao, & Yang, 2014	Qu et al., 2014	Gupta, Aseh, Rios, Aggarwal, & Mathur, 2009

Figure 3. Examples of silk fibroin nanoparticles loaded with different actives. Production techniques, nanosystem dimension and therapeutic effects are reported. PTX - Paclitaxel; DOX – Doxorubicin.

A coarse technique employed for SF nanoparticle production is the milling procedure also known as mechanical comminution: a simple physical method based on chopping, grinding and crushing the SF degummed fibers into smaller systems ⁶⁶. Unfortunately, this method required specific apparatus (such as cutter mill, rotary milling and planetary ball milling) and long time period, and generally results in big nanoparticle aggregates with a wide size range ⁸³. For these reasons it is not as commonly employed.

Desolvation represents the most common method for obtaining protein-based nanoparticles (Figure 4). Also known as simple coacervation, it is based on the reduction of the SF chain

solubility in the presence of organic solvents such as acetone³², ethanol⁸⁴, dimethyl sulfoxide (DMSO)⁴⁰ and methanol⁶⁵, leading to a phase separation⁸⁵. The organic solvent/dissolving agent leads to a sudden SF chain dehydration and packaging, leading to a change from Silk I to Silk II conformation and providing the nanosystem formation. Thanks to the electrostatic repulsion with the negative charge, the nanoparticle aggregation does not occur⁸⁶ even if the SF concentration plays a crucial role in controlling the final nanosystem dimension and stability. Therefore, finding the optimum SF/dissolving agent ratio is required. This easy process allows researchers to obtain nanosystems with controllable size; the inner core is composed of SF crystalline domains, while the core shell is characterized by the presence of hydrophilic tails⁸⁷.

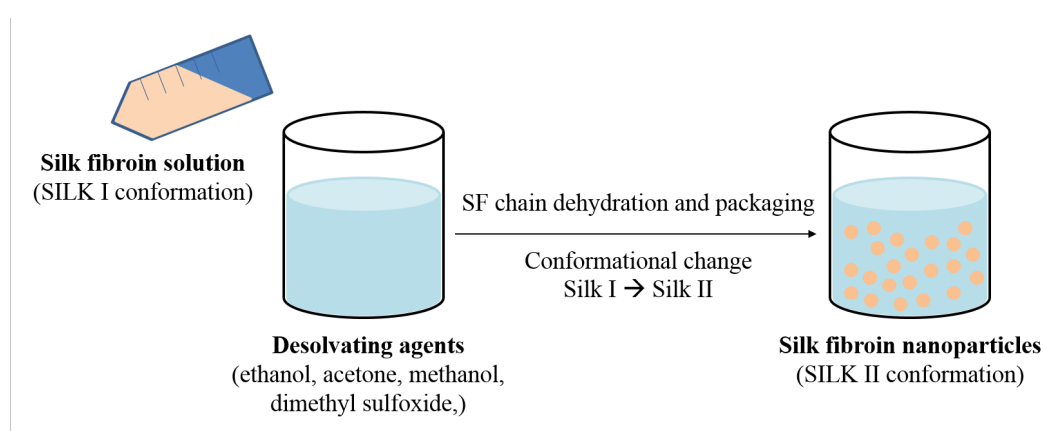


Figure 4. Representation of desolvation method for the production of silk fibroin nanoparticles.

The presence of organic solvents allows easy encapsulation of lipophilic active compounds by solubilizing them into the dissolving agents before carrying out the nanoparticle production. For example, curcumin- and 5-fluorouracil-loaded SF nanoparticles have been recently considered as innovative NDDS for breast cancer treatment⁸⁸. Notably, the nano-encapsulation of natural lipophilic drugs such as curcumin and resveratrol allows the drugs to overcome some of their typical hurdles including poor bioavailability and limited solubility, thus improving their therapeutic application potential⁸⁹.

The main drawback of dissolution is the presence of organic solvents, which must be removed by several centrifuge or strong dialysis cycles in order to avoid any cytotoxicity events.

In 2013, Wu and colleagues developed an innovative method to obtain nanoparticle production, exploiting the natural self-assembly of SF. Paclitaxel (PTX) ethanolic solution was added drop wise into the aqueous SF solution, limiting the amount of organic solvent and avoiding the use of surfactants. PTX-loaded nanosystems were round shape structures with a mean diameter of

130 nm and they were uptaken by gastric cancer cells, showing a higher antitumor efficacy than the systemic administration of free PTX⁹⁰. Seib and colleagues developed DOX-loaded SF nanoparticles by acetone nano-precipitation for the treatment of breast cancer and they showed a stimulus-responsiveness influenced by pH, highlighted in acidic conditions. Moreover, nanoparticles were taken up by breast cancer cells and DOX was released in a controlled manner once internalized in lysosomes³².

Salting out represents another valid approach employed for SF nanoparticle production (Figure 5), even if it results in SF nanoparticles with higher dimensional range (500-2000 nm). This process starts with the preparation of a salting bath, based on potassium phosphate salts, typically K_2HPO_4 - KH_2PO_4 . The nanosystems resulted by the hydrophobic interaction between the SF protein chains and the decreased water molecules, which are replaced by protein-protein interactions^{91, 82}. The salt, pH, ionic strength and SF concentration influence the process yield, particle morphology, zeta potential, secondary structure, and nanoparticle stability. Alkaline pH is preferred over acidic to avoid non-dispersible aggregates. Otherwise, the secondary structure of nanoparticles obtained by salting out technology could influence the drug release⁹¹. For example, Tian and colleagues developed doxorubicin (DOX)-loaded magnetic SF nanoparticles by a one-step salting out approach, effective for targeted cancer therapy purposes. Briefly, magnetic nanosystems were added to the potassium phosphate bath before adding the SF solution, providing both the drug targeting, by the application of magnetic field, and the nanoparticle formation⁹². The major drawback of this technique is related to the use of high amount of salts, difficult to remove with standard dialysis cycles.

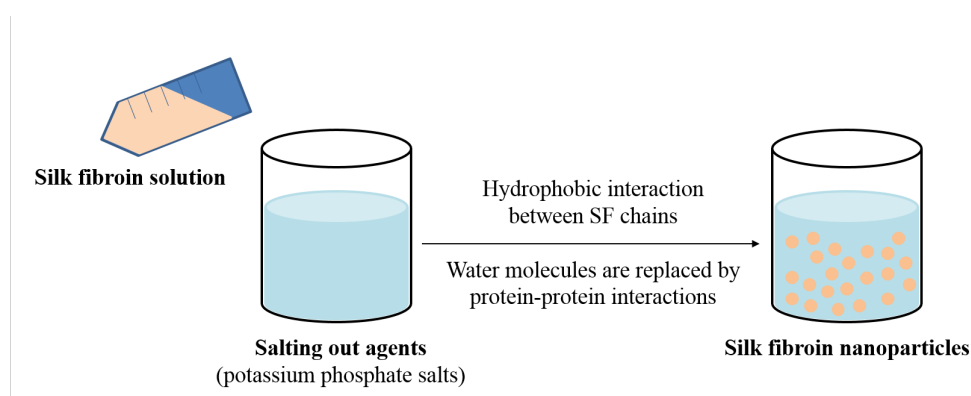


Figure 5. Representation of salting out method for the production of silk fibroin nanoparticles.

Electro-spraying provides the atomization of a starting SF solution via electrical field applications. A capillary nozzle passing through a high voltage field drops out silk solution. In

this way, electrostatic forces break down the flow into small droplets. The obtained SF nanoparticles, highly pure due to the absence of desolvating agents or salt solutions, have to be treated with organic solvents to induce the conformational transition into the stable conformation (Silk II)⁹³. Moreover, the presence of two coaxial needles allows the creation of SF bubbles in which air is encapsulated within the protein solution⁹⁴. Kim et al. prepared SF microparticles via electro-spraying and demonstrated that both the concentration and the shear viscosity of SF solution played the most crucial role in affecting microsystem round-shaped geometry. Regular particles were obtained with short dissolution times (5 minutes in Ajisawa's reagent at 80°C) and high concentration (10% weight) of SF⁹⁵.

Characterized by a similar technology, the laminar jet break-up represents a non-harsh condition method, similar to spray-drying and electro-spraying techniques, although it avoids high temperature. The method consists of a vibrating nozzle that breaks the aqueous SF flow into small droplets. Due to high voltage application, droplets are then frozen in nitrogen. Wenk and colleagues observed that the SF nanoparticle diameter was directly influenced by the nozzle diameter and the treatment employed to obtain Silk II conformation. Moreover, authors encapsulated labile biological drugs, such as insulin-like growth factor, without affecting their properties due to the mild process⁹⁶. An appealing technique is represented by supercritical fluid technology. CO₂ is the most employed supercritical fluid mainly due to a-toxicity and low cost⁹⁷, for more details on this topic see review⁹⁸. These three techniques, electrospray, laminar jet break up and supercritical fluid technology, need specific apparatus and for this reason are expensive.

For the first time in 2009, Gupta et al. used the capillary microdot technique to create SF nanoparticles loaded with curcumin, characterized by a dimensional range lower than 100 nm and showing appealing anti-tumoral activity. The blending between SF and chitosan, proposed by the authors as a promoter of in vivo tissue regeneration, decreased both curcumin entrapment and release. The introduction of chitosan triggered the hydrophilic properties of nanosystems, resulting in a reduction of curcumin entrapment, which is a highly hydrophobic active, and consequently in a lower drug release⁹⁹.

Recently, an intriguing strategy for preparing SF nanoparticles directly during the dissolution step was suggested by Xiao and colleagues. Briefly, using specific concentration of a combination between formic acid and lithium bromide permitted to control the dissolution degree of SF degummed fibers. The obtained SF nanoparticles showed a spherical shape, no aggregation phenomena and a dimension of about 100-200 nm¹⁰⁰.

Generally, different approaches are used to load active molecules into SF nanoparticles: the encapsulation method, also named entrapment, is achieved by the solubilization of drug into bath in which nanoparticles are obtained. The absorption method, also known as the co-incubation technique, is based on loading of drug only onto nanosystem surface. Finally, the covalent binding is reached through the creation of drug-fibroin interactions of different natures, including chemical/physical reactions or crosslinking approaches ¹⁰¹.

SF nanoparticles appeared suitable NDDS for the encapsulation of labile drugs, such as growth factors. For example, vascular endothelial growth factor (VEGF) was loaded in SF nanoparticles by the co-incubation technique and a sustained drug release has been observed for over 3 weeks without any burst release ⁴⁰. Similarly, bone morphogenetic protein-2 (BMP-2) was successfully encapsulated in SF nanoparticles, obtaining a controlled release of the encapsulated growth factor, making them effective for bone regeneration ⁴¹.

The absorption method is achieved by electrostatic bonds between the SF negatively charged nanoparticles and positively charged drugs by a simple incubation technique ^{40 102}, modifying the zeta potential of nanosystems ¹⁰³. The surface decoration with positively charged moieties including chitosan or polyethylenimine avoids aggregation phenomena, thus improving cellular uptake ¹⁰².

The SF nanoparticle surface could be modified, thus improving drug loading, specific targeting and controlled release. It has many active sites, such as tyrosine residues and RGD sequences, which could be considered suitable anchorage sites for the bio-conjugation of surface molecules ¹⁰⁴. PEGylation avoids nanoparticle aggregation phenomena by ameliorating their stability in suspension; this approach is commonly employed not only for SF, but also for all of the protein-based nanosystems ¹⁰⁵. Wang et al. evaluated the stability of SF nanoparticles by coating them with glycol chitosan, N,N,N-trimethyl chitosan, polyethylenimine and PEGylated polyethylenimine by exploiting electrostatic interactions. Results showed that those coated with glycol chitosan and PEGylated polyethylenimine were easily re-suspended after lyophilization due to steric repulsion of the polymer chains ¹⁰². Since SF is enriched in selective sites exploitable for PEG bonds, such as cysteine residues, this represents an interesting approach for overcoming the tendency of SF nanoparticles to aggregate after freeze-drying. Moreover, lyophilized nanoparticle aggregation problems could be overcome by adding cryo-protectants, such as glycine or mannitol, to the raw material ¹⁰⁶.

Recently, RGD motifs have been added to SF nanoparticles to increase their targeting abilities to reach intestinal tissue; in particular, results showed that RGD functionalization reduces pro-inflammatory molecule release in bowel disease murine models ¹⁰⁷.

4.1 SF blended nanoparticles

It is quite common in nanotechnology to combine polymers of different natures to exploit benefits from both of them, even if the obtained result will not meet the expectation. Although SF encloses a plethora of benefits, sometimes it is necessary to couple it in order to completely fulfill the desired target, even if the combination of different polymers could not lead to better results. For example, SF-albumin blended nanoparticles were developed for methotrexate delivery. The presence of albumin improved SF mechanical properties and biodegradability, while drug nano-encapsulation avoided methotrexate cytotoxicity effects, including hepatotoxicity and pulmonary diseases ¹⁰⁸.

Conversely, SF-chitosan non-covalently blended nanosystems were developed to deliver curcumin but the authors obtained worse results than when using the single polymer nanosystems. Curcumin entrapment reached 96% for SF nanoparticles and 64-73% for blended nanoparticles. This difference was also observed in terms of cellular uptake and efficacy against breast cancer cells ⁹⁹. Contrastingly, SF-PEG blended nanosystems loaded with curcumin were produced for anti-aging purposes and provided a suitable support for tissue regeneration ⁷⁷. Notably, the particle size of SF-PEG nanosystems was influenced by both PEG molecular weight and concentration. Moreover, when employing PEG with low molecular weight at a concentration between 40% and 60% w/v, hydrogels were formed ¹⁰¹. Similarly to PEG, poly vinyl alcohol (PVA), a FDA-approved polymer, was successfully employed for SF blended micro-nanosphere production because a natural phase separation occurred when the two polymers were combined to create films via a three step process ¹⁰⁹. Briefly, blended SF-PVA solutions were employed to prepare dried films dissolved in water, and then centrifuged in order to obtain SF nanoparticles ¹⁰⁸. Moreover, PVA is able to improve the nanoparticle superficial morphology in terms of smoothing and uniformity ¹¹⁰.

In this context, Numata and colleagues obtained a bimodular scaffold based on SF hydrogel, loaded with rhodamine B and containing SF nanoparticles loaded with fluorescein isothiocyanate (FITC). They observed a starting burst release for rhodamine B, whereas a sustained and controlled release for FITC was noted ¹¹¹. This approach could be employed not only for dye models, but also to couple API with different biological properties.

5 Silk Sericin

5.1 Silk sericin structure

SS is a hydrophilic-based glycoprotein synthesized by the labial gland of *B. mori*, with a molecular weight of about 200 kDa, highly enriched in polar amino acids. It consists of 18 types of amino acids including serine, glycine, glutamic acid, aspartic acid, threonine and tyrosine, with serine being the most prevalent^{29 112 113}.

Notably, it becomes enriched in flavonoids and carotenoids, responsible for antioxidant and anti-tyrosinase activities¹¹⁴. The typical globular shape of SS is due to the peculiar amino acid disposition and their properties confer it typical adhesive features. From an organic composition description, SS contains 46.5% carbon, 31% oxygen, 16.5% nitrogen, and 6% hydrogen¹¹⁵.

X-ray studies allow us to observe that SS structure is divided in three parts according to their different solubility and amino acid structure; each layer is produced and secreted by cells localized in different gland regions of the arthropods. Sericin A is the external layer and is easily removed by degumming silk cocoons by hot water; sericin B occupies the middle space and has lower polarity even if it contains the same amino acids as sericin A; finally, the inner layer is represented by sericin C, strictly close to the SF filaments and showing poor water solubility. In order to completely remove all three sericin layers, alkali solutions must be used during the degumming process¹¹⁶.

SS secondary structure retains a combination of β -sheets and random coil domains, thus giving it a double behavior, albeit the latter is often predominant. As occurs for SF, SS crystallinity could also be induced by the exposure to organic solvent (e.g. ethanol), increasing the mechanical or physical shear stresses or via the crosslinking with glutaraldehyde^{117 118}. Its polar structure explains its solubility in water, even if it depends on the ratio of random coil to β -sheet structures. Interestingly, SS is soluble in hot water, while its β -sheet conformation prevails at lower temperatures resulting in a gel formation¹¹⁹.

5.2 Silk sericin properties

SS has been considered for centuries as a silk waste product in textile industries, extracted and removed during the degumming process, in order to ameliorate the quality and biocompatibility of SF. Only recently, SS has been considered for biomedical, cosmetic and pharmaceutical purposes (Figure 6)²⁹.

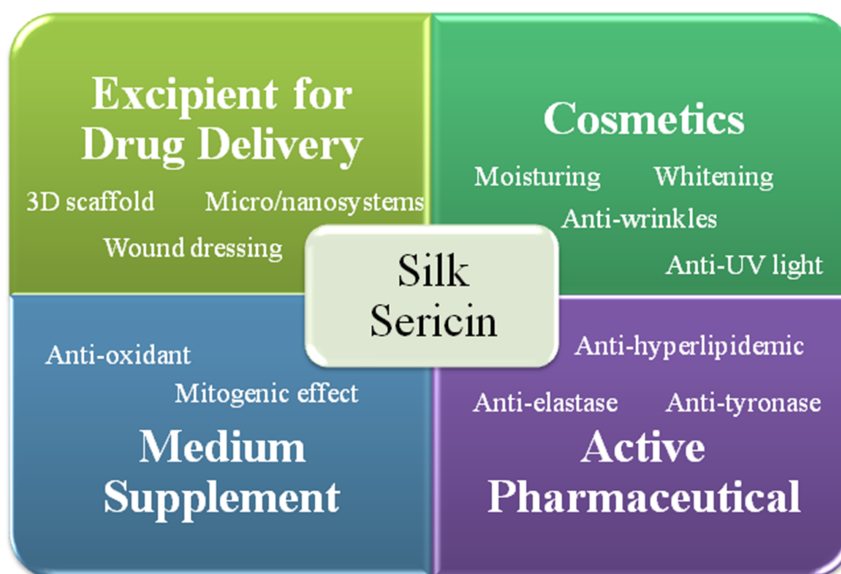


Figure 6. Possible application fields of silk sericin. Silk sericin is employed as an excipient for the development of drug delivery systems, in cosmetic field, as an effective active pharmaceutical ingredient or as a supplement for cell culture medium, as a substitute for fetal bovine serum.

It is difficult to recycle SS after classic degumming processes due to the presence of chemicals, although Wu and collaborators recently developed an innovative degumming process able to recover SS by employing ultrafiltration ¹²⁰.

SS shows several activities such as antioxidant ^{121, 122}, anti-aging (anti-wrinkle), whitening ¹²³ anti-tyrosinase, anti-elastase ¹²⁴, anti-bacterial (wound-healing), anti-coagulation ¹²⁵, anti-inflammatory ¹²⁶ and cryo-protection. For example, the antioxidant activity is related to SS amino acidic composition, enriched in –OH groups ¹²¹. Moreover, SS shows a hypoglycemic effect by increasing insulin production and secretion as observed in rat models, and also by ameliorating diabetes-related complications ^{127 128}.

As already discussed for SF, also SS retains an anti-inflammatory activity triggered by the inhibition of the proliferation of human peripheral blood mononuclear cells ¹²⁴.

Otherwise, its addition to cell culture media improves cell proliferation, showing a mitogenic effect on several cell lineages and avoiding oxidative stress ¹²⁹. In particular, Terada et al. reported positive results on four cellular lineages using low MW SS at a concentration between 0.01% and 0.1% weight/volume ¹³⁰. SS is increasingly introduced as fetal bovine serum substitute as cellular supplement due to lower cost and no risk of zoonosis ¹³¹.

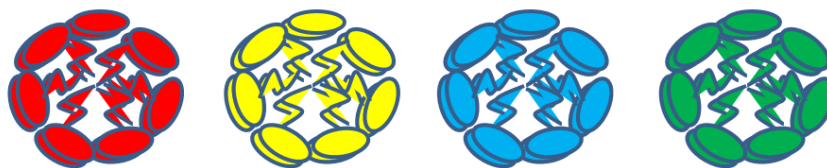
The potential of SS at a nanoscale level, for the design and development of nano-tools, has not been completely investigated. Based on our knowledge, results regarding the employment of SS “alone” for nanoparticle production, still lack, probably due to its instability influenced by extreme pH, water solubility and temperatures.

6. SS blended nanoparticles

SS is enriched in several polar side chains made of hydroxyl, carboxyl and amino groups providing a broad spectrum of functionalization, crosslinking and blending with other polymers to make it suitable for biomedical and therapeutic applications (Figure 7) ¹³². As already mentioned for SF, PEGylation technique was employed to improve SS nanoparticle stability in water, which is the principal goal during SS nanoparticle design. Notably, the introduction of PEG chains allowed the conformational change into SS structure, from random coil to β -sheet ¹³³. Similarly, genipin, a non-toxic, natural cross-linker, was introduced to develop SS nanoparticles for the delivery of atorvastatin. Close to what was reported for SF nanoparticles, dissolution technique in ethanol was exploited to obtain SS nanosystems, followed by its bond with the cross-linker. Briefly, nanosystems were characterized by a particle size of 166 nm with a high entrapment efficiency (91%) and a controlled drug release related to the cross-linking level; the higher the cross link with genipin, the slower drug release in 48 hours. Moreover, the anti-hyperlipidemic activity of SS potentiated the atorvastatin in vivo therapeutic potential maybe due to their synergic activity ¹³⁴.

SS-poly(ethyl cyanoacrylate) nanospheres were developed for delivery of fenofibrate, a lipophilic agent for lipid regulation. The presence of SS conferred muco-adhesive properties to poly(ethyl cyanoacrylate), creating stable NDDS able to stay for 6 hours in the gastric environment. These nanosystems were produced by interfacial polymerization, simply by adding dropwise cyanoacrylate to SS acidic solution, and then fenofibrate was loaded exploiting the incubation method (reported by the authors as soak method). The fenofibrate loading into SS nanospheres improved its oral bioavailability, increasing its in vivo activity and avoiding hepatic lipid accumulation ¹³⁵.

SS nanoparticles blended with Pluronic F-127 and F-87 were developed as bimodular NDDS for both hydrophilic and hydrophobic drugs (FITC and PTX, respectively). The obtained nanosystems showed high stability in aqueous solutions and were rapidly internalized by cells due to their small dimensions of 100-110 nm. Moreover, results showed the efficacy of nanosystems to deliver and release the encapsulated drug, inducing cancer cell apoptosis ¹³⁶.



Encapsulated Active	Silk Sericin - Atorvastatin	Silk Sericin - Fenofibrate	Silk Sericin - FITC & PTX	Silk Sericin - DOX
Composite Material	Genipin	Poly(ethyl cyanoacrylate)	Pluronic F-127 and F-87	Folate
Size	166 nm	175 nm	100-110 nm	≈ 50 nm
Therapeutic Effect	Increase of anti-hyperlipidemic activity	Increase of bioavailability/efficacy of fenofibrate	Bimodular device for both hydrophilic and hydrophobic drugs	Tumor targeting and pH responsiveness (acidic conditions)
Reference	Kanoujia, Singh, Singh, & Saraf, 2016	Parisi et al., 2015	Mandal & Kundu, 2009	Huang et al., 2016

Figure 7. Examples of silk sericin nanoparticles combined with different molecules, including non-toxic crosslinkers such as genipin, Pluronic, folate-based targeted moieties and poly(ethyl cyanoacrylate).

The blending of SS to obtain nanoparticles is necessary to stabilize the SS, avoiding rapid drug leakage and allowing the acquisition of targeting capabilities. However, despite these advantages, the blending approach could result in limitations/drawbacks due to the use of synthetic-no biodegradable polymers/cross linkers¹³⁷. In relation to tumor targeting decoration, Huang and colleagues developed folate-SS-DOX nanoparticles: these nanosystems showed the ability to reach tumoral tissues by conjugating them with folate moieties. The presence of hydrozone bonds, by which DOX is linked to SS structure, showed a pH responsiveness resulting in a controlled drug release only selective for acidic conditions, which are typical of tumor tissues. Moreover, the interaction between highly hydrophilic SS and lipophilic drugs, such as DOX, resulted in nanoparticle formation due to the self-assembly behavior of SS¹³⁷.

7. Pre-clinical and clinical trials

There are several in vitro or pre-clinical studies regarding silk nanosystems, showing their efficacy in the treatment of a broad spectrum of diseases, starting from cancer to inflammatory diseases. Very interesting was the efficacy of the combination between curcumin and 5-fluorouracil loaded SF nanoparticles for the treatment of breast cancer. They effectively reduced in vivo the tumor size, compared to free drug treatments, probably by inducing cell apoptosis mediated by reactive oxygen species secretion⁸⁸. Concerning SS, in vivo studies of fenofibrate-loaded SS nanosystems, obtained by blending it with poly-ethyl cyanoacrylate, showed an anti-hyperlipidemic effect by increasing fenofibrate poor solubility and bioavailability¹³⁵.

Unfortunately, these are not enough. Albeit silk-based polymers are capturing the interest of the scientific community, we are still far from their clinical application; this statement is enforced by the fact that until today there is no clinical trial based on silk-based polymers (searching for SF/SS nanoparticles, last access June 1st, 2017). Yet, different types of nano-carriers are commercially available, mainly liposomes and polymeric micelles, leading to good clinical results¹³⁸. The question arises spontaneously: “Why this diffidence in performing experiments on human beings?” “Why are clinical applications/trials based on silk nanosystems still missing?” One answer could be the fact that there are still several doubts concerning nanoparticle toxicity, regardless of their components, as occurred for Ferugulose ® (NC100150) and Resovist ®¹³⁹. Another possible response is that in vitro results related to silk nanoparticle employment do not completely match the prefixed target. Moreover, the tuning of a scalable and cheap production method could open the industrial production to silk nanosystems, thus opening their clinical applications. Nevertheless, we believe that silk nanoparticles will find their clinical applications, opening innovative, undiscovered and exciting perspectives for the treatment of fatal diseases to future generations.

8. Conclusions

Silk fibroin retains unique mechanical, physico-chemical and biological features, making it a suitable natural polymer for drug delivery system design and development. Otherwise, silk sericin shows lower structural properties but a higher number of biological activities, and thus applications, than silk fibroin. Silk fibroin nanoparticles could be developed by tuning the fibroin secondary structure, while silk sericin needs to be blended with other polymer(s) for the creation of nano drug delivery systems. All the nanoparticle production techniques show both

advantages and drawbacks, which must be overcome by exploring and developing new ones. Despite this, both nanosystems have been employed for drug delivery purposes including small molecules, proteins and genes to achieve the treatment of several fatal diseases. Nevertheless silk proteins have been deeply studied *in vitro*, their clinical applications are still lacking. Overall, silk proteins appeared as suitable and innovative natural-inspired excipients, exploitable for the development nano drug delivery systems in multidisciplinary fields, as well as bioactive compounds able to improve and support some active principle ingredient effects.

9. Acknowledgements

This paper was partially supported by Artefil S.R.L (Luisago, CO, Italy) and Innovhub, Stazioni Sperimentali per l'industria, sezione Seta (MI, Italy). The authors are grateful to Ryan Rogers, University of Michigan, for editorial help.

10. Notes and References

1. W. H. De Jong and P. J. A. Borm, *International Journal of Nanomedicine*, 2008, 3, 133-149.
2. F. Mottaghitlab, M. Farokhi, M. A. Shokrgozar, F. Atyabi and H. Hosseinkhani, *Journal of Controlled Release*, 2015, 206, 161-176.
3. S. S. Suri, H. Fenniri and B. Singh, *Journal of occupational medicine and toxicology (London, England)*, 2007, 2, 16-16.
4. D. Liu, F. Yang, F. Xiong and N. Gu, *Theranostics*, 2016, 6, 1306-1323.
5. C. LoPresti, V. Vetri, M. Ricca, V. Fodera, G. Tripodo, G. Spadaro and C. Dispenza, *Reactive & Functional Polymers*, 2011, 71, 155-167.
6. C. Dispenza, G. Tripodo, C. LoPresti, G. Spadaro and G. Giammona, *Reactive & Functional Polymers*, 2009, 69, 565-575.
7. D. Mandracchia, A. Trapani, G. Tripodo, M. G. Perrone, G. Giammona, G. Trapani and N. A. Colabufo, *Carbohydrate Polymers*, 2017, 166, 73-82.
8. A. MR, E. C, G. A, V. B and R. JS, *Smart polymers and their applications as biomaterials*, Pennsylvania, 2007.
9. H. Priya James, R. John, A. Alex and K. R. Anoop, *Acta pharmaceutica Sinica. B*, 2014, 4, 120-127.
10. L. A. L. Fliervoet and E. Mastrobattista, *Advanced Drug Delivery Reviews*, 2016, 106, 63-72.

11. S. Perteghella, B. Crivelli, L. Catenacci, M. Sorrenti, G. Bruni, V. Necchi, B. Vigani, M. Sorlini, M. L. Torre and T. Chlapanidas, *International journal of pharmaceutics*, 2017, 520, 86-97.
12. G. Tripodo, T. Chlapanidas, S. Perteghella, B. Vigani, D. Mandracchia, A. Trapani, M. Galuzzi, M. C. Tosca, B. Antonioli, P. Gaetani, M. Marazzi and M. L. Torre, *Colloids and Surfaces B-Biointerfaces*, 2015, 125, 300-308.
13. B. Crivelli, T. Chlapanidas, S. Perteghella, E. Lucarelli, L. Pascucci, A. T. Brini, I. Ferrero, M. Marazzi, A. Pessina, M. L. Torre and G. Italian Mesenchymal Stem Cell, *Journal of Controlled Release*, 2017, 262, 104-117.
14. D. Mandracchia, A. Rosato, A. Trapani, T. Chlapanidas, I. M. Montagner, S. Perteghella, C. Di Franco, M. L. Torre, G. Trapani and G. Tripodo, *Nanomedicine-Nanotechnology Biology and Medicine*, 2017, 13, 1245-1254.
15. D. Mandracchia, G. Tripodo, A. Trapani, S. Ruggieri, T. Annese, T. Chlapanidas, G. Trapani and D. Ribatti, *European Journal of Pharmaceutical Sciences*, 2016, 93, 141-146.
16. G. Tripodo, A. Trapani, M. L. Torre, G. Giammona, G. Trapani and D. Mandracchia, *European Journal of Pharmaceutics and Biopharmaceutics*, 2015, 97, 400-416.
17. J. E. Gagner, W. Kim and E. L. Chaikof, *Acta Biomaterialia*, 2014, 10, 1542-1557.
18. C. Fu, Z. Shao and V. Fritz, *Chemical Communications*, 2009, 6515-6529.
19. Y. Wang, H.-J. Kim, G. Vunjak-Novakovic and D. L. Kaplan, *Biomaterials*, 2006, 27, 6064-6082.
20. J. G. Hardy and T. R. Scheibel, *Biochemical Society Transactions*, 2009, 37, 677-681.
21. T.-T. Cao and Y.-Q. Zhang, *Materials Science & Engineering C-Materials for Biological Applications*, 2016, 61, 940-952.
22. G. H. Altman, F. Diaz, C. Jakuba, T. Calabro, R. L. Horan, J. S. Chen, H. Lu, J. Richmond and D. L. Kaplan, *Biomaterials*, 2003, 24, 401-416.
23. S. Inoue, K. Tanaka, F. Arisaka, S. Kimura, K. Ohtomo and S. Mizuno, *Journal of Biological Chemistry*, 2000, 275, 40517-40528.
24. C. Vepari and D. L. Kaplan, *Progress in Polymer Science*, 2007, 32, 991-1007.
25. G. Freddi, R. Mossotti and R. Innocenti, *Journal of Biotechnology*, 2003, 106, 101-112.
26. C. Z. Zhou, F. Confalonieri, M. Jacquet, R. Perasso, Z. G. Li and J. Janin, *Proteins-Structure Function and Genetics*, 2001, 44, 119-122.
27. H. Heslot, *Biochimie*, 1998, 80, 19-31.

28. A. Garel, G. Deleage and J. C. Prudhomme, *Insect Biochemistry and Molecular Biology*, 1997, 27, 469-477.
29. S. C. Kundu, B. C. Dash, R. Dash and D. L. Kaplan, *Progress in Polymer Science*, 2008, 33, 998-1012.
30. F. Lucas, J. T. Shaw and S. G. Smith, *Advances in protein chemistry*, 1958, 13, 107-242.
31. L. S. Wray, X. Hu, J. Gallego, I. Georgakoudi, F. G. Omenetto, D. Schmidt and D. L. Kaplan, *Journal of Biomedical Materials Research Part B-Applied Biomaterials*, 2011, 99B, 89-101.
32. F. P. Seib, G. T. Jones, J. Rnjak-Kovacina, Y. Lin and D. L. Kaplan, *Advanced Healthcare Materials*, 2013, 2, 1606-1611.
33. B. N.T. and A. S.M., *Journal of Polymer Science - Part A: Polymer Chemistry*, 1983, 21, 1273-1280.
34. T. Dyakonov, C. H. Yang, D. Bush, S. Gosangari, S. Majuru and A. Fatmi, *Journal of drug delivery*, 2012, 2012, 490514-490514.
35. A. A, *Journal of Sericulture Science of Japan*, 1998, 67, 91-97.
36. Z. Zheng, S. Guo, Y. Liu, J. Wu, G. Li, M. Liu, X. Wang and D. Kaplan, *Journal of Biomaterials Applications*, 2016, 31, 450-463.
37. E. Wenk, H. P. Merkle and L. Meinel, *Journal of Controlled Release*, 2011, 150, 128-141.
38. F. G. Omenetto and D. L. Kaplan, *Science*, 2010, 329, 528-531.
39. S. Perteghella, E. Martella, L. de Girolamo, C. P. Orfei, M. Pierini, V. Fumagalli, D. V. Pintacuda, T. Chlapanidas, M. Vigano, S. Farago, M. L. Torre and E. Lucarelli, *International Journal of Molecular Sciences*, 2017, 18.
40. J. Kundu, Y.-I. Chung, Y. H. Kim, G. Taeb and S. C. Kundu, *International Journal of Pharmaceutics*, 2010, 388, 242-250.
41. P. Shi, S. A. Abbah, K. Saran, Y. Zhang, J. Li, H.-K. Wong and J. C. H. Goh, *Biomacromolecules*, 2013, 14, 4465-4474.
42. T. M. Muffly, A. P. Tizzano and M. D. Walters, *Journal of the Royal Society of Medicine*, 2011, 104, 107-112.
43. H. J. Jin and D. L. Kaplan, *Nature*, 2003, 424, 1057-1061.
44. A. Matsumoto, A. Lindsay, B. Abedian and D. L. Kaplan, *Macromolecular Bioscience*, 2008, 8, 1006-1018.

45. X. Chen, Z. Shao, D. P. Knight and F. Vollrath, *Proteins-Structure Function and Bioinformatics*, 2007, 68, 223-231.
46. J. Rnjak-Kovacina, L. S. Wray, K. A. Burke, T. Torregrosa, J. M. Golinski, W. Huang and D. L. Kaplan, *Acs Biomaterials Science & Engineering*, 2015, 1, 260-270.
47. X. Hu, K. Shmelev, L. Sun, E.-S. Gil, S.-H. Park, P. Cebe and D. L. Kaplan, *Biomacromolecules*, 2011, 12, 1686-1696.
48. G. G. Leisk, T. J. Lo, T. Yucel, Q. Lu and D. L. Kaplan, *Advanced Materials*, 2010, 22, 711-+.
49. B. Marelli, M. A. Brenckle, D. L. Kaplan and F. G. Omenetto, *Scientific Reports*, 2016, 6.
50. F. Vollrath and D. P. Knight, *Nature*, 2001, 410, 541-548.
51. Q. Lu, H. Zhu, C. Zhang, F. Zhang, B. Zhang and D. L. Kaplan, *Biomacromolecules*, 2012, 13, 826-832.
52. S. Bai, S. Liu, C. Zhang, W. Xu, Q. Lu, H. Han, D. L. Kaplan and H. Zhu, *Acta Biomaterialia*, 2013, 9, 7806-7813.
53. M. D. Pierschbacher and E. Ruoslahti, *Nature*, 1984, 309, 30-33.
54. B. Kundu, N. E. Kurland, S. Bano, C. Patra, F. B. Engel, V. K. Yadavalli and S. C. Kundu, *Progress in Polymer Science*, 2014, 39, 251-267.
55. D. Yao, S. Dong, Q. Lu, X. Hu, D. L. Kaplan, B. Zhang and H. Zhu, *Biomacromolecules*, 2012, 13, 3723-3729.
56. T. Chlapanidas, S. Perteghella, S. Farago, A. Boschi, G. Tripodo, B. Vigani, B. Crivelli, S. Renzi, S. Dotti, S. Preda, M. Marazzi, M. L. Torre and M. Ferrari, *Journal of Applied Polymer Science*, 2016, 133.
57. B. Kundu, R. Rajkhowa, S. C. Kundu and X. Wang, *Advanced Drug Delivery Reviews*, 2013, 65, 457-470.
58. K. Luo, Y. Yang and Z. Shao, *Advanced Functional Materials*, 2016, 26, 872-880.
59. Q. Lu, X. Hu, X. Wang, J. A. Kluge, S. Lu, P. Cebe and D. L. Kaplan, *Acta Biomaterialia*, 2010, 6, 1380-1387.
60. J. Lee, S. H. Park, I. H. Seo, K. J. Lee and W. Ryu, *European Journal of Pharmaceutics and Biopharmaceutics*, 2015, 94, 11-19.
61. K. H. Kim, L. Jeong, H. N. Park, S. Y. Shin, W. H. Park, S. C. Lee, T. I. Kim, Y. J. Park, Y. J. Seol, Y. M. Lee, Y. Ku, I. C. Rhyu, S. B. Han and C. P. Chung, *Journal of Biotechnology*, 2005, 120, 327-339.

62. J. Melke, S. Midha, S. Ghosh, K. Ito and S. Hofmann, *Acta Biomaterialia*, 2016, 31, 1-16.
63. L. Meinel, S. Hofmann, V. Karageorgiou, C. Kirker-Head, J. McCool, G. Gronowicz, L. Zichner, R. Langer, G. Vunjak-Novakovic and D. L. Kaplan, *Biomaterials*, 2005, 26, 147-155.
64. D. W. Kim, H. S. Hwang, D.-S. Kim, S. H. Sheen, D. H. Heo, G. Hwang, S. H. Kang, H. Kweon, Y.-Y. Jo, S. W. Kang, K.-G. Lee, K. W. Park, K. H. Han, J. Park, W. S. Eum, Y.-J. Cho, H. C. Choi and S. Y. Choi, *Bmb Reports*, 2011, 44, 787-792.
65. A. Abel Lozano-Perez, A. Rodriguez-Nogales, V. Ortiz-Cullera, F. Algieri, J. Garrido-Mesa, P. Zorrilla, M. Elena Rodriguez-Cabezas, N. Garrido-Mesa, M. P. Utrilla, L. De Matteis, J. Martinez de la Fuente, J. Luis Cenis and J. Galvez, *International Journal of Nanomedicine*, 2014, 9, 4507-4520.
66. X. Cui, J. Wen, X. Zhao, X. Chen, Z. Shao and J. J. Jiang, *Journal of Biomedical Materials Research Part A*, 2013, 101, 1511-1517.
67. S. Farago, G. Lucconi, S. Perteghella, B. Vigani, G. Tripodo, M. Sorrenti, L. Catenacci, A. Boschi, M. Faustini, D. Vigo, T. Chlapanidas, M. Marazzi and M. L. Torre, *Pharmaceutical Development and Technology*, 2016, 21, 453-462.
68. T. Chlapanidas, M. C. Tosca, S. Farago, S. Perteghella, M. Galuzzi, G. Lucconi, B. Antonioli, F. Ciancio, V. Rapisarda, D. Vigo, M. Marazzi, M. Faustini and M. L. Torre, *International Journal of Immunopathology and Pharmacology*, 2013, 26, 43-49.
69. T. E. Bucknall, L. Teare and H. Ellis, *European surgical research. Europaische chirurgische Forschung. Recherches chirurgicales europeennes*, 1983, 15, 59-66.
70. Y. Cao and B. Wang, *International Journal of Molecular Sciences*, 2009, 10, 1514-1524.
71. Y. Wang, D. D. Rudym, A. Walsh, L. Abrahamsen, H.-J. Kim, H. S. Kim, C. Kirker-Head and D. L. Kaplan, *Biomaterials*, 2008, 29, 3415-3428.
72. R. L. Horan, K. Antle, A. L. Collette, Y. Z. Huang, J. Huang, J. E. Moreau, V. Volloch, D. L. Kaplan and G. H. Altman, *Biomaterials*, 2005, 26, 3385-3393.
73. P. A. Gunatillake and R. Adhikari, *European cells & materials*, 2003, 5, 1-16.
74. S. Perteghella, B. Vigani, L. Mastracci, F. Grillo, B. Antonioli, M. Galuzzi, M. C. Tosca, B. Crivelli, S. Preda, G. Tripodo, M. Marazzi, T. Chlapanidas and M. L. Torre, *Macromolecular Bioscience*, 2017, 17, 1700131.

75. B. Vigani, L. Mastracci, F. Grillo, S. Perteghella, S. Preda, B. Crivelli, B. Antonioli, M. Galuzzi, M. C. Tosca, M. Marazzi, M. L. Torre and T. Chlapanidas, *Journal of Bioactive and Compatible Polymers*, 2016, 31, 600-612.
76. M. Tsukada, G. Freddi and N. Minoura, *Journal of Applied Polymer Science*, 1994, 51, 823-829.
77. L. Yang, Z. Zheng, C. Qian, J. Wu, Y. Liu, S. Guo, G. Li, M. Liu, X. Wang and D. L. Kaplan, *Journal of Colloid and Interface Science*, 2017, 496, 66-77.
78. R. Elia, J. Guo, S. Budijono, V. Normand, D. Benczedi, F. Omenetto and D. L. Kaplan, *Journal of Coatings Technology and Research*, 2015, 12, 793-799.
79. Y. Kishimoto, H. Morikawa, S. Yamanaka and Y. Tamada, *Materials Science & Engineering C-Materials for Biological Applications*, 2017, 73, 498-506.
80. U. J. Kim, J. Y. Park, C. M. Li, H. J. Jin, R. Valluzzi and D. L. Kaplan, *Biomacromolecules*, 2004, 5, 786-792.
81. M. Lovett, C. Cannizzaro, L. Daheron, B. Messmer, G. Vunjak-Novakovic and D. L. Kaplan, *Biomaterials*, 2007, 28, 5271-5279.
82. Z. Zhao, Y. Li and M.-B. Xie, *International Journal of Molecular Sciences*, 2015, 16, 4880-4903.
83. R. Rajkhowa, L. Wang and X. Wang, *Powder Technology*, 2008, 185, 87-95.
84. C. P. Reis, R. J. Neufeld, A. J. Ribeiro and F. Veiga, *Nanomedicine-Nanotechnology Biology and Medicine*, 2006, 2, 8-21.
85. W. Lohcharoenkal, L. Wang, Y. C. Chen and Y. Rojanasakul, *BioMed research international*, 2014, 2014, 180549-180549.
86. Y.-Q. Zhang, W.-D. Shen, R.-L. Xiang, L.-J. Zhuge, W.-J. Gao and W.-B. Wang, *Journal of Nanoparticle Research*, 2007, 9, 885-900.
87. M. Chen, Z. Shao and X. Chen, *Journal of Biomedical Materials Research Part A*, 2012, 100A, 203-210.
88. H. Li, J. Tian, A. Wu, J. Wang, C. Ge and Z. Sun, *International Journal of Nanomedicine*, 2016, 11, 4373-4380.
89. J. E. Kipp, *International Journal of Pharmaceutics*, 2004, 284, 109-122.
90. P. Wu, Q. Liu, R. Li, J. Wang, X. Zhen, G. Yue, H. Wang, F. Cui, F. Wu, M. Yang, X. Qian, L. Yu, X. Jiang and B. Liu, *Acs Applied Materials & Interfaces*, 2013, 5, 12638-12645.
91. A. S. Lammel, X. Hu, S.-H. Park, D. L. Kaplan and T. R. Scheibel, *Biomaterials*, 2010, 31, 4583-4591.

92. Y. Tian, X. Jiang, X. Chen, Z. Shao and W. Yang, *Advanced Materials*, 2014, 26, 7393-7398.
93. J. Qu, Y. Liu, Y. Yu, J. Li, J. Luo and M. Li, *Materials Science & Engineering C-Materials for Biological Applications*, 2014, 44, 166-174.
94. Z. Ekemen, Z. Ahmad, E. Stride, D. Kaplan and M. Edirisinghe, *Biomacromolecules*, 2013, 14, 1412-1422.
95. M. K. Kim, J. Y. Lee, H. Oh, D. W. Song, H. W. Kwak, H. Yun, I. C. Um, Y. H. Park and K. H. Lee, *International Journal of Biological Macromolecules*, 2015, 79, 988-995.
96. E. Wenk, A. J. Wandrey, H. P. Merkle and L. Meinel, *Journal of Controlled Release*, 2008, 132, 26-34.
97. Z. Zhao, Y. Li, Y. Zhang, A.-Z. Chen, G. Li, J. Zhang and M.-B. Xie, *Powder Technology*, 2014, 268, 118-125.
98. K. Byrappa, S. Ohara and T. Adschiri, *Advanced Drug Delivery Reviews*, 2008, 60, 299-327.
99. V. Gupta, A. Aseh, C. N. Rios, B. B. Aggarwal and A. B. Mathur, *International Journal of Nanomedicine*, 2009, 4, 115-122.
100. L. Xiao, G. Lu, Q. Lu and D. L. Kaplan, *Acs Biomaterials Science & Engineering*, 2016, 2, 2050-2057.
101. J. Wu, Z. Zheng, G. Li, D. L. Kaplan and X. Wang, *Acta Biomaterialia*, 2016, 39, 156-168.
102. S. Wang, T. Xu, Y. Yang and Z. Shao, *Acs Applied Materials & Interfaces*, 2015, 7, 21254-21262.
103. A. Abel Lozano-Perez, H. Correa Rivero, M. d. C. Perez Hernandez, A. Pagan, M. G. Montalban, G. Villora and J. Luis Cenis, *International Journal of Pharmaceutics*, 2017, 518, 11-19.
104. B. Subia, S. Chandra, S. Talukdar and S. C. Kundu, *Integrative Biology*, 2014, 6, 203-214.
105. G. Pasut and F. M. Veronese, *Journal of Controlled Release*, 2012, 161, 461-472.
106. W. Abdelwahed, G. Degobert, S. Stainmesse and H. Fessi, *Advanced Drug Delivery Reviews*, 2006, 58, 1688-1713.
107. A. Rodriguez-Nogales, F. Algieri, L. De Matteis, A. Abel Lozano-Perez, J. Garrido-Mesa, T. Vezza, J. M. de la Fuente, J. Luis Cenis, J. Galvez and M. Elena Rodriguez-Cabezas, *International Journal of Nanomedicine*, 2016, 11, 5945-5958.

108. B. Subia and S. C. Kundu, *Nanotechnology*, 2013, 24.
109. X. Wang, T. Yucel, Q. Lu, X. Hu and D. L. Kaplan, *Biomaterials*, 2010, 31, 1025-1035.
110. P. Shi and J. C. H. Goh, *International Journal of Pharmaceutics*, 2011, 420, 282-289.
111. K. Numata, S. Yamazaki and N. Naga, *Biomacromolecules*, 2012, 13, 1383-1389.
112. R. Dash, S. K. Ghosh, D. L. Kaplan and S. C. Kundu, *Comparative Biochemistry and Physiology B-Biochemistry & Molecular Biology*, 2007, 147, 129-134.
113. S. Dhawan and K. P. Gopinathan, *Development Genes and Evolution*, 2003, 213, 435-444.
114. P. Aramwit, S. Damrongsakkul, S. Kanokpanont and T. Srichana, *Biotechnology and Applied Biochemistry*, 2010, 55, 91-98.
115. R. SK and K. M, *Journal of Polymer and Textile Engineering*, 2015, 2, 29-35.
116. Y.-J. Wang and Y.-Q. Zhang, *Silk: Inheritance and Innovation - Modern Silk Road*, 2011, 175-176, 158-+.
117. B. C. Dash, B. B. Mandal and S. C. Kundu, *Journal of Biotechnology*, 2009, 144, 321-329.
118. S. Nayak, S. Talukdar and S. C. Kundu, *Cell and Tissue Research*, 2012, 347, 783-794.
119. Z. LJ, Y. J and Y. L, *Zhejiang Nongye Daxue Xuebao*, 1998, 24, 268-272.
120. M.-H. Wu, J.-X. Yue and Y.-Q. Zhang, *Journal of Cleaner Production*, 2014, 76, 154-160.
121. N. Kato, S. Sato, A. Yamanaka, H. Yamada, N. Fuwa and M. Nomura, *Bioscience Biotechnology and Biochemistry*, 1998, 62, 145-147.
122. E. Bari, C. R. Arciola, B. Vigani, B. Crivelli, P. Moro, G. Marrubini, M. Sorrenti, L. Catenacci, G. Bruni, T. Chlapanidas, E. Lucarelli, S. Perteghella and M. L. Torre, *Materials*, 2017, 10.
123. H.-Y. Wang, Y.-J. Wang, L.-X. Zhou, L. Zhu and Y.-Q. Zhang, *Food & Function*, 2012, 3, 150-158.
124. T. Chlapanidas, S. Farago, G. Lucconi, S. Perteghella, M. Galuzzi, M. Mantelli, M. A. Avanzini, M. C. Tosca, M. Marazzi, D. Vigo, M. L. Torre and M. Faustini, *International Journal of Biological Macromolecules*, 2013, 58, 47-56.
125. Y. Tamada, M. Sano, K. Niwa, T. Imai and G. Yoshino, *Journal of Biomaterials Science-Polymer Edition*, 2004, 15, 971-980.
126. T. Chlapanidas, S. Perteghella, F. Leoni, S. Farago, M. Marazzi, D. Rossi, E. Martino, R. Gaggeri and S. Collina, *International Journal of Molecular Sciences*, 2014, 15, 13624-13636.

127. A. Ogawa, S. Terada, T. Kanayama, M. Miki, M. Morikawa, T. Kimura, A. Yamaguchi, M. Sasaki and H. Yamada, *Journal of Bioscience and Bioengineering*, 2004, 98, 217-219.
128. C. Song, Z. Yang, M. Zhong and Z. Chen, *Neural Regeneration Research*, 2013, 8, 506-513.
129. T. Isobe, Y. Ikebata, T. Onitsuka, M. Wittayarat, Y. Sato, M. Taniguchi and T. Otoi, *Theriogenology*, 2012, 78, 747-752.
130. S. Terada, T. Nishimura, M. Sasaki, H. Yamada and M. Miki, *Cytotechnology*, 2002, 40, 3-12.
131. T.-T. Cao and Y.-Q. Zhang, *Amino acids*, 2017.
132. X. Zhang, M. M. R. Khan, T. Yamamoto, M. Tsukada and H. Morikawa, *International Journal of Biological Macromolecules*, 2012, 50, 337-347.
133. K. Y. Cho, J. Y. Moon, Y. W. Lee, K. G. Lee, J. H. Yeo, H. Y. Kweon, K. H. Kim and C. S. Cho, *International Journal of Biological Macromolecules*, 2003, 32, 36-42.
134. J. Kanoujia, M. Singh, P. Singh and S. A. Saraf, *Materials Science & Engineering C-Materials for Biological Applications*, 2016, 69, 967-976.
135. O. I. Parisi, M. Fiorillo, L. Scrivano, M. S. Sinicropi, V. Dolce, D. Iacopetta, F. Puoci and A. R. Cappello, *Biomacromolecules*, 2015, 16, 3126-3133.
136. B. B. Mandal and S. C. Kundu, *Nanotechnology*, 2009, 20.
137. L. Huang, K. Tao, J. Liu, C. Qi, L. Xu, P. Chang, J. Gao, X. Shuai, G. Wang, Z. Wang and L. Wang, *Acs Applied Materials & Interfaces*, 2016, 8, 6577-6585.
138. S. Svenson, *Wiley Interdisciplinary Reviews-Nanomedicine and Nanobiotechnology*, 2014, 6, 125-135.
139. M. Kendall and I. Lynch, *Nature Nanotechnology*, 2016, 11, 206-+.



Contents lists available at ScienceDirect

Journal of Controlled Release

journal homepage: www.elsevier.com/locate/jconrel



Review article

Mesenchymal stem/stromal cell extracellular vesicles: From active principle to next generation drug delivery system



Barbara Crivelli^a, Theodora Chlapanidas^a, Sara Perteghella^{a,*}, Enrico Lucarelli^b, Luisa Pascucci^c, Anna Teresa Brini^{d,e}, Ivana Ferrero^{f,g}, Mario Marazzi^h, Augusto Pessina^d, Maria Luisa Torre^a, Italian Mesenchymal Stem Cell Group (GISM)¹

^a Department of Drug Sciences, University of Pavia, Viale Taramelli 12, 27100 Pavia, Italy

^b Osteoarticular Regeneration Laboratory, 3rd Orthopaedic and Traumatologic Clinic, Rizzoli Orthopedic Institute, Via di Barbiano 1/10, 40136 Bologna, Italy

^c Veterinary Medicine Department, University of Perugia, Via San Costanzo 4, 06126 Perugia, Italy

^d Department of Biomedical, Surgical and Dental Sciences, University of Milan, Via Pascal 36, 20100 Milan, Italy

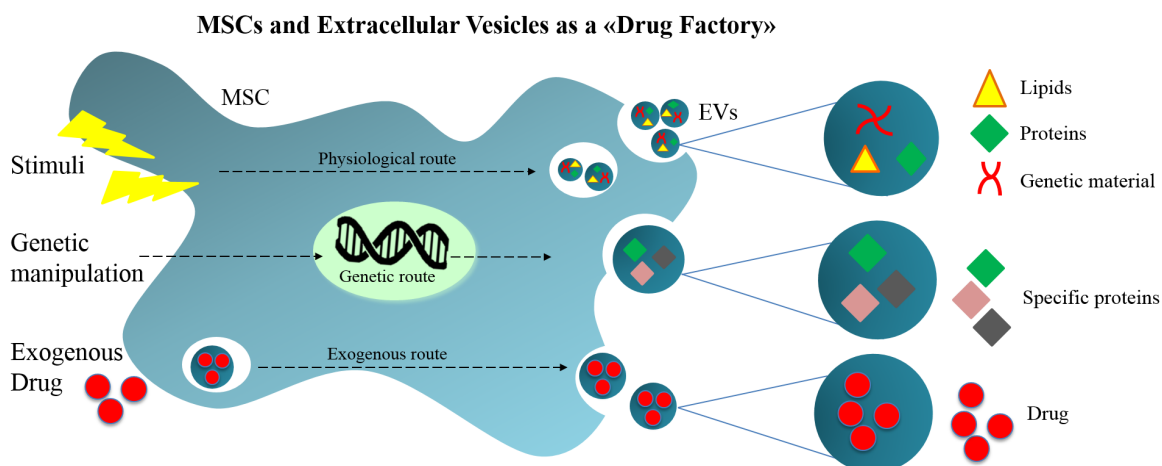
^e I.R.C.C.S. Galeazzi Orthopedic Institute, Via Riccardo Galeazzi 4, 20161 Milan, Italy

^f Paediatric Onco-Haematology, Stem Cell Transplantation and Cellular Therapy Division, City of Science and Health of Turin, Regina Margherita Children's Hospital, Piazza Polonia 94, 10126 Turin, Italy

^g Department of Public Health and Paediatrics, University of Turin, Piazza Polonia 94, 10126 Turin, Italy

^h Tissue Therapy Unit, ASST Niguarda Hospital, Piazza Ospedale Maggiore 3, 20162 Milan, Italy

Graphical abstract



Abstract

It has been demonstrated that the biological effector of mesenchymal stem/stromal cells (MSCs) is their secretome, which is composed of a heterogeneous pool of bioactive molecules, partially enclosed in extracellular vesicles (EVs). Therefore, the MSC secretome (including EVs) has been recently proposed as possible alternative to MSC therapy. The secretome can be considered as a protein-based biotechnological product, it is probably safer compared with living/cycling cells, it presents virtually lower tumorigenic risk, and it can be handled, stored and sterilized as an Active Pharmaceutical/Principle Ingredient (API). EVs retain some structural and technological analogies with synthetic drug delivery systems (DDS), even if their potential clinical application is also limited by the absence of reproducible/scalable isolation methods and Good Manufacturing Practice (GMP)-compliant procedures. Notably, EVs secreted by MSCs preserve some of their parental cell features such as homing, immunomodulatory and regenerative potential. This review focuses on MSCs and their EVs as APIs, as well as DDS, considering their ability to reach inflamed and damaged tissues and to prolong the release of encapsulated drugs. Special attention is devoted to the illustration of innovative therapeutic approaches in which nanomedicine is successfully combined with stem cell therapy, thus creating a novel class of “next generation drug delivery systems.”

Keywords

Mesenchymal stem/stromal cells; secretome; extracellular vesicles; drug delivery systems.

1. MSCs: therapeutic agents and drug carriers

The idea to employ MSC-derived EVs instead of their parent cells in clinical practice derives from their therapeutic efficacy [1] [2] [3]. MSC paternity can be attributed to the pathologist Julius Cohnheim, who, in 1867, was the first to hypothesize that non-hematopoietic bone marrow cells migrate to far injured tissues to take part in regenerative processes [4]. In 1966, Alexander Friedenstein observed the development of reticular tissue from a heterotopic transplantation of bone marrow fragments and cell suspensions [5]. Later, he reported the presence of fibroblastoid cells in rodent bone marrow, early named Colony Forming Unit Fibroblasts (CFU-F). These cells were morphologically different from marrow hematopoietic

cells with in vitro clonogenic potential that had previously never been attributed to other lineages [6]. In 1976, Friedenstein described the isolation procedure to separate CFU-F from whole bone marrow aspirate based on differential adhesion properties [7]. Over the years, other researchers confirmed his observations by demonstrating CFU-F ability to differentiate into osteoblast, chondrocyte, adipocyte and myoblast lineages [8] [9] [10] [11] [12]. In 1991, Caplan re-named these CFU-F cells into “Mesenchymal Stem Cells” (MSCs) to emphasize their ability to theoretically differentiate into end-stage cells of mesodermal tissues such as bone, cartilage, bone marrow stroma, adipose tissue, muscle, ligaments, and dermis. Two decades later, in an opinion paper, Caplan proposed to change their name to “Medicinal Signaling Cells” due to the secretion of a heterogeneous pool of bioactive compounds with an immunoregulatory and regenerative potential [13]. MSCs were first isolated from the bone marrow [7], then from several other adult tissues such as fat [14] [15] [16], dental pulp [17], synovial membrane [18] and tendons [19]. Moreover, MSCs populate lymphoid tissues [20] such as spleen and thymus [21], and perinatal sources including cord blood [22] [23], Wharton jelly [24], placenta [25] and amniotic fluid [26].

Currently, bone marrow still represents the most popular source of MSCs for clinical applications, even if the collection is painful for the patient and results in a low yield of recovered cells [27]. On the contrary, fat tissue represents a minimally-invasive source of MSCs, symbolized by stromal vascular fraction (SVF). Some authors have proposed the use of SVF instead of MSCs due to its heterogeneity reducing manufacturing times and preserving the regenerative potential [28] [29] [30] [31]. The MSCs derived from adipose tissue and other sources such as deciduous teeth, placenta or umbilical cord are characterized by features similar to bone marrow-derived MSCs in terms of morphology, multilineage potency and cell yield, despite specific differences in transcriptional and proteomic expression [32] [14] [33] [34] [35]. Due to the variability among MSC populations, a consensus document was written by the International Society for Cellular Therapy in order to establish minimal criteria to define MSCs and to facilitate their clinical application. Three minimal criteria were proposed: 1) adherence to plastic supports when cultured in standard conditions; 2) expression of specific surface markers, including positivity for CD105, CD73, CD90 and negativity for CD34, CD45, CD14 or CD11b, CD79 α or CD19 and HLA-Class II markers; 3) in vitro differentiation into osteoblasts, chondrocytes and adipocytes, named multipotency [36]. In addition, MSCs may express other positive markers such as embryonic stem cell markers, i.e. Oct-4, Rex-1, and Sox-

2, although their expression is strictly influenced by the source of the MSCs method of isolation and different culture stages [37].

MSCs are attractive candidates for several clinical applications, including oncohaematology and regenerative medicine, and currently several trials are recruiting patients in different countries to test the efficacy of MSCs in the treatment of several diseases. The translational application of MSCs means considering them as Advanced Therapy Medicinal Products, or drugs, thus their manufacturing process for clinical purposes should comply with Good Manufacturing Practice (GMP) to preserve the quality and safety standards of the final product. For this reason, all manufacturing steps, ranging from their collection to their clinical application, must be controlled and validated, as recently reported by Torre et al., on behalf of the Italian Mesenchymal Stem Cell Group (GISM) [38] [39].

In clinical practice, MSCs retain several drawbacks that can be classified into different categories. The first category is represented by risks associated with the intrinsic cellular properties mainly related to cell differentiation status, tumorigenic potential, proliferation ability and life span in culture. The second category comprises risks associated with extrinsic factors introduced by cell collection, handling, culturing and storage. Finally, MSC therapy suffers from risks associated with clinical features including exposure duration and administration route [40]. The biodistribution of the cells is a critical step because the majority of the systemically injected MSCs are trapped by the lung and liver microvasculature, and the consequent failure to reach the target site [41]. This limit may be overcome by tissue engineering approaches, either by implanting cells within a three-dimensional scaffold [42] [43] [44] [45] or by engineering their surface, resulting in an improvement in their ability to reach their native niche or injured tissues [46].

Due to their plasticity, MSCs were considered “ideal tools” for regenerative medicine, since originally it was assumed that their therapeutic potential depended upon their differentiation ability [47]. It is currently believed that the therapeutic potential of MSCs does not depend only by their regenerative capacity, but largely by the release of molecules possessing paracrine activity that are partially delivered by extracellular vesicles (EVs) [48] [49] [50].

1.1 Therapeutic effects of MSCs

MSCs are currently employed as “eclectic key players” in several clinical trials (730 clinical trials are available online on June 5th 2017; <http://www.clinicaltrials.gov>) either alone or in combination with scaffolds or biomolecules of different natures. However, it is still unclear how injected cells interact with the target site while maintaining their viability and phenotype [51]. Some authors suggested a strict interaction between exogenous and resident MSCs that would switch off the immune surveillance thus allowing tissue regeneration [47] [52]. In fact, MSCs suppress T cell proliferation and differentiation per se or by regulating the Treg cells activation by secreting immunosuppressive factors and chemokines [53] [54].

Nearly half of all registered clinical trials exploits the MSCs’ immune-modulatory and/or anti-inflammatory properties for the treatment of severe autoimmune diseases, organ transplantation and rejection, inflammatory conditions such as multiple sclerosis [55], diabetes [56], osteoarthritis [57], inflammatory bowel disease [58] and osteogenesis imperfecta [59] [60]. In particular, Graft versus Host Disease (GvHD) represents one of the major fields of application for MSCs, the data suggest that MSC therapy results in effective remission of the symptoms without serious side effects [61] [62] [63]. Similarly, MSCs have been tested in several other autoimmune disorders such as systemic lupus erythematosus (SLE), rheumatoid arthritis and Crohn’s disease [64] [65] [66].

The MSCs used in clinical trials have been isolated from different sources: the most common being bone marrow, but also adipose tissue, umbilical cord and placenta. Notably, even though both autologous and allogeneic MSC transplantations have shown to be safe, the latter is preferred due to the isolation source (young and healthy donors), availability off the shelf and the higher cost-effectiveness [67] [68].

Albeit clinical results are encouraging several concerns about MSC-based therapy including safety, long-term efficacy, route of administration, and cost-effectiveness still represent issues that need to be addressed. MSC engraftment at the target site also represents a limit and many studies support the lack of long-term MSC engraftment; this evidence lead to the hypothesis that the positive effects exerted by MSC therapy were mediated by paracrine mechanisms [69]. The use of tissue engineering approaches such as 3D scaffolds or injectable hydrogels has been proposed to increase cells’ retention [46]. Despite all these open issues, MSC therapy still represents an appealing opportunity to ameliorate the life of patients suffering from fatal diseases, such as GvHD [70], multiple sclerosis [71], diabetes [56] and spinal cord injury [72].

1.2 MSCs as drug delivery systems

In recent years, the design of suitable drug delivery systems (DDS), providing an optimization of both pharmacodynamic and pharmacokinetic properties of the drug [73], is at the leading edge. In particular, micro/nanotechnology occupies a great branch of the drug delivery field, with the development of several nano-sized DDS including microspheres, liposomes, nanoparticles, dendrimers and micelles that are able to carry various therapeutic molecules to target sites. One of the most desired features of DDS, in addition to safety, efficacy and controlled release, is the “smart targeting,” which can sometimes be difficult to achieve [74]. Advanced DDS must retain “smart targeting” capability, thus improving the therapeutic effects and minimizing the off-target biodistribution to avoid undesired side effects. Smart micro/nanoplatfroms can respond to both endogenous and exogenous stimuli, such as pH variations, enzyme concentration, temperature, ultrasound, and magnetic fields, which are applied to enhance the drug release at its target site [75]. In particular, nanosystems are widely used to deliver anti-cancer drugs, thanks to their ability to passively reach the tumor site, exploiting their Enhanced Permeability Retention effect [76]. Despite these advantages, there are still some concerning points with the use of nanodevices, such as rapid clearance from the bloodstream, lack of specificity followed by nonspecific biodistribution and insufficient data related to their acute and chronic cytotoxicity [77] [78]. For these reasons, the scientific community is still searching for smart DDS, and recently cells have been proposed as innovative DDS. Cells can be successfully exploited as drug carriers for their ability to prolong the circulation time of drugs and, exclusively for some cell lineages (immune cells, MSCs), for their capacity to reach inflamed and damaged tissues. Different approaches have been used to load drugs into cells: bioactive compounds (e.g. drugs or growth factors) can be easily loaded through passive diffusion or can be linked to the cell surface. Moreover, most cells can be engineered with non-viral and viral vectors to over-express genes of interest in order to achieve a steady production, and thus a sustained release, of a desired therapeutic product at the target site [79].

MSCs can be considered natural DDS, since they physiologically retain the “smart targeting”: their migratory/homing ability towards diseased tissues can be enhanced through the over-expression of membrane proteins responsible for binding chemo-attractive signaling molecules released by damaged tissues. For example, the over-expression of CXCR4 receptors resulted in beneficial effects for both kidney and liver grafts [80] [81]. Other overexpressed chemokine receptors such as CXCR7 and CXCR1, nuclear receptors such as Nur77 and Nurr1, as well as

aquaporin gene and adhesion molecules may increase the MSCs' migratory potential without affecting stemness genes [82]. Notably, the homing potential of MSCs could be strongly reduced in relation to the route of administration, due to their interaction with the mononuclear phagocyte system, if intravenously injected, or to their accumulation in pancreas and gastrointestinal tract, after intraperitoneal and subcutaneous injection [83].

Nowadays, the MSCs' innate homing has been reported in several studies of ischemic brain injury, myocardial infarction and acute renal failure, even though this mechanism has not yet been clearly understood and explained [84] [47]. Two main hypotheses have been described. The first is attributed to the direct cell-to-cell contact, while the other is related to the secretome of MSCs including chemokines, cytokines and growth factors (Figure 1) [33].

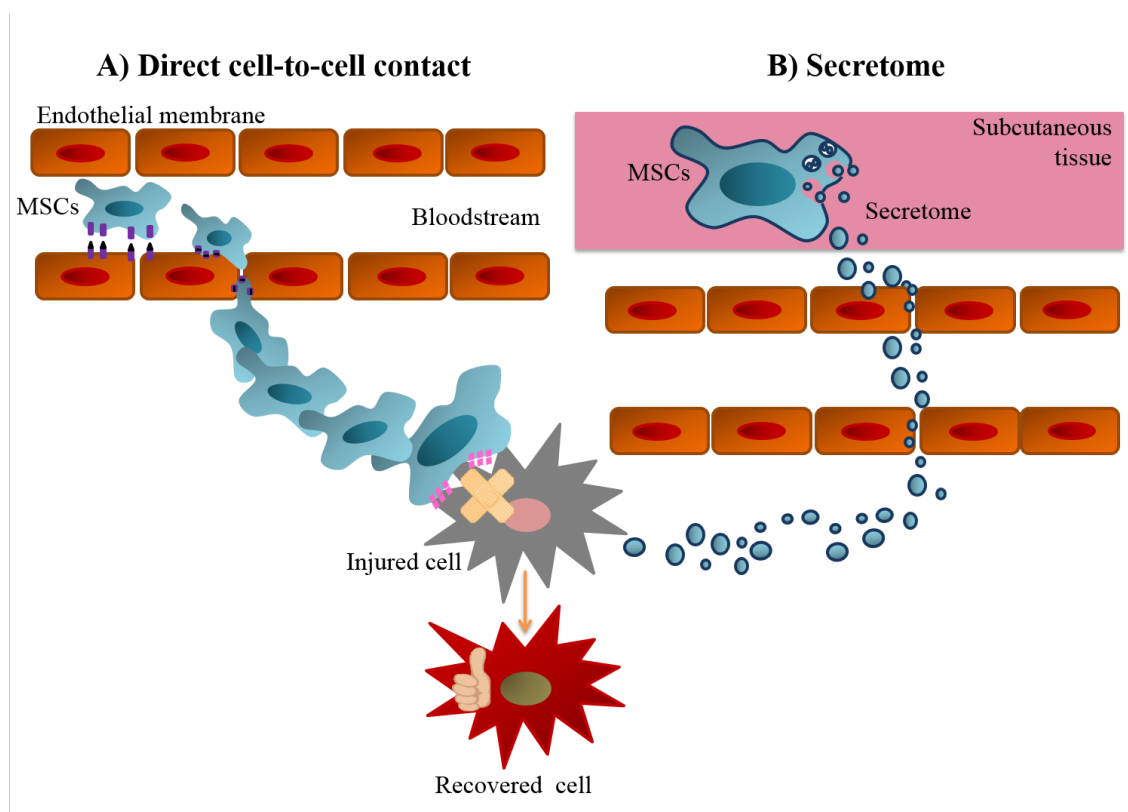


Figure 1. Hypothesis of the MSC homing mechanism: A) direct cell-to-cell contact: MSCs adhere and cross the endothelial membrane by expressing a restricted set of molecules, reaching the inflamed/damaged site; B) cell-secreted factors (secretome) able to cross the endothelial membrane, entering the bloodstream and finally reaching the injured cells.

In support of the first hypothesis, it has been shown that, similarly to leukocytes, MSCs are able to adhere and cross the endothelial membrane by expressing a restricted set of molecules (selectin-P, integrin B1, VCAM-1) that regulate their homing potential [47]. MSCs' migration towards the injured tissue increases under hypoxic conditions because low oxygen tension

changes their surface receptors and the interaction with the damaged tissue, even if it is strictly related to MSCs close to the injured site [85]. Unfortunately, it is still unclear whether MSCs isolated from various sources show differences in their homing potential [86]. Nevertheless, recent discoveries show that the therapeutic efficacy is no longer attributed to MSCs, but to their characteristic secreted bioactive soluble factors and vesicular systems (namely secretome) [87], as demonstrated in the treatment of cisplatin-induced acute kidney injury murine models [88].

Currently, great interest is focused on MSCs and other cell lineages such as red blood cells to deliver anti-cancer prodrugs because their cytoplasmic enzymes allow them to activate the encapsulated anti-cancer pro-drug once the desired site is reached [79] [89]. Moreover, MSCs can deliver pro-apoptotic proteins, such as tumor necrosis factor related apoptosis induced ligand (TRAIL), overcoming TRAIL-resistant tumor cells, with positive effects on colorectal carcinoma [90]. Similarly, adipose derived-MSCs over-expressing interferon-beta (IFN- β) showed efficacy for the treatment of experimental autoimmune encephalomyelitis [91].

For the treatment of critical limb ischemia and Huntington disease the use of genetically engineered MSCs able to secrete bioactive molecules such as vascular endothelial growth factor (VEGF) and brain-derived neurotrophic factor (BDNF) has been proposed [92]. The rationale for developing engineered MSCs expressing and thus secreting these bioactive factors is to increase their local expression and to potentiate their biological effects. Therefore, engineered MSCs represent ideal candidates for drug delivery, increasing the efficacy of drug therapies, albeit, based on our knowledge, there are no studies focusing on the therapeutic release mechanism from engineered-MSCs [93]. Furthermore as recently reviewed, some results are contradictory because factors released by modified MSCs have both pro- and anti-tumor effect [94].

In 2011, Pessina et al. showed the ability of MSCs to uptake and then release large amounts of the anti-cancer drug paclitaxel (PTX), thus acquiring potent anti-tumor and anti-angiogenic activity in vitro without applying any genetic manipulation. Results confirmed that the drug encapsulated into cells did not elicit side effects, but at the same time maintained its activity [95]. Recently, the same procedure was employed to deliver PTX into MSCs isolated from other sources (human placenta and interdental papilla), confirming previous observations [96] [97]. The use of MSCs as chemotherapeutic delivery agents to tumors must be considered positively in the context of the controversial role of between MSCs and tumor associated fibroblasts (TAFs) on tumor growth. For example, tumors resistant to anti-VEGF therapy stimulate TAFs

to express pro-angiogenic platelet derived growth factor-C (PDGF-C) by suggesting to use it as a new potential therapeutic target [98] [99]. Furthermore, when massive stroma is present as in pancreatic cancer [100] a possible therapeutic strategy could be the use of the same MSCs as a “trojan horse” that can be integrated into the tumor mass and deliver the drug in situ at very high concentration difficult to obtain by intravenous injection.

As MSCs, neuronal and hematopoietic stem cells could also be DDS in the treatment of different neurological disorders and cancer conditions. Indeed, Song et al. induced TRAIL overexpression in hematopoietic stem cells, and in a murine model it led to a significant inhibition of tumor growth without affecting normal tissues [101].

Up to now, cell-based DDS stands out as an innovative approach in the drug delivery field, even if it is dramatically different from the classical pharmaceutical technology approach.

2. Mesenchymal stem cell-extracellular vesicles

EVs are membranous vesicular systems released by different cell types [102] [103]. Chargaff and West observed EVs, for the first time in 1946, as pro-coagulant platelet-derived particles in plasma [104]. Few years later, in 1967, Peter Wolf described them as “platelet dust” [105]. Since they are present both in unicellular and multicellular organisms, they can be considered highly conserved in both prokaryotes and eukaryotes [106] [107]. EVs can be isolated from body fluids such as blood, saliva [108], urine [109] [110], breast milk [111] [112], synovial fluid [113], bile [114], seminal fluid [115] and cerebrospinal fluid [116] [117].

Formerly, EVs were considered as secreted systems implicated in cellular waste disposal mechanisms; nowadays, it is known that they act as mediators in distant cell-to-cell communication [118] [119]. In particular, the EV ability to transfer genetic information between cells has deeply changed the genetic manipulation of cells: it is now possible to regulate the genetic expression at post-transcriptional level, since the information is encoded in EV-miRNAs [120]. This process may have some limitations, since it was also reported that functional RNA delivered to target cells via EVs is rapidly degraded without being translated [121]. EVs could be used as new effective diagnostic biomarkers for tumor investigation [76], including breast and prostate tumors in their early stage [122] [123]. EV payload and surface markers are strictly related to their parent cell lineage and are influenced by their metabolic state during vesicle biogenesis [124], giving them a double role in physiological and pathological conditions. In fact, EVs equally contribute to suppress or support a pathological

condition [125]. This led to the introduction of the complex concept of “good and bad” vesicles [126] that will be discussed in a specific section below.

Several complex extracellular vesicles have been described and variously named (multivesicular cargo, macrovesicles, multivesicular spheres) [127] [128] [129]. Cells secrete a heterogeneous mixture of EVs whose morphology and size may be deeply altered by manipulation methods (such as ultracentrifugation, aldehyde fixation and dehydration). Thus, the different types of EVs are indistinguishable by electron microscopic observation except, theoretically, by their biogenesis [128]; in fact, size cannot be used to distinguish between different types of EVs [121] [130] [131].

Multivesicular bodies (MVBs) contain intra-luminal nanovesicles, namely exosomes (Ex), mainly ranging from 30 to 100 nm that increase in number with the progressive maturation of MVBs. The high amount of MVBs suggests that Ex strongly contribute to the formation of EV progeny. MVBs fuse with the cell membrane releasing Ex to the extracellular environment (Figure 2).

Ex, first observed by Rose Johnstone and colleagues in 1970 in maturing reticulocytes [132] [133], show a phospholipid bilayer characterized by ceramides, sphingolipids, tetraspanins (CD9, CD63, CD81), Alix and TSG101, considered as exosomal markers. Moreover, exosome membrane retains the same protein content of their parent cells, thus proving an identity card of Ex origin [134] [135]. Ex are abundant in biological fluids such as blood, urine and saliva, which allow their interaction with distant tissues and possible applications in the diagnostic field. Ex may represent an innovative, sensitive and minimally-invasive method to detect tumors at early stages, although so far the only strong evidence supporting this hypothesis has been provided for pancreatic cancer [136] [137].

Shedding vesicles (SVs), also named ectosomes, microvesicles or microparticles [138], ranging from 60 nm to 1 μ m in diameter, originate from direct outward budding of the plasma membrane in response to differing physiological or artificial stimuli, such as an increase in cytosolic calcium levels, ionophore treatment or changes in bloodstream conditions. They are surrounded by the cellular membrane, thus keeping the same parent cell moieties [139] [48]. SVs may be observed both by transmission and scanning electron microscopy, TEM and SEM. When observed by TEM, SVs characteristically display an electron-dense limiting membrane and slightly to moderately electron-dense contents (Figure 2). However, vesicles showing a cytoplasm-like texture may be occasionally seen as a consequence of the apocrine-like mechanism of release.

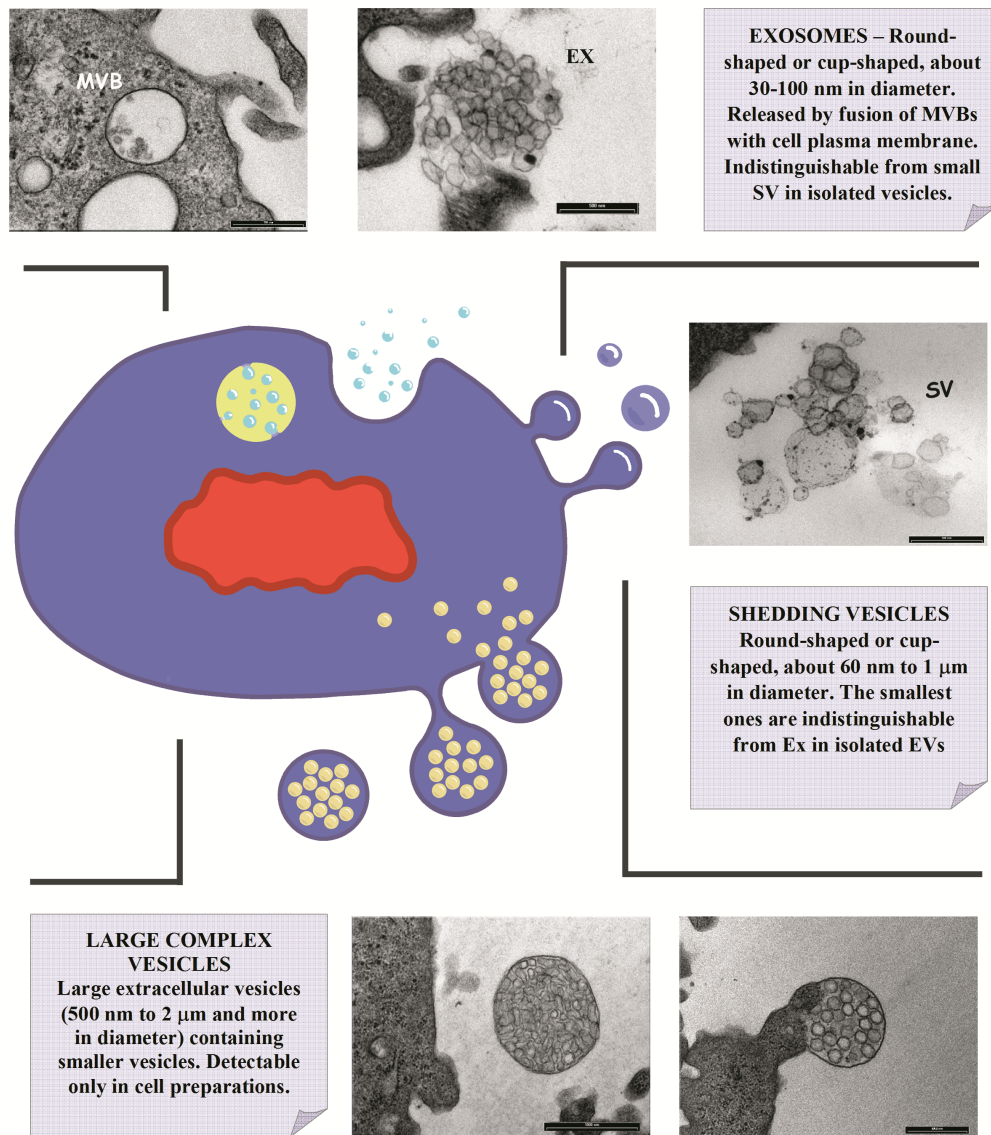


Figure 2. Main classes of EVs: Exosomes (Ex) are the smallest membrane-enclosed vesicles released by cells; they are enclosed in multivesicular bodies (MVBs) before being released in the extracellular environment. Shedding vesicles (SV) represents the most heterogeneous pool of extracellular vesicles, touching a dimensional range between 60 and 1000 nm; they are formed via outward budding of the cellular membrane. Finally, large complex vesicles are exocytosed through a sort of micro-apocrine secretion.

Finally, large complex EVs budding from the cell surface of different cell lineages and containing nanovesicles have been described [127, 128, 140]. It has been speculated that enclosed nano-vesicles, in a first phase, converge underneath a distinctive region of the plasma membrane and are then exocytosed through a sort of micro-apocrine secretion. The functional significance of these vesicles still needs to be clarified (Figure 2).

Unfortunately, there is not yet an optimized and standardized EV product and the therapeutic potential may vary among independent EV preparations, even if isolated from the same cell lineage [69]. The common isolation method is based on differential centrifugation, whereby apoptotic bodies, cell debris and SVs are pelleted using centrifugal forces among 200 and 10,000 g and Ex are isolated applying 100,000 g of ultracentrifugation forces [141]. However, this technique is time consuming, very expensive (it needs specialized equipment), difficult to scale up and requires a large amount of starting cells. Moreover, ultracentrifugation can damage EV integrity [142] and induce the formation of aggregates [143]. The most drawbacks associated to ultracentrifugation are overlapped by size-exclusion chromatography (SEC), which is able to sort particles in relation to their size, preserving the EV integrity, albeit it requires long time to collect pure samples [144]. Indeed, the SEC approach must be coupled with ion-exchange chromatography (IEC) to achieve a pure EV population [145]. Moreover, other innovative isolation techniques are reported in literature including the microfluidics-based technique, with faster time of analysis but low collection efficiency [146]. Finally, the commercially available isolation kits, based on polymer-induced precipitation (Optiprep®, ExoQuick®) and available only for lab-scale production, are not efficient in isolating populations of EVs (for example only Ex) [147].

EVs act as cellular “logistic shuttles” and their cargo contains lipids, proteins, enzymes, growth factors, receptors, metabolites and genetic material such as DNA and RNA [148]. Recently, high-resolution lipidomic and proteomic analyses conducted on EVs isolated from different cell lineages (glioblastoma cells, carcinoma cells and MSCs) showed differences in their lipid and protein content: Ex proteins did not mirror the proteomic profile of their parental cells, whereas SV proteins belonged to the cell endoplasmic reticulum and mitochondria. Finally, considering their lipid composition, Ex are highly enriched in glycolipids and free fatty acids, while SVs show more ceramides and sphingomyelins [149].

Once released into the extracellular environment, EVs are taken up via multiple mechanisms by neighboring cells or reach distant sites through biological fluids [150], modulating the target cell phenotype and the cellular biological properties [151]. EVs interact with the target cell through surface receptors or integrins, or by fusing with the plasma membrane (endocytosis) [152]. This last mechanism, environmentally controlled, often occurs under acidic conditions, and consequently is more frequent in cancer conditions [153].

EVs act either by regulating the expression of several receptors of targeted cells including tumor necrosis factor (TNF), MHC Class I/II molecules and CCR5 chemokine receptors [154], or by

transferring bioactive compounds (e.g. growth factors, lipids and proteins) into target cells after cell membrane fusion [48] [155] [156]. Moreover, the horizontal transfer of genetic products via EVs induces transient or permanent phenotype changes in target cells [157], making RNA a “key” cell fate modulator. This observation supports the possibility that MSCs modulate their biological effects by delivering genetic information that might affect gene expression in the target cells through EV-mediated transfer of mRNAs and various non-coding RNAs [48] [158]. Thanks to their strong potential, EVs have been tested in phase I clinical trials for the treatment of different types of cancer including metastatic melanoma, advanced non-small lung cancer and malignant glioma leading to conflicting conclusions [159] [160] (NCT01550523). Tumor-derived EVs were used in a phase I clinical study for the treatment of colorectal cancer in association with appropriate immune stimulatory adjuvant to exert an immunotherapeutic anti-tumor activity; they showed the safety but not the efficacy of EV treatment [161]. EVs derived from natural killer lymphocytes possess an in vitro immune-stimulatory activity similar to that mediated by EVs of dendritic cells [162].

Given the absence of a consensus [163], in order to standardize isolation and characterization protocols, the International Society for Extracellular Vesicles (ISEV) has dictated the minimal criteria required to distinguish “the real” EVs from other non-vesicular complexes, such as the presence of protein AGO2. Briefly, the criteria are: 1) EVs must be isolated from body fluids or cell culture supernatants; 2) at least one of the three different protein categories (transmembrane, cytosolic or intracellular proteins) must be quantified; and 3) vesicles must be characterized in terms of morphology and dimensional range; 4) markers to evaluate EV contamination should be provided i.e. proteins associated with compartments other than plasma membrane or endosomes (e.g. endoplasmic reticulum, mitochondria) and extracellular proteins binding specifically or non-specifically to membranes, co-isolating with EVs (e.g. acetylcholinesterase, albumin) [120].

In relation of what reported in the 4th criterion, proteins and soluble factors are considered as contaminating factors even though they are essential components of the cellular secretion that shows, as a whole, high biological activity. Evidence of this, is the consolidated use of the conditioned medium by many research groups. The vesicular fraction has a qualitative/quantitative composition that is definitely different from the whole conditioned medium [164] [165]. Moreover, depending on the isolation method of EVs, Ex or shedding vesicles with different cargos are obtained.

Nowadays, cytokines and growth factors released by MSCs are quite well defined even if no data are actually available about what kinds of factors are released as free cytokines/growth factors or packaged in EVs [156] (Figure 3). Finally, at the best of our knowledge, secretome studies able to distinguish between soluble factors and vesicles, have not been published.

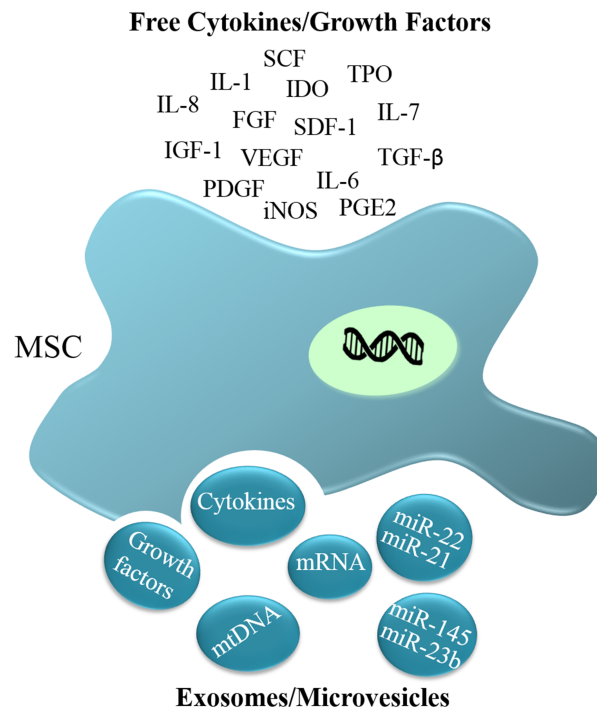


Figure 3. Representation of free or packaged cytokines/growth factors secreted by MSCs.

EVs derived from MSCs can be considered as unique tools in the control of tissue regeneration: they mimic the effect of MSCs on target tissues, displaying long-term tissue reprogramming. In this case, their mechanism of action is strongly related to their cargo, which is able to activate specific regenerative cellular programs; moreover, MSC-derived EVs showed fewer limitations than their parent cells.

MSC-EVs are characterized by more than 150 miRNAs and 938 different genes (www.exocarta.org), and they can interact with either adjacent cells or cells resident in remote areas to trigger appropriate cellular responses. MSC-secreted bioactive factors act as paracrine or endocrine mediators able to influence cell behavior [166]. In particular, MSC-EVs play a bi-directional role between damaged and their own progenitor cells: those derived from injured cells stimulate stem cells to differentiate; whereas EVs released by MSCs promote regenerative mechanisms in cells that survived the injury [152] [124].

This paracrine effect was first described by Haynesworth SE et al. (1996), observing that MSCs secrete a heterogeneous pool of growth factors, chemokines and cytokines that are able to exert similar effects as those of their parent cells on neighboring tissues [164]. For instance, it was demonstrated that the beneficial effects exerted by the MSC in the setting of acute myocardial infarction were mediated by the conditioned medium of MSC via cytoprotective pathways, particularly when the cells were transduced with the pro-survival gene Akt (Akt-MSCs) [167]. Similar results have been described in hepatic regeneration [168] and in acute kidney injury models, where MSCs provide a paracrine support to the repair of local damaged cells [88]. Moreover, MSC-EVs have promoted neo-angiogenesis processes by stimulating the Wnt4/beta-catenin pathway [169]. In the central nervous system (CNS), MSC secretome showed neurogenesis, inhibition of glial scar formation and a neuroprotective effect in the presence of different brain pathophysiological conditions [170] [171].

Immunosuppressive and immunomodulatory effects exerted by MSCs were first attributed to different molecules, including interferon gamma (IFN- γ) and inducible nitric-oxide synthase (iNOS), but Bruno et al. demonstrated that the protective effect against induced acute tubular injury was properly exerted by encapsulated growth factors in MSC-EVs [48] [1]. MSC-EVs exhibit many of the immune modulatory properties of their cells of origin, inhibiting proliferation, differentiation and antibody production of activated B cells [172] and inducing the apoptosis of activated T cells, while increasing the proliferation of regulatory T cells and the immunosuppressive cytokine IL-10 concentration in culture medium [173]. Recently, Di Trapani and colleagues observed MSC-EV ability to suppress also NK cells [174] meanwhile Zhang et al confirmed MSC-EVs activity on macrophage polarization leading to an immune suppressive M2 phenotype, inducing the differentiation of CD4⁺ T cells to Treg and the production of IL-10 [54]. Thus, MSC-EVs exert their immune modulatory activity both on innate and on adaptive immunity. Of note, a case of successful treatment with MSC-EVs in a patient with steroid-resistant gastrointestinal GVHD was reported [175].

Using EVs as smaller cellular “alter ego” effectors, with similar superficial markers and possibly enriched in genetic material, it may be possible to achieve an innovative cell-free strategy [176] with promising therapeutic effects in myocardial infarct size reduction [2], musculoskeletal disabilities [177], acute and chronic kidney injury [178], tissue repair and regeneration (wound healing) treatments [179]. In addition, the use of MSC-EVs instead of MSCs overcomes the main obstacles of cell therapy, in particular regarding safety, regulation and complexity issues [152], including the intravascular administration drawbacks typical of

cellular therapy, which can cause vascular clotting [180], even if there are actually indications that EVs derived by endothelial cells can induce thrombosis effect, by stimulating coagulation and inflammation, when employed at high concentrations [181].

As clearly suggested by Lener and colleagues, it is crucial to list EVs as APIs or next drug delivery systems in order to define standard requirements for isolation, safety, quality and therapeutic purposes. Since EV production requires the use of living cells, they must be cultured following GMP regulations; in fact, changes in cell culture can result in alterations of EV biological properties and therapeutic effects. Different therapeutic potentials could be observed both when employing heterogeneous (harvested from different cellular lineages) and also homogeneous (when using EV obtained from independent preparation collected from the same cellular type) EV populations, resulting in safety issues. Moreover, purification protocols could alter the EV biological activity, due to the loss of effectors, thus resulting in lower therapeutic potential [63]. In our opinion, to obtain a standard product with reproducible features, as required for APIs, a "fingerprint" should be carried out fixing the limits of the product acceptability (for example, proteomic profile and lipid content). This represents the typical pharmaceutical approach for the production of biologicals, or extractive phyto-complexes.

The majority of clinical trials use EVs isolated from several different cell lineages and only one study thus far aims to test the effect of MSC-derived microvesicles and Ex therapy on β -cell mass in type I diabetes mellitus patients (NCT02138331, last access June 5th 2017 <http://www.clinicaltrials.gov>).

As they are complex carriers that can transfer a variety of biological molecules, the functional implications of their biodiversity should be investigated in detail, viewing their exploitation in therapeutic settings per se or as drug delivery nano-systems.

2.1 EVs as DDS: analogies with liposomes

EVs show a strong similarity to liposomes but they possess additional favorable features such as stability in the bloodstream, slower clearance, low immunogenicity and the ability to deliver therapeutic agents of various sizes, ranging from small molecules (such as anti-inflammatory or chemotherapeutic agents), to genetic fragments (e.g. mRNAs, miRNAs and siRNAs) and other nanosystems [130, 175]. In particular, miRNA and siRNA delivery by EVs allows them to change the cellular genetic expression [176].

Liposomes are synthetic, bimodular, phospholipid bilayer-enclosed vesicular systems of about 100 nm in diameter, able to encapsulate both hydrophilic molecules in their aqueous core and lipophilic drugs, exploiting their hydrophobic phospholipid bilayer, as well as amphipathic compounds by distributing them between both phases. Thanks to their bimodular nature, different therapeutic molecules can be encapsulated, including anti-cancer molecules, vaccines, chelating agents, peptides, hormones, genetic moieties, proteins and many others for cosmetic, nutraceutical and pharmaceutical purposes [182]. For the production of liposomes, there are several techniques available, providing optimal encapsulation efficiency, narrow particle size distribution and long-term stability: 1) mechanical dispersion, 2) solvent dispersion, and 3) detergent removal methods [183]. Thanks to knowledge gleaned throughout the last 40 years, therapeutic liposomes are produced with an industrial approach, underlining the scalability of the process, which yet lacks in the EV field [152]. Liposomes have been employed in different clinical trials for the treatment of cancer, inflammatory and fungal diseases [184]. The first liposome formulation commercially available was Doxil®, approved in 1995 by the US Food and Drug Administration (FDA) for the treatment of chemotherapy refractory acquired immune deficiency syndrome (AIDS)-related Kaposi's sarcoma [185]. Nowadays, more than a dozen of liposomal packaged drugs are commercially available and more than twenty formulations are currently under investigation in several clinical trials [186]. Some formulations, such as Doxil® and Lipodox®, are commercially available as suspension forms, but the majority of liposomal “ready to use” formulations are lyophilized products due to their long-term stability with an adequate cryoprotectant [186]. Liposome formulations are preferentially administered intravenously, even if intramuscular (Epaxal® and Inflexal V®), spinal (Depocyt®) or epidural (DepoDur®) administrations have been approved [186].

Different liposome types, including uni-lamellar and multi-lamellar vesicles (in relation to their bilayer structure) have been developed and these structures influence the nanoparticle biodistribution and cellular uptake mechanisms [187]. The liposomal surface charge can be positive, negative or neutral [188]; this feature is exploited in gene therapy thanks to the attraction between the negatively charged DNA and the cationic liposomes [189]. The liposome phospholipid membrane is usually based on phosphatidylcholine (lecithin), phosphatidylserine and cholesterol, compounds able to self-assemble in an aqueous environment, creating the typical liposomal structure and preventing physical instability [190].

Despite these many advantages, liposomes present some drawbacks including instability, oxidation, poor targeting and drug leakage [191]; in fact, when intravenously injected, they

accumulate both in liver and spleen macrophages or result in quick clearance from the bloodstream by opsonization and mononuclear phagocyte activation. Opsonization is a physiological defense mechanism of the human body which facilitates foreign body recognition and removal, avoiding at the same time DDS targeting and efficacy [192]. Even though it could decrease the targeting capabilities of liposomes by interfering with the interactions between the nanosystem and the target cell, PEGylation is often applied on artificial liposomal coronas to avoid fast clearance from the circulation, thus prolonging bloodstream permanence [193].

For these reasons, smart liposomes, able to respond to different endogenous or exogenous stimuli, represent one of the most attractive topic in the nanomedicine field [75]. Based on the deep knowledge acquired in liposomal field, it has been possible to better understand the complex EV structure, their drug loading and release properties, their stability and potentiality as DDS [138] [192]. On the other hand, new discoveries in the EV field could be successfully applied to improve current liposomal delivery systems.

Since liposomes are synthetic nanosystems, it remains challenging to perfectly mimic the cellular phospholipid bilayer: this hurdle could be overcome using EVs as drug vehicles, since their double-lipid bilayer retains the same structure as natural cellular corona, essential to preserve the physiological cargo from bloodstream degradation [176]. Moreover, the phospholipid bilayer is composed of the same proteins, markers and potential targeting moieties as their parent cells [138] [152]. For example, Ohno et al. recently employed an artificial peptide (GE11), which is less mitogenic than Epidermal Growth Factor (EGF), for targeting EGFR-expressing cancer tissues, providing new approaches for miRNA replacement therapies [194]. Notably, EVs can encapsulate both hydrophilic and lipophilic therapeutics and deliver them even through “hard to cross barriers” such as the Blood Brain Barrier (BBB), avoiding phagocytosis or degradation mediated by macrophages [195] [196] [197].

Notably, EVs show less toxicity than synthetic liposomes or metal-based nanoparticles, such as gold nanoparticles, and higher stability in the bloodstream as well as specific targeting capabilities [198]. In particular, EVs derived from MSCs retain their instinctive homing to injured tissues, thus helping in recovery processes, as observed by Grange et al. in acute kidney injury models [199]. This natural tropism is essential for a suitable “smart” DDS to avoid off target side effects and enhance the specific uptake by target cells [200].

Therefore, when compared to synthetic nanosystems, EVs can be considered “ideal” DDS retaining several desirable features including cytocompatibility, biocompatibility, intrinsic targeting and high bloodstream stability [201] [202].

2.2 Drug encapsulation in EVs

Two approaches have currently been employed for drug loading in EVs, each with different advantages and disadvantages. The exogenous approach provides drug encapsulation after EV isolation and purification, while the endogenous approach is carried out during EV biogenesis (Figure 4). Moreover, cells could be transfected with genetic material to induce EV loaded secretion [203].

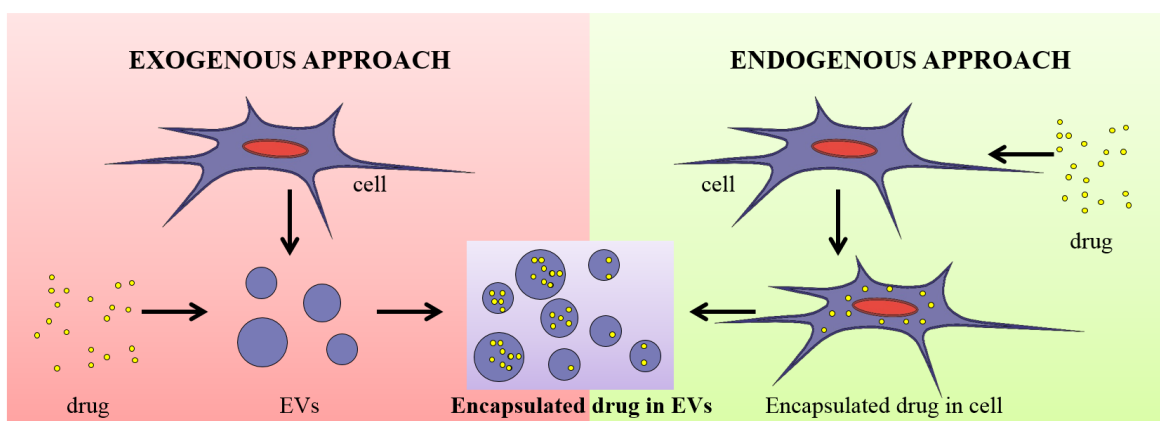


Figure 4. Schematic representation of drug encapsulation in EVs: in the exogenous approach, EVs are loaded after their isolation, while the endogenous approach is based on active molecules encapsulation during EV biogenesis.

The endogenous approach is applied to encapsulate molecules of different natures, including genetic material, lipids and proteins [106]. Cells are briefly cultured with the selected compound until its internalization occurs; then, the cells are stressed to induce the release of drug-enriched EVs in the extracellular milieu [204].

Some authors proposed the transfection-based method to achieve the secretion of EVs loaded with miRNAs, as a result of endogenous secretory mechanisms. Similarly, another endogenous technique exploited for EV loading is based on the transfection of donor cells with drug-encoding DNA, thus applying a genetic engineering approach. Alvarez-Erviti et al. highlighted the EV potential as innovative DDS for the first time. Specifically, they engineered autologous DC, obtaining EVs characterized by linking the Rabies Viral Glycoprotein (RVG) sequence to Lamp2b, an exosomal membrane protein, resulting in an increase in brain targeting. They

isolated EVs expressing RVG sequences on their membrane surface, causing a decrease brain protein expression associated to Alzheimer's disease [197]. In addition, the engineered glycosylation of the RVG peptides enhanced EV in vitro internalization when compared to non-glycosylated peptides, ameliorating EV target capabilities [205]. Similarly, Batrakova et al. used this method to achieve Ex loading with different protein cargos for the treatment of neurodegenerative diseases, utilizing their peculiar ability to overcome the BBB [206]. The main limitation of this approach is represented by the amount of encapsulated drug, related to its properties [106] [207]. The expression of physiologically therapeutic molecules produced by cells and packaged into EVs is influenced by cell lineage, genetic manipulation, but may also depend on culture conditions (e.g. hypoxia and type of supplement). The optimal strategy for achieving an increased route of the expressed therapeutic to EVs depends on the final target. In 2014, Pascucci et al. successfully obtained MSC-EVs loaded with Paclitaxel (PTX) by incubating cells at 37°C with high drug dosage. PTX-loaded EVs showed a high in vitro efficacy against pancreatic cancer cell growth [208]. Del Fattore et al. observed that both bone marrow-derived and umbilical cord-derived MSC-EVs decreased glioblastoma cell proliferation in vitro, while an opposite effect was observed with adipose tissue-derived MSC-EVs. Moreover, both bone marrow- and umbilical cord-MSC-EVs induced apoptosis of glioblastoma cells, while adipose tissue-MSC-EVs had no effect. Loading umbilical cord-MSC-EVs with Vincristine further increased cytotoxicity when compared both to the free drug and to unloaded EVs [209]. Similarly, Tang et al. showed the ability of tumor cells to encapsulate chemotherapeutic agents into EVs [210]. Both studies suggested that anticancer drug delivery via physiologically secreted vesicles could solve the main drawback of chemotherapy, *id est* side effects. Vehiculating chemotherapeutics into MSC-EVs achieves smart drug targeting, avoiding its biodistribution toward healthy tissues. To further improve the EV targeting, Arginine-glycine-asparagine (RGD) sequences were added to doxorubicin (DOX)-loaded EVs by cell transfection with the vector expressing RGD sequence to selectively target breast cancer cells due to their high expression of peculiar integrins with high affinity for engineered EVs, without accumulation in undesired tissues (i.e. liver and spleen) [211]. In contrast, Federici et al. demonstrated that malignant melanoma cancer cells are resistant to cisplatin treatment by a double mechanism of extracellular acidification and EV-mediated removal [212], suggesting that Ex, by encapsulating and removing anticancer drugs from cancer cells, play a crucial role in chemoresistance.

The exogenous method carries out the EV loading after vesicle isolation from body fluids or cell culture media; this approach can be applied for both hydrophobic and hydrophilic molecules. The encapsulation of hydrophobic drugs is achieved after direct blending: small lipophilic molecules passively diffuse through the EV membrane, while other molecules, such as PXT, are entrapped in EV double lipid bilayer [204]. A hydrophobic interaction occurs between the hydrophobic tails of EV phospholipid layer and the hydrophobic drug, thus achieving a physical entrapment and protecting the encapsulated drug from degradation phenomena in the extracellular environment. For example, Sun et al. isolated EVs from murine lymphoma cells and incubated curcumin at room temperature for a few minutes. Their results confirmed that curcumin-loaded EVs enhanced in vitro drug solubility, stability and in vivo bioavailability; importantly, this approach improved curcumin anti-inflammatory activity when compared to free drug [213]. The same technique was used by Zhuang et al. to obtain drug-loaded Ex exploitable for the treatment of brain inflammatory diseases. The intranasal administration of EVs, enriched by a transcription factor inhibitor (JSI124), showed a quick and specific targeted uptake by microglial cells, confirming the EV ability to cross the BBB [196].

The loading of hydrophilic compounds (such as RNA and genetic material) is more challenging due to the presence of the EV phospholipid bilayer structure, which constitutes the major obstacle to passive loading [204]. Different methods have been exploited to load hydrophilic compounds in EVs. Electroporation is a technique based on high voltage application to induce the spontaneous pore formation in membranous structures; this approach allows the cross of hydrophilic compounds through EV membrane without affecting EV integrity, morphology or functionality [197]. However, the electroporation process must be controlled to avoid drug precipitation and aggregation [214]: membrane stabilizer addition, such as trehalose, helps to avoid EV aggregation and fusion, a common phenomenon observed when applying electroporation procedures to liposomes [215]. Wahlgren et al. exploited an optimized electroporation technique, preceded by the pre-complexation of siRNAs with cationic liposomes, to achieve Ex loading. With this proof of concept, they demonstrated the possible role of Ex as gene therapy vehicles, overcoming the limiting step represented by the negative surface charges of both EVs and siRNAs [216].

Other approaches have been exploited for exogenous EV loading, such as repeated freeze-thaw cycles, sonication, treatment with saponins to increase EV permeability, and extrusion [217]. The highest drug loading capacity is reached using the sonication technique instead of

incubation at room temperature or electroporation reaching drug loading (%) of 28.29 %, 1.44 % and 5.3 % [76]. Haney et al. combined sonication and extrusion procedures to load catalase, an antioxidant molecule, in Ex; the authors confirmed that this approach enhanced the drug loading (by roughly 26 %) and preserved the catalase activity [217].

Harnessing exogenous techniques, drugs can also adhere to the exosome surface, thus being available for a fast release. This approach could be exploited when a sustained release of the drug is needed since the whole encapsulated drug is not entrapped in the intracellular matrix but is partially linked to the external surface, thus providing a starting-burst release effect. Moreover, both targeting and retention time could be increased by the addition of PEG moieties to the EV surface, allowing the attachment of other targeting molecules [218].

Based on our knowledge, an important issue that could be further investigated is the possible interaction between EV “natural” cargo and the encapsulated molecules that could either enhance or reduce the biological and pharmacological activity of these nanosystems.

2.3 “Good and bad” vesicles

EVs can be considered the middle ground between cell-based therapy and nanomedicine, since they retain the best qualities of both systems [204]. The existence of “good and bad” vesicles is related to their double role in physiological and pathological conditions, leading a bidirectional flow of information [126]. In particular, EVs participate in the maintenance of the homeostatic balance as well as modulate angiogenic, inflammatory and coagulatory conditions. The crucial role of EVs in pathological conditions, such as in cancer and autoimmune diseases, has been deeply studied; however, their role in homeostasis and physiological functions is not fully explored yet [158].

EVs can affect immune responses, promote tumor invasiveness, metastasis and drug resistance, promote endothelial cell migration, and participate in neovascularization acting as carriers of angiogenic stimuli [219]. Diseased cells exploit EVs as carriers to spread infections and diseases, such as in the case of spongiform encephalopathies [220] and Hepatitis C (HCV) [221]. Moreover, macrophages infected by *Mycobacterium tuberculosis* deliver glycopeptidolipids into Ex, which exert a pro-inflammatory activity [222].

In osteoarthritis and rheumatoid arthritis, EVs secreted by IL-1 β -stimulated fibroblast-like synoviocytes induce extracellular matrix degradation, improve inflammation and change the chondrocyte morphology and activity [223] [224]. Cancerous cells secrete Ex enriched in

oncogenic RNA, miRNA and transcription factors responsible for mediating metastasis neo-formation in targeted tissues by promoting neo-angiogenesis and immune suppression [225]. Melanoma cells secrete Ex enriched in RNA that are able to transform poorly metastatic tumor cells into highly metastatic cells; this exosome-mediated information exchange provides a hypothetical mechanism for dissemination of cancer phenotypes. Moreover, cancer cell-derived EVs promote angiogenesis and facilitate tumor-immune surveillance escape [226].

Degenerative disease exacerbation is also influenced by exosome-mediated mechanisms. Neurons from Parkinson's and Alzheimer's patients secrete Ex containing α -synuclein and amyloid beta (A β), the main hallmarks of these pathologies. These Ex contribute to the nucleation and physical diffusion of the α -synuclein and A β aggregates [227].

One of the first therapeutic applications of "good" vesicles was to create EV-based vaccines able to suppress the tumor expansion in immune-competent mice. EV-based vaccines have been tested also for the treatment of infectious diseases, to trigger a more efficient immune response than that mediated by standard vaccines in the recipient organism (for more details see review [200]). The positive results achieved using EV-based vaccines, which could be considered an innovative cell-free vaccine approach, have paved the way to their intensive study in clinical trials [228] [229].

Since MSC-EVs retained the same beneficial properties of their parent cells, they have been widely used as "ideal" cell substitutes in different therapeutic fields, in particular for the treatment of several pathological conditions including pulmonary hypertension [230], myocardial ischemia [231] [232], hepatic failure [233], acute renal injury [88], tumor [208] [211] [234], bone [235] [236] and CNS degeneration [237].

The role of MSC-EVs, and also of their parent cells, in tumorigenesis and metastatization creation is still an open question. There are studies reporting the ability of MSC-EVs to inhibit cancer cell proliferation and research suggesting their role in tumour growth and drug resistance. This double behavior must be cleared before entering the clinical application, by characterizing the MSC-EV effective payload [229].

In order to achieve EV clinical application, it is essential to define their parent cell culture conditions, which must be in line with GMP standards. Additionally, the purification and isolation technologies can also substantially alter the composition of the finished product. The resulting heterogeneity represents a translational issue regarding regulatory approval concerning to safety. The only way to enter clinical trials is to obtain a standardized product with specific quality requirements using a repeatable and validated process. On a reproducible

product, it will be possible to carry out the safety and efficacy checks required for regulatory approval.

3. Novel therapeutic approach: next generation drug delivery system

Today, MSC-derived EVs could replace MSC therapy due to their comparable regenerative potential with even better features. MSCs and their secreted EVs retain great potential as targeted drug delivery vehicles thanks to their ability to encapsulate several therapeutic molecules and to their physiological tropism to reach injured sites. Notably, the combination of MSCs with nanoparticles allows stem cell therapy and nanomedicine advantages to be coupled for the treatment of several disease, such as brain tumors [238] or osteosarcoma [239].

As innovative and “smart” DDS, MSC tropism could be employed also for tumor tracking by encapsulating iron oxide nanoparticles, which are commonly used as contrast agents [240]. Another non-invasive targeting strategy is represented by metallic nanosystems combined to a magnetic field: the incubation of iron oxide nanoparticles with cells results in the production of EVs loaded with nanosystems. These double systems based on EV enriched in iron nanoparticles, were able to be taken up by naive cells, and to disseminate throughout the body [241]. In 2015, Tripodo et al. introduced a novel integrated biological-pharmaceutical approach to improve the therapeutic potential of MSC-EVs as innovative DDS. This idea deals with the fusion of a more classical technological approach, based on bio-inspired nanoparticles, with the more innovative EV application as physiological nanosystems for drug delivery purposes. A carrier-in-carrier system using an endogenous loading technique has been developed: the first carrier was represented by micelles based on vitamin E and inulin, able to encapsulate high curcumin content but at the same time preventing its cytotoxicity, while the second carrier was based on MSC-EVs. This study demonstrated the micelles’ ability to cross MSC membrane within few minutes, protecting them from curcumin cytotoxicity, and that MSCs were able to release the entrapped drug, protecting curcumin from degradation [242].

This biological-pharmaceutical approach has been tested on other pharmaceutical carriers; in 2017, Perteghella et al. investigated a novel carrier-in-carrier system composed of MSC-EVs loaded with silk/curcumin nanoparticles. The first carrier is represented by silk nanoparticles, able to encapsulate high curcumin content, while the second carrier is represented by MSC-EVs. Qualitative analyses on released product highlighted a higher MSC ability to release nanoparticles within SV systems than in Ex, probably due to nanosystem size [243].

These “next generation drug delivery systems” combine beneficial effects of both regenerative cell therapies and pharmaceutical nanomedicine, providing a tool that could lead to avoid the use of viable MSCs and their regulatory affairs.

Given the complex nature, multiple-component of biologically active contents and the cellular origin of EVs, it is debatable what kind of pharmaceutical category they belong to. Food and Drug Administration (FDA) and European Medicinal Agency (EMA), at the best of our knowledge, have not yet classified secretome and/or EVs. We agree with the position of Lener and colleagues that distinguish between EVs, obtained from genetically modified cells, considered as Advanced Therapy Medicinal Product (ATMPs), and native EVs, from genetically non-manipulated cells, considered as acellular biological medicinal product [69].

4. Conclusions

EVs are nano-sized vesicles physiologically released by cells and actively involved in cell-to-cell communication. The innate ability of EVs to deliver their cargo to target cells represents the basis of their suitable application as innovative DDS. MSC-derived EVs provide an intriguing tool exploitable for regenerative medicine and for treatment of diseases refractory to conventional therapies.

EVs have peculiar properties which make them unique DDS: the main strengths of EVs are a lack of toxicity and lower antigenicity when compared with synthetic nanosystems, while they could virtually exert higher safety profile, higher stability in the bloodstream, and lower cost of production than cell therapy.

Still today, EVs are in a regulatory gap: they are not cells, but cellular products, thus they cannot be considered as Cell Therapy or Tissue Engineering Products. For this reason, regulatory authorities are requested to give an urgent opinion about all of these issues, which strongly influences the product’s final quality. Moreover, a universally accepted protocol for EV isolation is missing, as well as validated methods for the quantification and the potency of EVs are lacking.

EVs seem to act as “Doctor Jekyll and Mister Hyde”, with a double identity played in both physiological and pathophysiological conditions. EVs’ complex structure and mechanism of action still need to be elucidated to achieve effective clinical and pharmaceutical applications. Finally, further studies are required to confirm their safety and to prove their efficacy both in

vitro but mainly in vivo, even if currently no side effects related to their pre-clinical and clinical use have been described yet.

In conclusion, we reiterate the requirement of clear regulatory guidance, adopting of EVs as therapeutic entities and defining their classification (are EVs considered ATMPs or not?), as well as the requirement of standards in terms of isolation protocols, as well as nomenclature to assist with developing EVs as therapeutic entities and enabling better group-to-group comparisons of EV studies. Scientific progress in this field and group-to-group comparisons could be achieved through the availability of a highly pure, “ready-off-the-shelf,” well-characterized and stable powder-based EV standard, with a low cost-benefit ratio.

5. Acknowledgements

We are grateful to Ryan Rogers, University of Michigan, for editorial help.

Conflict of interest

The authors disclose any actual or potential conflict of interest.

6. References

- [1] S. Bruno, C. Grange, M.C. Deregibus, R.A. Calogero, S. Saviozzi, F. Collino, L. Morando, A. Busca, M. Falda, B. Bussolati, C. Tetta, G. Camussi, Mesenchymal Stem Cell-Derived Microvesicles Protect Against Acute Tubular Injury, *Journal of the American Society of Nephrology*, 20 (2009) 1053-1067.
- [2] R.C. Lai, F. Arslan, M.M. Lee, S.K. Sze, A. Choo, T.S. Chen, M. Salto-Tellez, L. Timmers, C.N. Lee, R.M. El Oakley, G. Pasterkamp, D.P.V. de Kleijn, S.K. Lim, Exosome secreted by MSC reduces myocardial ischemia/reperfusion injury (vol 4, pg 214, 2010), *Stem Cell Research*, 5 (2010) 170-171.
- [3] L. Timmers, S.K. Lim, F. Arslan, J.S. Armstrong, I.E. Hofer, P.A. Doevendans, J.J. Piek, R.M. El Oakley, A. Choo, C.N. Lee, G. Pasterkamp, D.P.V. de Kleijn, Reduction of myocardial infarct size by human mesenchymal stem cell conditioned medium, *Stem Cell Research*, 1 (2008) 129-137.
- [4] C.J. F., Ueber entzündung und eiterung, in, 1867, pp. 1-79.

- [5] A.J. Friedenstein, I.I. Piatetzky-Shapiro, K.V. Petrakova, Osteogenesis in transplants of bone marrow cells, *Journal of embryology and experimental morphology*, 16 (1966) 381-390.
- [6] A.J. Friedenstein, R.K. Chailakhjan, K.S. Lalykina, The development of fibroblast colonies in monolayer cultures of guinea-pig bone marrow and spleen cells, *Cell and tissue kinetics*, 3 (1970) 393-403.
- [7] A.J. Friedenstein, J.F. Gorskaja, N.N. Kulagina, Fibroblast precursors in normal and irradiated mouse hematopoietic organs, *Experimental hematology*, 4 (1976) 267-274.
- [8] D.J. Prockop, Marrow stromal cells as stem cells for nonhematopoietic tissues, *Science*, 276 (1997) 71-74.
- [9] M.F. Pittenger, A.M. Mackay, S.C. Beck, R.K. Jaiswal, R. Douglas, J.D. Mosca, M.A. Moorman, D.W. Simonetti, S. Craig, D.R. Marshak, Multilineage potential of adult human mesenchymal stem cells, *Science*, 284 (1999) 143-147.
- [10] A.I. Caplan, Adult mesenchymal stem cells for tissue engineering versus regenerative medicine, *Journal of Cellular Physiology*, 213 (2007) 341-347.
- [11] C.M. Kolf, E. Cho, R.S. Tuan, Mesenchymal stromal cells - Biology of adult mesenchymal stem cells: regulation of niche, self-renewal and differentiation, *Arthritis Research & Therapy*, 9 (2007).
- [12] P. Bianco, P.G. Robey, P.J. Simmons, Mesenchymal stem cells: Revisiting history, concepts, and assays, *Cell Stem Cell*, 2 (2008) 313-319.
- [13] A.I. Caplan, What's in a Name?, *Tissue Engineering Part A*, 16 (2010) 2415-2417.
- [14] P.A. Zuk, M. Zhu, P. Ashjian, D.A. De Ugarte, J.I. Huang, H. Mizuno, Z.C. Alfonso, J.K. Fraser, P. Benhaim, M.H. Hedrick, Human adipose tissue is a source of multipotent stem cells, *Molecular Biology of the Cell*, 13 (2002) 4279-4295.
- [15] L. de Girolamo, S. Lopa, E. Arrigoni, M.F. Sartori, F.W.B. Preis, A.T. Brini, Human adipose-derived stem cells isolated from young and elderly women: their differentiation potential and scaffold interaction during in vitro osteoblastic differentiation, *Cytotherapy*, 11 (2009) 793-803.

- [16] E. Arrigoni, S. Lopa, L. de Girolamo, D. Stanco, A.T. Brini, Isolation, characterization and osteogenic differentiation of adipose-derived stem cells: from small to large animal models, *Cell and Tissue Research*, 338 (2009) 401-411.
- [17] S. Shi, S. Gronthos, Perivascular niche of postnatal mesenchymal stem cells in human bone marrow and dental pulp, *Journal of Bone and Mineral Research*, 18 (2003) 696-704.
- [18] C. De Bari, F. Dell'Accio, P. Tylzanowski, F.P. Luyten, Multipotent mesenchymal stem cells from adult human synovial membrane, *Arthritis and Rheumatism*, 44 (2001) 1928-1942.
- [19] Y.M. Bi, D. Ehirchiou, T.M. Kilts, C.A. Inkson, M.C. Embree, W. Sonoyama, L. Li, A.I. Leet, B.M. Seo, L. Zhang, S.T. Shi, M.F. Young, Identification of tendon stem/progenitor cells and the role of the extracellular matrix in their niche, *Nature Medicine*, 13 (2007) 1219-1227.
- [20] P. Ame-Thomas, H. Maby-El Hajjami, C. Monvoisin, R. Jean, D. Monnier, S. Caulet-Maugendre, T. Guillaudeau, T. Lamy, T. Fest, K. Tarte, Human mesenchymal stem cells isolated from bone marrow and lymphoid organs support tumor B-cell growth: role of stromal cells in follicular lymphoma pathogenesis, *Blood*, 109 (2007) 693-702.
- [21] M. Krampera, S. Sartoris, F. Liotta, A. Pasini, R. Angeli, L. Cosmi, A. Andreini, F. Mosna, B. Bonetti, E. Rebellato, M.G. Testi, F. Frosali, G. Pizzolo, G. Tridente, E. Maggi, S. Romagnani, F. Annunziato, Immune regulation by mesenchymal stem cells derived from adult spleen and thymus, *Stem Cells and Development*, 16 (2007) 797-810.
- [22] I. Rogers, R.F. Casper, Umbilical cord blood stem cells, *Best Practice & Research in Clinical Obstetrics & Gynaecology*, 18 (2004) 893-908.
- [23] K. Bieback, H. Kluter, Mesenchymal stromal cells from umbilical cord blood, *Current stem cell research & therapy*, 2 (2007) 310-323.
- [24] R.R. Taghizadeh, K.J. Cetrulo, C.L. Cetrulo, Wharton's Jelly stem cells: Future clinical applications, *Placenta*, 32 (2011) S311-S315.
- [25] K. Igura, X. Zhang, K. Takahashi, A. Mitsuru, S. Yamaguchi, T.A. Takahashi, Isolation and characterization of mesenchymal progenitor cells from chorionic villi of human placenta, *Cytherapy*, 6 (2004) 543-553.

- [26] M.S. Tsai, J.L. Lee, Y.J. Chang, S.M. Hwang, Isolation of human multipotent mesenchymal stem cells from second-trimester amniotic fluid using a novel two-stage culture protocol, *Human Reproduction*, 19 (2004) 1450-1456.
- [27] A. Schaffler, C. Buchler, Concise review: Adipose tissue-derived stromal cells - Basic and clinical implications for novel cell-based therapies, *Stem Cells*, 25 (2007) 818-827.
- [28] P. Gaetani, M.L. Torre, M. Klinger, M. Faustini, F. Crovato, M. Bucco, M. Marazzi, T. Chlapanidas, D. Levi, F. Tancioni, D. Vigo, R. Rodriguez Y Baena, Adipose-derived stem cell therapy for intervertebral disc regeneration: An in vitro reconstructed tissue in alginate capsules, *Tissue Engineering Part A*, 14 (2008) 1415-1423.
- [29] M. Faustini, M. Bucco, T. Chlapanidas, G. Luconi, M. Marazzi, M.C. Tosca, P. Gaetani, M. Klinger, S. Villani, V.V. Ferretti, D. Vigo, M.L. Torre, Nonexpanded Mesenchymal Stem Cells for Regenerative Medicine: Yield in Stromal Vascular Fraction from Adipose Tissues, *Tissue Engineering Part C-Methods*, 16 (2010) 1515-1521.
- [30] T. Chlapanidas, S. Farago, F. Mingotto, F. Crovato, M.C. Tosca, B. Antonioli, M. Bucco, G. Luconi, A. Scalise, D. Vigo, M. Faustini, M. Marazzi, M.L. Torre, Regenerated Silk Fibroin Scaffold and Infrapatellar Adipose Stromal Vascular Fraction as Feeder-Layer: A New Product for Cartilage Advanced Therapy, *Tissue Engineering Part A*, 17 (2011) 1725-1733.
- [31] B. Vigani, L. Mastracci, F. Grillo, S. Perteghella, S. Preda, B. Crivelli, B. Antonioli, M. Galuzzi, M.C. Tosca, M. Marazzi, M.L. Torre, T. Chlapanidas, Local biological effects of adipose stromal vascular fraction delivery systems after subcutaneous implantation in a murine model, *Journal of Bioactive and Compatible Polymers*, 31 (2016) 600-612.
- [32] L. de Girolamo, E. Lucarelli, G. Alessandri, M.A. Avanzini, M.E. Bernardo, E. Biagi, A.T. Brini, G. D'Amico, F. Fagioli, I. Ferrero, F. Locatelli, R. Maccario, M. Marazzi, O. Parolini, A. Pessina, M.L. Torre, G. Italian Mesenchymal Stem Cell, *Mesenchymal Stem/Stromal Cells: A New "Cells as Drugs" Paradigm. Efficacy and Critical Aspects in Cell Therapy*, *Current Pharmaceutical Design*, 19 (2013) 2459-2473.
- [33] V.B.R. Konala, M.K. Mamidi, R. Bhonde, A.K. Das, R. Pochampally, R. Pal, The current landscape of the mesenchymal stromal cell secretome: A new paradigm for cell-free regeneration, *Cytotherapy*, 18 (2016) 13-24.

- [34] M. Strioga, S. Viswanathan, A. Darinskas, O. Slaby, J. Michalek, Same or Not the Same? Comparison of Adipose Tissue-Derived Versus Bone Marrow-Derived Mesenchymal Stem and Stromal Cells, *Stem Cells and Development*, 21 (2012) 2724-2752.
- [35] N. Quirici, C. Scavullo, L. de Girolamo, S. Lopa, E. Arrigoni, G.L. Deliliers, A.T. Brini, Anti-L-NGFR and-CD34 Monoclonal Antibodies Identify Multipotent Mesenchymal Stem Cells in Human Adipose Tissue, *Stem Cells and Development*, 19 (2010) 915-925.
- [36] M. Dominici, K. Le Blanc, I. Mueller, I. Slaper-Cortenbach, F.C. Marini, D.S. Krause, R.J. Deans, A. Keating, D.J. Prockop, E.M. Horwitz, Minimal criteria for defining multipotent mesenchymal stromal cells. The International Society for Cellular Therapy position statement, *Cytotherapy*, 8 (2006) 315-317.
- [37] R. Izadpanah, C. Trygg, B. Patel, C. Kriedt, J. Dufour, J.M. Gimble, B.A. Bunnell, Biologic properties of mesenchymal stem cells derived from bone marrow and adipose tissue, *Journal of Cellular Biochemistry*, 99 (2006) 1285-1297.
- [38] M.L. Torre, E. Lucarelli, S. Guidi, M. Ferrari, G. Alessandri, L. De Girolamo, A. Pessina, I. Ferrero, Gism, Ex Vivo Expanded Mesenchymal Stromal Cell Minimal Quality Requirements for Clinical Application, *Stem Cells and Development*, 24 (2015) 677-685.
- [39] EudraLex. Volume 4: Good manufacturing practice (GMP) Guidelines for medicinal products for human and veterinary use, laid down in Commission Directives 91/356/EEC, as amended by Directive 2003/94/EC, and 91/412/EEC.
- [40] C.A. Herberts, M.S.G. Kwa, H.P.H. Hermsen, Risk factors in the development of stem cell therapy, *Journal of Translational Medicine*, 9 (2011).
- [41] S. Schrepfer, T. Deuse, H. Reichenspurner, M.P. Fischbein, R.C. Robbins, M.P. Pelletier, Stem cell transplantation: The lung barrier, *Transplantation Proceedings*, 39 (2007) 573-576.
- [42] T. Chlapanidas, S. Perteghella, S. Farago, A. Boschi, G. Tripodo, B. Vigani, B. Crivelli, S. Renzi, S. Dotti, S. Preda, M. Marazzi, M.L. Torre, M. Ferrari, Platelet lysate and adipose mesenchymal stromal cells on silk fibroin nonwoven mats for wound healing (vol 133, 42942, 2016), *Journal of Applied Polymer Science*, 133 (2016).
- [43] T. Chlapanidas, M.C. Tosca, S. Farago, S. Perteghella, M. Galuzzi, G. Lucconi, B. Antonioli, F. Ciancio, V. Rapisarda, D. Vigo, M. Marazzi, M. Faustini, M.L. Torre,

FORMULATION AND CHARACTERIZATION OF SILK FIBROIN FILMS AS A SCAFFOLD FOR ADIPOSE-DERIVED STEM CELLS IN SKIN TISSUE ENGINEERING, *International Journal of Immunopathology and Pharmacology*, 26 (2013) 43-49.

[44] L. de Girolamo, E. Arrigoni, D. Stanco, S. Lopa, A. Di Giancamillo, A. Addis, S. Borgonovo, C. Dellavia, C. Domeneghini, A.T. Brini, Role of Autologous Rabbit Adipose-Derived Stem Cells in the Early Phases of the Repairing Process of Critical Bone Defects, *Journal of Orthopaedic Research*, 29 (2011) 100-108.

[45] L. de Girolamo, S. Niada, E. Arrigoni, A. Di Giancamillo, C. Domeneghini, M. Dadsetan, M.J. Yaszemski, D. Gastaldi, P. Vena, M. Taffetani, A. Zerbi, V. Sansone, G.M. Peretti, A.T. Brini, Repair of osteochondral defects in the minipig model by OPF hydrogel loaded with adipose-derived mesenchymal stem cells, *Regenerative Medicine*, 10 (2015) 135-151.

[46] F.M. Chen, X.H. Liu, Advancing biomaterials of human origin for tissue engineering, *Progress in Polymer Science*, 53 (2016) 86-168.

[47] D.M. Patel, J. Shah, A.S. Srivastava, Therapeutic Potential of Mesenchymal Stem Cells in Regenerative Medicine, *Stem Cells International*, (2013).

[48] L. Biancone, S. Bruno, M.C. Deregibus, C. Tetta, G. Camussi, Therapeutic potential of mesenchymal stem cell-derived microvesicles, *Nephrology Dialysis Transplantation*, 27 (2012) 3037-3042.

[49] T. Katsuda, N. Kosaka, F. Takeshita, T. Ochiya, The therapeutic potential of mesenchymal stem cell-derived extracellular vesicles, *Proteomics*, 13 (2013) 1637-1653.

[50] M. Gnecci, Z. Zhang, A. Ni, V.J. Dzau, Paracrine Mechanisms in Adult Stem Cell Signaling and Therapy, *Circulation Research*, 103 (2008) 1204-1219.

[51] D.J. Prockop, D.J. Kota, N. Bazhanov, R.L. Reger, Evolving paradigms for repair of tissues by adult stem/progenitor cells (MSCs), *Journal of Cellular and Molecular Medicine*, 14 (2010) 2190-2199.

[52] C.E.P. Aronin, R.S. Tuan, Therapeutic Potential of the Immunomodulatory Activities of Adult Mesenchymal Stem Cells, *Birth Defects Research Part C-Embryo Today-Reviews*, 90 (2010) 67-74.

- [53] N. Li, J. Hua, Interactions between mesenchymal stem cells and the immune system, *Cellular and Molecular Life Sciences*, 74 (2017) 2345-2360.
- [54] B. Zhang, Y. Yin, R.C. Lai, S.S. Tan, A.B.H. Choo, S.K. Lim, Mesenchymal Stem Cells Secrete Immunologically Active Exosomes, *Stem Cells and Development*, 23 (2014) 1233-1244.
- [55] T. Tanna, V. Sachan, Mesenchymal Stem Cells: Potential in Treatment of Neurodegenerative Diseases, *Current Stem Cell Research & Therapy*, 9 (2014) 513-521.
- [56] J.Q. Cai, Z.X. Wu, X.M. Xu, L.M. Liao, J. Chen, L.H. Huang, W.Z. Wu, F. Luo, C.G. Wu, A. Pugliese, A. Pileggi, C. Ricordi, J.M. Tan, Umbilical Cord Mesenchymal Stromal Cell With Autologous Bone Marrow Cell Transplantation in Established Type 1 Diabetes: A Pilot Randomized Controlled Open-Label Clinical Study to Assess Safety and Impact on Insulin Secretion, *Diabetes Care*, 39 (2016) 149-157.
- [57] Y.M. Pers, L. Rackwitz, R. Ferreira, O. Pullig, C. Delfour, F. Barry, L. Sensebe, L. Casteilla, S. Fleury, P. Bourin, D. Noel, F. Canovas, C. Cyteval, G. Lisignoli, J. Schrauth, D. Haddad, S. Domergue, U. Noeth, C. Jorgensen, A. Consortium, Adipose Mesenchymal Stromal Cell-Based Therapy for Severe Osteoarthritis of the Knee: A Phase I Dose-Escalation Trial, *Stem Cells Translational Medicine*, 5 (2016) 847-856.
- [58] D. Garcia-Olmo, M. Garcia-Arranz, D. Herreros, I. Pascual, C. Peiro, J.A. Rodriguez-Montes, A phase I clinical trial of the treatment of Crohn's fistula by adipose mesenchymal stem cell transplantation, *Diseases of the Colon & Rectum*, 48 (2005) 1416-1423.
- [59] E.M. Horwitz, D.J. Prockop, L.A. Fitzpatrick, W.W.K. Koo, P.L. Gordon, M. Neel, M. Sussman, P. Orchard, J.C. Marx, R.E. Pyeritz, M.K. Brenner, Transplantability and therapeutic effects of bone marrow-derived mesenchymal cells in children with osteogenesis imperfecta, *Nature Medicine*, 5 (1999) 309-313.
- [60] X. Wei, X. Yang, Z.P. Han, F.F. Qu, L. Shao, Y.F. Shi, Mesenchymal stem cells: a new trend for cell therapy, *Acta Pharmacologica Sinica*, 34 (2013) 747-754.
- [61] K. Le Blanc, I. Rasmusson, B. Sundberg, C. Gotherstrom, M. Hassan, M. Uzunel, O. Ringden, Treatment of severe acute graft-versus-host disease with third party haploidentical mesenchymal stem cells, *Lancet*, 363 (2004) 1439-1441.

- [62] K. LeBlanc, F. Frassoni, L. Ball, F. Locatelli, H. Roelofs, I. Lewis, E. Lanino, B. Sundberg, M.E. Bernardo, M. Remberger, G. Dini, R.M. Egeler, A. Bacigalupo, W. Fibbe, O. Ringden, M. Dev Committee European Grp Blood, Mesenchymal stem cells for treatment of steroid-resistant, severe, acute graft-versus-host disease: a phase II study, *Lancet*, 371 (2008) 1579-1586.
- [63] F. Baron, R. Storb, Mesenchymal Stromal Cells: A New Tool against Graft-versus-Host Disease?, *Biology of Blood and Marrow Transplantation*, 18 (2012) 822-840.
- [64] R. Ciccocioppo, M.E. Bernardo, A. Sgarella, R. Maccario, M.A. Avanzini, C. Ubezio, A. Minelli, C. Alvisi, A. Vanoli, F. Calliada, P. Dionigi, C. Perotti, F. Locatelli, G.R. Corazza, Autologous bone marrow-derived mesenchymal stromal cells in the treatment of fistulising Crohn's disease, *Gut*, 60 (2011) 788-798.
- [65] G.I.A. MacDonald, A. Augello, C. De Bari, Role of Mesenchymal Stem Cells in Reestablishing Immunologic Tolerance in Autoimmune Rheumatic Diseases, *Arthritis and Rheumatism*, 63 (2011) 2547-2557.
- [66] L.Y. Sun, D.D. Wang, J. Liang, H.Y. Zhang, X.B. Feng, H. Wang, B.Z. Hua, B.J. Liu, S.Q. Ye, X.A. Hu, W.R. Xu, X.F. Zeng, Y.Y. Hou, G.S. Gilkeson, R.M. Silver, L.W. Lu, S.T. Shi, Umbilical Cord Mesenchymal Stem Cell Transplantation in Severe and Refractory Systemic Lupus Erythematosus, *Arthritis and Rheumatism*, 62 (2010) 2467-2475.
- [67] I. Martin, H. Ireland, H. Baldomero, M. Dominici, D.B. Saris, J. Passweg, The Survey on Cellular and Engineered Tissue Therapies in Europe in 2013, *Tissue Engineering Part A*, 22 (2016) 5-16.
- [68] M.K. Mamidi, S. Dutta, R. Bhonde, A.K. Das, R. Pal, Allogeneic and autologous mode of stem cell transplantation in regenerative medicine: Which way to go?, *Medical Hypotheses*, 83 (2014) 787-791.
- [69] T. Lener, M. Gimona, L. Aigner, V. Borger, E. Buzas, G. Camussi, N. Chaput, D. Chatterjee, F.A. Court, H.A. del Portillo, L. O'Driscoll, S. Fais, J.M. Falcon-Perez, U. Felderhoff-Mueser, L. Fraile, Y.S. Gho, A. Gorgens, R.C. Gupta, A. Hendrix, D.M. Hermann, A.F. Hill, F. Hochberg, P.A. Horn, D. de Kleijn, L. Kordelas, B.W. Kramer, E.M. Kramer-Albers, S. Laner-Plamberger, S. Laitinen, T. Leonardi, M.J. Lorenowicz, S.K. Lim, J. Lotvall, C.A. Maguire, A. Marcilla, I. Nazarenko, T. Ochiya, T. Patel, S. Pedersen, G. Pocsfalvi, S.

Pluchino, P. Quesenberry, I.G. Reischl, F.J. Rivera, R. Sanzenbacher, K. Schallmoser, I. Slaper-Cortenbach, D. Strunk, T. Tonn, P. Vader, B.W.M. van Balkom, M. Wauben, S. El Andaloussi, C. Thery, E. Rohde, B. Giebel, Applying extracellular vesicles based therapeutics in clinical trials - an ISEV position paper, *Journal of Extracellular Vesicles*, 4 (2015).

[70] B. Amorin, A.P. Alegretti, V. Valim, A. Pezzi, A.M. Laureano, M.A. Lima da Silva, A. Wieck, L. Silla, Mesenchymal stem cell therapy and acute graft-versus-host disease: a review, *Human Cell*, 27 (2014) 137-150.

[71] J.-F. Li, D.-J. Zhang, T. Geng, L. Chen, H. Huang, H.-L. Yin, Y.-z. Zhang, J.-Y. Lou, B. Cao, Y.-L. Wang, The Potential of Human Umbilical Cord-Derived Mesenchymal Stem Cells as a Novel Cellular Therapy for Multiple Sclerosis, *Cell Transplantation*, 23 (2014) S113-S122.

[72] H.S. Satti, A. Waheed, P. Ahmed, K. Ahmed, Z. Akram, T. Aziz, T.M. Satti, N. Shahbaz, M.A. Khan, S.A. Malik, Autologous mesenchymal stromal cell transplantation for spinal cord injury: A Phase I pilot study, *Cytotherapy*, 18 (2016) 518-522.

[73] F. Mottaghitalab, M. Farokhi, M.A. Shokrgozar, F. Atyabi, H. Hosseinkhani, Silk fibroin nanoparticle as a novel drug delivery system, *Journal of Controlled Release*, 206 (2015) 161-176.

[74] R. Langer, Drug delivery and targeting, *Nature*, 392 (1998) 5-10.

[75] D. Liu, F. Yang, F. Xiong, N. Gu, The Smart Drug Delivery System and Its Clinical Potential, *Theranostics*, 6 (2016) 1306-1323.

[76] M.S. Kim, M.J. Haney, Y. Zhao, V. Mahajan, I. Deygen, N.L. Klyachko, E. Inskoe, A. Piroyan, M. Sokolsky, O. Okolie, S.D. Hingtgen, A.V. Kabanov, E.V. Batrakova, Development of exosome-encapsulated paclitaxel to overcome MDR in cancer cells, *Nanomedicine-Nanotechnology Biology and Medicine*, 12 (2016) 655-664.

[77] R.J.C. Bose, S.H. Lee, H. Park, Biofunctionalized nanoparticles: an emerging drug delivery platform for various disease treatments, *Drug Discovery Today*, 21 (2016) 1303-1312.

[78] A. El-Ansary, S. Al-Daihan, On the toxicity of therapeutically used nanoparticles: an overview, *Journal of toxicology*, 2009 (2009) 754810-754810.

- [79] L.A.L. Fliervoet, E. Mastrobattista, Drug delivery with living cells, *Advanced Drug Delivery Reviews*, 106 (2016) 63-72.
- [80] Z.Q. Cao, G. Zhang, F.L. Wang, H.B. Liu, L. Liu, Y.L. Han, J. Zhang, J.L. Yuan, Protective Effects of Mesenchymal Stem Cells with CXCR4 Up-Regulation in a Rat Renal Transplantation Model, *Plos One*, 8 (2013).
- [81] N.M. Liu, A. Patzak, J.Y. Zhang, CXCR4-overexpressing bone marrow-derived mesenchymal stem cells improve repair of acute kidney injury, *American Journal of Physiology-Renal Physiology*, 305 (2013) F1064-F1073.
- [82] A. Nowakowski, P. Walczak, B. Lukomska, M. Janowski, Genetic Engineering of Mesenchymal Stem Cells to Induce Their Migration and Survival, *Stem Cells International*, (2016).
- [83] O.P.B. Wiklander, J.Z. Nordin, A. O'Loughlin, Y. Gustafsson, G. Corso, I. Maeger, P. Vader, Y. Lee, H. Sork, Y. Seow, N. Heldring, L. Alvarez-Erviti, C.E. Smith, K. Le Blanc, P. Macchiarini, P. Jungebluth, M.J.A. Wood, S. El Andaloussi, Extracellular vesicle in vivo biodistribution is determined by cell source, route of administration and targeting, *Journal of Extracellular Vesicles*, 4 (2015).
- [84] A. De Becker, I.V. Riet, Homing and migration of mesenchymal stromal cells: How to improve the efficacy of cell therapy?, *World journal of stem cells*, 8 (2016) 73-87.
- [85] B. Annabi, Y.T. Lee, S. Turcotte, E. Naud, R.R. Desrosiers, M. Champagne, N. Eliopoulos, J. Galipeau, R. Beliveau, Hypoxia promotes murine bone-marrow-derived stromal cell migration and tube formation, *Stem Cells*, 21 (2003) 337-347.
- [86] D.A. De Ugarte, Z. Alfonso, P.A. Zuk, A. Elbarbary, M. Zhu, P. Ashjian, P. Benhaim, M.H. Hedrick, J.K. Fraser, Differential expression of stem cell mobilization-associated molecules on multi-lineage cells from adipose tissue and bone marrow, *Immunology Letters*, 89 (2003) 267-270.
- [87] D.J. Prockop, "Stemness" does not explain the repair of many tissues by mesenchymal stem/multipotent stromal (MSCs), *Clinical Pharmacology & Therapeutics*, 82 (2007) 241-243.

- [88] B. Bi, R. Schmitt, M. Israilova, H. Nishio, L.G. Cantley, Stromal cells protect against acute tubular injury via an endocrine effect, *Journal of the American Society of Nephrology*, 18 (2007) 2486-2496.
- [89] S. Biagiotti, M.F. Paoletti, A. Fraternali, L. Rossi, M. Magnani, Drug Delivery by Red Blood Cells, *Iubmb Life*, 63 (2011) 621-631.
- [90] K. Shah, Mesenchymal stem cells engineered for cancer therapy, *Advanced Drug Delivery Reviews*, 64 (2012) 739-748.
- [91] A. Mohammadzadeh, A.A. Pourfathollah, S. Shahrokhi, A. Fallah, M.T. Tahoori, A. Amari, M. Forouzandeh, M. Soleimani, Evaluation of AD-MSC (adipose-derived mesenchymal stem cells) as a vehicle for IFN-beta delivery in experimental autoimmune encephalomyelitis, *Clinical Immunology*, 169 (2016) 98-106.
- [92] J.A. Nolte, "Next-generation" mesenchymal stem or stromal cells for the in vivo delivery of bioactive factors: progressing toward the clinic, *Transfusion*, 56 (2016) 15S-17S.
- [93] L.S. Sherman, M. Shaker, V. Mariotti, P. Rameshwar, Mesenchymal stromal/stem cells in drug therapy: New perspective, *Cytotherapy*, (2016).
- [94] A. Nowakowski, K. Drela, J. Rozycka, M. Janowski, B. Lukomska, Engineered Mesenchymal Stem Cells as an Anti-Cancer Trojan Horse, *Stem Cells and Development*, 25 (2016) 1513-1531.
- [95] A. Pessina, A. Bonomi, V. Cocce, G. Invernici, S. Navone, L. Cavicchini, F. Sisto, M. Ferrari, L. Vigano, A. Locatelli, E. Ciusani, G. Cappelletti, D. Cartelli, C. Arnaldo, E. Parati, G. Marfia, R. Pallini, M.L. Falchetti, G. Alessandri, Mesenchymal Stromal Cells Primed with Paclitaxel Provide a New Approach for Cancer Therapy, *Plos One*, 6 (2011).
- [96] A.T. Brini, V. Cocce, L.M.J. Ferreira, C. Giannasi, G. Cossellu, A.B. Gianni, F. Angiero, A. Bonomi, L. Pascucci, M.L. Falchetti, E. Ciusani, G. Bondiolotti, F. Sisto, G. Alessandri, A. Pessina, G. Farronato, Cell-mediated drug delivery by gingival interdental papilla mesenchymal stromal cells (GinPa-MSCs) loaded with paclitaxel, *Expert Opinion on Drug Delivery*, 13 (2016) 789-798.
- [97] A. Bonomi, A. Silini, E. Vertua, P.B. Signoroni, V. Cocce, L. Cavicchini, F. Sisto, G. Alessandri, A. Pessina, O. Parolini, Human amniotic mesenchymal stromal cells (hAMSCs) as

potential vehicles for drug delivery in cancer therapy: an in vitro study, *Stem Cell Research & Therapy*, 6 (2015).

[98] Y. Crawford, I. Kasman, L. Yu, C. Zhong, X. Wu, Z. Modrusan, J. Kaminker, N. Ferrara, PDGF-C Mediates the Angiogenic and Tumorigenic Properties of Fibroblasts Associated with Tumors Refractory to Anti-VEGF Treatment, *Cancer Cell*, 15 (2009) 21-34.

[99] G. Francia, U. Emmenegger, R.S. Kerbel, Tumor-Associated Fibroblasts as "Trojan Horse" Mediators of Resistance to Anti-VEGF Therapy, *Cancer Cell*, 15 (2009) 3-5.

[100] A. Bonomi, V. Sordi, E. Dugnani, V. Ceserani, M. Dossena, V. Cocce, L. Cavicchini, E. Ciusanj, G. Bondiolotti, G. Piovani, L. Pascucci, F. Sisto, G. Alessandri, L. Piemonti, E. Parati, A. Pessina, Gemcitabine-releasing mesenchymal stromal cells inhibit in vitro proliferation of human pancreatic carcinoma cells, *Cytotherapy*, 17 (2015) 1687-1695.

[101] K.L. Song, N. Benhaga, R.L. Anderson, R. Khosravi-Fari, Transduction of tumor necrosis factor-related apoptosis-inducing ligand into hematopoietic cells leads to inhibition of syngeneic tumor growth in vivo, *Cancer Research*, 66 (2006) 6304-6311.

[102] S. Rani, A.E. Ryan, M.D. Griffin, T. Ritter, Mesenchymal Stem Cell-derived Extracellular Vesicles: Toward Cell-free Therapeutic Applications, *Molecular Therapy*, 23 (2015) 812-823.

[103] G. Raposo, W. Stoorvogel, Extracellular vesicles: Exosomes, microvesicles, and friends, *Journal of Cell Biology*, 200 (2013) 373-383.

[104] E. Chargaff, R. West, The biological significance of the thromboplastic protein of blood, *The Journal of biological chemistry*, 166 (1946) 189-197.

[105] P. Wolf, The nature and significance of platelet products in human plasma, *British journal of haematology*, 13 (1967) 269-288.

[106] P. Vader, E.A. Mol, G. Pasterkamp, R.M. Schiffelers, Extracellular vesicles for drug delivery, *Advanced Drug Delivery Reviews*, 106 (2016) 148-156.

[107] M.A. Lopez-Verrilli, F.A. Court, Exosomes: mediators of communication in eukaryotes, *Biological Research*, 46 (2013) 5-11.

- [108] Y. Ogawa, Y. Miura, A. Harazono, M. Kanai-Azuma, Y. Akimoto, H. Kawakami, T. Yamaguchi, T. Toda, T. Endo, M. Tsubuki, R. Yanoshita, Proteomic Analysis of Two Types of Exosomes in Human Whole Saliva, *Biological & Pharmaceutical Bulletin*, 34 (2011) 13-23.
- [109] F. Royo, P. Zuniga-Garcia, V. Torrano, A. Loizaga, P. Sanchez-Mosquera, A. Ugalde-Olano, E. Gonzalez, A.R. Cortazar, L. Palomo, S. Fernandez-Ruiz, I. Lacasa-Viscasillas, M. Berdasco, J.D. Sutherland, R. Barrio, A. Zabala-Letona, N. Martin-Martin, A. Arruabarrena-Aristorena, L. Valcarcel-Jimenez, A. Caro-Maldonado, J. Gonzalez-Tampan, G. Cachi-Fuentes, M. Esteller, A.M. Aransay, M. Unda, J.M. Falcon-Perez, A. Carracedo, Transcriptomic profiling of urine extracellular vesicles reveals alterations of CDH3 in prostate cancer, *Oncotarget*, 7 (2016) 6835-6846.
- [110] A.J. Tompkins, D. Chatterjee, M. Maddox, J. Wang, E. Arciero, G. Camussi, P.J. Quesenberry, J.F. Renzulli, The emergence of extracellular vesicles in urology: fertility, cancer, biomarkers and targeted pharmacotherapy, *Journal of Extracellular Vesicles*, 4 (2015).
- [111] M.I. Zonneveld, A.R. Brisson, M.J.C. van Herwijnen, S. Tan, C.H.A. van de Lest, F.A. Redegeld, J. Garssen, M.H.M. Wauben, E.N.M. Nolte-'t Hoen, Recovery of extracellular vesicles from human breast milk is influenced by sample collection and vesicle isolation procedures, *Journal of extracellular vesicles*, 3 (2014).
- [112] C. Admyre, S.M. Johansson, K.R. Qazi, J.J. Filen, R. Lahesmaa, M. Norman, E.P.A. Neve, A. Scheynius, S. Gabrielsson, Exosomes with immune modulatory features are present in human breast milk, *Journal of Immunology*, 179 (2007) 1969-1978.
- [113] E.I. Buzas, B. Gyorgy, G. Nagy, A. Falus, S. Gay, Emerging role of extracellular vesicles in inflammatory diseases, *Nature Reviews Rheumatology*, 10 (2014) 356-364.
- [114] A.I. Masyuk, B.Q. Huang, C.J. Ward, S.A. Gradilone, J.M. Banales, T.V. Masyuk, B. Radtke, P.L. Splinter, N.F. LaRusso, Biliary exosomes influence cholangiocyte regulatory mechanisms and proliferation through interaction with primary cilia, *American Journal of Physiology-Gastrointestinal and Liver Physiology*, 299 (2010) G990-G999.
- [115] S. Keller, J. Ridinger, A.K. Rupp, J.W.G. Janssen, P. Altevogt, Body fluid derived exosomes as a novel template for clinical diagnostics, *Journal of Translational Medicine*, 9 (2011).

- [116] J.M. Street, P.E. Barran, C.L. Mackay, S. Weidt, C. Balmforth, T.S. Walsh, R.T.A. Chalmers, D.J. Webb, J.W. Dear, Identification and proteomic profiling of exosomes in human cerebrospinal fluid, *Journal of Translational Medicine*, 10 (2012).
- [117] L.J. Vella, R.A. Sharples, V.A. Lawson, C.L. Masters, R. Cappai, A.F. Hill, Packaging of prions into exosomes is associated with a novel pathway of PrP processing, *Journal of Pathology*, 211 (2007) 582-590.
- [118] J.M. Silverman, N.E. Reiner, Exosomes and other microvesicles in infection biology: organelles with unanticipated phenotypes, *Cellular Microbiology*, 13 (2011) 1-9.
- [119] T.N. Ellis, M.J. Kuehn, Virulence and Immunomodulatory Roles of Bacterial Outer Membrane Vesicles, *Microbiology and Molecular Biology Reviews*, 74 (2010) 81-+.
- [120] J. Lotvall, A.F. Hill, F. Hochberg, E.I. Buzas, D. Di Vizio, C. Gardiner, Y.S. Gho, I.V. Kurochkin, S. Mathivanan, P. Quesenberry, S. Sahoo, H. Tahara, M.H. Wauben, K.W. Witwer, C. Thery, Minimal experimental requirements for definition of extracellular vesicles and their functions: a position statement from the International Society for Extracellular Vesicles, *Journal of extracellular vesicles*, 3 (2014) 26913-26913.
- [121] M. Kanada, M.H. Bachmann, J.W. Hardy, D.O. Frimansson, L. Bronsart, A. Wang, M.D. Sylvester, T.L. Schmidt, R.L. Kaspar, M.J. Butte, A.C. Matin, C.H. Contag, Differential fates of biomolecules delivered to target cells via extracellular vesicles, *Proceedings of the National Academy of Sciences of the United States of America*, 112 (2015) E1433-E1442.
- [122] C. Corcoran, A.M. Friel, M.J. Duffy, J. Crown, L. O'Driscoll, Intracellular and Extracellular MicroRNAs in Breast Cancer, *Clinical Chemistry*, 57 (2011) 18-32.
- [123] J. Nilsson, J. Skog, A. Nordstrand, V. Baranov, L. Mincheva-Nilsson, X.O. Breakefield, A. Widmark, Prostate cancer-derived urine exosomes: a novel approach to biomarkers for prostate cancer, *British Journal of Cancer*, 100 (2009) 1603-1607.
- [124] C. Tetta, E. Ghigo, L. Silengo, M.C. Deregibus, G. Camussi, Extracellular vesicles as an emerging mechanism of cell-to-cell communication, *Endocrine*, 44 (2013) 11-19.
- [125] N. Chaput, C. Thery, Exosomes: immune properties and potential clinical implementations, *Seminars in Immunopathology*, 33 (2011) 419-440.

- [126] A. Lo Cicero, P.D. Stahl, G. Raposo, Extracellular vesicles shuffling intercellular messages: for good or for bad, *Current Opinion in Cell Biology*, 35 (2015) 69-77.
- [127] E.T. Fertig, M. Gherghiceanu, L.M. Popescu, Extracellular vesicles release by cardiac telocytes: electron microscopy and electron tomography, *Journal of Cellular and Molecular Medicine*, 18 (2014) 1938-1943.
- [128] L. Pascucci, C. Dall'Aglio, C. Bazzucchi, F. Mercati, M.G. Mancini, A. Pessina, G. Alessandri, M. Giammarioli, S. Dante, G. Brunati, P. Ceccarelli, Horse adipose-derived mesenchymal stromal cells constitutively produce membrane vesicles: a morphological study, *Histology and Histopathology*, 30 (2015) 549-557.
- [129] C. Junquera, T. Castiella, G. Munoz, R. Fernandez-Pacheco, M. Jose Luesma, M. Monzon, Biogenesis of a new type of extracellular vesicles in gastrointestinal stromal tumors: ultrastructural profiles of spherosomes, *Histochemistry and Cell Biology*, 146 (2016) 557-567.
- [130] E. Willms, H.J. Johansson, I. Mager, Y. Lee, K.E.M. Blomberg, M. Sadik, A. Alaarg, C.I.E. Smith, J. Lehtio, S.E.L. Andaloussi, M.J.A. Wood, P. Vader, Cells release subpopulations of exosomes with distinct molecular and biological properties, *Scientific Reports*, 6 (2016).
- [131] J. Kowal, G. Arras, M. Colombo, M. Jouve, J.P. Morath, B. Primdal-Bengtson, F. Dingli, D. Loew, M. Tkach, C. Thery, Proteomic comparison defines novel markers to characterize heterogeneous populations of extracellular vesicle subtypes, *Proceedings of the National Academy of Sciences of the United States of America*, 113 (2016) E968-E977.
- [132] R.M. Johnstone, Revisiting the road to the discovery of exosomes, *Blood Cells Molecules and Diseases*, 34 (2005) 214-219.
- [133] B.T. Pan, R.M. Johnstone, Fate of the transferrin receptor during maturation of sheep reticulocytes in vitro: selective externalization of the receptor, *Cell*, 33 (1983) 967-978.
- [134] Z. Andreu, M. Yanez-Mo, Tetraspanins in extracellular vesicle formation and function, *Frontiers in Immunology*, 5 (2015).
- [135] S.S. Tan, Y. Yin, T. Lee, R.C. Lai, R.W.Y. Yeo, B. Zhang, A. Choo, S.K. Lim, Therapeutic MSC exosomes are derived from lipid raft microdomains in the plasma membrane, *Journal of extracellular vesicles*, 2 (2013).

- [136] S.A. Melo, L.B. Luecke, C. Kahlert, A.F. Fernandez, S.T. Gammon, J. Kaye, V.S. LeBleu, E.A. Mittendorf, J. Weitz, N. Rahbari, C. Reissfelder, C. Pilarsky, M.F. Fraga, D. Piwnica-Worms, R. Kalluri, Glypican-1 identifies cancer exosomes and detects early pancreatic cancer, *Nature*, 523 (2015) 177-U182.
- [137] J. De Toro, L. Herschlik, C. Waldner, C. Mongini, Emerging roles of exosomes in normal and pathological conditions: new insights for diagnosis and therapeutic applications, *Frontiers in Immunology*, 6 (2015).
- [138] M. Kotmakci, V.B. Cetintas, Extracellular Vesicles as Natural Nanosized Delivery Systems for Small-Molecule Drugs and Genetic Material: Steps towards the Future Nanomedicines, *Journal of Pharmacy and Pharmaceutical Sciences*, 18 (2015) 396-413.
- [139] J. Stephen, E.L. Bravo, D. Colligan, A.R. Fraser, J. Petrik, J.D.M. Campbell, Mesenchymal stromal cells as multifunctional cellular therapeutics - a potential role for extracellular vesicles, *Transfusion and Apheresis Science*, 55 (2016) 62-69.
- [140] C. Junquera, T. Castiella, G. Munoz, R. Fernandez-Pacheco, M.J. Luesma, M. Monzon, Biogenesis of a new type of extracellular vesicles in gastrointestinal stromal tumors: ultrastructural profiles of spherosomes, *Histochemistry and Cell Biology*, 146 (2016) 557-567.
- [141] H.G. Lamparski, A. Metha-Damani, J.Y. Yao, S. Patel, D.H. Hsu, C. Ruegg, J.B. Le Pecq, Production and characterization of clinical grade exosomes derived from dendritic cells, *Journal of Immunological Methods*, 270 (2002) 211-226.
- [142] R. Grant, E. Ansa-Addo, D. Stratton, S. Antwi-Baffour, S. Jorfi, S. Kholia, L. Krige, S. Lange, J. Inal, A filtration-based protocol to isolate human Plasma Membrane-derived Vesicles and exosomes from blood plasma, *Journal of Immunological Methods*, 371 (2011) 143-151.
- [143] R. Linares, S. Tan, C. Gounou, N. Arraud, A.R. Brisson, High-speed centrifugation induces aggregation of extracellular vesicles, *Journal of Extracellular Vesicles*, 4 (2015).
- [144] J.Z. Nordin, Y. Lee, P. Vader, I. Maeger, H.J. Johansson, W. Heusermann, O.P.B. Wiklander, M. Hallbrink, Y. Seow, J.J. Bultema, J. Gilthorpe, T. Davies, P.J. Fairchild, S. Gabrielsson, N.C. Meisner-Kober, J. Lehtio, C.I.E. Smith, M.J.A. Wood, S.E.L. Andaloussi, Ultrafiltration with size-exclusion liquid chromatography for high yield isolation of

extracellular vesicles preserving intact biophysical and functional properties, *Nanomedicine-Nanotechnology Biology and Medicine*, 11 (2015) 879-883.

[145] V. Luga, L. Zhang, A.M. Vilorio-Petit, A.A. Ogunjimi, M.R. Inanlou, E. Chiu, M. Buchanan, A.N. Hosein, M. Basik, J.L. Wrana, Exosomes Mediate Stromal Mobilization of Autocrine Wnt-PCP Signaling in Breast Cancer Cell Migration, *Cell*, 151 (2012) 1542-1556.

[146] P. Li, M. Kaslan, S.H. Lee, J. Yao, Z. Gao, Progress in Exosome Isolation Techniques, *Theranostics*, 7 (2017) 789-804.

[147] D.D. Taylor, S. Shah, Methods of isolating extracellular vesicles impact down-stream analyses of their cargoes, *Methods*, 87 (2015) 3-10.

[148] D.S. Choi, D.K. Kim, Y.K. Kim, Y.S. Gho, Proteomics, transcriptomics and lipidomics of exosomes and ectosomes, *Proteomics*, 13 (2013) 1554-1571.

[149] R.A. Haraszti, M.C. Didiot, E. Sapp, J. Leszyk, S.A. Shaffer, H.E. Rockwell, F. Gao, N.R. Narain, M. DiFiglia, M.A. Kiebish, N. Aronin, A. Khvorova, High-resolution proteomic and lipidomic analysis of exosomes and microvesicles from different cell sources, *Journal of Extracellular Vesicles*, 5 (2016).

[150] A. Marote, F.G. Teixeira, B. Mendes-Pinheiro, A.J. Salgado, MSCs-Derived Exosomes: Cell-Secreted Nanovesicles with Regenerative Potential, *Frontiers in Pharmacology*, 7 (2016).

[151] G. Turturici, R. Tinnirello, G. Sconzo, F. Geraci, Extracellular membrane vesicles as a mechanism of cell-to-cell communication: advantages and disadvantages, *American Journal of Physiology-Cell Physiology*, 306 (2014) C621-C633.

[152] O.G. De Jong, B.W.M. Van Balkom, R.M. Schiffelere, C.V.C. Bouten, M.C. Verhaar, Extracellular vesicles: potential roles in regenerative medicine, *Frontiers in Immunology*, 5 (2014) 1-13.

[153] I. Parolini, C. Federici, C. Raggi, L. Lugini, S. Palleschi, A. De Milito, C. Coscia, E. Iessi, M. Logozzi, A. Molinari, M. Colone, M. Tatti, M. Sargiacomo, S. Fais, Microenvironmental pH Is a Key Factor for Exosome Traffic in Tumor Cells, *Journal of Biological Chemistry*, 284 (2009) 34211-34222.

- [154] M. Mack, A. Kleinschmidt, H. Bruhl, C. Klier, P.J. Nelson, J. Cihak, J. Plachy, M. Stangassinger, V. Erfle, D. Schlondorff, Transfer of the chemokine receptor CCR5 between cells by membrane-derived microparticles: A mechanism for cellular human immunodeficiency virus 1 infection, *Nature Medicine*, 6 (2000) 769-+.
- [155] A. Sarkar, S. Mitra, S. Mehta, R. Raices, M.D. Wewers, Monocyte Derived Microvesicles Deliver a Cell Death Message via Encapsulated Caspase-1, *Plos One*, 4 (2009).
- [156] G. Taraboletti, S. D'Ascenzo, I. Giusti, D. Marchetti, P. Borsotti, D. Millimaggi, R. Giavazzi, A. Pavan, V. Dolo, Bioavailability of VEGF in tumor-shed vesicles depends on vesicle burst induced by acidic pH, *Neoplasia*, 8 (2006) 96-103.
- [157] J. Ratajczak, K. Miekus, M. Kucia, J. Zhang, R. Reca, P. Dvorak, M.Z. Ratajczak, Embryonic stem cell-derived microvesicles reprogram hematopoietic progenitors: evidence for horizontal transfer of mRNA and protein delivery, *Leukemia*, 20 (2006) 847-856.
- [158] M. Yanez-Mo, P.R.M. Siljander, Z. Andreu, A.B. Zavec, F.E. Borrás, E.I. Buzas, K. Buzas, E. Casal, F. Cappello, J. Carvalho, E. Colas, A. Cordeiro-da Silva, S. Fais, J.M. Falcon-Perez, I.M. Ghobrial, B. Giebel, M. Gimona, M. Graner, I. Gursel, M. Gursel, N.H.H. Heegaard, A. Hendrix, P. Kierulf, K. Kokubun, M. Kosanovic, V. Kralj-Iglic, E.M. Kramer-Albers, S. Laitinen, C. Lasser, T. Lener, E. Ligeti, A. Line, G. Lipps, A. Llorente, J. Lotvall, M. Mancek-Keber, A. Marcilla, M. Mittelbrunn, I. Nazarenko, E.N.M. Nolte-t' Hoen, T.A. Nyman, L. O'Driscoll, M. Olivan, C. Oliveira, E. Pallinger, H.A. del Portillo, J. Reventos, M. Rigau, E. Rohde, M. Sammar, F. Sanchez-Madrid, N. Santarem, K. Schallmoser, M.S. Ostendorf, W. Stoorvogel, R. Stukelj, S.G. Van der Grein, M.H. Vasconcelos, M.H.M. Wauben, O. De Wever, Biological properties of extracellular vesicles and their physiological functions, *Journal of Extracellular Vesicles*, 4 (2015).
- [159] B. Escudier, T. Dorval, N. Chaput, F. Andre, M.P. Caby, S. Novault, C. Flament, C. Leboulleire, C. Borg, S. Amigorena, C. Boccaccio, C. Bonnerot, O. Dhellin, M. Movassagh, S. Piperno, C. Robert, V. Serra, N. Valente, J.B. Le Pecq, A. Spatz, O. Lantz, T. Tursz, E. Angevin, L. Zitvogel, Vaccination of metastatic melanoma patients with autologous dendritic cell (DC) derived-exosomes: results of the first phase I clinical trial, *Journal of Translational Medicine*, 3 (2005).

- [160] M.A. Morse, J. Garst, T. Osada, S. Khan, A. Hobeika, T.M. Clay, N. Valente, R. Shreeniwas, M.A. Sutton, A. Delcayre, D.H. Hsu, J.B. Le Pecq, H.K. Lyerly, A phase I study of dexosome immunotherapy in patients with advanced non-small cell lung cancer, *Journal of Translational Medicine*, 3 (2005).
- [161] S. Dai, D. Wei, Z. Wu, X. Zhou, X. Wei, H. Huang, G. Li, Phase I clinical trial of autologous ascites-derived exosomes combined with GM-CSF for colorectal cancer, *Molecular Therapy*, 16 (2008) 782-790.
- [162] L. Lugini, S. Cecchetti, V. Huber, F. Luciani, G. Macchia, F. Spadaro, L. Paris, L. Abalsamo, M. Colone, A. Molinari, F. Podo, L. Rivoltini, C. Ramoni, S. Fais, Immune Surveillance Properties of Human NK Cell-Derived Exosomes, *Journal of Immunology*, 189 (2012) 2833-2842.
- [163] J.M. Gudbergsson, K.B. Johnsen, M.N. Skov, M. Duroux, Systematic review of factors influencing extracellular vesicle yield from cell cultures, *Cytotechnology*, 68 (2016) 579-592.
- [164] M. Gnechi, H.M. He, N. Noiseux, O.D. Liang, L.M. Zhang, F. Morello, H. Mu, L.G. Melo, R.E. Pratt, J.S. Ingwall, V.J. Dzau, Evidence supporting paracrine hypothesis for Akt-modified mesenchymal stem cell-mediated cardiac protection and functional improvement, *Faseb Journal*, 20 (2006) 661-669.
- [165] X. Teng, L. Chen, W. Chen, J. Yang, Z. Yang, Z. Shen, Mesenchymal Stem Cell-Derived Exosomes Improve the Microenvironment of Infarcted Myocardium Contributing to Angiogenesis and Anti-Inflammation, *Cellular Physiology and Biochemistry*, 37 (2015) 2415-2424.
- [166] A.I. Caplan, J.E. Dennis, Mesenchymal stem cells as trophic mediators, *Journal of Cellular Biochemistry*, 98 (2006) 1076-1084.
- [167] M. Gnechi, H.M. He, O.D. Liang, L.G. Melo, F. Morello, H. Mu, N. Noiseux, L.N. Zhang, R.E. Pratt, J.S. Ingwall, V.J. Dzau, Paracrine action accounts for marked protection of ischemic heart by Akt-modified mesenchymal stem cells, *Nature Medicine*, 11 (2005) 367-368.
- [168] S.M.G. Fouraschen, Q.W. Pan, P.E. de Ruiter, W.R.R. Farid, G. Kazemier, J. Kwekkeboom, J.N.M. Ijzermans, H.J. Metselaar, H.W. Tilanus, J. de Jonge, L.J.W. van der Laan, Secreted Factors of Human Liver-Derived Mesenchymal Stem Cells Promote Liver

Regeneration Early After Partial Hepatectomy, *Stem Cells and Development*, 21 (2012) 2410-2419.

[169] B. Zhang, X.D. Wu, X. Zhang, Y.X. Sun, Y.M. Yan, H. Shi, Y.H. Zhu, L.J. Wu, Z.J. Pan, W. Zhu, H. Qian, W.R. Xu, Human Umbilical Cord Mesenchymal Stem Cell Exosomes Enhance Angiogenesis Through the Wnt4/beta-Catenin Pathway, *Stem Cells Translational Medicine*, 4 (2015) 513-522.

[170] F.G. Teixeira, M.M. Carvalho, N. Sousa, A.J. Salgado, Mesenchymal stem cells secretome: a new paradigm for central nervous system regeneration?, *Cellular and Molecular Life Sciences*, 70 (2013) 3871-3882.

[171] H.Q. Xin, Y. Li, B. Buller, M. Katakowski, Y. Zhang, X.L. Wang, X. Shang, Z.G. Zhang, M. Chopp, Exosome-Mediated Transfer of miR-133b from Multipotent Mesenchymal Stromal Cells to Neural Cells Contributes to Neurite Outgrowth, *Stem Cells*, 30 (2012) 1556-1564.

[172] M. Budoni, A. Fierabracci, R. Luciano, S. Petrini, V. Di Ciommo, M. Muraca, The Immunosuppressive Effect of Mesenchymal Stromal Cells on B Lymphocytes Is Mediated by Membrane Vesicles, *Cell Transplantation*, 22 (2013) 369-379.

[173] A. Del Fattore, R. Luciano, L. Pascucci, B.M. Goffredo, E. Giorda, M. Scapaticci, A. Fierabracci, M. Muraca, Immunoregulatory Effects of Mesenchymal Stem Cell-Derived Extracellular Vesicles on T Lymphocytes, *Cell Transplantation*, 24 (2015) 2615-2627.

[174] M. Di Trapani, G. Bassi, M. Midolo, A. Gatti, P.T. Kanga, A. Cassaro, R. Carusone, A. Adamo, M. Krampera, Differential and transferable modulatory effects of mesenchymal stromal cell-derived extracellular vesicles on T, B and NK cell functions, *Scientific Reports*, 6 (2016).

[175] L. Kordelas, V. Rebmann, A.K. Ludwig, S. Radtke, J. Ruesing, T.R. Doeppner, M. Epple, P.A. Horn, D.W. Beelen, B. Giebel, MSC-derived exosomes: a novel tool to treat therapy-refractory graft-versus-host disease, *Leukemia*, 28 (2014) 970-973.

[176] S. Ohno, G.P.C. Drummen, M. Kuroda, Focus on Extracellular Vesicles: Development of Extracellular Vesicle-Based Therapeutic Systems, *International Journal of Molecular Sciences*, 17 (2016).

- [177] H.R. Hofer, R.S. Tuan, Secreted trophic factors of mesenchymal stem cells support neurovascular and musculoskeletal therapies, *Stem Cell Research & Therapy*, 7 (2016).
- [178] S. Bruno, S. Porta, B. Bussolati, Extracellular vesicles in renal tissue damage and regeneration, *European Journal of Pharmacology*, 790 (2016) 83-91.
- [179] S. Rani, T. Ritter, The Exosome - A Naturally Secreted Nanoparticle and its Application to Wound Healing, *Advanced Materials*, 28 (2016) 5542-5552.
- [180] C.-H. Wang, W.-J. Cherng, S. Verma, Drawbacks to stem cell therapy in cardiovascular diseases, *Future cardiology*, 4 (2008) 399-408.
- [181] V. Combes, A.C. Simon, G.E. Grau, D. Arnoux, L. Camoin, F. Sabatier, M. Mutin, M. Sanmarco, J. Sampol, F. Dignat-George, In vitro generation of endothelial microparticles and possible prothrombotic activity in patients with lupus anticoagulant, *Journal of Clinical Investigation*, 104 (1999) 93-102.
- [182] A. Akbarzadeh, R. Rezaei-Sadabady, S. Davaran, S.W. Joo, N. Zarghami, Y. Hanifehpour, M. Samiei, M. Kouhi, K. Nejati-Koshki, Liposome: classification, preparation, and applications, *Nanoscale Research Letters*, 8 (2013).
- [183] P. Yingchoncharoen, D.S. Kalinowski, D.R. Richardson, Lipid-Based Drug Delivery Systems in Cancer Therapy: What Is Available and What Is Yet to Come, *Pharmacological Reviews*, 68 (2016) 701-787.
- [184] H.E. Gendelman, V. Anantharam, T. Bronich, S. Ghaisas, H. Jin, A.G. Kanthasamy, X. Liu, J. McMillan, R.L. Mosley, B. Narasimhan, S.K. Mallapragada, Nanoneuromedicines for degenerative, inflammatory, and infectious nervous system diseases, *Nanomedicine-Nanotechnology Biology and Medicine*, 11 (2015) 751-767.
- [185] S.E. Krown, D.W. Northfelt, D. Osoba, J.S. Stewart, Use of liposomal anthracyclines in Kaposi's sarcoma, *Seminars in Oncology*, 31 (2004) 36-52.
- [186] H.I. Chang, M.K. Yeh, Clinical development of liposome-based drugs: formulation, characterization, and therapeutic efficacy, *International Journal of Nanomedicine*, 7 (2012) 49-60.

- [187] J.O. Eloy, M.C. de Souza, R. Petrilli, J.P. Abriata Barcellos, R.J. Lee, J.M. Marchetti, Liposomes as carriers of hydrophilic small molecule drugs: Strategies to enhance encapsulation and delivery, *Colloids and Surfaces B-Biointerfaces*, 123 (2014) 345-363.
- [188] G. Bozzuto, A. Molinari, Liposomes as nanomedical devices, *International Journal of Nanomedicine*, 10 (2015) 975-999.
- [189] S. Li, X.A. Gao, K.G. Son, F. Sorigi, H. Hofland, L. Huang, DC-Chol lipid system in gene transfer, *Journal of Controlled Release*, 39 (1996) 373-381.
- [190] L. Sercombe, T. Veerati, F. Moheimani, S.Y. Wu, A.K. Sood, S. Hua, Advances and Challenges of Liposome Assisted Drug Delivery, *Frontiers in Pharmacology*, 6 (2015).
- [191] Z.S. Bayindir, N. Yuksel, Provesicles as Novel Drug Delivery Systems, *Current Pharmaceutical Biotechnology*, 16 (2015) 344-364.
- [192] R. van der Meel, M.H.A.M. Fens, P. Vader, W.W. van Solinge, O. Eniola-Adefeso, R.M. Schiffelers, Extracellular vesicles as drug delivery systems: Lessons from the liposome field, *Journal of Controlled Release*, 195 (2014) 72-85.
- [193] J.S. Suk, Q.G. Xu, N. Kim, J. Hanes, L.M. Ensign, PEGylation as a strategy for improving nanoparticle-based drug and gene delivery, *Advanced Drug Delivery Reviews*, 99 (2016) 28-51.
- [194] S. Ohno, M. Takanashi, K. Sudo, S. Ueda, A. Ishikawa, N. Matsuyama, K. Fujita, T. Mizutani, T. Ohgi, T. Ochiya, N. Gotoh, M. Kuroda, Systemically Injected Exosomes Targeted to EGFR Deliver Antitumor MicroRNA to Breast Cancer Cells, *Molecular Therapy*, 21 (2013) 185-191.
- [195] S. El-Andaloussi, Y. Lee, S. Lakhali-Littleton, J.H. Li, Y. Seow, C. Gardiner, L. Alvarez-Erviti, I.L. Sargent, M.J.A. Wood, Exosome-mediated delivery of siRNA in vitro and in vivo, *Nature Protocols*, 7 (2012) 2112-2126.
- [196] X.Y. Zhuang, X.Y. Xiang, W. Grizzle, D.M. Sun, S.Q. Zhang, R.C. Axtell, S.W. Ju, J.Y. Mu, L.F. Zhang, L. Steinman, D. Miller, H.G. Zhang, Treatment of Brain Inflammatory Diseases by Delivering Exosome Encapsulated Anti-inflammatory Drugs From the Nasal Region to the Brain, *Molecular Therapy*, 19 (2011) 1769-1779.

- [197] L. Alvarez-Erviti, Y.Q. Seow, H.F. Yin, C. Betts, S. Lakhali, M.J.A. Wood, Delivery of siRNA to the mouse brain by systemic injection of targeted exosomes, *Nature Biotechnology*, 29 (2011) 341-U179.
- [198] S.A.A. Kooijmans, P. Vader, S.M. van Dommelen, W.W. van Solinge, R.M. Schiffelers, Exosome mimetics: a novel class of drug delivery systems, *International Journal of Nanomedicine*, 7 (2012) 1525-1541.
- [199] C. Grange, M. Tapparo, S. Bruno, D. Chatterjee, P.J. Quesenberry, C. Tetta, G. Camussi, Biodistribution of mesenchymal stem cell-derived extracellular vesicles in a model of acute kidney injury monitored by optical imaging, *International Journal of Molecular Medicine*, 33 (2014) 1055-1063.
- [200] B. Gyorgy, M.E. Hung, X.O. Breakefield, J.N. Leonard, Therapeutic Applications of Extracellular Vesicles: Clinical Promise and Open Questions, *Annual Review of Pharmacology and Toxicology*, Vol 55, 55 (2015) 439-464.
- [201] D. Ha, N. Yang, V. Nadihe, Exosomes as therapeutic drug carriers and delivery vehicles across biological membranes: current perspectives and future challenges, *Acta Pharmaceutica Sinica B*, 6 (2016) 287-296.
- [202] D. Zocco, P. Ferruzzi, F. Cappello, W.P. Kuo, S. Fais, Extracellular vesicles as shuttles of tumor biomarkers and anti-tumor drugs, *Frontiers in oncology*, 4 (2014) 267-267.
- [203] D.S. Sutaria, M. Badawi, M.A. Phelps, T.D. Schmittgen, Achieving the Promise of Therapeutic Extracellular Vesicles: The Devil is in Details of Therapeutic Loading, *Pharmaceutical Research*, 34 (2017) 1053-1066.
- [204] E.V. Batrakova, M.S. Kim, Using exosomes, naturally-equipped nanocarriers, for drug delivery, *Journal of Controlled Release*, 219 (2015) 396-405.
- [205] M.E. Hung, J.N. Leonard, Stabilization of Exosome-targeting Peptides via Engineered Glycosylation, *Journal of Biological Chemistry*, 290 (2015) 8166-8172.
- [206] Y.L. Zhao, M.J. Haney, R. Gupta, J.P. Bohnsack, Z.J. He, A.V. Kabanov, E.V. Batrakova, GDNF-Transfected Macrophages Produce Potent Neuroprotective Effects in Parkinson's Disease Mouse Model, *Plos One*, 9 (2014).

- [207] N. Kosaka, H. Iguchi, Y. Yoshioka, F. Takeshita, Y. Matsuki, T. Ochiya, Secretory Mechanisms and Intercellular Transfer of MicroRNAs in Living Cells, *Journal of Biological Chemistry*, 285 (2010) 17442-17452.
- [208] L. Pascucci, V. Cocce, A. Bonomi, D. Ami, P. Ceccarelli, E. Ciusani, L. Vigano, A. Locatelli, F. Sisto, S.M. Doglia, E. Parati, M.E. Bernardo, M. Muraca, G. Alessandri, G. Bondiolotti, A. Pessina, Paclitaxel is incorporated by mesenchymal stromal cells and released in exosomes that inhibit in vitro tumor growth: A new approach for drug delivery, *Journal of Controlled Release*, 192 (2014) 262-270.
- [209] A. Del Fattore, R. Luciano, R. Saracino, G. Battafarano, C. Rizzo, L. Pascucci, G. Alessandri, A. Pessina, A. Perrotta, A. Fierabracci, M. Muraca, Differential effects of extracellular vesicles secreted by mesenchymal stem cells from different sources on glioblastoma cells, *Expert Opinion on Biological Therapy*, 15 (2015) 495-504.
- [210] K. Tang, Y. Zhang, H.F. Zhang, P.W. Xu, J. Liu, J.W. Ma, M. Lv, D.P. Li, F. Katirai, G.X. Shen, G.M. Zhang, Z.H. Feng, D.Y. Ye, B. Huang, Delivery of chemotherapeutic drugs in tumour cell-derived microparticles, *Nature Communications*, 3 (2012).
- [211] Y.H. Tian, S.P. Li, J. Song, T.J. Ji, M.T. Zhu, G.J. Anderson, J.Y. Wei, G.J. Nie, A doxorubicin delivery platform using engineered natural membrane vesicle exosomes for targeted tumor therapy, *Biomaterials*, 35 (2014) 2383-2390.
- [212] C. Federici, F. Petrucci, S. Caimi, A. Cesolini, M. Logozzi, M. Borghi, S. D'Illo, L. Lugini, N. Violante, T. Azzarito, C. Majorani, D. Brambilla, S. Fais, Exosome Release and Low pH Belong to a Framework of Resistance of Human Melanoma Cells to Cisplatin, *Plos One*, 9 (2014).
- [213] D.M. Sun, X.Y. Zhuang, X.Y. Xiang, Y.L. Liu, S.Y. Zhang, C.R. Liu, S. Barnes, W. Grizzle, D. Miller, H.G. Zhang, A Novel Nanoparticle Drug Delivery System: The Anti-inflammatory Activity of Curcumin Is Enhanced When Encapsulated in Exosomes, *Molecular Therapy*, 18 (2010) 1606-1614.
- [214] S.A.A. Kooijmans, S. Stremersch, K. Braeckmans, S.C. de Smedt, A. Hendrix, M.J.A. Wood, R.M. Schiffelers, K. Raemdonck, P. Vader, Electroporation-induced siRNA precipitation obscures the efficiency of siRNA loading into extracellular vesicles, *Journal of Controlled Release*, 172 (2013) 229-238.

- [215] J.L. Hood, M.J. Scott, S.A. Wickline, Maximizing exosome colloidal stability following electroporation, *Analytical Biochemistry*, 448 (2014) 41-49.
- [216] J. Wahlgren, T.D. Karlson, M. Brisslert, F.V. Sani, E. Telemo, P. Sunnerhagen, H. Valadi, Plasma exosomes can deliver exogenous short interfering RNA to monocytes and lymphocytes, *Nucleic Acids Research*, 40 (2012).
- [217] M.J. Haney, N.L. Klyachko, Y.L. Zhaoa, R. Gupta, E.G. Plotnikova, Z.J. He, T. Patel, A. Piroyan, M. Sokolsky, A.V. Kabanov, E.V. Batrakova, Exosomes as drug delivery vehicles for Parkinson's disease therapy, *Journal of Controlled Release*, 207 (2015) 18-30.
- [218] S.A.A. Kooijmans, L.A.L. Fliervoet, R. van der Meel, M. Fens, H.F.G. Heijnen, P. Henegouwen, P. Vader, R.M. Schiffelers, PEGylated and targeted extracellular vesicles display enhanced cell specificity and circulation time, *Journal of Controlled Release*, 224 (2016) 77-85.
- [219] T.H. Lee, E. D'Asti, N. Magnus, K. Al-Nedawi, B. Meehan, J. Rak, Microvesicles as mediators of intercellular communication in cancer-the emerging science of cellular 'debris', *Seminars in Immunopathology*, 33 (2011) 455-467.
- [220] B. Fevrier, G. Raposo, Exosomes: endosomal-derived vesicles shipping extracellular messages, *Current Opinion in Cell Biology*, 16 (2004) 415-421.
- [221] T.N. Bukong, F. Momen-Heravi, K. Kodys, S. Bala, G. Szabo, Exosomes from Hepatitis C Infected Patients Transmit HCV Infection and Contain Replication Competent Viral RNA in Complex with Ago2-miR122-HSP90, *Plos Pathogens*, 10 (2014).
- [222] S. Bhatnagar, K. Shinagawa, F.J. Castellino, J.R.S. Schorey, Exosomes released from macrophages infected with intracellular pathogens stimulate a proinflammatory response in vitro and in vivo, *Blood*, 110 (2007) 3234-3244.
- [223] J. Withrow, C. Murphy, Y.T. Liu, M. Hunter, S. Fulzele, M.W. Hamrick, Extracellular vesicles in the pathogenesis of rheumatoid arthritis and osteoarthritis, *Arthritis Research & Therapy*, 18 (2016).
- [224] T. Kato, S. Miyaki, H. Ishitobi, Y. Nakamura, T. Nakasa, M.K. Lotz, M. Ochi, Exosomes from IL-1 beta stimulated synovial fibroblasts induce osteoarthritic changes in articular chondrocytes, *Arthritis Research & Therapy*, 16 (2014).

- [225] L. Balaj, R. Lessard, L.X. Dai, Y.J. Cho, S.L. Pomeroy, X.O. Breakefield, J. Skog, Tumour microvesicles contain retrotransposon elements and amplified oncogene sequences, *Nature Communications*, 2 (2011).
- [226] A. Clayton, J.P. Mitchell, J. Court, M.D. Mason, Z. Tabi, Human tumor-derived exosomes selectively impair lymphocyte responses to interleukin-2, *Cancer Research*, 67 (2007) 7458-7466.
- [227] L. Rajendran, M. Honsho, T.R. Zahn, P. Keller, K.D. Geiger, P. Verkade, K. Simons, Alzheimer's disease beta-amyloid peptides are released in association with exosomes, *Proceedings of the National Academy of Sciences of the United States of America*, 103 (2006) 11172-11177.
- [228] E.Y. Lee, K.S. Park, Y.J. Yoon, J. Lee, H.G. Moon, S.C. Jang, K.H. Choi, Y.K. Kim, Y.S. Gho, Therapeutic Effects of Autologous Tumor-Derived Nanovesicles on Melanoma Growth and Metastasis, *Plos One*, 7 (2012).
- [229] L. Zitvogel, A. Regnault, A. Lozier, J. Wolfers, C. Flament, D. Tenza, P. Ricciardi-Castagnoli, G. Raposo, S. Amigorena, Eradication of established murine tumors using a novel cell-free vaccine: dendritic cell-derived exosomes, *Nature Medicine*, 4 (1998) 594-600.
- [230] C. Lee, S.A. Mitsialis, M. Aslam, S.H. Vitali, E. Vergadi, G. Konstantinou, K. Sdrimas, A. Fernandez-Gonzalez, S. Kourembanas, Exosomes Mediate the Cytoprotective Action of Mesenchymal Stromal Cells on Hypoxia-Induced Pulmonary Hypertension, *Circulation*, 126 (2012) 2601-+.
- [231] L.N. Huang, W.Y. Ma, Y.D. Ma, D. Feng, H.Y. Chen, B.Z. Cai, Exosomes in Mesenchymal Stem Cells, a New Therapeutic Strategy for Cardiovascular Diseases?, *International Journal of Biological Sciences*, 11 (2015) 238-245.
- [232] F. Arslan, R.C. Lai, M.B. Smeets, L. Akeroyd, A. Choo, E.N.E. Aguor, L. Timmers, H.V. van Rijen, P.A. Doevendans, G. Pasterkamp, S.K. Lim, D.P. de Kleijn, Mesenchymal stem cell-derived exosomes increase ATP levels, decrease oxidative stress and activate PI3K/Akt pathway to enhance myocardial viability and prevent adverse remodeling after myocardial ischemia/reperfusion injury, *Stem Cell Research*, 10 (2013) 301-312.

- [233] B. Parekkadan, A.W. Tilles, M.L. Yarmush, Bone marrow-derived mesenchymal stem cells ameliorate autoimmune enteropathy independently of regulatory T cells, *Stem Cells*, 26 (2008) 1913-1919.
- [234] J.K. Lee, S.R. Park, B.K. Jung, Y.K. Jeon, Y.S. Lee, M.K. Kim, Y.G. Kim, J.Y. Jang, C.W. Kim, Exosomes Derived from Mesenchymal Stem Cells Suppress Angiogenesis by Down-Regulating VEGF Expression in Breast Cancer Cells, *Plos One*, 8 (2013).
- [235] R. Narayanan, C.-C. Huang, S. Ravindran, Hijacking the Cellular Mail: Exosome Mediated Differentiation of Mesenchymal Stem Cells, *Stem Cells International*, (2016).
- [236] Y. Nakamura, S. Miyaki, H. Ishitobi, S. Matsuyama, T. Nakasa, N. Kamei, T. Akimoto, Y. Higashi, M. Ochi, Mesenchymal-stem-cell-derived exosomes accelerate skeletal muscle regeneration, *Febs Letters*, 589 (2015) 1257-1265.
- [237] A.D. Pusic, R.P. Kraig, Youth and Environmental Enrichment Generate Serum Exosomes Containing miR-219 that Promote CNS Myelination, *Glia*, 62 (2014) 284-299.
- [238] M. Roger, A. Clavreul, M.C. Venier-Julienne, C. Passirani, L. Sindji, P. Schiller, C. Montero-Menei, P. Menei, Mesenchymal stem cells as cellular vehicles for delivery of nanoparticles to brain tumors, *Biomaterials*, 31 (2010) 8393-8401.
- [239] S. Duchi, G. Sotgiu, E. Lucarelli, M. Ballestri, B. Dozza, S. Santi, A. Guerrini, P. Dambrosio, S. Giannini, D. Donati, C. Ferroni, G. Varchi, Mesenchymal stem cells as delivery vehicle of porphyrin loaded nanoparticles: Effective photoinduced in vitro killing of osteosarcoma, *Journal of Controlled Release*, 168 (2013) 225-237.
- [240] M.R. Loebinger, P.G. Kyrtatos, M. Turmaine, A.N. Price, Q. Pankhurst, M.F. Lythgoe, S.M. Janes, Magnetic Resonance Imaging of Mesenchymal Stem Cells Homing to Pulmonary Metastases Using Biocompatible Magnetic Nanoparticles, *Cancer Research*, 69 (2009) 8862-8867.
- [241] A.K.A. Silva, C. Wilhelm, J. Kolosnjaj-Tabi, N. Luciani, F. Gazeau, Cellular Transfer of Magnetic Nanoparticles Via Cell Microvesicles: Impact on Cell Tracking by Magnetic Resonance Imaging, *Pharmaceutical Research*, 29 (2012) 1392-1403.
- [242] G. Tripodo, T. Chlapanidas, S. Perteghella, B. Vigani, D. Mandracchia, A. Trapani, M. Galuzzi, M.C. Tosca, B. Antonioli, P. Gaetani, M. Marazzi, M.L. Torre, Mesenchymal stromal

cells loading curcumin-INVITE-micelles: A drug delivery system for neurodegenerative diseases, *Colloids and Surfaces B-Biointerfaces*, 125 (2015) 300-308.

[243] S. Perteghella, B. Crivelli, L. Catenacci, M. Sorrenti, G. Bruni, V. Necchi, B. Vigani, M. Sorlini, M.L. Torre, T. Chlapanidas, Stem cell-extracellular vesicles as drug delivery systems: New frontiers for silk/curcumin nanoparticles, *International journal of pharmaceutics*, 520 (2017) 86-97.

Aim

The final aim of my PhD thesis was the development of a novel integrated nanobiological-nanotechnological approach able to improve the therapeutic potential of mesenchymal stem cells derived extracellular vesicles by exploiting the carrier-in-carrier concept: the first pharmaceutical/technological carrier was represented by silk fibroin nanoparticles into which selected drugs have been loaded, while the second biological carrier was represented by the mesenchymal stem cells secreted membrane vesicles able to ensure an adequate drug targeting to pathological tissue by their innate tropism. In particular, the nanotechnological approach wants to avoid the intracellular drug hydrolytic or enzymatic degradation, to improve its water solubility, to achieve a controlled release and to protect the mesenchymal stem cells from cytotoxic effects of the drug itself. The biological approach wants to exploit not only the homing capacity of the mesenchymal stem cell-derived extracellular vesicles but also their innate immunosuppressive and regenerative potentials. Using extracellular vesicles instead of mesenchymal stem cells as biological nanocarriers allows to avoid all the complications related to cellular therapy: in fact, they show similar features of their parent cells with virtually lower tumorigenic risk compared to viable/replicating cells and for this reason probably higher safety and easy of handle, storage and application if we consider extracellular vesicles as conventional active principle ingredients.

By coupling this two complementary approaches, the development of a “Next Generation Drug Delivery System” was proposed in this PhD thesis for the regeneration of musculoskeletal system. To achieve this final goal subsequent actions were carried out: firstly, silk fibroin nanoparticle technique was developed (First Action); therefore, *in vitro* nanosystem anti-inflammatory efficacy was defined (Second Action), and, finally a procedure to obtain the nanostructured carrier-in-carrier delivery system has been designed (Third Action).

Results

The present PhD thesis is organized in three parts. First were developed bio-inspired nanoparticles made of silk fibroin (**First Action Results**), the protein composing the inner core of silk, into which two different drug models have been encapsulated for the treatment of musculoskeletal diseases. In particular, we focused our attention on osteoarthritis, a disabling disease affecting people worldwide characterized by a plethora of pathways involving cytokines, chemokines, proteins, inflammatory and immune system cells. Curcumin was chosen because of its natural anti-oxidant and anti-inflammatory properties while celecoxib because it is considered as the “first choice treatment” for osteoarthritis. Unfortunately, both drugs, when employed as naked, suffer from both severe cytotoxic phenomena and poor biopharmaceutical properties, which can be overcome by harnessing a nanotechnological approach. Silk fibroin nanoparticle-based delivery systems are suitable for highly hydrophobic agents, circumventing the pitfalls of their poor aqueous solubility thus revealing their great biological effects. Since osteoarthritis is characterized by pro-oxidant agent production and pro-inflammatory cytokine release, leading to cartilage degradation and associated pain, therefore, firstly, cytocompatibility and hemocompatibility studies have been performed to assess the nanosystem compatibility compared to that of their equivalent free drug formulations; secondly, the evaluation of their anti-oxidant and anti-inflammatory activity was carried out in an *in vitro* model of osteoarthritis to verify their potential application for the treatment of musculoskeletal pathologies (**Second Action, Paper 3**).

The previously developed silk fibroin bio-inspired nanosystems have been employed to create an effective and versatile “next generation drug delivery system”, named carrier-in-carrier, by combining a nano-technological with a nano-biological approach, exploiting simultaneously both of their remarkable features; this combination could open new horizons for the treatment of musculoskeletal diseases and inflammatory pathologies. The first carrier is composed of silk fibroin nanoparticles, already deeply studied and employed for the development of a plethora of scaffolds and drug supports, characterized by an intrinsic anti-inflammatory activity, as demonstrated in **Paper 3**. The second delivery system is composed of extracellular systems physiologically secreted by mesenchymal stem/stromal cells, already proposed and tested as drug vehicles. The EVs will be loaded with drug models, previously internalized by nanoparticles exploiting the exogenous technique: a carrier-in-carrier approach wants to ensure a physiological drug targeting to pathological tissues, by exploiting mesenchymal stem cell derived extracellular vesicles innate homing to injured tissues (**Third Action, Paper 4**).

First Action Results

1. Introduction

Silk is a protein naturally produced by insects and spiders; its architecture shows that the inner core is composed of two filaments, the heavy chain (≈ 250 kDa) and the light chain (≈ 25 kDa) respectively, entirely coated by a sericin “glue like” layer showing a protective activity (Vollrath F 2001). The polarity of this external coating make it easily removed by boiling the cocoons in hot water, or in presence of carbonate (Altman GH 2002). Once obtained pure silk fibroin fibers, it is possible to develop silk fibroin nanoparticles exploiting a broad spectrum of different techniques, by exploiting silk self-assembly behavior ruled by hydrophilic and hydrophobic chain interactions (Jin HJ 2003).

Desolvation, also known as coacervation, is the preferred method to obtain protein-based nanoparticles. It is based on the dehydration of SF chains in the presence of several organic solvents such as acetone, ethanol, dimethyl sulfoxide (DMSO) and methanol. The main drawbacks are the presence of high volumes of organic solvents, which must be removed using several centrifuges or strong dialysis cycles, in order to avoid any cytotoxic events. Another valid approach employed for SF nanoparticle production is salting out, resulting in particles with higher dimensional range (Lammel AS 2010). The process is similar to desolvation, but instead of using an organic solvent, a highly concentrated salt solution is employed. As reported by Lammel, the key parameters of the process are the pH of the salting solution, the kind of salt employed, the SF concentration, the ratio between it and the salt bath (Lammel AS 2010). Other techniques are the mechanical comminution (Rajkhowa R 2008), electro-spraying (which provides the atomization of a starting SF solution via electrical field applications) (Qu J 2014) and the capillary microdot technique (Gupta V 2009).

The aim of this work was to obtain silk fibroin nanoparticles able to deliver hydrophic drugs and to study their technological and physico-chemical characterization.

2. Material and Methods

2.1 Silk fibroin extraction and solubilization

Silk Fibroin (SF), from the *Bombyx mori* cocoons, was degummed in autoclave at 120 °C for 1 hour, to remove the “glue like” coating made of sericin; next, degummed fibers were rinsed with deionized water at 60°C, dried at room temperature, cut in small pieces and solubilized using Ajisawa’s reagent (CaCl₂/EtOH/H₂O, molar ratio 1:2:8) for 5 minutes at 70 °C under magnetic stirring to obtain a raw SF solution. The silk solution was filtered (70 μ m) and

dialyzed against distilled water using a cellulose membrane (MWCO, cut-off 12-14 KDa) at room temperature. The final concentration of silk fibroin was about 3% w/v, and it has been diluted to 1.5% w/v before carrying out the nanoparticle production.

2.2 Tuning of the production technique for silk fibroin nanoparticles

Silk fibroin nanoparticles can be prepared by exploiting different methods (as deeply discussed in the introduction) in relation to the selected drug and its chemical-physical properties (Zhao Z 2015). Each method shows pros and cons, so the selection of the appropriate production technique is essential to obtain SF-based nanoparticles for drug delivery applications. The high molecular weight and the protein nature of SF make the preparation of nanoparticles and the reproducibility of the method difficult to control. Moreover, SF tends to self-assemble into fibers or gels upon exposure to heat, salt, pH change and high shear stress.

Three different methods were performed to obtain SF nanoparticles:

1. **Salting out:** the SF aqueous solution was added to a salting solution (volumetric ratio 1:5), prepared by mixing in deionized water both K_2HPO_4 and KH_2PO_4 with pH 8, under mild magnetic stirring. Increasing the salt concentration resulted in the removal of the water barrier between protein molecules leading to higher protein-protein interactions (Figure 1). Therefore, the protein molecules aggregate together by forming hydrophobic interactions with each other and precipitate from the solution. The resulting particles were collected and dialyzed against deionized water before freeze-drying process.

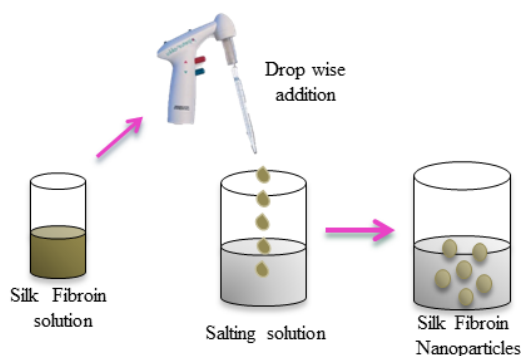


Figure 1. Salting out schematic representation.

2. **Desolvation with ethanol:** SF aqueous solution was mixed with an ethanol 96% solution (ratio 1:5), under vigorous magnetic stirring at room temperature. The process reduces the protein solubility leading to a phase separation. The addition of the

desolvating agent leads to conformational changes within the protein structure resulting in coacervation or precipitation of the protein. By a phase separation, a phase with a coacervate and a second phase with a solvent/non-solvent mixture are formed. In this process, the organic solvent must be miscible with the non-solvent. The obtained coacervate was centrifuged (3000 g) or dialyzed to remove the organic solvent residues and finally freeze-dried.

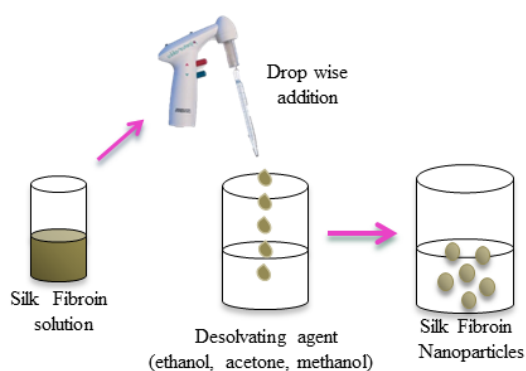


Figure 2. Desolvation schematic representation. Ethanol or acetone could be employed as desolvating agents, triggering the silk fibroin nanoprecipitation.

- 3. Desolvation with acetone:** similarly to what reported previously, SF solution was added drop wise into acetone, maintaining $>75\%$ v/v acetone volume, under mild magnetic stirring at room temperature (Seib PF 2013). Precipitated nanoparticles were gathered and then dialyzed using cellulose membranes (MWCO 12-14 KDa) at room temperature against distilled water to remove the solvent phase.

Once chosen the best technique to obtain silk nanoparticles, curcumin was loaded to verify its ability once encapsulated in them. Due to its marked solubility in acetone, curcumin was directly solubilized in the organic solvent before performing the nanoparticle production.

Once obtained, the nanosystem suspensions (blank or curcumin-loaded) were dialyzed for 3 days in distilled water using cellulose tubes (MWCO 3,000–5,000 Da) until complete solvent removal. Finally, aqueous suspension was freeze-dried at 8×10^{-1} mbar and -50°C for 72 hours before carrying out their characterization.

2.3 Nanoparticle characterization

2.3.1 Granulometric analysis

Granulometric analysis (Beckman, Coulter counter LS230, Miami, Florida, USA) was performed to evaluate the particle size distribution, considering both the volume and the number percentages.

Freeze-dried samples were re-suspended in deionized water (0,1 mg/mL), bar stirred for almost 1 hour and filtered using 0.22 μ m before carrying out the analysis. Samples were put into the measurement cell and ran in five replicates of 90 seconds each. The refractive index was set at 1 for deionized water. Results were expressed as the average of at least five replicates for each formulation.

2.3.2 Scanning Electron Microscopy (SEM)

A morphological analysis by SEM (Zeiss EVO MA10, Carl Zeiss, Oberkochen, Germany) was carried out to confirm the particle dimensions and external aspect. The samples were gold sputter coated under argon to make them electrically conductive prior to microscopy.

2.3.3 Drug loading evaluation

The curcumin loading (%) in SF nanoparticles, obtained via acetone desolvation technique, was evaluated using a direct spectrophotometer method (Uvikon 860, Kontron Instruments, Switzerland) by reading its absorbance at 425 nm. Briefly, freeze-dried nanoparticles were dissolved in 96% v/v ethanol (0.1 mg/ml), maintaining mild magnetic stirring. Curcumin concentration was measured from a calibration curve of nine curcumin solutions in ethanol (96%v/v) at the concentration range of $8 \cdot 10^{-3}$ – $6.25 \cdot 10^{-4}$ mg/ml, with a correlation coefficient $r^2 > 0.9895$. Ethanol was considered as control solution. Each measurement was performed in triplicate.

2.3.4 Determination of the process yield

The nanoparticle yield (Y%) was evaluated by measuring the ratio between the final weight of the nanoparticle recovered after freeze-drying process and the starting amount of raw material.

2.4 Solid-state characterization

Nanoparticles were then characterized in terms of Differential Scanning Calorimetry, Thermogravimetric Analysis and Fourier Transform Infrared Spectroscopy.

2.4.1 Differential Scanning Calorimetry (DSC)

Temperature and enthalpy values were measured with a Mettler STARE system (Mettler Toledo, Novate Milanese, Mi, Italy) equipped with DSC81e Module and an Intracooler device for sub-ambient temperature analysis (Jukabo FT 900) on 1-2 mg (Mettler TG 50 Thermobalance) samples in 40 μ L sealed aluminium pans with pierced lid (method: 10-400 $^{\circ}$ C temperature range; heating rate 10 K/min; nitrogen air atmosphere flux 50 mL/min). The instrument was previously calibrated with Indium, as standard reference, and measurement were carried out at least in triplicate.

2.4.2 Simultaneous Thermogravimetric Analysis (TGA/DSC 1)

Mass losses were recorded with a Mettler STARe system (Mettler Toledo, Novate Milanese, MI, Italy) TGA on 2-3 mg samples in 70 μ L alumina crucibles with lid (30-400 °C temperature range; heating rate 10 K/min; nitrogen air atmosphere flux 50 mL/min). The instrument was previously calibrated with Indium, as standard reference, and measurement were carried out at least in triplicate.

2.4.3 Fourier Transform Infrared (FT-IR) spectroscopy

Mid-IR (650-4000 cm^{-1}) spectra (4 cm^{-1} resolution) were recorded on powder samples using a Spectrum One Perkin-Elmer spectrophotometer (Perkin Elmer, Wellesley, MA, USA) equipped with a MIRacle™ ATR device (Pike Technologies, Madison, WI, USA).

3. Results and Discussion

Three different techniques were performed to verify the silk fibroin nanoparticle production: in particular salting out, desolvation via ethanol and via acetone were considered. Results showed that the final product quality and dimension are strictly influenced by the set parameters of the production technique performed.

During salting out process, the hydrophobic interactions between SF chains and water molecules decrease, and they are replaced by protein-protein interactions, leading to particle formation. Exploiting the salting out method, represented in the granulometric analysis graph by the red curve, particles with a size distribution range of 1-10 μm could be obtained (Figure 3); diluting the starting SF solution (ratio SF/saline solution 1:50, 1:70, 1:100) before carrying out the experiment did not influence the particle size. This results could be due to the kind of employed salts (in this case potassium phosphate salts) and by the salting solution pH, which, as reported in literature, is able to influence the particle size (Lammel AS, 2010).

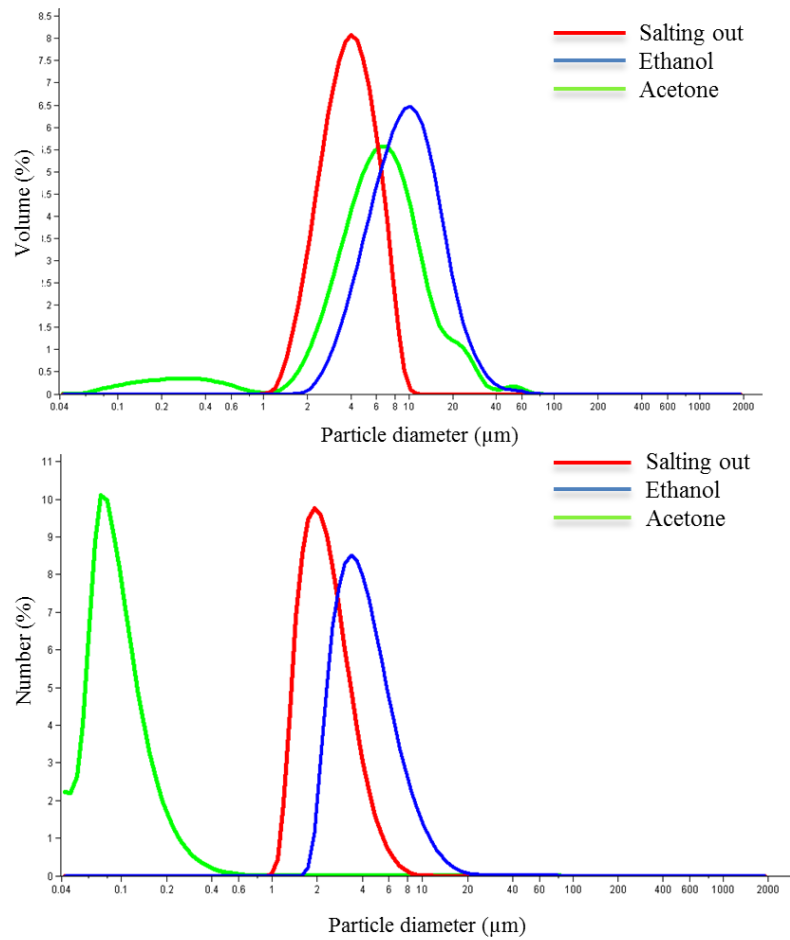


Figure 3. The granulometric analysis showed that it is possible to obtain nanoparticles only via acetone desolvation, represented by the green line. In fact, the green curve reported in the number % graph is shifted to smaller particle diameter values (range 40-400 nm) while the curves of the other two methods employed (blue for ethanol desolvation and red for salting out, respectively) are still in micrometric ranges.

SEM morphological investigation showed the presence of round-shaped particle aggregates, highlighting the micrometric dimension (Figure 4).

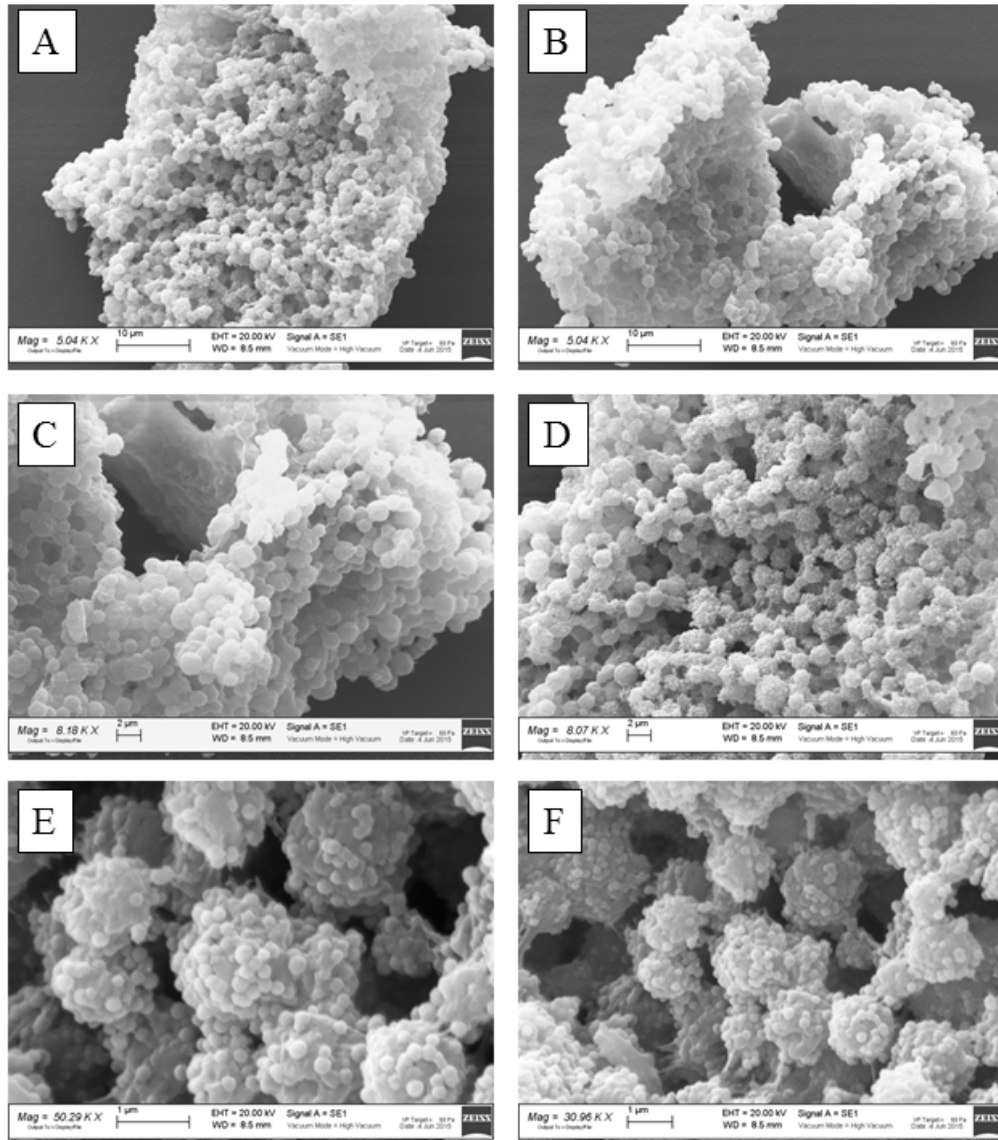


Figure 4. Scanning electron microscopy (SEM) images captured at different magnifications of silk fibroin particles obtained with the salting out technique.

Through desolvation via ethanol, particles with a size distribution range between 2-100 μm were obtained, as confirmed by the granulometric analysis (Figure 3, blue curve); similarly of what observed for particles produced via salting out, diluting the SF solution did not change the particle size. SEM microscopy showed the presence of fused material resulting in smooth surfaces, sometimes characterized by spherical structures (Figure 5).

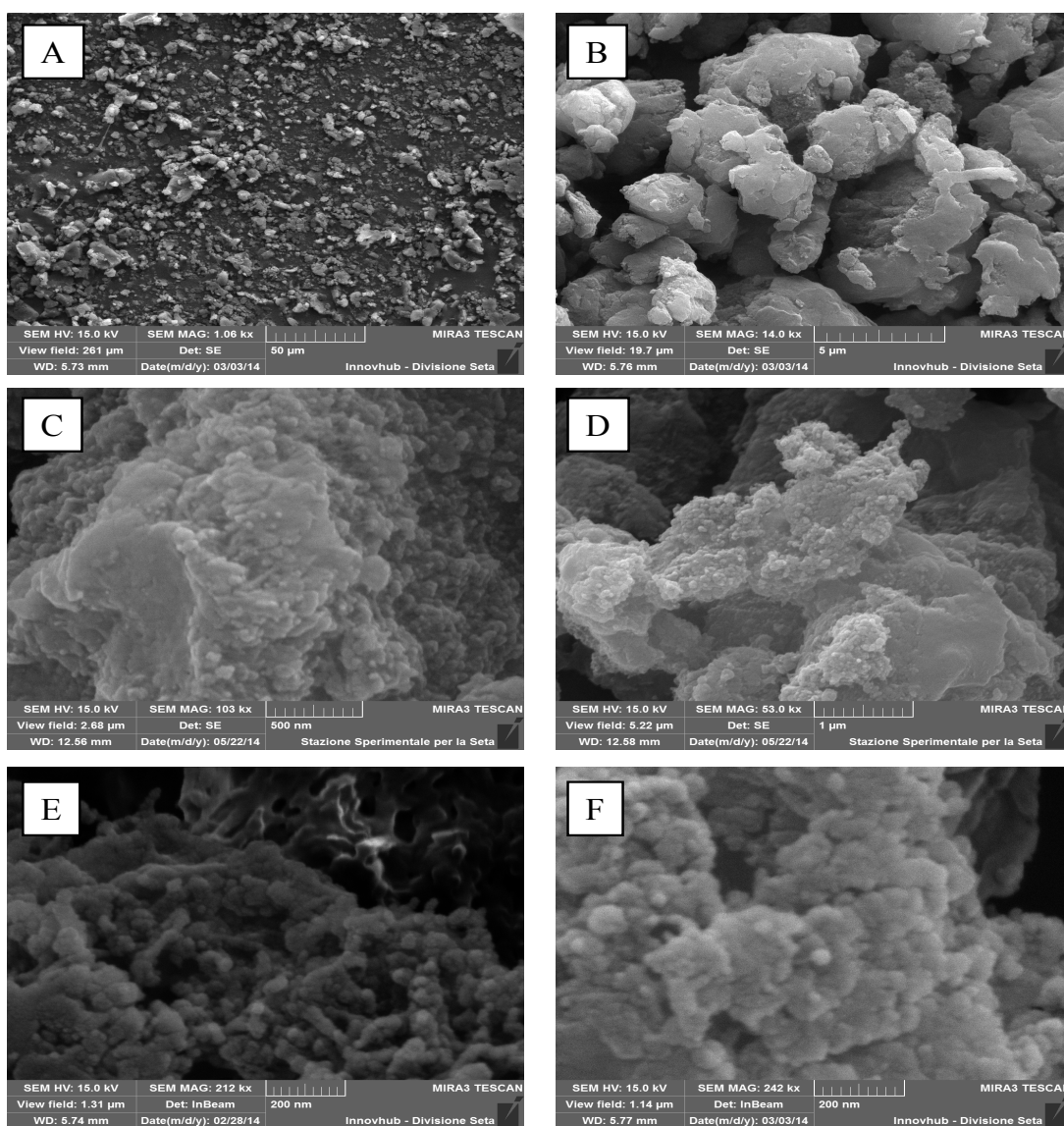


Figure 5. Scanning electron microscopy (SEM) images captured at different magnifications of silk fibroin particles obtained with the desolvation via ethanol.

Finally, exploiting the acetone as desolvating agent, silk fibroin based nanosystems with a diameter of about 100 nm were obtained, as clearly indicated by the number percentage graphic (Figure 3). The acetone succeeded in triggering the silk fibroin nanoprecipitation:

Starting from these results, the acetone desolvation technique was adopted to encapsulate first curcumin, and then celecoxib, in silk fibroin nanoparticles: briefly, different amounts of the considered active were incorporated in the starting acetone bath before carrying out the desolvation process.

Both the granulometric analysis and the SEM morphological investigations were performed as reported above considering curcumin loaded and blank silk fibroin nanoparticles obtained via acetone desolvation method.

A mean particle size of about 6 μm in both curcumin loaded and blank nanoparticles could be observed in the volume % graph (Figure 6A); despite a particle aggregation was observed, the number percentage graph clearly showed a nanoparticle diameter of about 100 nm for both samples (Figure 6B, the green curve is perfectly overlapped by the blue curve).

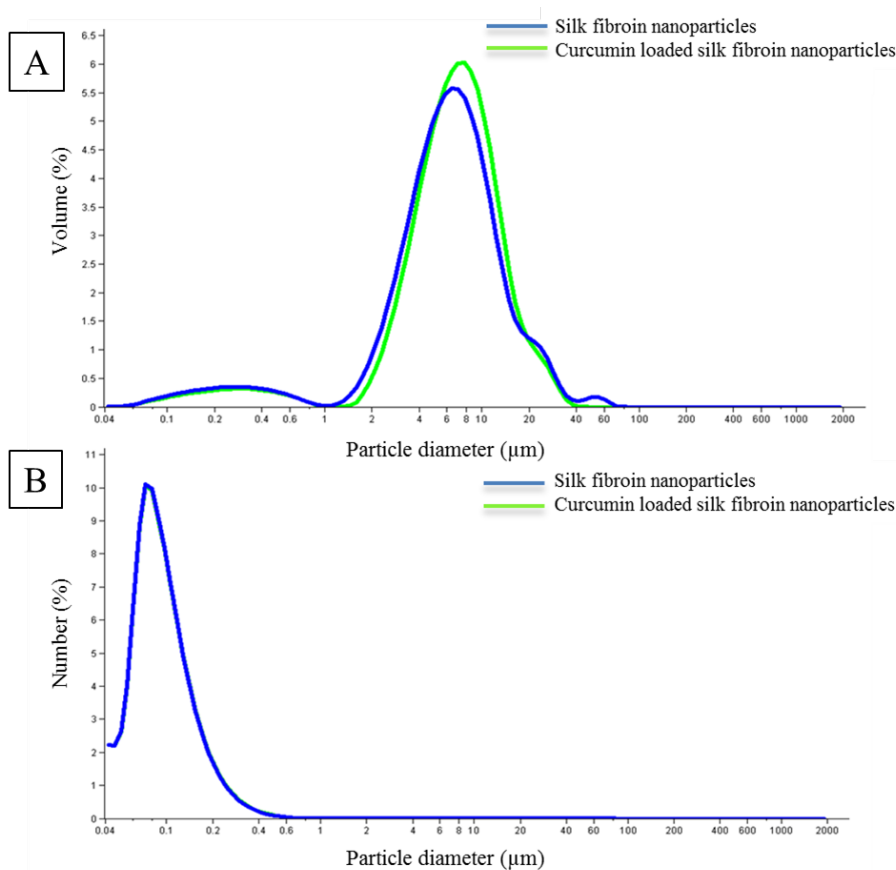


Figure 6. Granulometric analysis of silk fibroin nanoparticles obtained with the desolvation technique, loaded with curcumin (green curve) or blank (blue curve). The volume % graph shows a mean particle size of 6 μm (A), while the number % graph indicates a mean particle size of 100 nm (B).

SEM results confirmed the nanoparticles size distribution and their spherical geometry (Figure 7A), highlighting that the encapsulation of curcumin did not alter the nanostructure morphology (Figure 7B).

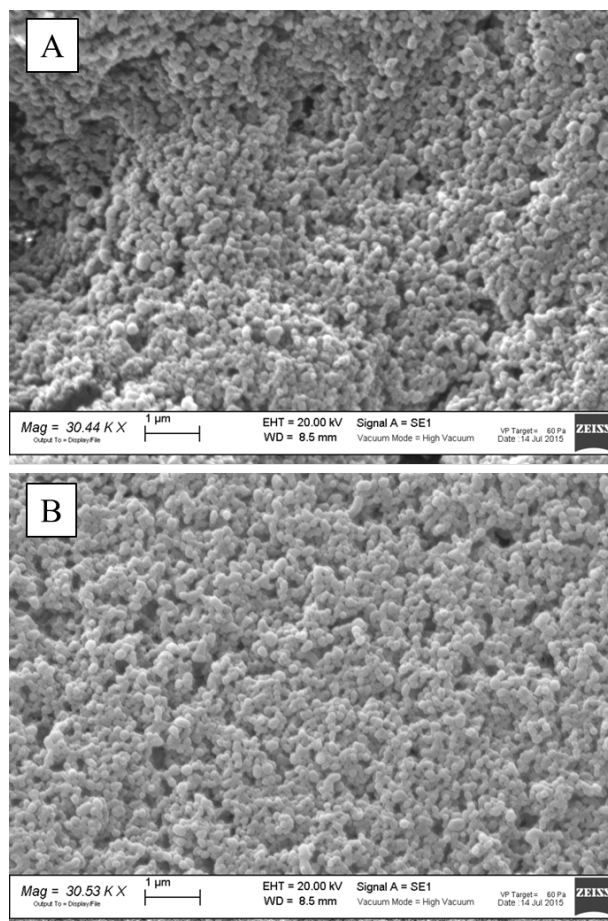


Figure 7. SEM images of silk fibroin nanoparticles unloaded (A) and loaded with curcumin (B) obtained employing acetone as the desolvating agent during the coacervation process.

3.1 Drug loading evaluation

Curcumin was chosen as a drug model due to its anti-oxidant and anti-inflammatory properties exploitable for musculoskeletal pathologies and was loaded in SF nanoparticles obtained via acetone desolvating technique. The drug content in SF nanoparticles was about $0.14\% \pm 0.04$ w/w.

3.2 Solid state characterization

Infrared spectroscopy was performed on both blank and curcumin loaded silk fibroin nanoparticles, as well as on free curcumin. FT-IR spectra, reported in Figure 8, confirmed the presence of silk in its stable conformation characterized by crystalline β -sheet domains. In fact, silk fibroin can exist in three structural models, resulting in different stability: Silk I is referred to water-soluble structure, Silk II to β -sheet conformation and Silk III to the air-water interface. β -sheet structure can be identified in the spectra region of Amide I (at about 1620 cm^{-1}) and Amide II (at about 1520 cm^{-1}) (Um IC, 2001).

Our results demonstrated that the main absorption bands of crystalline β -sheet domains of silk fibroin were detected at 1622 cm^{-1} , 1516 cm^{-1} and 1231 cm^{-1} , indicating that silk fibroin existed in its stable conformation in both blank (spectrum a) and curcumin loaded nanoparticles (spectrum b).

Particular regard should be given to the FT-IR spectrum of curcumin loaded silk fibroin nanoparticles (spectrum b), which was perfectly overlapped to that of blank nanoparticles (spectrum a). The typical absorption bands of curcumin at 1626 cm^{-1} and 1508 cm^{-1} due to C=O stretching, 1601 cm^{-1} due to C=C aromatic ring, 1273 cm^{-1} due to C-O enol stretching, 1025 cm^{-1} due to C-O-C stretching, 962 cm^{-1} and 713 cm^{-1} due to cis-trans CH vibration of aromatic ring, appeared only in the free curcumin sample (spectrum c). This was probably due to the very low percent of the active loaded in silk fibroin nanoparticles, which was lower than 1 % w/w.

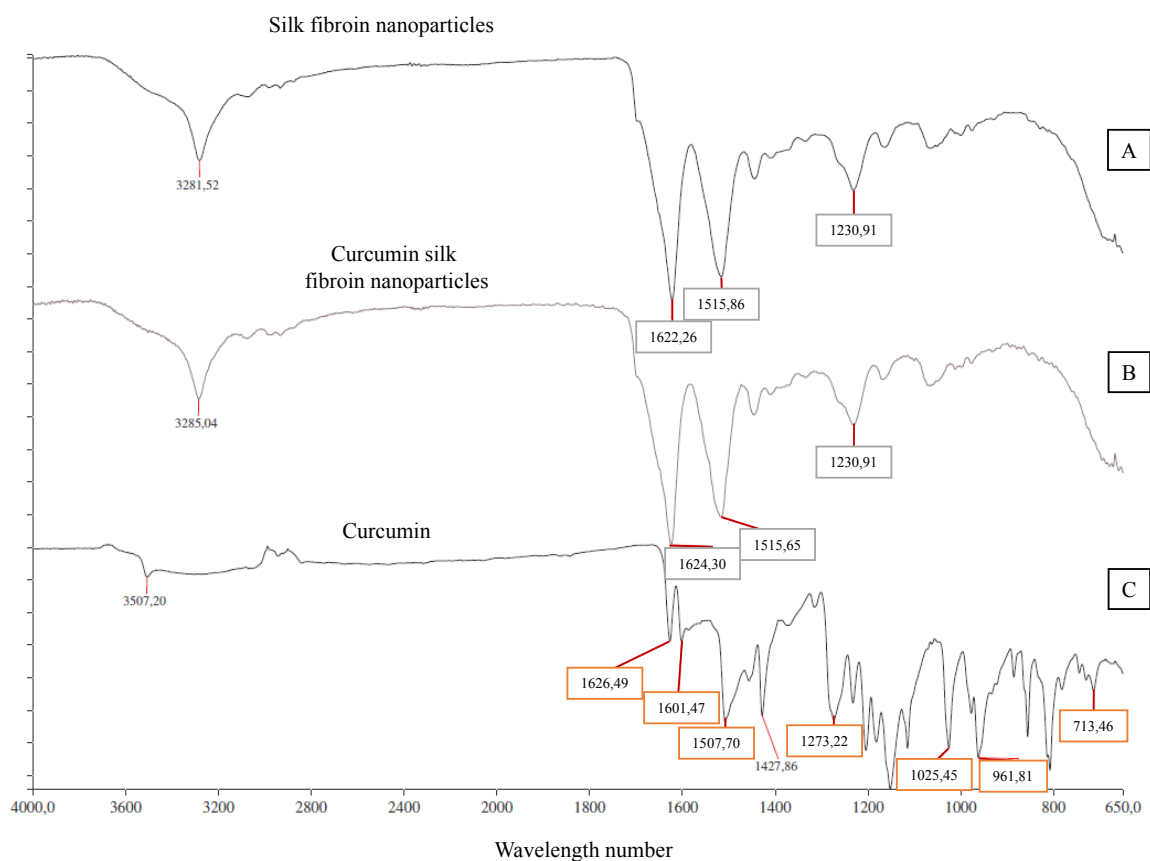


Figure 8. FTIR characterization of A) silk fibroin nanoparticles, B) curcumin-loaded silk fibroin nanoparticles and C) free curcumin. Grey frames show the typical absorption bands of the stable conformation of silk fibroin; orange frames highlight the curcumin typical absorption bands.

DSC analysis of silk fibroin (Figure 9A, curve a) evidenced the absence of glass transition at about 175 °C and exothermic event of crystallization at about 210 °C, because of the conformational transition of silk fibroin, and the presence of a broad endothermic effect between 30 and 100 °C due to dehydration (mass loss in TGA curve of about 8%, Figure 6B, curve a) followed by the sample decomposition at about 295 °C, as confirmed by mass loss recorded in TGA curve. DSC analysis of curcumin loaded fibroin nanoparticles showed thermal behavior superimposable to silk fibroin, without any evidence of presence of the active (Figure 9A, curve b) with a mass loss in TGA curve, in the range of temperature 30-100 °C, of about 7% (Figure 9B, curve b). Curcumin showed a typical DSC profile of an anhydrous crystalline sample ($T_{\text{onset,m}} = 168.2 \pm 0.2$ °C; $T_{\text{peak,m}} = 174.4 \pm 0.1$ °C; $\Delta H_m = 103 \pm 1$ Jg⁻¹) with a mass loss recorded in TGA curve starting at around 220 °C corresponding to the decomposition of the sample. Then, also in thermal analysis, the presence of active in the loaded nanoparticles was not appreciable due to the very low mass percent loaded (0,14% w/w).

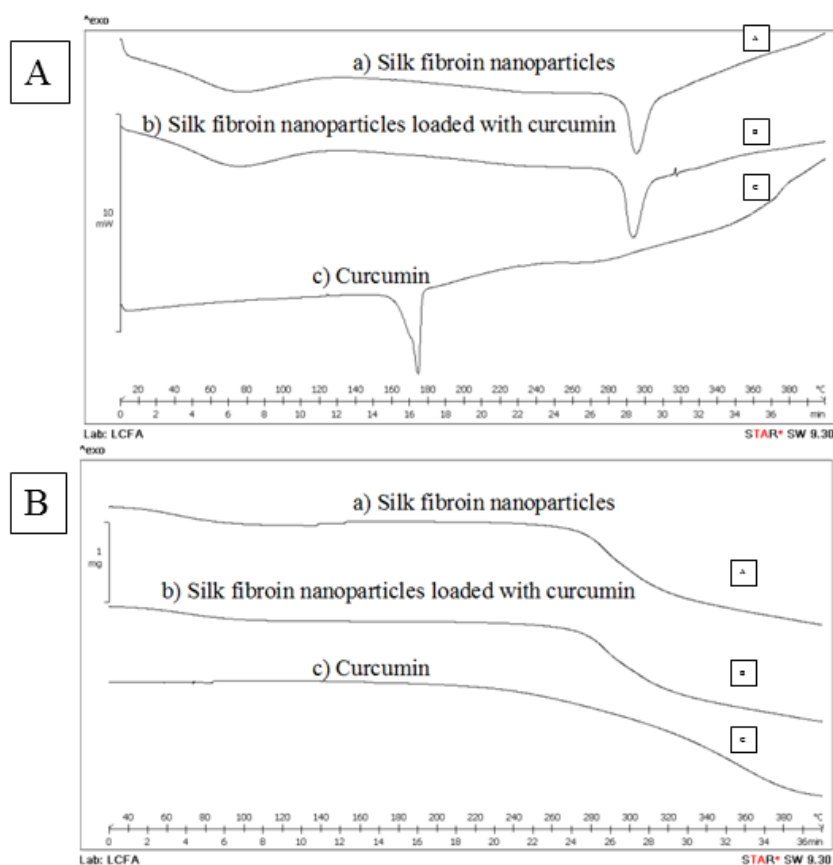


Figure 9. DSC (A) and TGA (B) characterization of a) silk fibroin nanoparticles, b) curcumin-loaded silk fibroin nanoparticles and c) free curcumin.

Conclusion

Desolvation method via acetone was the optimal method to obtain silk fibroin nanoparticles. Through this technique it was possible to load curcumin in silk fibroin nanoparticles, even if the drug loading was very low (about 0.14% w/w). As reported in the future works, increasing loading of curcumin were achieved by varying the starting drug amount solubilized in the acetone bath (*Paper 4*); additionally, also celecoxib was successfully encapsulated in silk fibroin nanoparticles (*Paper 3*).

References

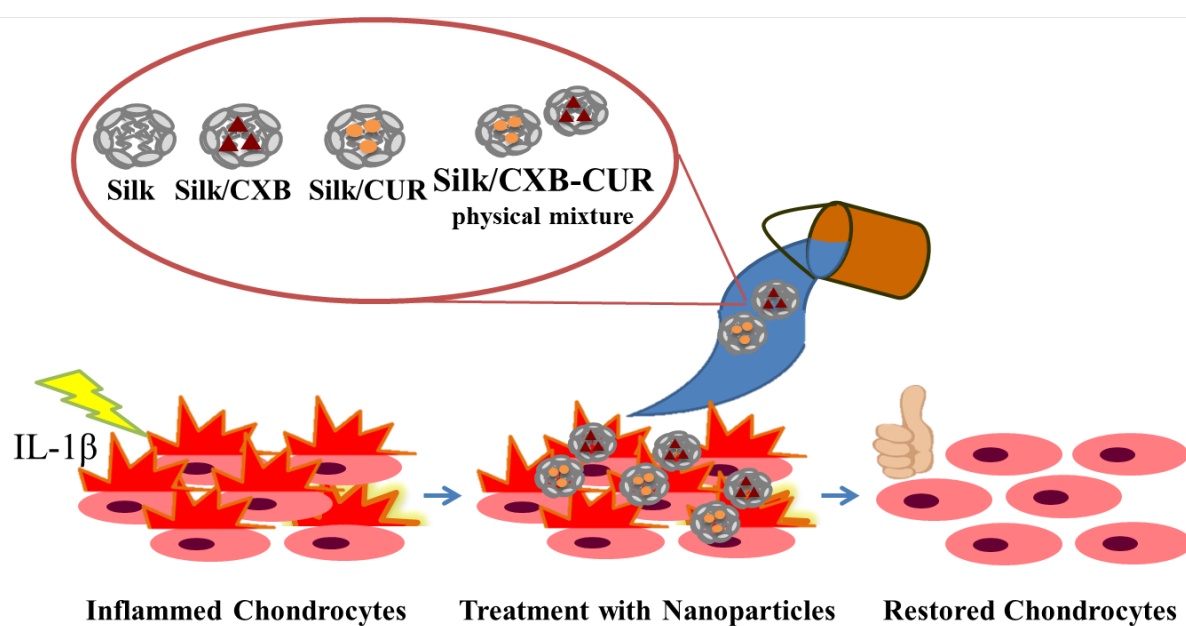
- Altman G.H., 2002. Silk matrix for tissue engineered anterior cruciate ligaments. *Biomaterials* 23, 4131-41.
- Gupta V., Aseh A., Rios C.N., Aggarwal B.B., Mathur A.B., 2009. Fabrication and characterization of silk fibroin-derived curcumin nanoparticles for cancer therapy. *International journal of nanomedicine* 4, 115-122.
- Hin H.J., Kaplan D.L., 2003. Mechanism of silk processing in insects and spiders. *Nature* 424, 1057-61.
- Lammel A.S., Hu X., Park S.-H., Kaplan D.L., Scheibel T.R., 2010. Controlling silk fibroin particle features for drug delivery. *Biomaterials* 31, 4583-4591.
- Qu J., Liu Y., Yu Y., Li J., Luo J., Li M., 2014. Silk fibroin nanoparticles prepared by electrospray as controlled release carriers of cisplatin. *Materials science and engineering C, Materials for biological applications* 44, 166-174.
- Rajkhowa R., Wang L., Wang X., 2008. Ultra-fine silk powder preparation through rotary and ball milling. *Powder technology* 185, 87-95.
- Seib F.P., Jones G.T., Rnjak-Kovacina J., Lin Y., Kaplan D.L., 2013. pH-Dependent anticancer drug release from silk nanoparticles. *Advanced Healthcare Materials* 2, 1606-1611.
- Um I.C., Kweon H.Y., Park Y.H., Hudson S., 2001. Structural characteristics and properties of the regenerated silk fibroin prepared from formic acid. *International Journal of Biological Macromolecules* 29, 91-97.
- Vollrath F. & Knight D. P., 2001. Liquid crystalline spinning of spider silk. *Nature* 410, 541–548.
- Zhao Z., Li Y., Xie M.-B., 2015. Silk fibroin-based nanoparticles for drug delivery. *International Journal of Molecular Sciences* 16, 4880-4903.

Silk fibroin nanoparticles reduced cytotoxicity and showed anti-inflammatory efficacy in IL-1 β stimulated human chondrocytes

Authors

Barbara Crivelli, Elia Bari, Sara Perteghella, Laura Catenacci, Milena Sorrenti, Giovanna Bruni, Giuseppe Tripodo, Theodora Chlapanidas and Maria Luisa Torre.

Graphical abstract



Abstract

This work aimed to verify the hypothesis that nano-encapsulated celecoxib (CXB) and curcumin (CUR) showed higher safety and efficacy profiles in an *in vitro* model of osteoarthritis (OA) than free drugs.

CUR showed a high antioxidant activity, further increased by its nano-encapsulation, due to the slightly antioxidant activity of silk fibroin. The nano-encapsulation avoided both the severe cytotoxic and the hemolytic effects evoked by free drugs, confirming the efficiency of the nanotechnological approach. All nanoparticles, at the higher tested concentration, were able to inhibit the inflammatory condition; surprisingly, silk nanoparticles possessed an intrinsic anti-inflammatory activity comparable to that of nano-encapsulated drugs and the physical mixture of Silk/CXB-CUR revealed more effective than Silk/CXB or Silk/CUR.

In conclusion, nanoparticles loaded with curcumin and celecoxib appeared the promising formulation for the treatment of osteoarthritis and silk fibroin cannot be considered anymore as an inert polymer, but it must be listed as a “real” active principle ingredient with suitable therapeutic application in inflammatory diseases.

Keywords

Musculoskeletal diseases; nanoparticles; silk fibroin; curcumin; celecoxib; anti-inflammatory activity.

Introduction

Osteoarthritis (OA) represents a pathological condition characterized by both inflammation and chronic degeneration of the musculoskeletal compartment, which is triggered by an overproduction of interleukin-1 β (IL-1 β) and tumour necrosis factor- α (TNF- α), leading to extracellular matrix degradation and cartilage tissue damage. Moreover, cytokine-activated chondrocytes, in inflammatory conditions, over-expressed several cytokines and chemokines including Regulated on Activation, Normal T cell Expressed and Secreted (RANTES) [1].

Currently, a standard therapy for treating OA does not exist: the available pharmacological strategies are several, diverse and aimed to reach and modify different biological targets, albeit the majority is targeted to pain relief. Among these, non-steroidal anti-inflammatory drugs (NSAIDs) and cyclooxygenase-2 (COX-2) selective inhibitors such as celecoxib (CXB), are employed for symptomatic pain, inflammation and swelling treatment. They are preferred to cyclooxygenase-1 (COX-1) selective inhibitors due to their limited gastro-enteric and renal side

effects [2], even if they have been associated to cardiovascular hazards caused by their high dosage and long-term administration [3] [4].

Since the established pharmacological therapy covers the entire patient lifespan and is characterized by severe long-term side effects or expensiveness, natural herbal compounds have been recently introduced. Among these, curcumin (CUR), a natural hydrophobic polyphenol extracted from the *Curcuma longa* rhizome, has been shown to retain remarkable anti-inflammatory and antioxidant properties exploitable not only in musculoskeletal pathologies but in other many chronic disorders [5] [6].

OA is commonly treated with systemic therapies based on free drugs albeit they are still suffering from several drawbacks due to their limited solubility [7], poor *in vivo* bioavailability, fast metabolism and bloodstream clearance, which could be easily overcome by encapsulating them in nanosystems [8]. Therefore, nanoparticles have gained much attention in biomedical and biotechnological fields thanks to their capability to efficiently control the drug release and targeting while protecting them from degradation activities and avoiding undesired side effects, when compared to conventional formulations [9] [10]. In this context, silk fibroin nanoparticles (Silk) stand out for their remarkable biocompatibility, controllable biodegradability, functional modification potential (due to amino and carboxylic groups placed on their surface), appropriate mechanical properties and therapeutic retention at the target site [11] [12].

Recently, our research group developed a novel drug delivery system coupling silk fibroin nanoparticles loaded with curcumin (Silk/CUR) and extracellular vesicles secreted by mesenchymal stem cells (MSCs). Silk/CUR were successfully uptaken by MSCs within 60 minutes, showing a cytoplasmic localization; notably, the application of a nanotechnological approach avoided CUR cytotoxic events. Finally, MSCs were able to release extracellular vesicles entrapping Silk/CUR, achieving a novel carrier-in-carrier system [13].

The aim of the present study is to evaluate the anti-inflammatory activity of nano-encapsulated CXB and CUR in an *in vitro* model of OA. First, Silk and Silk/CXB were developed and characterized from a technological point of view; subsequently, they were *in vitro* tested on human inflamed articular chondrocytes, in comparisons with Silk/CUR, evaluating the effects on inflammatory mediators such as nitrite, IL-6 and RANTES production. Finally, the *in vitro* efficacy was also evaluated on the physical mixture of Silk/CXB and Silk/CUR to demonstrate their possible synergism on inflamed chondrocytes.

2. Experimental

2.1 Materials

Sodium carbonate, lithium bromide, acetone, CUR, CXB, ethanol, methanol, collagenase, 3-(4,5-dimethylthiazol-2-yl)-2,5-diphenyl-tetrazolium bromide (MTT) and dimethyl sulfoxide (DMSO) were purchased from Sigma-Aldrich (Milan, Italy). Dialysis cellulose tubes (MWCO 3,000–5,000 Da) were obtained from Visking (London, United Kingdom). 70 µm nylon meshes were obtained from Greiner Bio-One GmbH (Kremsmunster, Austria). Griess Reagent kit was purchased from Biotium (Fremont, California, USA) while human RANTES and human IL-16 enzyme-linked immunosorbent assays (ELISA) were obtained from PeproTech, Rocky Hill, USA. All reagents used for cell cultures were purchased from Euroclone (Milan, Italy).

2.2 Silk fibroin extraction

Bombyx mori cocoons were cut in dime-sized pieces and subjected to a degumming process in aqueous Na₂CO₃ (0.02M) for 30 minutes; next, degummed fibers were washed in distilled water to completely remove sericin and dried at room temperature. Finally, silk fibroin (SF) fibers were solubilized in LiBr solution (9.3M) at 60 °C for 4 hours [14] [15] and silk solution was dialyzed against distilled water using cellulose tubes at room temperature for 72 hours, to assure the complete removal of the employed salts. The SF final concentration, calculated by freeze-drying (Modulyo® Edwards Freeze dryer, Kingston, NY) of known SF volumes was about 8% w/v.

2.3 Nanoparticle preparation

Aqueous SF solution was diluted (1.5 % w/v) before carrying out the nanoparticle preparation by desolvation [16]. Briefly, an acetone bath was prepared, maintaining a volume ratio between the considered organic solvent and the SF solution > 75% v/v; SF solution was added drop wise into the acetone, leading to a separation phase and thus to nanoparticle formation (named Silk). Three dialysis cycles were needed to completely remove the employed solvent. Silk were stored at 4 °C or subjected to freeze dried process at $8 \cdot 10^{-1}$ mbar and -50° C for 72 hours for further investigations.

Silk nanoparticles loaded with CXB (Silk/CXB) and loaded with CUR (Silk/CUR) were obtained via the same technique, exploiting their high solubility into acetone. Table 1 reports nanoparticle formulations referred to Silk and Silk/CXB (named Silk/CXB 5 and Silk/CXB 11 considering the different drug loading), while Silk/CUR 1.5 (due to CUR loading) were obtained according to Perteghella S (2017) [13] At least three batches of each formulation have been obtained.

Table 1. Composition and characterization of Silk/CXB nanoparticles: two different drug loadings were achieved by solubilizing different concentrations of CXB into the starting acetone bath. The drug loading, the process yield and the encapsulation efficiency percentages are reported as mean values \pm standard errors (ES).

Nanoparticles	Drug concentration in acetone (mg/ml)	Drug Loading (%) (mean \pm SE)	Process Yield (%) (mean \pm SE)	Encapsulation Efficiency (%) (mean \pm SE)
Silk	0	0	88.46 \pm 7.832	0
Silk/CXB 5	0.1	5.29 \pm 0.308	82.58 \pm 8.388	11.14 \pm 5.847
Silk/CXB 11	0.5	11.40 \pm 0.764	71.62 \pm 10.689	5.14 \pm 1.936

2.4 Characterization of Silk and Silk/CXB

2.4.1 Drug loading

CXB actual loaded amount in silk nanoparticles was evaluated by UV-Vis at 254 nm (CXB maximum absorption wavelength) via a direct spectrophotometer method (Uvikon 860, Kontron Instruments, Switzerland). Briefly, 1 mg of freeze-dried nanoparticles was dissolved in 10 ml of 96 % v/v ethanol, maintaining mild magnetic stirring for fixed times. The total drug content was evaluated from a standard calibration curve ($r^2 > 0.9824$), characterized by a concentration range between $40 \cdot 10^{-3}$ and $10 \cdot 10^{-3}$ mg/ml. Ethanol was considered as blank. Each experiment was performed in triplicate.

Nanoparticle yield (Y%) was evaluated according to the following equation:

$$Y(\%) = \frac{\text{total weight nanoparticles}}{\text{weight of polymer} + \text{weight of CXB}} \times 100$$

The encapsulation efficiency (EE%) was determined as percentage ratio between the actual entrapped drug and the theoretical drug content.

2.4.2 Nanoparticle dimensions and evaluation of polydispersity index

The size distribution of Silk and Silk/CXB 11, including the mean diameter (Z-average) and the polydispersity index (Pdi), was determined by using a Malvern Zetasizer Nano ZSP (Malvern Instruments, Malvern, UK). Samples were sonicated and filtered before carrying out the analysis. All experiments were performed in quintuplicate in distilled water at 25°C.

2.4.3 Morphological evaluation by scanning electron microscopy (SEM)

Nanoparticles were observed using SEM (Zeiss EVO MA10, Carl Zeiss, Oberkochen, Germany). Briefly, freeze-dried samples were gold-sputter coated under argon to render them electrically conductive prior to perform the morphological analysis.

2.4.4 Fourier Transform Infrared (FT-IR) spectroscopy

FT-IR spectra of the lyophilized samples were obtained using a Spectrum One Perkin-Elmer spectrophotometer (Perkin Elmer, Wellesley, MA, USA) equipped with a MIRacle™ ATR device (Pike Technologies, Madison, WI, USA). The IR spectra in transmittance mode were recorded in the spectral region of 650-4000 cm^{-1} with a resolution of 4 cm^{-1} . Each experiment was performed in triplicate.

2.4.5 Differential Scanning Calorimetry (DSC)

Temperature and enthalpy values were measured with a Mettler STARE system (Mettler Toledo, Italy) equipped with DSC81° Module and an Intracooler device for sub-ambient temperature analysis (Jukabo FT 900) on about 3 mg of samples in 40 μL sealed aluminium pans with pierced lid (method: -10-400 $^{\circ}\text{C}$ temperature range; heating rate 10 K min^{-1} ; nitrogen air atmosphere flux 50 mL min^{-1}). The instrument was previously calibrated with Indium, as standard reference. Each experiment was performed in triplicate.

2.4.6 Simultaneous Thermogravimetric Analysis (TGA/DSC 1)

Mass losses were recorded with a Mettler STARE system (Mettler Toledo, Italy) TGA on 3-4 mg samples in 70 μL alumina crucibles with lid (30-400 $^{\circ}\text{C}$ temperature range; heating rate 10 K min^{-1} ; nitrogen air atmosphere flux 50 mL min^{-1}). The instrument was previously calibrated with Indium, as standard reference and experiments were performed at least in triplicate.

2.4.7 In vitro drug release studies

The dialysis technique was applied to investigate the CXB *in vitro* cumulative release [17]. Briefly, a fixed volume of nanoparticle suspension (10 ml), equivalent to 0.04 mg of CXB, was dialyzed (MWCO 12,000–14,000 Da) against an ethanol bath 50 % v/v, maintained under mild magnetic stirring. At each considered time point, fixed volumes of the release medium were withdrawn and replaced by the same amount of fresh medium to ensure sink conditions. The drug concentration was determined via a spectrophotometer method, by reading the withdrawn volume from the release medium at 254 nm.

2.5 Determination of the ROS-scavenging activity by DPPH assay

The ROS-scavenging activity was evaluated by the DPPH (2,2-diphenyl-2-picrylhydrazyl hydrate) assay, according to Chlapanidas and colleagues, with some modifications [18]. Briefly, samples were tested considering three different nanoparticle concentrations (200, 400 and 800 $\mu\text{g/ml}$) and their free drug equivalent concentrations (11, 22 and 44 $\mu\text{g/ml}$ for CXB; 3, 6 and 12 $\mu\text{g/ml}$ for CUR) (see Table 2).

Table 2. Relative amount of free drugs (CXB, CUR and their mixture CXB-CUR) corresponding to their equivalent concentration loaded in nanoparticles. The CXB-CUR physical mix contains 50% of each considered active.

Free drugs	Nanoparticle concentrations		
	200 µg/ml	400 µg/ml	800 µg/ml
CXB	11 µg/ml	22 µg/ml	44 µg/ml
CUR	3 µg/ml	6 µg/ml	12 µg/ml
CXB-CUR	5.5 + 1.5 µg/ml	11 + 3 µg/ml	22 + 6 µg/ml

Analysis was also performed on the physical mixture of Silk/CXB 5 and Silk/CUR 1.5 or CXB-CUR with a weight ratio 50:50. Samples were dissolved in 70% v/v methanol under magnetic stirring. 50 µl of each sample were mixed with 1950 µl of methanolic solution of DPPH (stock solution 1 mM) and incubated at room temperature for 60 minutes avoiding light exposure. Finally, samples were centrifuged at 3000 g for 10 minutes and the scavenging activity was analyzed by measuring the optical density (OD) at 515 nm.

As negative control, a reaction mixture composed by 50 µl of 70% v/v methanol and 1950 µl of DPPH solution was prepared.

The percentage of ROS-scavenging activity was calculated according to the following formula:

$$\text{Antioxidant activity (\%)} = \frac{(\text{OD blank} - \text{OD sample})}{\text{OD blank}} \times 100$$

where OD blank is the absorbance of negative control and OD sample is that of samples.

2.6 Hemolytic assay

Hemolytic assay was carried out to study the toxicity of nanoparticles and free drugs (Silk, Silk/CXB 5 and CXB) on red blood cells (RBCs). Fresh human blood samples were collected from consent healthy individuals (female blood) and centrifuged at 1500 g for 5 min, to separate RBCs from plasma serum. The obtained pellet containing RBCs was washed twice with PBS without Ca^{2+} and Mg^{2+} (pH = 7.4). The RBC suspension was treated with 200-800 µg/ml of freeze-dried nanoparticles or with the equivalent free drug concentration, previously re-suspended in PBS, and incubated at room temperature for 60 min. The volume ratio between RBCs and tested samples was set at 90:10. RBCs treated with PBS were used as negative control, while RBCs treated with distilled water were used as positive control (considered as 100% of hemolysis). After incubation, samples were centrifuged at 3000 g for 10 minutes. The

recovered supernatants were analyzed by reading their OD at 540 nm (Synergy HT, Biotech, United Kingdom), which corresponds to the absorption maxima of hemoglobin. Hemolysis % was evaluated with the follow equation:

$$\text{Hemolysis (\%)} = \frac{(\text{OD sample} - \text{OD blank})}{\text{OD positive CTRL}} \times 100$$

where OD sample is the absorbance of samples, OD blank is the absorbance of negative control (RBCs treated with PBS) and OD positive CTRL is the optical density RBCs treated with distilled water.

2.7 In vitro biological assays

2.7.1 Knee tissue collection and primary human articular chondrocytes isolation and culture

Cartilage samples, obtained during arthroplasty surgery, were cut into 1-2 mm³ segments and washed three times with PBS before being digested with trypsin-EDTA 1X, for 30 minutes at 37°C, 5% CO₂, followed by overnight incubation with 200 IU type IA collagenase. The resulting cell suspension was filtered using 70 µm nylon meshes to completely remove undigested tissue and cells were centrifuged at 300 g for 5 min. Obtained chondrocytes were seeded onto flasks (7,000 cells/cm²) with Dulbecco's Modified Eagle's Medium High Glucose (DMEM-HG) enriched in 10% fetal bovine serum (FBS), penicillin (100 IU/ml), streptomycin (100 µg/ml), amphotericin B (2.5 µg/ml), Fibroblast Growth Factor-2 (FGF-2, 10 µg/ml) and Transforming Growth Factor beta1 (TGF-β1, 10 µg/ml) at 37°C, 5% CO₂. Each cell line was used until third passage of culture.

2.7.2 Chondrocyte stimulation and treatments

Chondrocytes were seeded in 24-well plates with a density of 1.25*10⁴ cells/cm² and cultured for 24 hours; then, cells were stimulated with IL-1β (10 ng/ml) in FBS deprived medium, to reproduce the mechanisms involved in OA raise, and simultaneously treated with samples for 72 hours [19]. Freeze-dried nanoparticle formulations were previously re-suspended in cell culture medium and sonicated for 1 hour before carrying out the incubation, while free drugs were solubilized in DMSO (2 mg/ml) and diluted in cell culture medium, achieving the same drug concentration loaded in the considered nanosystems. For biological tests, Silk, Silk/CXB 5, Silk/CUR 1.5 and Silk/CXB-CUR physical mixture were considered at three different concentrations (200, 400 and 800 µg/ml). Notably, the physical mixture concentration is obtained by mixing a half amount of both Silk/CXB 5 and Silk/CUR 1.5.

Supernatants were collected and stored at -80°C for further enzyme-linked immunosorbent assay (ELISA), while nitric oxide (NO) release by Griess method was detected immediately on fresh supernatants.

2.7.3 Cell viability

Cellular viability was examined using the 3-(4,5-dimethylthiazol-2-yl)-2,5-diphenyl-tetrazolium bromide (MTT) assay on un-stimulated chondrocytes, cultured without FBS, after 72 hours of incubation with samples, at the same concentrations reported in paragraph 2.7.2. Briefly, 100 µL of MTT solution (0.5 mg/ml) was added to each well for 3 hours. After the incubation, MTT-medium was removed and formazan crystals were solubilized with 100 µl of DMSO in each well, mixing the solution to completely dissolve the reacted dye. The OD was measured using a microplate reader (Synergy HT) at 570 nm and 670 nm (reference wavelength). Cell viability (%) was calculated as follows: $100 \times (\text{ODs}/\text{ODc})$, where ODs represents the mean value of the measured optical density of the tested sample and ODc is the mean value of the measured optical density of untreated cells (control).

2.7.4 Determination of nitrite levels (NO) by Griess

The NO released in cell culture supernatants was detected by using the Griess method, following the manufacturer's instructions. IL-1β stimulated cells, not treated with nanoparticles were considered as positive CTRL, while untreated chondrocytes as negative CTRL.

2.7.5 RANTES and IL-6 determination by ELISA

The secretion of IL-6 and RANTES by human articular chondrocytes was evaluated using a quantitative ELISA kits, according to manufacturer's instructions.

2.8 Statistical analysis

Raw data of *in vitro* drug release, antioxidant activity, hemolytic assay, cellular viability and *in vitro* biological assays (NO, IL-6 and RANTES) were processed using STATGRAPHICS XVII (Statpoint Technologies, Inc., Warrenton, Virginia, U.S.) and a linear generalized Analysis of Variance model (ANOVA) was used to evaluate the data. The *post-hoc* LSD's test for multiple comparisons was employed to analyze the differences between groups. Unless differently specified, data are expressed as mean ± standard deviation. The statistical significance was fixed at $p \leq 0.05$.

3. Results and Discussion

In this research paper, we compared the anti-inflammatory activity of two different actives: CUR, a natural polyphenol extracted from the rhizome of *Curcuma Longa*, characterized by an anti-inflammatory and antioxidant activity exploited in the treatment of chronic disorders, and

CXB, a sulfonamide synthetic compound belonging to the COX-2 selective inhibitors class, which is actually employed as the “first choice” for OA treatment. Albeit CXB is still considered as the best therapeutic option in treating OA pain, its long-term use in high-dosage could trigger severe cardio-toxicity and renal complications [20]. Conversely, CUR showed the ability to attenuate the inflammatory condition related to OA [21] [22].

Unfortunately, both drugs suffer from low solubility, thus showing low bioavailability, after oral administration, thus limiting their therapeutic applications. For this reason, their encapsulation should be actuated to trigger a perceivable biological response, limiting their cytotoxic effects.

Based on our knowledge, it is the first time that CXB has been nano-encapsulated in Silk, even if it has been loaded in other nanosystems including liposomes [23], solid lipid nanoparticles [24] and micelles [25]. Silk and Silk/CXB formulations were obtained via desolvation method, exploiting the marked solubility of CXB in acetone. In particular, different loadings were achieved (Table 1) with respect to the starting drug concentration solubilized in the acetone bath.

The process yield (%) ranged from 71.62 ± 10.689 to 88.46 ± 7.832 , while the EE (%) ranged from 5.14 ± 1.936 to 11.14 ± 5.847 (Table 1).

Silk and Silk/CXB 11 showed a Z-average diameter of about 100 nm (Figure 1A), characterized by a monomodal distribution, confirming our previous results [13]. The Pdi was about 0.15, indicating a highly homogeneous population of nanoparticles. SEM morphological investigation (reported for Silk/CXB 11, Figure 1B) showed a spherical shape characterizing the nanosystems. As already reported for Silk/CUR [13], the encapsulation of the active did not change the shape of nanosystems. The particle size distribution and morphology of the obtained nanoparticles (Figure 1) were in agreement with that reported by other researchers: the use of acetone allows to obtain nanoparticles with a diameter of about 100 nm and a defined spherical geometry [26] [16] [24].

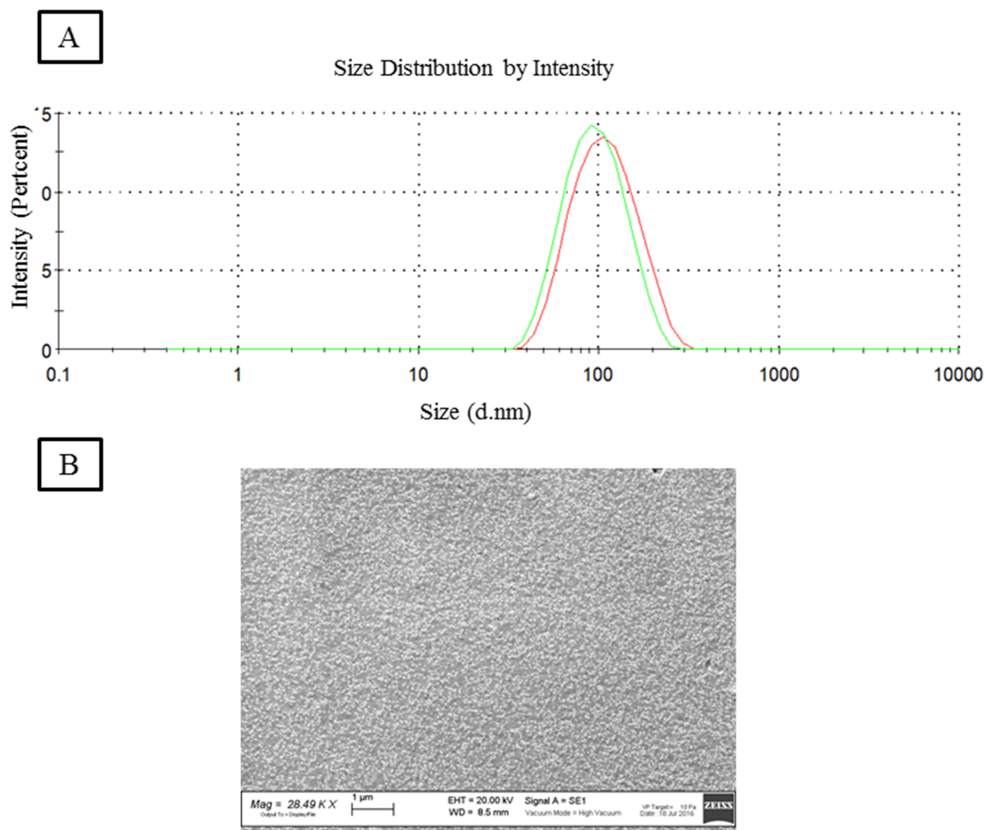


Figure 1. Particle size distribution (A) and morphology obtained by scanning electron microscopy (B) of Silk/CXB 11. Scale bar represents 1 μm .

We chose desolvation via acetone, due to the nanoparticle size achieved exploiting the reaction occurring between SF chains in presence of organic solvents. The exposure of SF chains to acetone, allowed the silk conformational change, increasing the presence of β -sheet domains [27] [28]. Similarly, we prepared Silk/CUR [13], obtaining lower drug loading than Silk/CXB even if the starting conditions were preserved. This could be probably due to the different interaction occurring between SF and the considered drugs (CUR and CXB): in fact, SF has a lot of functional groups (carboxyl and amino) able to differently interact and create chemical reactions with the encapsulated molecule during nanoparticle biogenesis [29]. Other anti-inflammatory drugs, such as ibuprofen (neutral) and its sodium salt (negative) for example, were successfully loaded in Silk by charge-charge interactions; obviously, the employment of positive charge molecules, such as Doxorubicin, led to higher drug loading considering that Silk retain a negative charge [30].

The low EE% achieved for CXB in Silk could be justified by the fact that the obtained nanoparticles were very small size (≈ 100 nm); in fact, as described by some authors, a size lower than 100 nm is related to high surface to volume ratio with a higher probability of drug loss in the external medium. Moreover, this parameter is strictly influenced by the nature of both nanoparticles and encapsulating active and the method of drug loading employed. Also Lozano-Perez achieved a low EE% of resveratrol (13%) in Silk, obtaining anyway effective nanoparticles for both *in vitro* and *in vivo* colitis models [31].

The FTIR analysis was carried out to confirm the effective nanoencapsulation of the considered active (CXB) into nanosystems and to assure the conformational change of SF. In the Figure 2A are reported the FT-IR spectra of CXB, Silk, and Silk/CXB at two different drug concentrations, 5% and 11%, respectively. In particular, the IR spectrum of SF showed characteristic peaks that can be identified in the spectra region of amide I (at about 1620 cm^{-1} , C=O stretching), amide II (at about 1520 cm^{-1} , N-H bending) and amide III (at about 1230 cm^{-1} , C-N and N-H functionalities), in all tested formulations (Figure 2). The FTIR spectrum of CXB showed the characteristic S=O symmetric and asymmetric stretching in the region 1130 and 1345 cm^{-1} , and the bands of N-H stretching vibration of SO_2NH_2 group at 3330 and 3231 cm^{-1} . The typical absorption bands of CXB are completely hidden for Silk/CXB 5, meanwhile they started to appear in Silk/CXB 11, related to its higher drug loading. To better compare the spectra of unloaded and loaded nanoparticles, the region between 1500 and 700 cm^{-1} was amplified (Figure 2B). This has allowed to identify some typical bands of CXB (1345 and 1133 cm^{-1}) only in the spectrum of nanoparticles with higher active content. FT-IR data were supported by thermal analysis.

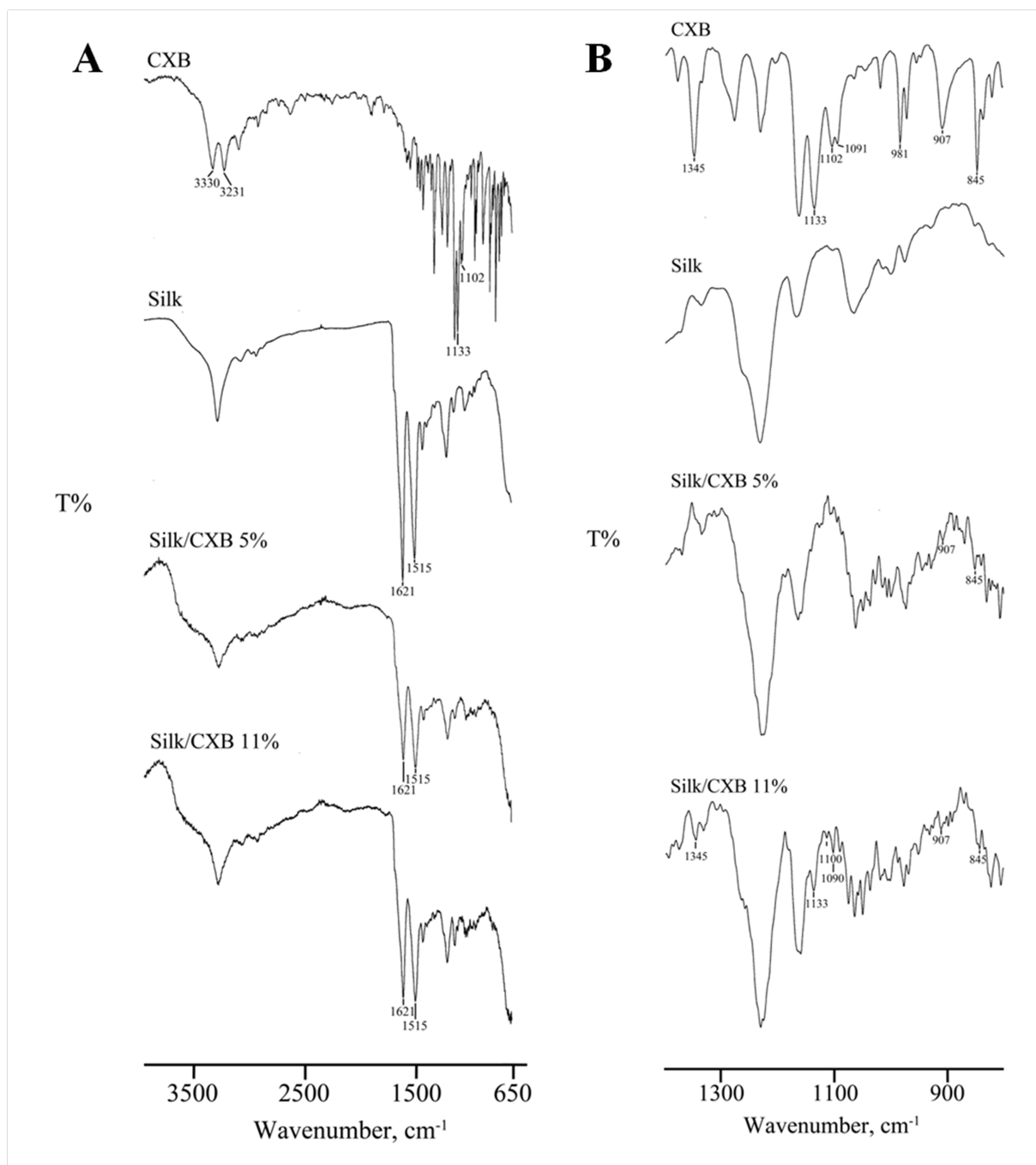


Figure 2. Fourier transform infrared (FT-IR) spectra of CXB, Silk, Silk/CXB5 and Silk/CXB11 in the spectral region of $4000 - 800 \text{ cm}^{-1}$ (A) and the region where typical CXB bands appeared ($1400 - 800 \text{ cm}^{-1}$) (B).

Concerning with DSC analysis, CXB is an anhydrous crystalline compound characterized by melting endothermic peak at $162.6 \pm 0.4 \text{ }^\circ\text{C}$ (Tonset, $m = 161.1 \pm 0.2 \text{ }^\circ\text{C}$; $\Delta H_m = 92 \pm 1 \text{ J g}^{-1}$) with a mass loss recorded in TGA (curve not reported) starting at around $300 \text{ }^\circ\text{C}$, due to drug decomposition. The unloaded Silk nanoparticles showed a typical profile of amorphous sample

with an endothermic effect at around 270 °C, associated to TGA mass loss, due to decomposition. As in the FT-IR spectra, the presence of CXB was observed in the thermal trace of nanoparticles at the higher drug content, as a small endothermic peak at 161.2 ± 0.6 °C. The broad endothermic effects between 30 and 100 °C in the DSC of Silk/CXB nanoparticles were due to dehydration (mass loss in TGA analyses of about $5.7 \pm 0.3\%$) (figure not shown).

The cumulative profiles of CXB released from nanoparticles showed that both time and formulation were statistically significant ($p < 0.0001$). No differences were observed about CXB release from both formulations (Silk/CXB 5 and Silk/CXB 11) within three hours, meanwhile, after that time, a different release was highlighted (Figure 3). A higher amount of CXB was released by Silk/CXB 11, reaching about 40% after 24 hours; conversely, only 14% of CXB was released by Silk/CXB 5 in the same frame time. Surprisingly, both Silk/CXB formulations achieved a plateau conditions after 24 hours, albeit their different drug loading (Figure 3).

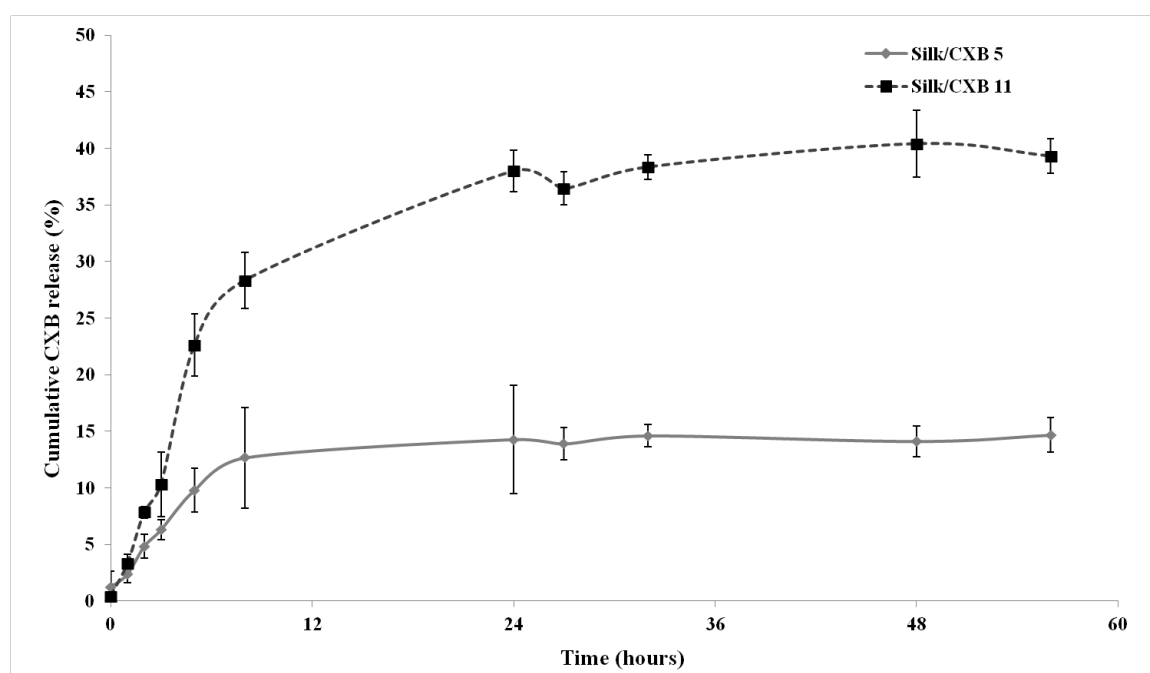


Figure 3. *In vitro* CXB release profiles from nanoparticles by a dialysis method in ethanol 50 % v/v at room temperature. Each data is expressed as mean value \pm standard deviations of at least three independent experiments.

CXB release profiles of both considered formulations (Silk/CXB 5 and Silk/CXB 11) were characterized by a biphasic profile, in which the first phase of burst release is principally due to drug desorption from the surface of nanosystems or by the diffusion of the drug portion entrapped near the nanosystem surface [17] [32].

The degradation of articular chondrocytes is governed by a combination of several mechanisms including an increasing in ROS production, leading to an imbalance between oxidant and antioxidant systems. For this reason, employing therapeutic molecules with antioxidant properties could allow to ameliorate the symptoms of OA or to prevent structural changes in damaged cartilage [33].

Briefly, different concentrations of nanoparticles (Silk, Silk/CUR 1.5, Silk/CXB 5 or Silk/CXB-CUR) or the equivalent free drug (CUR, CXB or CXB-CUR) (Table 2) were considered. ANOVA results showed that both formulation and concentration were statistically significant ($p < 0.0001$); in particular, a dose related response was appreciated for Silk/CUR 1.5, CUR and Silk/CXB-CUR (Figure 4).

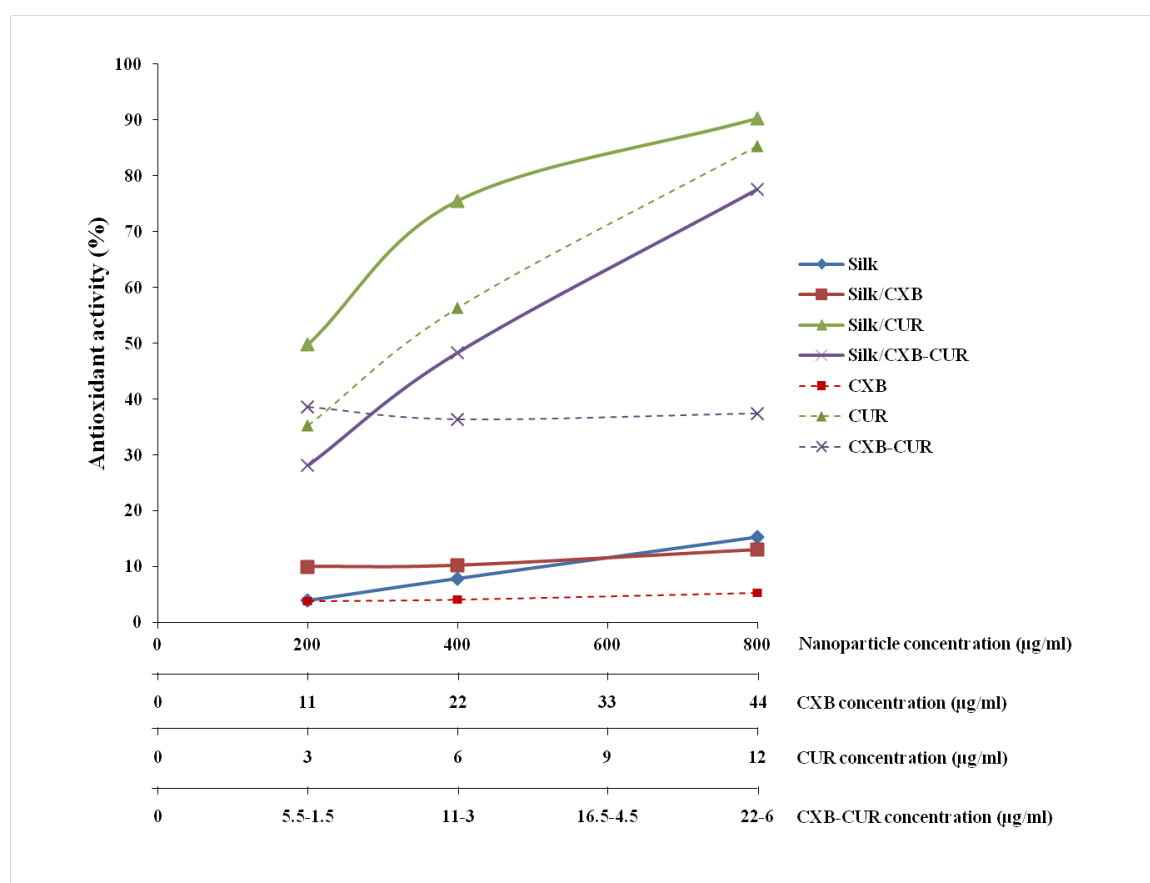


Figure 4. Antioxidant activity (%) of nanosystems (solid lines) and free drugs (dotted lines), correlated by the same colors (blue for Silk, red for Silk/CXB 5 and CXB, green for Silk/CUR 1.5 and CUR and purple for Silk/CXB-CUR and CXB-CUR). X axis reports the nanoparticle concentration and the equivalent drug concentration encapsulated into nanosystems. Data are reported as mean values of at least three independent experiments; standard deviations are not showed to better understand the graph.

The nanoencapsulation of CUR increased its antioxidant properties, reaching 90% with the higher concentration considered (800 µg/ml), due to the slightly antioxidant activity of SF. No statistical difference was observed among Silk/CXB 5, CXB and Silk, which showed a ROS scavenging activity lower than 10% [34]. Finally, when considering CXB-CUR physical mix, an antioxidant activity of 40% was observed independently by sample concentration (Figure 4). Our results confirmed CUR strong antioxidant property, both free and nano-encapsulated in Silk [35]. CXB does not possess a scavenging activity, but probably it could influence the expression of anti or pro-oxidant enzymes [47]. Surprisingly, the physical combination of Silk/CXB-CUR allowed to obtain a similar, dose-response, antioxidant activity of what reported for Silk/CUR 1.5 and CUR. This could be due to a synergism between the two compounds, even if, based on the obtained results, the main anti-oxidant effect is exerted by CUR.

Nanoparticles tested at 200 and 400 µg/ml showed a high hemocompatibility, meanwhile this decreased when they were employed at 800 µg/ml; this behavior was observed for both Silk and Silk/CXB 5. Conversely, CXB showed a hemotoxicity at all the considered concentrations ($p < 0.0001$). The nano-encapsulation of CXB into Silk dramatically reduced its hemotoxicity, as already reported for paclitaxel loaded chitosan nanosystems [36].

In order to reproduce the typical environment of OA condition, an *in vitro* model, based on human articular chondrocytes stimulated with IL-1 β , was created to test the efficacy of each nanoparticle formulation. In fact, IL-1 β , an inhibitor of collagen II synthesis and proteoglycan production and a promoter of IL-6, NO and ROS secretion, is commonly employed to effectively mimic the cartilage degradation [37]. Concerning cartilage degradation, NO promotes chondrocyte apoptosis, the release of pro-inflammatory cytokines and the reduction of both collagen II and proteoglycan synthesis [33]. IL-6 plays a pivotal role in inflammatory pathway by activating T cells and leading to pro-inflammatory chemokines production [38]. Finally, also RANTES is a key mediator in inflammatory conditions; it is expressed by normal chondrocytes both at messenger RNA (mRNA) and at protein levels, and this effect is highlighted in OA or IL-1 β stimulated chondrocytes [39] [40]. The role of RANTES was understood in 1997, when Plater-Zyberk observed that the injection of a CC receptor antagonist, ameliorated the pathological condition of arthritic mice [41]. Until today, very few studies evaluated RANTES in OA conditions [42]. For example, Alaeddine in 2001 highlighted RANTES influence on gene expression of other inflammatory mediators directly involved in cartilage degradation [1].

In primis, cell mitochondrial activity was measured by MTT on chondrocytes cultured with nanoparticles or with their equivalent free drugs (Table 2) to evaluate the cytotoxicity of considered samples with respect to not treated cells. ANOVA results highlighted that both formulations and concentrations were statistically significant ($p < 0.0001$). Drug nanoencapsulation avoided cytotoxicity phenomena, showing viability higher than 70% for all nanoparticle formulations, independently by the concentration employed; conversely, free drugs affected cellular viability in relation to their concentration employed. A special attention should be given to CXB which dramatically decreased chondrocyte viability when employed at 22 or 44 $\mu\text{g/ml}$, reaching a viability lower than 3%. Conversely, CUR exerted a cytotoxic effect only when employed at 12 $\mu\text{g/ml}$. Consequently to these results, only nanoparticles at all concentrations were considered for succeeding analyses.

In treating OA, cytotoxic events must be avoided because an increase in IL-1 β secretion leads to a higher apoptotic events % [43]. Tripodo et al. demonstrated that the incorporation of CUR in micelles avoided free drug cytotoxic phenomena, which were observed when employing “naked” CUR [44]. Also CXB showed severe cytotoxic effects on several cellular lineages, reaching a viability of 50% when employed at 100 μM [45].

As reported in Figure 5A, the treatment with IL-1 β (without nanoparticles and considered as positive control) increased the production of NO ($21.09 \pm 2.561 \mu\text{M}$) with respect to unstimulated cells ($2.63 \pm 3.639 \mu\text{M}$), confirming the efficacy of the *in vitro* model.

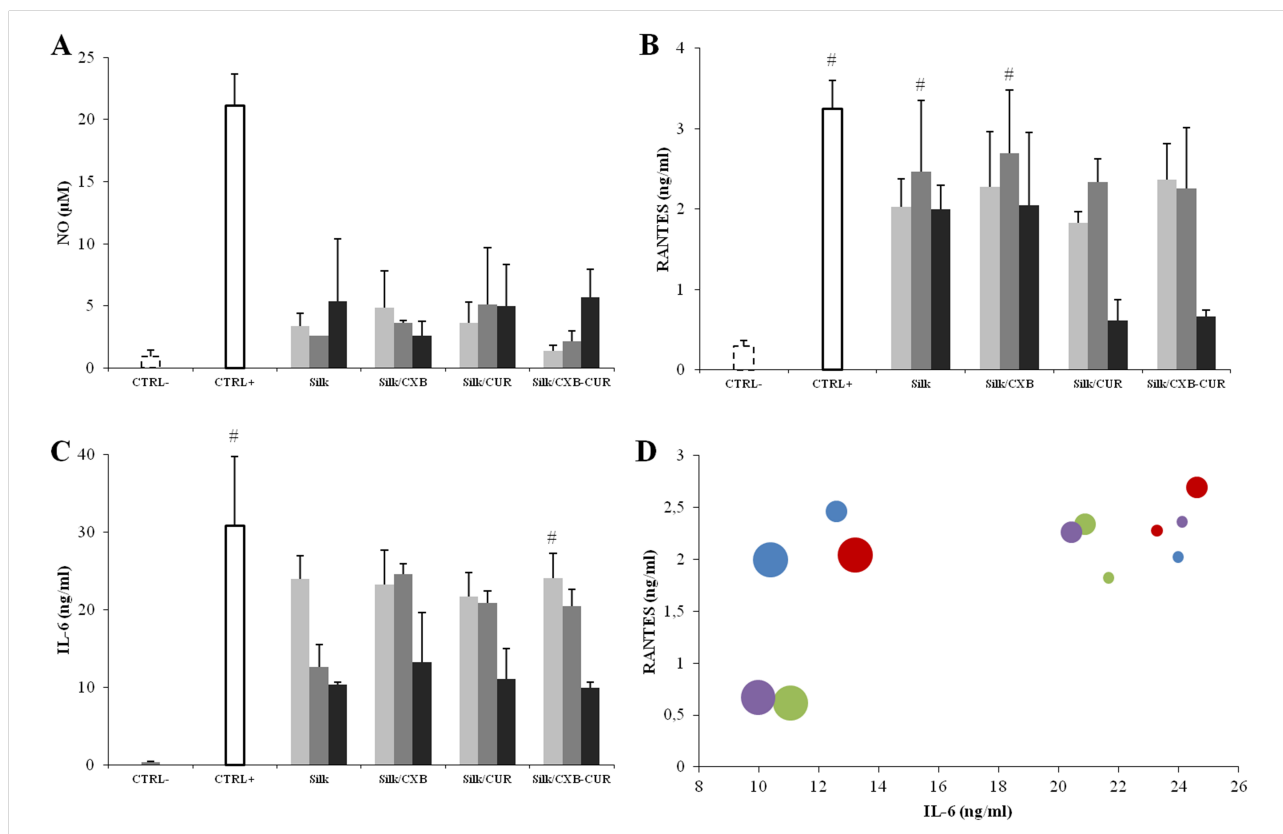


Figure 5. Effects of nanoparticle formulations on IL-1 β induced NO (A), RANTES (B), IL-6 (C) and the correlation between IL-6 and RANTES (D). Data are expressed as mean values \pm standard deviations (n=3). Different grey intensities correspond to different nanoparticle concentrations: light grey 200 μ g/ml, medium grey 400 μ g/ml and dark grey 800 μ g/ml. Positive CTRL (solid line) is represented by IL-1 β stimulated cells (not treated with samples), while negative CTRL (dotted line) is composed of un-stimulated cells. In figure D the relationship between IL-6 and RANTES is represented by different colored circles, related to different nanoparticle samples (Silk – blue, Silk/CXB – red, Silk/CUR – green and Silk/CXB-CUR purple); the diameter of the circles is proportional to the nanoparticle concentration: the larger circles correspond to the 800 μ g/mL, the intermediate to 400 μ g/mL, while the smaller circles to 200 μ g/mL.

indicates no significant differences between groups ($p < 0.05$).

The inhibition of the secretion of 3 mediators of the inflammatory pathway, in particular, NO, IL-6 and RANTES, was studied. We observed that the secretion of NO, RANTES and IL-6 was significantly reduced ($p < 0.0001$) by all nanoparticles, with a dose-response observed only for IL-6 production. This confirmed the nanoparticle effective anti-inflammatory activity, independently by their encapsulated active. Silk/CXB reduced NO levels in inflamed chondrocytes, without a significant effect of the nanoparticle concentration. Silk/CXB-CUR at the concentrations of 200 and 400 μ g/ml decreased NO levels, reaching an effect comparable to that observed for not-treated cells. Notably, Silk showed the same efficacy in decreasing NO

levels with respect to loaded nanoparticles, thus showing an intrinsic anti-inflammatory activity (Figure 5A).

ANOVA analysis underlined that both formulation and concentration were statistically significant for RANTES secretion ($p < 0.0001$); the RANTES levels were significantly reduced by all nanoparticle formulations. In particular, Silk/CUR and Silk/CXB-CUR, incubated at the concentration of 800 $\mu\text{g/ml}$, showed a marked reduction of RANTES (lower than 1 ng/ml) with respect to the other considered groups (Figure 5B).

Concerning the production of IL-6 by stimulated chondrocytes, ANOVA results evidenced a dose-response for all nanoparticles, with a marked effect when considering the higher concentration (800 $\mu\text{g/ml}$) ($p < 0.0001$) as reported in Figure (Figure 5C). Similarly to NO secretion, the amount of IL-6 significantly decreased when employing Silk, highlighting its anti-inflammatory potential; in particular the inhibition of IL-6 production was similarly detected with Silk at 400 $\mu\text{g/ml}$ and all other nanoparticles at the higher concentration (800 $\mu\text{g/ml}$) (Figure 5C).

In Figure 5D the relationship between IL-6 and RANTES is reported (Figure 5D). Nanoparticles, at the higher concentration (800 $\mu\text{g/ml}$), were able to decrease both IL-6 and RANTES production, which expression is regulated by the PKC δ /c-Src/c-Jun and AP-1 signaling pathways, as demonstrated by Tang and colleagues in human synovial fibroblasts [46].

The physical mixture of Silk/CXB and Silk/CUR decreased the production of all the considered markers in stimulated chondrocytes, with an effect comparable to that of un-stimulated cells. This effect can be explained as the result of their synergism, already tested in different therapeutic fields. For example, Gugulothu evaluated the combination between CUR and CXB within pH sensitive nanoparticles for the treatment of ulcerative colitis, showing a synergistic activity. CXB-CUR nano-encapsulation avoided their overall cytotoxicity phenomena, enhancing their therapeutic action [47]. Moreover, the presence of CUR allowed to reduce the CXB amount, and thus its related severe side effects. CUR was able to potentiate CXB activity by inhibiting in different way the expression of both COX-2 and prostaglandin E2 [35]. This synergism was also observed in the treatment of colorectal cancer cells, highlighting an inhibitory effect on cellular growth when using both drugs [48]. Moreover, CUR is able to reduce iNOS and NO radicals in lipopolysaccharide stimulated rats [49], both when employed as free or encapsulated in solid lipid nanoparticles [50].

Silk showed an anti-inflammatory activity comparable to that of Silk/CXB and Silk/CUR in our *in vitro* model, highlighting its great potential in treating inflammatory diseases. This effect was reported in several biomedical fields: SF peptides, obtained during biodegradation, are the main effectors of anti-inflammatory property [51] [52]. SF cannot be considered anymore as an inert polymer, but it must be listed as a “real” active principle ingredient able to effectively inhibit the expression of pro-inflammatory markers, with suitable therapeutic application in inflammatory diseases, as confirmed by previous observations [31].

Conclusions

This study supported the efficacy of the nanotechnological approach avoiding hemolysis and cytotoxic effects on human articular chondrocytes. We demonstrated that silk fibroin represents an active compound able to significantly reduce the secretion of inflammatory mediators including NO, IL-6 and RANTES with an effect comparable to that of nano-encapsulated CXB, which is considered as the first drug choice for OA treatment. Notably, promising results were obtained when employing the physical mixture of Silk/CXB-CUR, due to a synergistic activity between the two active principles for the treatment of osteoarthritis. Silk nanosystems could be considered as an innovative treatment for OA conditions.

Authors contribution

BC, EB, SP, and MLT conceived of the study, participated in its design and coordination. BC, and TC wrote the first draft of the manuscript; SP, EL, TC and GT wrote the final paper; BC and EB carried out the nanoparticle production. SP performed the experiments on cell cultures. MS and LC carried out FTIR and TGA. GB performed SEM analysis. MLT performed the statistical analysis. All authors revised and approved the final manuscript.

Acknowledgments

Authors thank Nembri Industrie Tessili S.r.l. (Capriolo (BG), Italy) for certified *Bombyx mori* cocoons, Prof. Sergio Schinelli and Dott. Mayra Paolillo (Drug Sciences Dept., Pavia University, Italy) for willingness on the use of Synergy HT (BioTek).

Conflict of interest disclosure

The authors declare no conflict of interest in this work.

References

- [1] N. Alaaeddine, T. Olee, S. Hashimoto, L. Creighton-Achermann, M. Lotz, Production of the chemokine RANTES by articular chondrocytes and role in cartilage degradation, *Arthritis and Rheumatism*, 44 (2001) 1633-1643.
- [2] F.E. Silverstein, G. Faich, J.L. Goldstein, L.S. Simon, T. Pincus, A. Whelton, R. Makuch, G. Eisen, N.M. Agarwal, W.F. Stenson, A.M. Burr, W.W. Zhao, J.D. Kent, J.B. Lefkowitz, K.M. Verburg, G.S. Geis, Gastrointestinal toxicity with celecoxib vs nonsteroidal anti-inflammatory drugs for osteoarthritis and rheumatoid arthritis - The CLASS study: A randomized controlled trial, *Jama-Journal of the American Medical Association*, 284 (2000) 1247-1255.
- [3] E.J. Topol, Arthritis medicines and cardiovascular events - "House of coxibs", *Jama-Journal of the American Medical Association*, 293 (2005) 366-368.
- [4] C.H. Hennekens, S. Borzak, Cyclooxygenase-2 inhibitors and most traditional nonsteroidal anti-inflammatory drugs cause similar moderately increased risks of cardiovascular disease, *Journal of Cardiovascular Pharmacology and Therapeutics*, 13 (2008) 41-50.
- [5] B.B. Aggarwal, K.B. Harikumar, Potential therapeutic effects of curcumin, the anti-inflammatory agent, against neurodegenerative, cardiovascular, pulmonary, metabolic, autoimmune and neoplastic diseases, *International Journal of Biochemistry & Cell Biology*, 41 (2009) 40-59.
- [6] O. Naksuriya, S. Okonogi, R.M. Schiffelers, W.E. Hennink, Curcumin nanoformulations: A review of pharmaceutical properties and preclinical studies and clinical data related to cancer treatment, *Biomaterials*, 35 (2014) 3365-3383.
- [7] S.K. Paulson, M.B. Vaughn, S.M. Jessen, Y. Lawal, C.J. Gresk, B. Yan, T.J. Maziasz, C.S. Cook, A. Karim, Pharmacokinetics of celecoxib after oral administration in dogs and humans: Effect of food and site of absorption, *Journal of Pharmacology and Experimental Therapeutics*, 297 (2001) 638-645.
- [8] S. Onoue, S. Yamada, H.-K. Chan, Nanodrugs: pharmacokinetics and safety, *International Journal of Nanomedicine*, 9 (2014) 1025-1037.
- [9] K. Roy, R.K. Kanwar, J.R. Kanwar, Molecular targets in arthritis and recent trends in nanotherapy, *International Journal of Nanomedicine*, 10 (2015) 5407-5420.
- [10] E. Nogueira, A. Gomes, A. Preto, A. Cavaco-Paulo, Update on Therapeutic Approaches for Rheumatoid Arthritis, *Current Medicinal Chemistry*, 23 (2016) 2190-2203.

- [11] B. Kundu, R. Rajkhowa, S.C. Kundu, X. Wang, Silk fibroin biomaterials for tissue regenerations, *Advanced Drug Delivery Reviews*, 65 (2013) 457-470.
- [12] D. Yao, H. Liu, Y. Fan, Silk scaffolds for musculoskeletal tissue engineering, *Experimental Biology and Medicine*, 241 (2016) 238-245.
- [13] S. Perteghella, B. Crivelli, L. Catenacci, M. Sorrenti, G. Bruni, V. Necchi, B. Vigani, M. Sorlini, M.L. Torre, T. Chlapanidas, Stem cell-extracellular vesicles as drug delivery systems: New frontiers for silk/curcumin nanoparticles, *International journal of pharmaceutics*, 520 (2017) 86-97.
- [14] D.N. Rockwood, R.C. Preda, T. Yucel, X. Wang, M.L. Lovett, D.L. Kaplan, Materials fabrication from *Bombyx mori* silk fibroin, *Nature Protocols*, 6 (2011) 1612-1631.
- [15] D.M. Phillips, L.F. Drummy, D.G. Conrady, D.M. Fox, R.R. Naik, M.O. Stone, P.C. Trulove, H.C. De Long, R.A. Mantz, Dissolution and regeneration of *Bombyx mori* Silk fibroin using ionic liquids, *Journal of the American Chemical Society*, 126 (2004) 14350-14351.
- [16] F.P. Seib, G.T. Jones, J. Rnjak-Kovacina, Y. Lin, D.L. Kaplan, pH-Dependent Anticancer Drug Release from Silk Nanoparticles, *Advanced Healthcare Materials*, 2 (2013) 1606-1611.
- [17] J. Shaikh, D.D. Ankola, V. Beniwal, D. Singh, M.N.V.R. Kumar, Nanoparticle encapsulation improves oral bioavailability of curcumin by at least 9-fold when compared to curcumin administered with piperine as absorption enhancer, *European Journal of Pharmaceutical Sciences*, 37 (2009) 223-230.
- [18] T. Chlapanidas, S. Farago, G. Luccioni, S. Perteghella, M. Galuzzi, M. Mantelli, M.A. Avanzini, M.C. Tosca, M. Marazzi, D. Vigo, M.L. Torre, M. Faustini, Sericins exhibit ROS-scavenging, anti-tyrosinase, anti-elastase, and in vitro immunomodulatory activities, *International Journal of Biological Macromolecules*, 58 (2013) 47-56.
- [19] C. Cannava, S. Tommasini, R. Stancanelli, V. Cardile, F. Cilurzo, I. Giannone, G. Puglisi, C.A. Ventura, Celecoxib-loaded PLGA/cyclodextrin microspheres: Characterization and evaluation of anti-inflammatory activity on human chondrocyte cultures, *Colloids and Surfaces B-Biointerfaces*, 111 (2013) 289-296.
- [20] L.J. Marnett, The COXIB Experience: A Look in the Rearview Mirror, *Annual Review of Pharmacology and Toxicology*, 49 (2009) 265-290.
- [21] D.-O. Moon, M.-O. Kim, Y.H. Choi, Y.-M. Park, G.-Y. Kim, Curcumin attenuates inflammatory response in IL-1 beta-induced human synovial fibroblasts and collagen-induced arthritis in mouse model, *International Immunopharmacology*, 10 (2010) 605-610.

- [22] Z. Zhang, D.J. Leong, L. Xu, Z. He, A. Wang, M. Navati, S.J. Kim, D.M. Hirsh, J.A. Hardin, N.J. Cobelli, J.M. Friedman, H.B. Sun, Curcumin slows osteoarthritis progression and relieves osteoarthritis-associated pain symptoms in a post-traumatic osteoarthritis mouse model, *Arthritis Research & Therapy*, 18 (2016).
- [23] E. Moghimipour, S. Handali, Utilization of thin film method for preparation of celecoxib loaded liposomes, *Advanced pharmaceutical bulletin*, 2 (2012) 93-98.
- [24] S. Sharma, S. Bano, A.S. Ghosh, M. Mandal, H.-W. Kim, T. Dey, S.C. Kundu, Silk fibroin nanoparticles support in vitro sustained antibiotic release and osteogenesis on titanium surface, *Nanomedicine-Nanotechnology Biology and Medicine*, 12 (2016) 1193-1204.
- [25] D. Mandracchia, G. Tripodo, A. Trapani, S. Ruggieri, T. Annese, T. Chlapanidas, G. Trapani, D. Ribatti, Inulin based micelles loaded with curcumin or celecoxib with effective anti-angiogenic activity, *European Journal of Pharmaceutical Sciences*, 93 (2016) 141-146.
- [26] Y.-Q. Zhang, W.-D. Shen, R.-L. Xiang, L.-J. Zhuge, W.-J. Gao, W.-B. Wang, Formation of silk fibroin nanoparticles in water-miscible organic solvent and their characterization, *Journal of Nanoparticle Research*, 9 (2007) 885-900.
- [27] C. Weber, C. Coester, J. Kreuter, K. Langer, Desolvation process and surface characterisation of protein nanoparticles, *International Journal of Pharmaceutics*, 194 (2000) 91-102.
- [28] S. Azarmi, Y. Huang, H. Chen, S. McQuarrie, D. Abrams, W. Roa, W.H. Finlay, G.G. Miller, R. Lobenberg, Optimization of a two-step desolvation method for preparing gelatin nanoparticles and cell uptake studies in 143B osteosarcoma cancer cells, *Journal of Pharmacy and Pharmaceutical Sciences*, 9 (2006) 124-132.
- [29] J. Qu, Y. Liu, Y. Yu, J. Li, J. Luo, M. Li, Silk fibroin nanoparticles prepared by electrospray as controlled release carriers of cisplatin, *Materials Science & Engineering C-Materials for Biological Applications*, 44 (2014) 166-174.
- [30] J. Wang, Z. Yin, X. Xue, S.C. Kundu, X. Mo, S. Lu, Natural Non-Mulberry Silk Nanoparticles for Potential-Controlled Drug Release, *International Journal of Molecular Sciences*, 17 (2016).
- [31] A. Abel Lozano-Perez, A. Rodriguez-Nogales, V. Ortiz-Cullera, F. Algieri, J. Garrido-Mesa, P. Zorrilla, M. Elena Rodriguez-Cabezas, N. Garrido-Mesa, M.P. Utrilla, L. De Matteis, J. Martinez de la Fuente, J. Luis Cenis, J. Galvez, Silk fibroin nanoparticles constitute a vector for controlled release of resveratrol in an experimental model of inflammatory bowel disease in rats, *International Journal of Nanomedicine*, 9 (2014) 4507-4520.

- [32] R. Singh, J.W. Lillard, Jr., Nanoparticle-based targeted drug delivery, *Experimental and Molecular Pathology*, 86 (2009) 215-223.
- [33] S.B. Abramson, Nitric oxide in inflammation and pain associated with osteoarthritis, *Arthritis Research & Therapy*, 10 (2008).
- [34] S. Sozer, G. Diniz, F. Lermioglu, Effects of Celecoxib in Young Rats: Histopathological Changes in Tissues and Alterations of Oxidative Stress/Antioxidant Defense System, *Archives of Pharmacal Research*, 34 (2011) 253-259.
- [35] S. Lev-Ari, L. Strier, D. Kazanov, O. Elkayam, D. Lichtenberg, D. Caspi, N. Arber, Curcumin synergistically potentiates the growth-inhibitory and pro-apoptotic effects of celecoxib in osteoarthritis synovial adherent cells, *Rheumatology*, 45 (2006) 171-177.
- [36] U. Gupta, S. Sharma, I. Khan, A. Gothwal, A.K. Sharma, Y. Singh, M.K. Chourasia, V. Kumar, Enhanced apoptotic and anticancer potential of paclitaxel loaded biodegradable nanoparticles based on chitosan, *International Journal of Biological Macromolecules*, 98 (2017) 810-819.
- [37] M. Daheshia, J.Q. Yao, The Interleukin 1 beta Pathway in the Pathogenesis of Osteoarthritis, *Journal of Rheumatology*, 35 (2008) 2306-2312.
- [38] J. Kikuchi, M. Hashizume, Y. Kaneko, K. Yoshimoto, N. Nishina, T. Takeuchi, Peripheral blood CD4(+) CD25(+) CD127(low) regulatory T cells are significantly increased by tocilizumab treatment in patients with rheumatoid arthritis: increase in regulatory T cells correlates with clinical response, *Arthritis Research & Therapy*, 17 (2015).
- [39] R.M. Borzi, I. Mazzetti, S. Macor, T. Silvestri, A. Bassi, L. Cattini, A. Facchini, Flow cytometric analysis of intracellular chemokines in chondrocytes in vivo: constitutive expression and enhancement in osteoarthritis and rheumatoid arthritis, *Febs Letters*, 455 (1999) 238-242.
- [40] L. Pulsatelli, P. Dolzani, A. Piacentini, T. Silvestri, R. Ruggeri, G. Gualtieri, R. Meliconi, A. Facchini, Chemokine production by human chondrocytes, *Journal of Rheumatology*, 26 (1999) 1992-2001.
- [41] C. PlaterZyberk, A.J. Hoogewerf, A.E.I. Proudfoot, C.A. Power, T.N.C. Wells, Effect of a CC chemokine receptor antagonist on collagen induced arthritis in DBA/1 mice, *Immunology Letters*, 57 (1997) 117-120.
- [42] Y.H. Hsu, M.S. Hsieh, Y.C. Liang, C.Y. Li, M.T. Sheu, D.T. Chou, T.F. Chen, C.H. Chen, Production of the chemokine eotaxin-1 in osteoarthritis and its role in cartilage degradation, *Journal of Cellular Biochemistry*, 93 (2004) 929-939.

- [43] F. Heraud, A. Heraud, M.F. Harmand, Apoptosis in normal and osteoarthritic human articular cartilage, *Annals of the Rheumatic Diseases*, 59 (2000) 959-965.
- [44] G. Tripodo, T. Chlapanidas, S. Perteghella, B. Vigani, D. Mandracchia, A. Trapani, M. Galuzzi, M.C. Tosca, B. Antonioli, P. Gaetani, M. Marazzi, M.L. Torre, Mesenchymal stromal cells loading curcumin-INVITE-micelles: A drug delivery system for neurodegenerative diseases, *Colloids and Surfaces B-Biointerfaces*, 125 (2015) 300-308.
- [45] M.A. Hashemipour, H. Mehrabizadeh Honarmand, F. Falsafi, M. Tahmasebi Arashlo, S. Rajabalian, S.A.H. Gandjalikhan Nassab, In Vitro Cytotoxic Effects of Celecoxib, Mefenamic Acid, Aspirin and Indometacin on Several Cells Lines, *Journal of dentistry (Shiraz, Iran)*, 17 (2016) 219-225.
- [46] C.-H. Tang, C.-J. Hsu, Y.-C. Fong, The CCL5/CCR5 Axis Promotes Interleukin-6 Production in Human Synovial Fibroblasts, *Arthritis and Rheumatism*, 62 (2010) 3615-3624.
- [47] D. Gugulothu, A. Kulkarni, V. Patravale, P. Dandekar, pH-Sensitive Nanoparticles of Curcumin-Celecoxib Combination: Evaluating Drug Synergy in Ulcerative Colitis Model, *Journal of Pharmaceutical Sciences*, 103 (2014) 687-696.
- [48] B. Shpitz, N. Giladi, E. Sagiv, S. Lev-Ari, E. Liberman, D. Kazanov, N. Arber, Celecoxib and curcumin additively inhibit the growth of colorectal cancer in a rat model, *Digestion*, 74 (2006) 140-144.
- [49] M. Onoda, H. Inano, Effect of curcumin on the production of nitric oxide by cultured rat mammary gland, *Nitric Oxide-Biology and Chemistry*, 4 (2000) 505-515.
- [50] R. Arora, A. Kuhad, I.P. Kaur, K. Chopra, Curcumin loaded solid lipid nanoparticles ameliorate adjuvant-induced arthritis in rats, *European Journal of Pain*, 19 (2015) 940-952.
- [51] A. Rodriguez-Nogales, F. Algieri, L. De Matteis, A. Abel Lozano-Perez, J. Garrido-Mesa, T. Vezza, J.M. de la Fuente, J. Luis Cenis, J. Galvez, M. Elena Rodriguez-Cabezas, Intestinal anti-inflammatory effects of RGD-functionalized silk fibroin nanoparticles in trinitrobenzenesulfonic acid-induced experimental colitis in rats, *International Journal of Nanomedicine*, 11 (2016) 5945-5958.
- [52] D.W. Kim, H.S. Hwang, D.-S. Kim, S.H. Sheen, D.H. Heo, G. Hwang, S.H. Kang, H. Kweon, Y.-Y. Jo, S.W. Kang, K.-G. Lee, K.W. Park, K.H. Han, J. Park, W.S. Eum, Y.-J. Cho, H.C. Choi, S.Y. Choi, Effect of silk fibroin peptide derived from silkworm *Bombyx mori* on the anti-inflammatory effect of Tat-SOD in a mice edema model, *Bmb Reports*, 44 (2011) 787-792.



Contents lists available at ScienceDirect

International Journal of Pharmaceutics

journal homepage: www.elsevier.com/locate/ijpharm



Stem cell-extracellular vesicles as drug delivery systems: New frontiers for silk/curcumin nanoparticles



Sara Perteghella^{a,1}, Barbara Crivelli^{a,1}, Laura Catenacci^a, Milena Sorrenti^a,
Giovanna Bruni^b, Vittorio Necchi^{c,d}, Barbara Vigani^a, Marzio Sorlini^e, Maria Luisa Torre^a,
Theodora Chlapanidas^{a,*}

^aUniversity of Pavia, Department of Drug Sciences, Viale Taramelli 12, 27100 Pavia, Italy

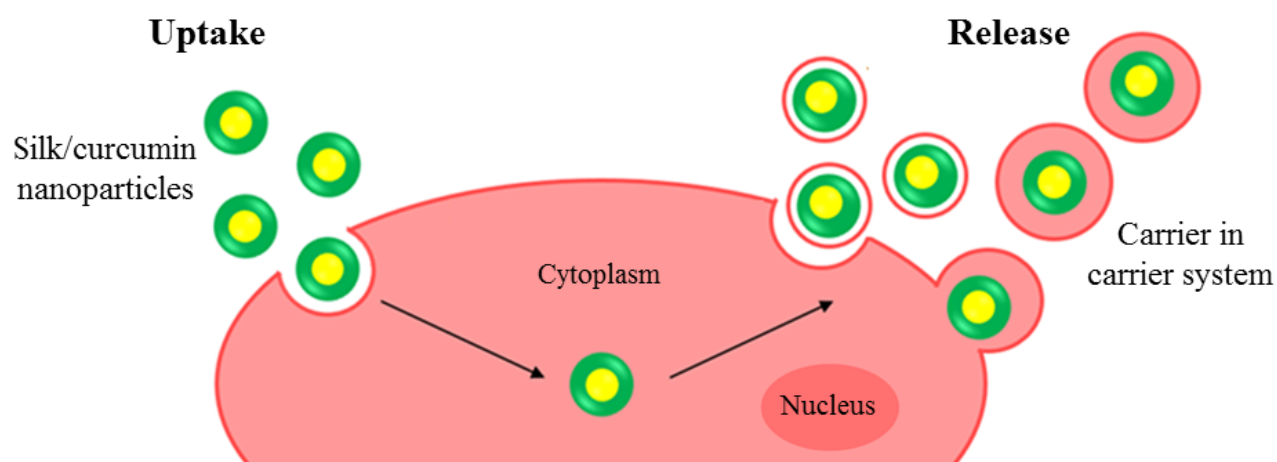
^bUniversity of Pavia, Department of Chemistry, Viale Taramelli 16, 27100 Pavia, Italy

^cUniversity of Pavia, Department of Molecular Medicine, Via Forlanini 6, 27100 Pavia, Italy

^dUniversity of Pavia, Centro Grandi Strumenti, Via Bassi 21, 27100 Pavia, Italy

^eSUPSI, University of Applied Sciences and Arts of Southern Switzerland, Innovative Technologies Department, Via Poblette 11, 6928 Manno, Switzerland

Graphical abstract



Abstract

The aim of this work was to develop a novel carrier-in-carrier system based on stem cell-extracellular vesicles loaded of silk/curcumin nanoparticles by endogenous technique. Silk nanoparticles were produced by desolvation method and curcumin has been selected as drug model because of its limited water solubility and poor bioavailability. Nanoparticles were stable, with spherical geometry, 100 nm in average diameter and the drug content reached about 30 %. Cellular uptake studies, performed on mesenchymal stem cells (MSCs), showed the accumulation of nanoparticles in the cytosol around the nuclear membrane, without cytotoxic effects. Finally, MSCs were able to release extracellular vesicles entrapping silk/curcumin nanoparticles. This combined biological-technological approach represents a novel class of nanosystems, combining beneficial effects of both regenerative cell therapies and pharmaceutical nanomedicine, avoiding the use of viable replicating stem cells.

Keywords

Mesenchymal stem cells; silk fibroin; curcumin; extracellular vesicles; nanoparticles; drug delivery systems.

1. Introduction

In recent years, novel drug delivery systems have been developed to optimize the efficacy of therapeutics enhancing their bioavailability, reducing their degradation rate, allowing targeting and thus their control release, cellular uptake and reducing side effects (Mottaghitlab et al., 2015). Nanotechnology is giving a great impact in drug delivery field and nanoparticles are at the leading edge, since they can improve solubility, stability and efficacy of drugs, achieving a reduction in administration frequency and lower risks of toxicity in patients (Mishra et al., 2013; Parveen et al., 2012). Thanks to their tunable properties (particle size, surface charge, chemical modifications) nanoparticles can be envisioned as the future of drug delivery technology as their “nanosize” is crucial to their cellular internalization, which is the key to achieve a “real” therapeutic efficacy (Kumari et al., 2010). Bio-inspired nanoparticles, based on natural polymers or bio-macromolecules, mirror natural compounds. Among them, silk fibroin is a natural polymer widely studied for tissue engineering and drug delivery (Altman et al., 2002; Chlapanidas et al., 2011; Chlapanidas et al., 2016; Chlapanidas et al., 2013; Farago et al., 2016; Vepari and Kaplan, 2007; Vigani et al., 2016). Silk fibroin is an effective polymer for the delivery of therapeutic agents because it has shown biocompatibility, controllable

biodegradability, low toxicity/immunogenicity, chemical modification potential, appropriate mechanical properties and therapeutic retention at target sites (Kundu et al., 2013; Wang and Zhang, 2015). Moreover, silk nanoparticles can be prepared by different techniques, mainly desolvation and salting out, selected on drug physicochemical properties (Zhao et al., 2015).

Extracellular vesicles (EVs) are small membrane bound-vesicles, ranging in size from 40 to 1000 nm, produced by most of mammalian cell lineages both under physiological and pathological conditions. EVs can be found in body fluids such as in saliva, urine, bile, cerebrospinal fluid (Kim et al., 2016; Tompkins et al., 2015), and can act as physiological delivery nanosystems. The main advantages of EV-based drug delivery than synthetic delivery nanosystems (e.g. liposomes) are lower immunogenicity and toxicity and higher stability in circulation and tissues (van der Meel et al., 2014). Moreover, EVs mirror the genetic and proteomic content of their secreting cells, thus those derived from mesenchymal stem/stromal cells (MSCs) retain several biological activities that are able to reproduce the beneficial effects of stem cells (Camussi and Quesenberry, 2013) including migration to injured tissues (i.e. homing), inflammatory and immune response modulation through the secretion of cytokines and trophic factors (Caplan, 2010; de Girolamo et al., 2013; Torre et al., 2015).

Recently, our research group has developed an innovative carrier-in-carrier system for hydrophobic drugs mediated by micelle-loaded MSCs: micelles were considered as the first drug carrier, while the second carrier were constituted by MSCs that could also assure an adequate drug targeting due to their innate homing. We demonstrated that the uptake of micelles by MSCs has resulted effective and quick without any relevant cytotoxic effects and cells, loaded of micelles, were able to release the entrapped drug (Tripodo et al., 2015a).

The aim of this study was to evolve a novel carrier-in-carrier delivery system based on EVs loaded of silk/curcumin nanoparticles. Silk nanoparticles were produced by desolvation method and curcumin has been selected as drug model because of its limited water solubility and poor bioavailability. This natural polyphenolic compound, isolated from the rhizome of *Curcuma longa*, could be used in the treatment of many chronic diseases, such as multiple sclerosis, rheumatoid arthritis, colitis, Alzheimer's disease and potentially in cancer prevention and therapy (Aggarwal and Harikumar, 2009) due to its proved antioxidant, anti-inflammatory, apoptosis-inducing and anti-angiogenic activities. Thus, nanoparticles were uptaken by adipose-derived MSCs and subsequently MSC-EVs, loaded of silk/curcumin nanoparticles, were secreted and characterized. Our idea represents a novel approach, coupling stem cell therapy and nanomedicine.

2. Material and Methods

2.1 Materials

Sodium carbonate, lithium bromide, calcium chloride, acetone, curcumin, ethanol, collagenase, 3-(4,5-dimethylthiazol-2-yl)-2,5-diphenyl-tetrazolium bromide (MTT), Nile red, sodium alginate and dimethyl sulfoxide were obtained from Sigma-Aldrich (Milan, Italy). Dialysis tubes were purchased from Visking (London, United Kingdom). All reagents used for cell cultures were purchased from Euroclone (Milan, Italy).

2.2 Silk fibroin extraction and nanoparticle preparation

Bombyx mori cocoons were cut into pieces, added to a boiling 0.02 M Na₂CO₃ solution for 30 minutes and then rinsed four times in distilled water. Degummed fibers were dried at room temperature and dissolved in 9.3 M LiBr solution at 60 °C for 4 hours (Aggarwal and Harikumar, 2009). The raw silk solution was dialyzed against distilled water using cellulose tubes (MWCO 3,000–5,000 Da) at room temperature for 72 hours to remove the residual LiBr chaotropic salts. The final concentration of aqueous silk solution was about 8 % w/v, determined by freeze-drying (Modulyo® Edwards Freeze dryer, Kingston, NY) of known silk volumes.

Silk nanoparticles were prepared by acetone desolvation method (Seib et al., 2013). Briefly, aqueous silk solution was diluted to achieve the concentration 1.5 % w/v and it was added drop wise in acetone under gentle stirring for 1 minute at room temperature (volume ratio silk:acetone 1:5). Silk/curcumin nanoparticles were obtained adding silk solution into acetone, in which previous curcumin powder was solubilized in different concentrations (Table 1). Nanoparticles were then dialyzed against distilled water using cellulose tubes (MWCO 3,000–5,000 Da) until complete solvent removal. Nanoparticles were stored at 4 °C or subjected to freeze dried process at $8 \cdot 10^{-1}$ mbar and -50° C for 72 hours for further investigations. Five different formulations, consisting of silk nanoparticles or silk/curcumin nanoparticles, were prepared (Table 1).

2.3 Characterization of silk and silk/curcumin nanoparticles

2.3.1 Drug loading determination

The quantification of curcumin content in silk nanoparticles was evaluated using a direct spectrophotometer method (Uvikon 860, Kontron Instruments, Switzerland) at 425 nm. Briefly, 1 mg of freeze-dried nanoparticles was dissolved in 10 ml of 96 % v/v ethanol, maintaining mild magnetic stirring. Curcumin concentration was measured from a calibration curve of nine curcumin solutions in ethanol at the concentration range of $8 \cdot 10^{-3}$ – $6.25 \cdot 10^{-4}$ mg/ml, with a

correlation coefficient $r^2 > 0.9895$. Ethanol was considered as control solution. Each measurement was performed in triplicate.

2.3.2 Nanoparticle-tracking analysis (NTA)

Nanoparticle mean diameter was determined by nanoparticle tracking using NanoSight (NS300, Malvern Instruments, Malvern, Italy), fitted with a NS300 flow-cell top plate and a 405 nm laser. The NanoSight sample pump was used in conjunction with 1 ml syringes. Fresh nanoparticles were diluted 1:100 in phosphate buffer saline (PBS) immediately prior to analysis. All measurements were carried out at 26.4 °C with detection angle of 90° and done in triplicate. A single analysis represented a fresh dilution of the stock particle solution and consisted of three 30 seconds video captures. Results were analyzed with the NTA software 3.0 (Malvern Instruments, Malvern, Italy).

2.3.3 Morphological evaluation

A Zeiss EVO MA10 (Carl Zeiss, Oberkochen, Germany) was used to analyze the morphology of nanoparticles. The samples were gold-sputter coated under argon to render them electrically conductive prior to microscopy.

2.3.4 Differential Scanning Calorimetry (DSC)

Temperature and enthalpy values were measured with a Mettler STARe system (Mettler Toledo, Italy) equipped with DSC81° Module and an Intracooler device for sub-ambient temperature analysis (Jukabo FT 900) on 2-3 mg samples in 40 µL sealed aluminium pans with pierced lid (method: 10-400 °C temperature range; heating rate 10 K min⁻¹; nitrogen air atmosphere flux 50 mL min⁻¹). The instrument was previously calibrated with Indium, as standard reference, and measurements were carried out at least in triplicate.

2.3.5 Simultaneous Thermogravimetric Analysis (TGA/DSC 1)

Mass losses were recorded with a Mettler STARe system (Mettler Toledo, Italy) TGA on 3-4 mg samples in 70 µL alumina crucibles with lid (30-400 °C temperature range; heating rate 10 K min⁻¹; nitrogen air atmosphere flux 50 mL min⁻¹). The instrument was previously calibrated with Indium, as standard reference, and measurements were carried out at least in triplicate.

2.3.6 Fourier Transform Infrared (FT-IR) spectroscopy

FT-IR spectra of the lyophilized silk fibroin nanoparticles were obtained using a Spectrum One Perkin-Elmer spectrophotometer (Perkin Elmer, Wellesley, MA, USA) equipped with a MIRacle™ ATR device (Pike Technologies, Madison, WI, USA). The IR spectra in transmittance mode were obtained in the spectral region of 650-4000 cm⁻¹ with a resolution of 4 cm⁻¹ and measurements were carried out at least in triplicate.

2.3.7 In vitro curcumin release study

The release of curcumin from the silk/curcumin nanoparticles was carried out by dialysis membrane method (Shaikh et al., 2009). Briefly, 10 ml of silk/curcumin nanoparticle suspension in distilled water (equivalent to 0.08 mg of curcumin) was put in a dialysis tube (MWCO 12,000–14,000 Da) and suspended in 100 ml of ethanol (50 % v/v) at room temperature under mild magnetic stirring. At fixed time intervals, predetermined volumes of the release medium were withdrawn and replaced by an equivalent amount of fresh medium. The curcumin concentration was spectrophotometrically determined at 425 nm. Each measurement was performed in triplicate.

2.4 Nanoparticle uptake by adipose-derived mesenchymal stem cells (MSCs)

2.4.1 Isolation and culture of MSCs

An adipose tissue sample, obtained from an informed donor during abdominoplastic surgery, was washed with PBS without Ca^{2+} and Mg^{2+} , mechanically minced with surgical scissors and digested with 0.075 % w/v type II collagenase solubilized in PBS with Ca^{2+} and Mg^{2+} at 37 °C. After 1 hour, the digested tissue was filtered on 70 μm cell strainer (Greiner Bio-One, Austria); cell suspension was added of Dulbecco's modified Eagle's Medium (DMEM) and Ham's medium F12, ratio 1:1, supplemented by 10 % v/v Fetal Bovine serum (FBS) and centrifuged (Thermo-Fisher Scientific, Italy) at 600 x g for 5 minutes (Faustini et al., 2010; Gaetani et al., 2008). The recovered stromal vascular fraction was cultured in monolayer condition (100,000 cells/cm²) in DMEM/F12, 10 % FBS, 1 % penicillin/streptomycin (100 UI/ml – 100 $\mu\text{g}/\text{ml}$) and 1 % amphotericin B (2.5 $\mu\text{g}/\text{ml}$). Once the MSCs reached sub-confluence, they were treated with 0.05 % trypsin-EDTA, re-suspended in culture medium and seeded onto flasks (10,000 cells/cm²) till the 2nd passage at 37 °C and 5 % CO₂.

2.4.2 Nanoparticle uptake by MSCs

MSCs were seeded in 96-well plates at a density of 10,000 cells/cm² and incubated with culture medium for 24 hours at 37 °C, 5 % CO₂. Then, all formulations were added to each well (200 $\mu\text{g}/\text{ml}$ in culture medium) and incubated with cells for 30, 60 or 120 minutes (Kundu et al., 2010; Tripodo et al., 2015a). At the established times, cells were washed with PBS and cellular uptake was evaluated in term of fluorescence intensity, exploiting the auto-fluorescence property of curcumin (Gupta et al., 2009), using a microplate reader (Synergy HT, BioTek, United Kingdom), equipped by an excitation filter at 485 nm and an emission filter at 528 nm. As a control, cells were cultured and assessed in absence of samples. Each condition was performed in triplicate.

2.4.3 Cell viability evaluation by MTT test

After exposure to nanoparticles, MSC viability was performed by adding 100 μ L of 3-(4,5-dimethylthiazol-2-yl)-2,5-diphenyl-tetrazolium bromide (MTT) solution (0.5 mg/ml) in each well. After 3 hours of incubation with the MTT dye solution, medium was removed and the formazan crystals were solubilized with 100 μ l of DMSO in each well, mixing the solution to completely dissolve the reacted dye. The optical density was read using a microplate reader (Synergy HT) at 570 nm and 670 nm (reference wavelength). Each condition was tested in triplicate. Cell viability (%) was calculated as follows: $100 \times (\text{ODs}/\text{ODc})$, where ODs represents the mean value of the measured optical density of the tested sample and ODc is the mean value of the measured optical density of untreated cells (control).

2.4.4 Nile Red staining and confocal microscopy evaluation

The fluorescent dye Nile Red was exploited as a probe for the identification of phospholipids. Nile Red powder was solubilized in acetone and stored at 4 °C, avoiding light exposure. The stock solution (3.14 M) was diluted 100x in PBS before use. MSCs were cultured in chamber slide (Nunc® Lab-Tek® II, Sigma-Aldrich) and incubated with nanoparticles (Np0, Np1.5 and Np14, see Table 1 for different curcumin loading); after 60 minutes, media were discarded and cells were washed with PBS. Adherent cells were treated with Nile Red solution and fluorescence emission was recorded with a laser scanning confocal microscope (TCS SP5 II, Leica, Germany), considering different Excitation/Emission filters to detect silk (Ex 488 nm; Em 500-550 nm), curcumin (Ex 405 nm; Em 430-500 nm) and lipids (Ex 543 nm; Em 580-660 nm).

2.5 Release and characterization of MSC-EVs enriched by silk/curcumin nanoparticles

Cells (10,000 cells/cm²) were incubated with nanoparticles (Np14, see Table 1 for curcumin loading) for 60 minutes. After uptake, medium was removed and MSCs were cultured in serum free medium overnight to induce EV release (L Ramos et al., 2016). Supernatant was collected and characterized by confocal and transmission electron microscopy (see below). Not treated MSCs were considered as control. Each experiment was carried out in triplicate.

2.5.1 Confocal microscopy evaluation

Supernatant (90 μ l) was incubated with 10 μ l of Nile Red solution (see paragraph 2.4.4) for 5 minutes. Nile Red is a non-fluorescent dye in water solution, but undergoes fluorescence when internalized in phospholipid bilayer (e.g. cell and EV membranes). Samples were put on a glass and observed under a laser scanning confocal microscope, considering different Excitation/Emission filters to detect silk (Ex 488 nm; Em 500-550 nm), curcumin (Ex 405 nm;

Em 430-500 nm) and lipids (Ex 543 nm; Em 580-660 nm). Nile Red solution (without supernatant) was considered as negative control. A representative region of acquired images was selected to draw the line profile. The related stack profile charts were obtained by a image analyzer (LAS-AF, Leica) to determine fluorescence intensity of each fluorophore.

2.5.2 Transmission electron microscopy

Medium viscosity alginate was solubilized in physiological saline solution (2% w/v) and sterilized by filtration. Supernatant was suspended in alginate solution (volume ratio 1:3) and extruded drop by drop through a 22G-needle into an isotonic saline solution containing 50 mM CaCl₂ under magnetic stirring. The calcium ions diffused into the droplets, reacting with the alginate chains and forming alginate beads (Vigani et al., 2016). This alginate matrix has been employed to provide a tridimensional scaffold in which MSC-EVs were immobilized, preserving their morphology. Encapsulated MSC-EVs were fixed in a solution of 2.5 % paraformaldehyde and 2% glutaraldehyde, followed by 1% osmium tetroxide, embedded in Epon812/Araldite mixture and processed for TEM. The samples were sectioned with Reichert Ultracut S Ultramicrotome. The ultrathin sections were observed for transmission electron microscopy with a JEOL JEM 1200 EX instrument. Supernatant, based on MSC-EVs not treated with nanoparticles, was processed using the same procedure.

2.6 Statistical analysis

The effect of formulation on curcumin release was assessed by a multifactor ANOVA, considering the time and the formulation as factors and the cumulative curcumin release as dependent variable.

Results of nanoparticle uptake were processed by a multifactor ANOVA, considering the time of incubation (30, 60 and 120 minutes) and formulation as fixed factors, the fluorescence intensity and the viability % as dependent variables.

The differences between groups were analyzed with the *post-hoc* LSD's test for multiple comparisons. Unless differently specified, data are expressed as mean \pm standard deviation. The statistical significance was fixed at $p \leq 0.05$.

3. Results

3.1 Characterization of silk and silk/curcumin nanoparticles

Five different nanoparticle formulations were obtained by desolvation method. The curcumin loading ranged between 1 and 30 % (Table 1), varying the concentration of curcumin in the starting acetone solution.

Table 1. Composition of silk and silk/curcumin nanoparticles (Np): five formulations were obtained after solubilization of different curcumin amount in acetone. The percentage of curcumin loading is reported as mean values and standard error (SE).

Nanoparticles	Curcumin concentration in acetone (mg/ml)	Curcumin loading (%) (mean \pm SE)
Np0	-	-
Np1	0.03	0.95 \pm 0.127
Np1.5	0.1	1.50 \pm 0.111
Np14	0.5	13.66 \pm 1.518
Np32	1.5	31.97 \pm 1.522

Silk and silk/curcumin nanoparticles were analyzed in terms of particle size distribution and morphology: NTA showed a hydrodynamic diameter of about 100 nm and 90 % of nanoparticles had a diameter less than 150 nm (Figure 1A). Morphological studies, carried out by SEM analysis on freeze-dried products, indicated that nanoparticles appeared as round-shaped structures; moreover, the presence of curcumin did not alter the particle size and the morphological structure of nanoparticles (Figure 1B-F).

The solid-state characterization by FT-IR showed that silk existed in its stable conformation, characterized by high content of crystalline β -sheets, that can be identified in the spectra region of amide I (at about 1620 cm^{-1} , C=O stretching), amide II (at about 1520 cm^{-1} , N-H bending) and amide III (at about 1230 cm^{-1} , C-N and N-H functionalities) (Figure 2, spectra b-e). Moreover, the FT-IR spectrum of Np1 was superimposable to that of Np0; this is probably due to the very low drug content in nanoparticles. Typical absorption bands of curcumin appeared in spectra of samples with higher active content, in particular at 1624 cm^{-1} and 1509 cm^{-1} due to C=O stretching, and at 962 cm^{-1} due to cis-trans C-H vibration of aromatic ring (Figure 2).

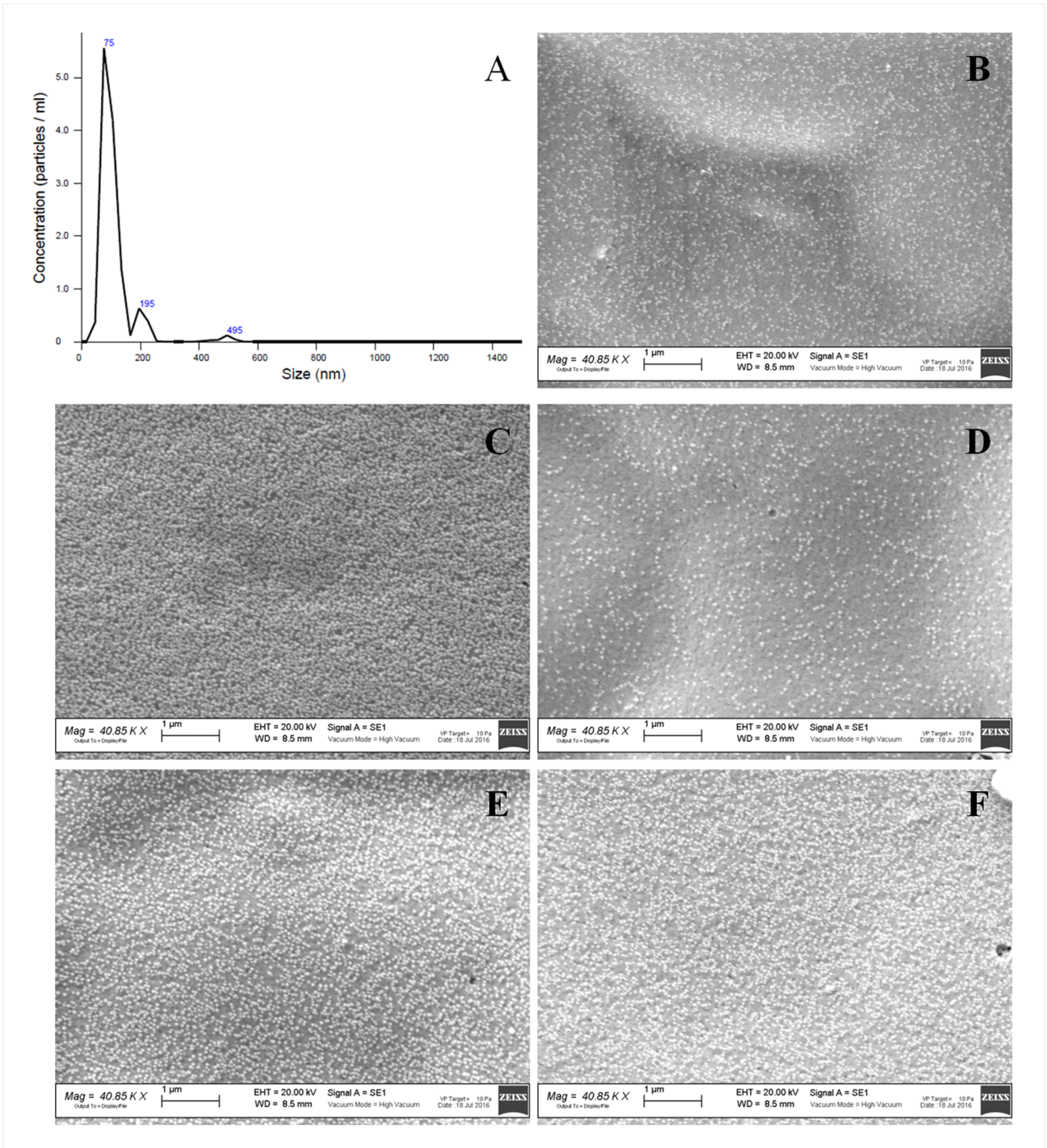


Fig. 1. Particle size distribution (A) and morphology obtained by scanning electron microscopy (B-F) of Np0 (A and B), Np1 (C), Np1.5 (D), Np14 (E) and Np32 (F). A magnification of Np0 is reported in the onset (B). Scale bar represents 1 μm.

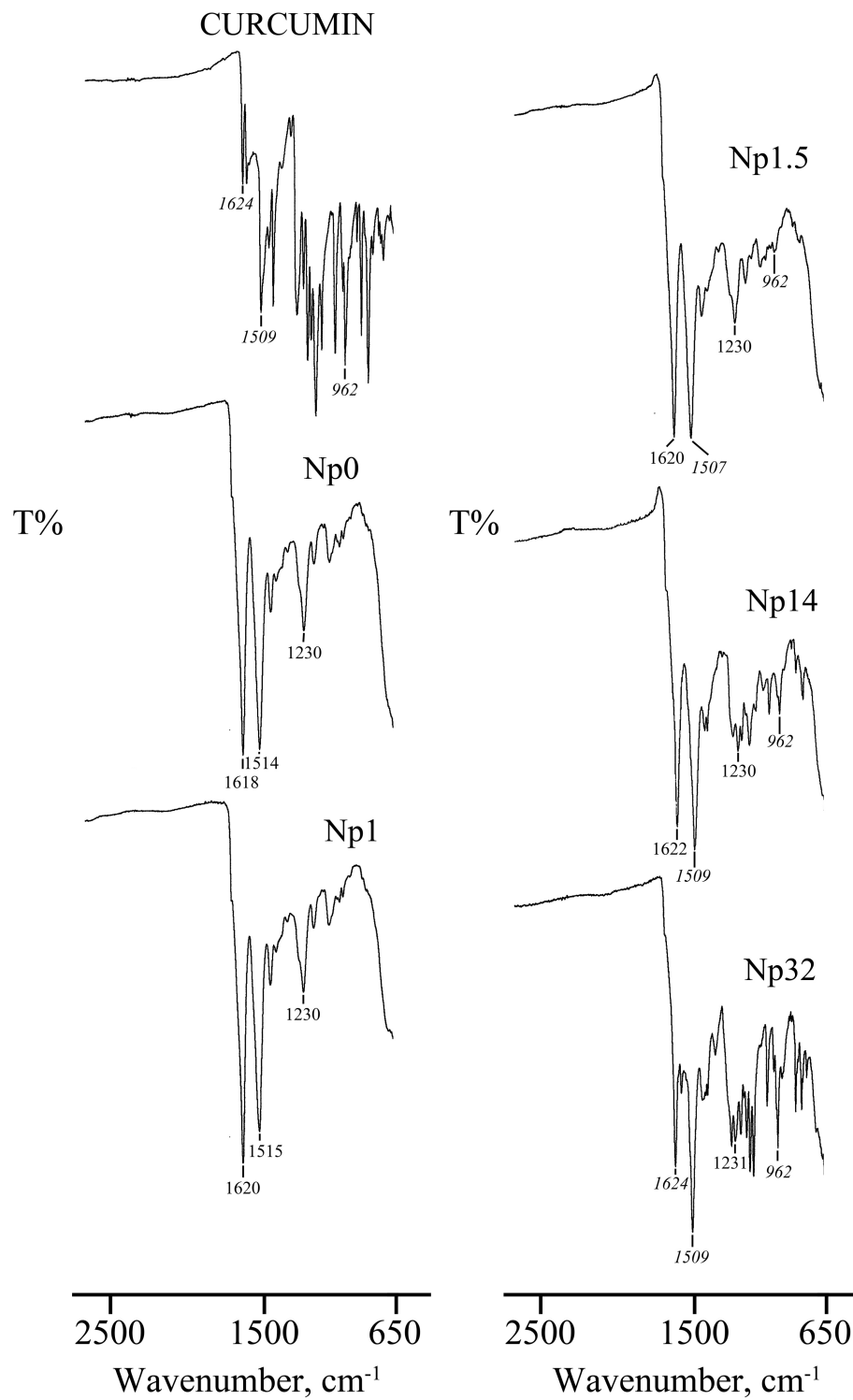


Fig. 2. Fourier transform infrared (FT-IR) spectra of curcumin, Np0, Np1, Np1.5, Np14 and Np32 in the spectral region of 650–2500 cm^{-1} .

DSC and TGA analyses of silk and silk/curcumin nanoparticles are reported in Figs. 3 and 4, respectively. Curcumin is an anhydrous crystalline compound characterized in DSC by $T_{\text{onset,m}} = 168.2 \pm 0.2 \text{ }^{\circ}\text{C}$; $T_{\text{peak,m}} = 174.4 \pm 0.1 \text{ }^{\circ}\text{C}$ and $\Delta H_{\text{m}} = 103 \pm 1 \text{ Jg}^{-1}$ with a mass loss recorded in TGA curve starting at around $220 \text{ }^{\circ}\text{C}$, corresponding to the sample decomposition (Fig. 4). A broad endothermic effect between 30 and $100 \text{ }^{\circ}\text{C}$ in the DSC profiles was observed in all formulations (Fig. 3), due to dehydration (mass loss in TGA analyses of about 6% , Fig. 4), followed by the sample decomposition at about $290 \text{ }^{\circ}\text{C}$. An endothermic effect at $176.3 \pm 0.8 \text{ }^{\circ}\text{C}$ was observed in silk/curcumin nanoparticles, confirming the presence of the active compound, and the area of this effect increased proportionally with the drug content (Figure 3).

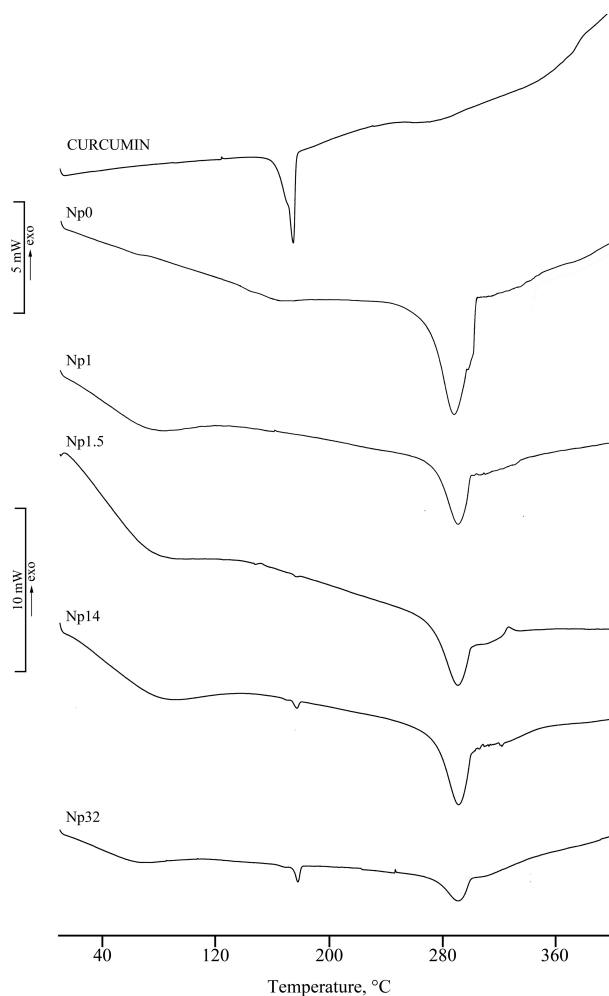


Fig. 3. Differential scanning calorimetry (DSC) profiles of curcumin, Np0, Np1, Np1.5, Np14 and Np32.

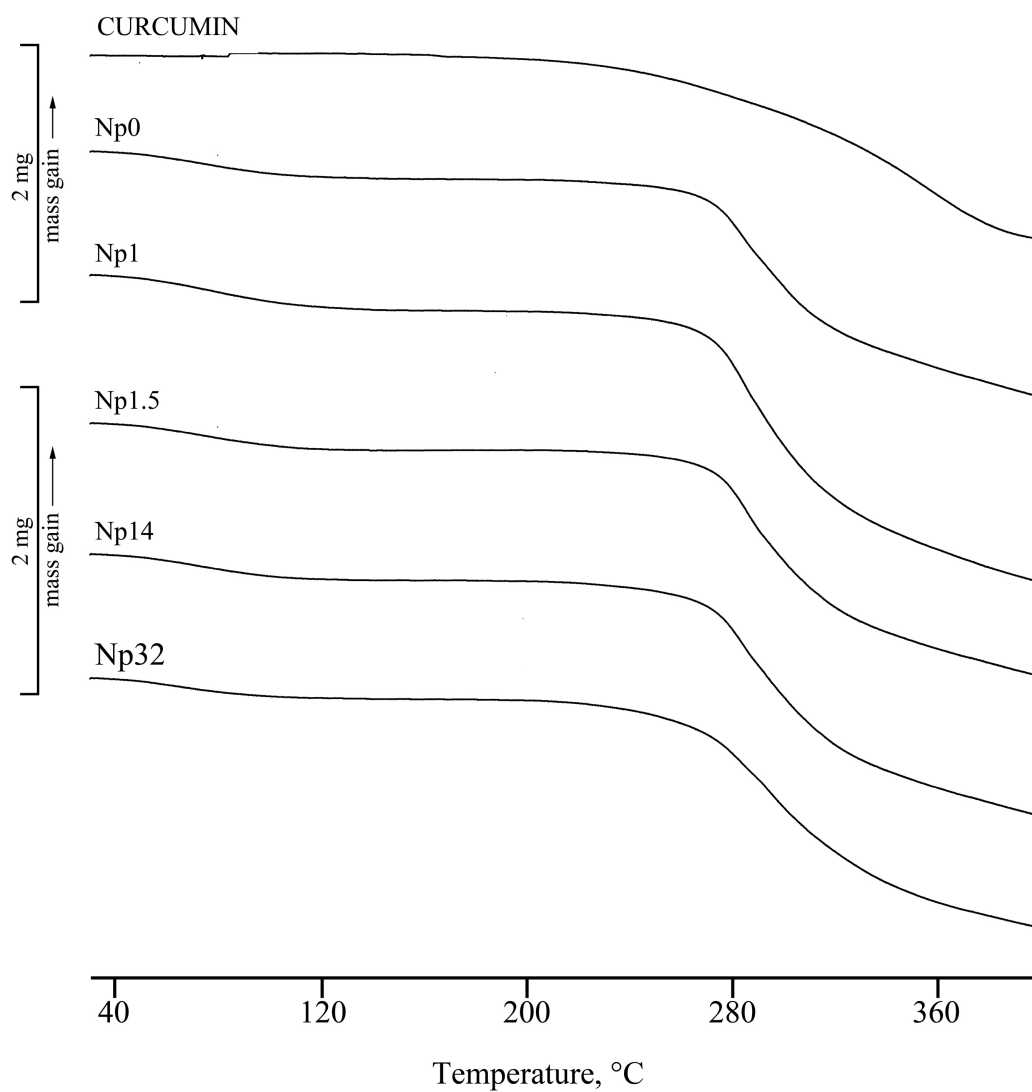


Fig. 4. Thermogravimetric Analysis (TGA) of curcumin, Np0, Np1, Np1.5, Np14 and Np32.

The cumulative release of curcumin from nanoparticles showed an initial burst release of about 15 % for Np1, Np1.5 and Np14 and about 25 % for Np32 within 7 hours, reaching a plateau after 1 day (Figure 5). The curcumin release profiles showed significant differences among formulations ($p < 0.0001$): lower and higher drug releases were observed for Np1 and Np32 respectively, whereas no differences were found between Np1.5 and Np14 (Figure 5).

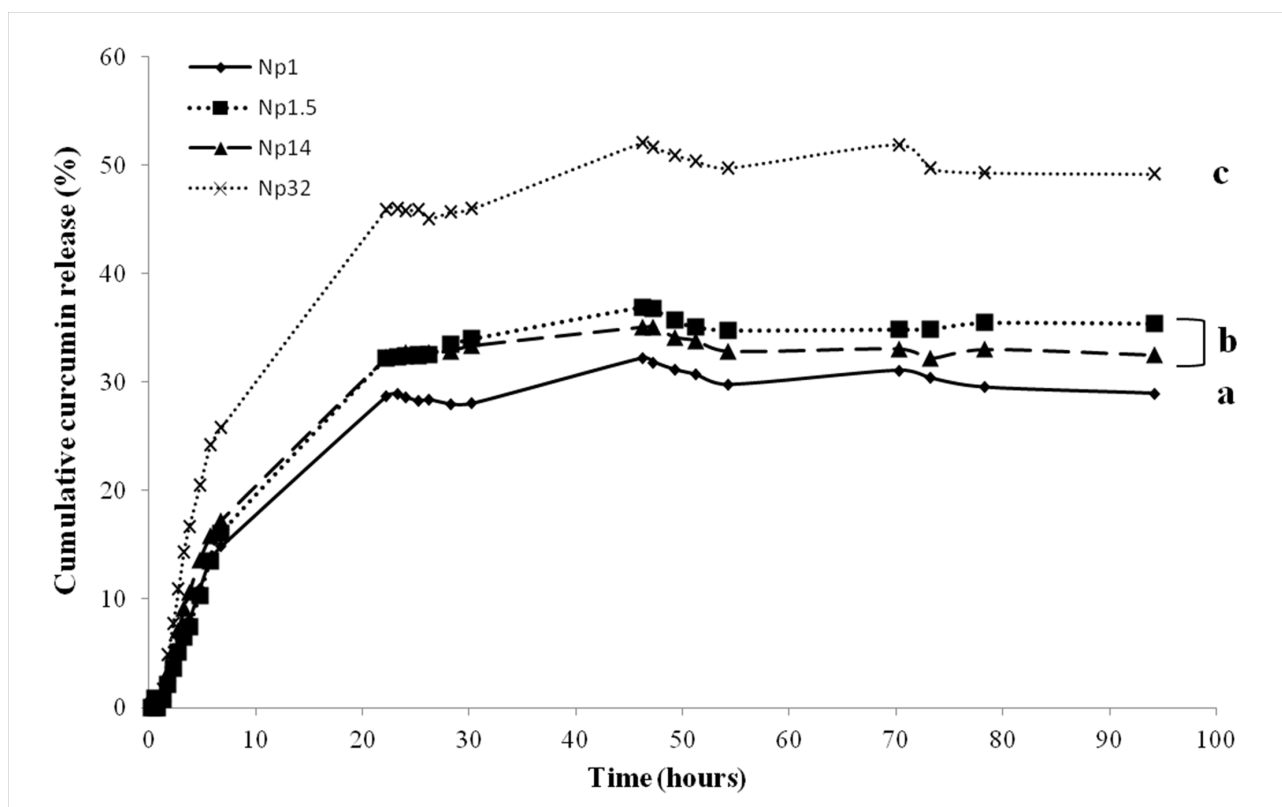


Fig. 5. *In vitro* curcumin release profiles from nanoparticles by a dialysis method in ethanol 50% v/v at room temperature. Each data is expressed as mean value of at least three independent experiments. Error bars are not indicated for a better readability of the graph. Different letters indicate significant differences between formulations ($p < 0.05$).

3.2 Nanoparticle uptake by mesenchymal stem cells

MSCs were incubated with nanoparticles for 120 minutes and fluorescence intensity of adherent cells was evaluated as uptake index: the auto-fluorescence of curcumin has been exploited for a quantitative analysis of nanoparticle uptake by MSCs, with a direct correlation between curcumin internalization and fluorescence intensity. ANOVA results indicated that both incubation time and formulation were statistically significant ($p < 0.0001$). In particular, we observed that the fluorescence intensity significantly increased with the curcumin content in nanoparticles (from Np1 to Np32), and the treatment for 60 minutes resulted in higher values; in fact, after 30 minutes the cellular uptake was incomplete, while the fluorescence intensity

was not increased after 120 minutes (Figure 6A). As expected, not treated cells (CTR) and cells treated with silk nanoparticles (Np0) showed lower fluorescence values than silk/curcumin nanoparticles (Figure 6A).

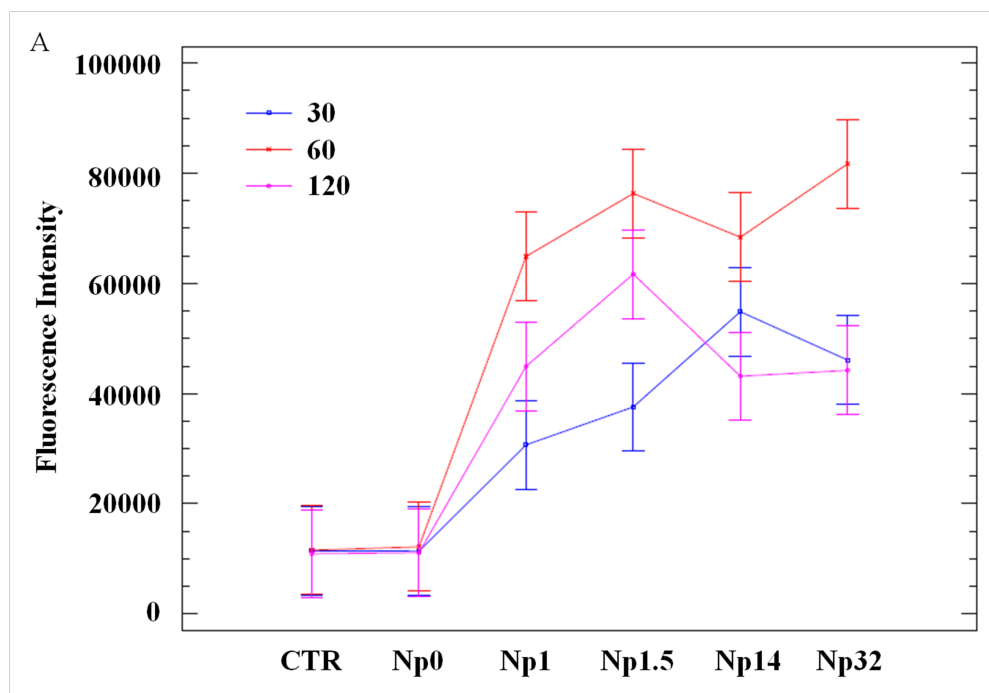


Fig. 6. Nanoparticle uptake by mesenchymal stem cells. Results are reported as mean values and 95.0% least significance difference (LSD) intervals of fluorescence intensity of MSCs incubated with nanoparticles for 30, 60 and 120 min (CTR: cells not treated with nanoparticles).

Metabolic activity of MSCs was measured by MTT assay immediately after incubation with nanoparticles. MTT assay provides a direct measure of cell mitochondrial activity and is considered as cell viability index with respect to not treated cells. Results are reported in Figure 6B; ANOVA indicated that both incubation time and formulation were statistically significant ($p = 0.0005$ and $p = 0.0026$, respectively). Silk nanoparticles (Np0) did not influence MSC viability at all tested incubation times, while silk/curcumin nanoparticles slightly decreased the cell viability. On the other side, the MSC viability significantly decreased after incubation with free-curcumin (about 20 % after 24 hours of treatment), confirming the efficient encapsulation system (Figure 6B).

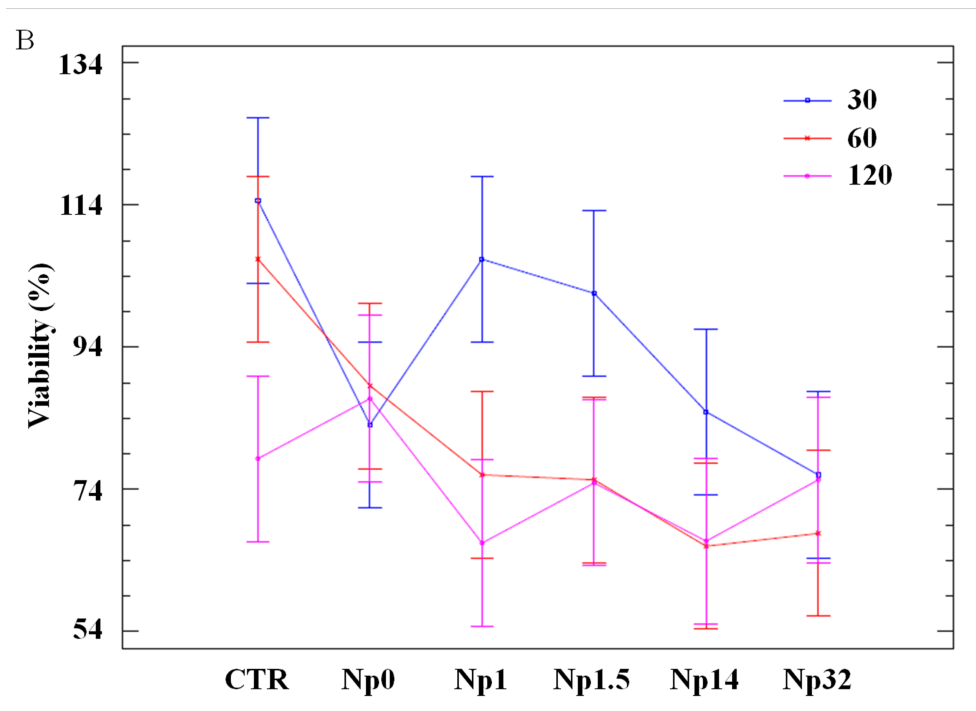


Fig. 6. Nanoparticle uptake by mesenchymal stem cells. Results are reported as mean values and 95.0% least significance difference (LSD) intervals of viability of MSCs incubated with nanoparticles for 30, 60 and 120 min (CTR: cells not treated with nanoparticles).

Three nanoparticle formulations (Np0, Np1.5 and Np14) have been selected excluding end points (Np1 and Np32), and their intracellular localization was evaluated by confocal microscopy. After nanoparticle uptake, MSCs were treated with Nile red solution, a probe for phospholipid detection (e.g. cell and EV phospholipid membranes), and the auto-fluorescence of both curcumin and silk have been exploited. Three specific excitation/emission filters were used for the simultaneous detection of each fluorophore (silk, curcumin and phospholipid bilayer). Results indicated that the curcumin fluorescence (Figure 7, blue images) increased enhancing the drug content in nanoparticles, confirmed by higher fluorescence in MSCs treated with Np14 than Np1.5. The fluorescence related to nanoparticle internalization (Figure 7, green images) was similar in all treated MSCs. Moreover, the localization of nanoparticles occurred in the cytoplasmic environment around the nuclear membrane (Figure 7, green images). The silk nanoparticles appeared an efficient encapsulation system, as confirmed by these confocal images in which we observed the same localization of curcumin and silk into cells. The same fluorescence, related to Nile Red staining, was observed in all MSCs, indicating that this probe has been internalized in phospholipid bilayer (Figure 7, red images).

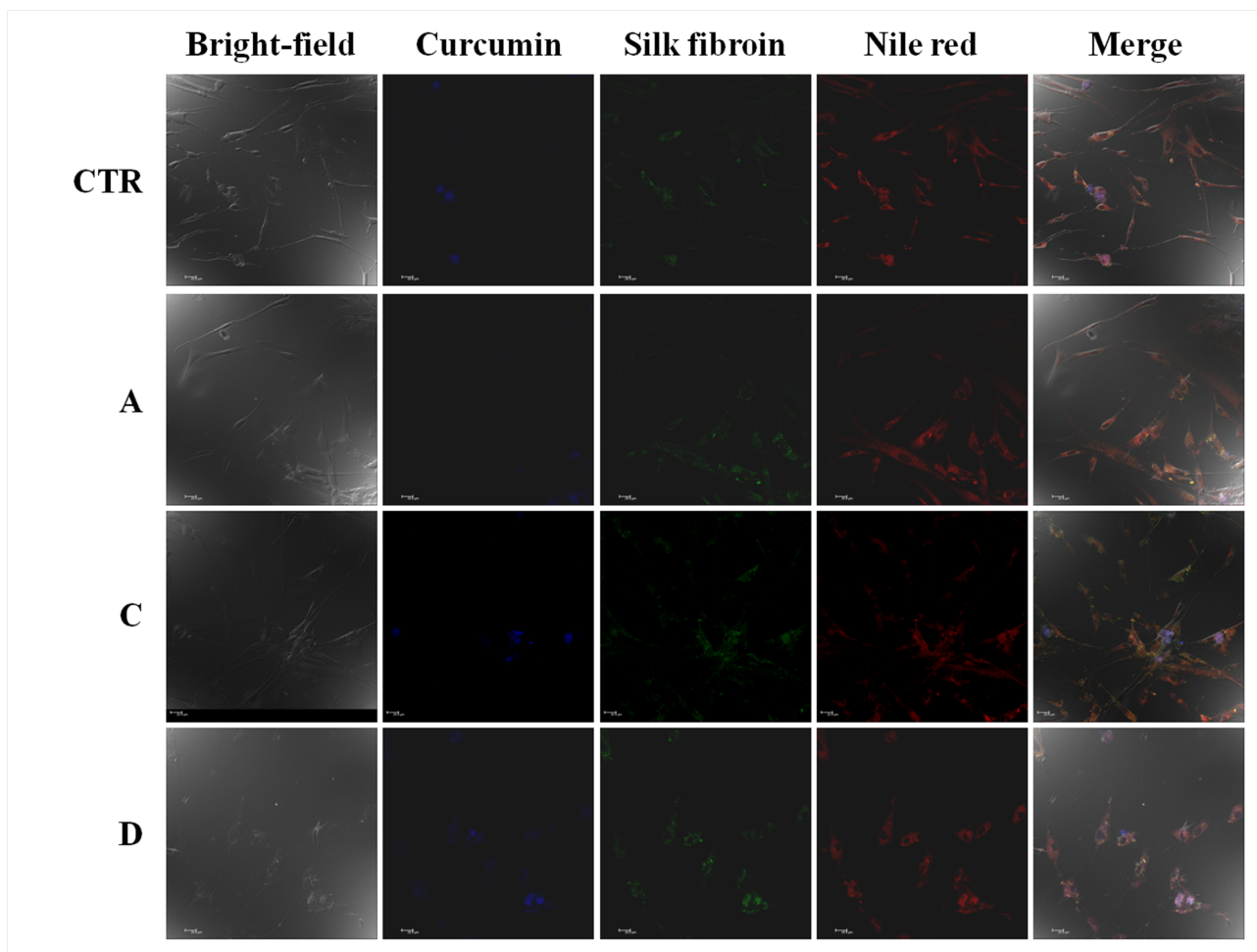


Fig. 7. Confocal microscopy images of MSCs incubated with Np0, Np1.5 and Np14 for 60 min (CTR: cells not treated with nanoparticles). For each group, adherent MSCs were observed in bright-field (left column) and considering three specific excitation/emission filters for curcumin (blue fluorescence), silk (green fluorescence) and phospholipid bilayer by Nile red (red fluorescence). These three fluorescent images were merged and reported in the right column. (For interpretation of the references to color in this figure legend and text, the reader is referred to the web version of this article.)

3.3 Release and characterization of MSC-EVs enriched by silk/curcumin nanoparticles

After cellular uptake, MSCs were cultured 24 hours in serum free condition to induce EV secretion. Our aim was not only to obtain MSC-EVs, but also to develop a carrier-in-carrier delivery system based on EVs loaded of silk/curcumin nanoparticles. For this reason, a morphological investigation was carried out on supernatant culture media. The line profile was marked on a specific region of images acquired by confocal microscopy. Stack profile charts are histograms of the emitted fluorescence intensity along the line profile. Histograms showed narrow peaks for all fluorophores and localized in the same position; this result confirmed the

co-localization of curcumin, silk and MSC-EVs, underlining the ability of MSCs to secrete the carrier-in-carrier system (Figure 8).

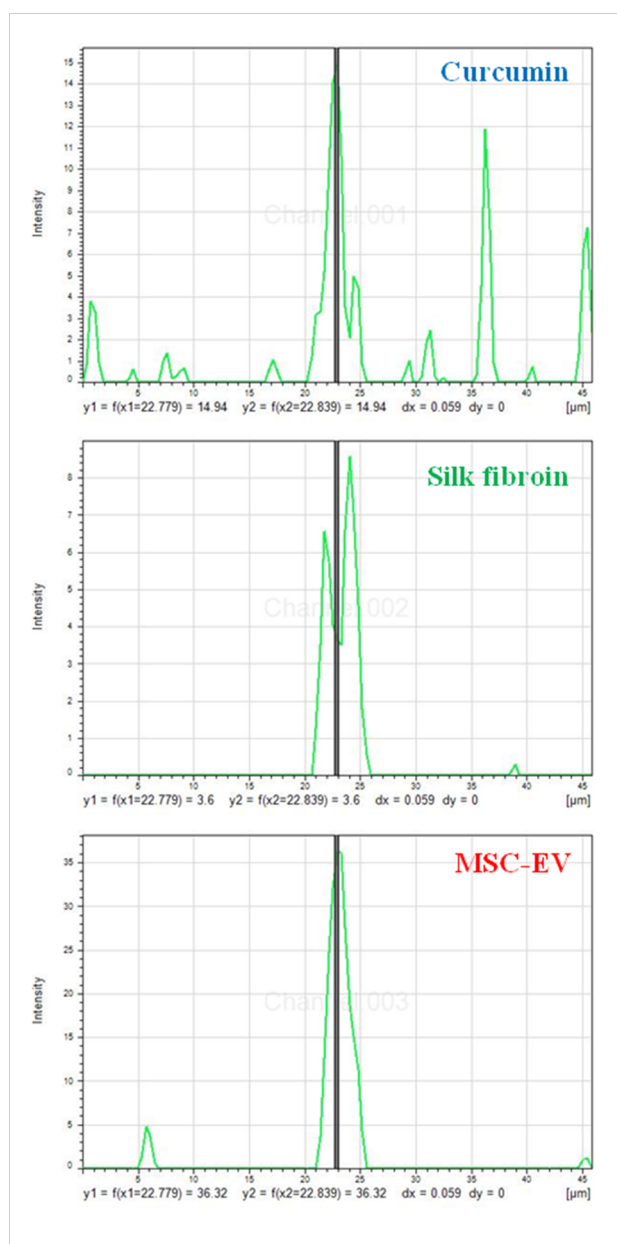


Fig. 8. Histograms of the fluorescence intensity along the line segment, drawn on a specific region of acquired images under confocal microscopy. Three specific excitation/emission filters were considered to detect curcumin, silk and Nile Red.

This result was highlighted by ultrastructural analysis: MSCs were able to release EVs (Figure 9A), spherical membranous systems characterized by a well-defined phospholipid bilayer with a thickness of about 5 nm, and to deliver nanosystems, visible as electron dense particles (Figure 9B). The adopted EV immobilization in alginate for TEM analysis could be an alternative to

cryo-electron microscopy, commonly used for the EV morphological investigation: in fact, EVs were surrounded by typical gel network characterized by alginate strands.

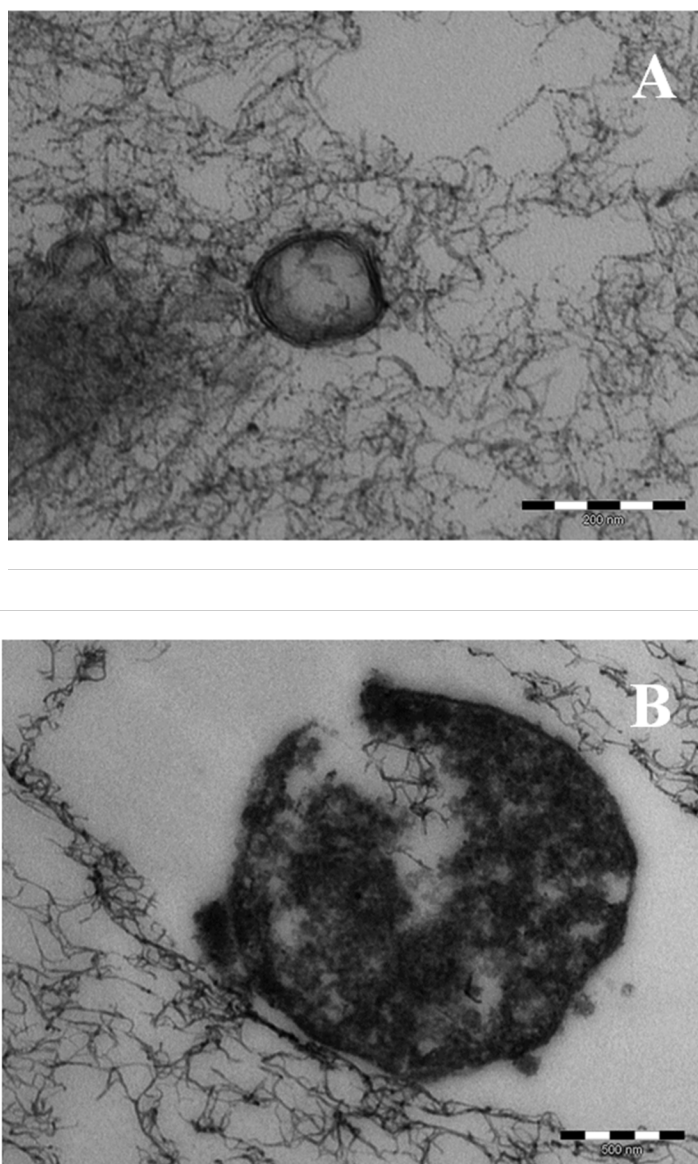


Fig. 9. Transmission electron microscope images of MSC-EVs (A) and carrier-in-carrier system (B).

4. Discussion

In this study, we evolved a new carrier-in-carrier device based on silk/curcumin nanoparticles loaded in MSC-EVs. In our previous work, we coined the “carrier-in-carrier” drug delivery system: micelles based on vitamin E and inulin, loaded with curcumin, were able to cross MSC membrane in few minutes, protecting them from curcumin cytotoxicity. Moreover, MSCs were able to release the entrapped curcumin (Tripodo et al., 2015a). Finally, pharmacokinetic studies

showed the presence of curcumin in the blood after intravenous injection up to 6 hours when it was encapsulated in micelles, while it was quickly removed from the bloodstream when we used free curcumin (Tripodo et al., 2015b). The same approach has been exploited in this paper, using a different biopolymer/nanosystem, namely silk nanoparticles. In literature, different methods have been reported for the preparation of silk nanoparticles, such as salting out (Lammel et al., 2010), electrospraying (Qu et al., 2014), microemulsion method (Myung et al., 2008), capillary microdot-technique (Gupta et al., 2009) and supercritical fluid technology (Zhao et al., 2012); we selected the desolvation method (Seib et al., 2013) because of the peculiar solubility of curcumin in acetone. It is known that the presence of a desolvating agent reduces the hydration of silk chains, leading to protein precipitation as nanoparticles (Azarmi et al., 2006; Weber et al., 2000). The particle size distribution and morphology of our nanoparticles (Figure 1) were in agreement with that reported by other researchers: the use of acetone allows to obtain nanoparticles with a diameter of about 100 nm and a spherical geometry (Seib et al., 2013; Sharma et al., 2016; Zhang et al., 2007).

Two main approaches are usually employed for the drug loading in nanoparticles, 1) the drug encapsulation during nanoparticle production, and 2) the drug surface absorption after nanoparticle formation (Soppimath et al., 2001). We selected the first technique since higher drug loading is reached and we observed that it depends on curcumin starting concentration (Table 1).

The solid-state characterization demonstrated that silk existed in its stable conformation, characterized by high content of crystalline β -sheets. In fact, fibroin can exist in three structural models: Silk I referred to water-soluble structure, Silk II to β -sheet conformation and Silk III at air-water interface (Hu et al., 2006). β -sheet structure can be identified in the spectral region of Amide I (at about 1620 cm^{-1}) and Amide II (at about 1520 cm^{-1}) (Um et al., 2001). Moreover, typical absorption bands of curcumin appeared in samples characterized by higher drug content. The stable conformation of silk fibroin and the increased drug loading in nanoparticles were also confirmed by DSC analyses.

Several methods are reported in literature to study *in vitro* drug release, such as side-by-side diffusion cells with artificial or biological membranes, diffusion technique with dialysis bags, reverse dialysis sac technique, ultracentrifugation and ultrafiltration (Soppimath et al., 2001). We used dialysis tubes in ethanol 50 % v/v to provide sink conditions because of curcumin poor solubility in water (Shaikh et al., 2009). Curcumin *in vitro* release profiles (Figure 5) showed an initial burst release, followed by a plateau condition. The starting burst release could be

attributed to the curcumin amount on the nanosystem surface (Faisant et al., 2002; Soppimath et al., 2001; Tsai et al., 2011). This biphasic release behavior is cohesive with previous researches: for example, Shaikh and colleagues encapsulated curcumin in PLGA nanoparticles and the drug release from nanoparticles occurred by diffusion followed by degradation of the polymer matrix (Shaikh et al., 2009). Lozano-Pérez and colleagues developed silk nanoparticles loaded with resveratrol by adsorption and they observed an initial burst release, reaching the saturation of the aqueous medium in few hours (Abel Lozano-Perez et al., 2014). A burst release was observed in the first 8 hours also using paclitaxel loaded silk nanoparticles (Wu et al., 2013).

In pharmaceutical field, nanoparticle-based approaches aim to improve safety and efficacy of Active Principle Ingredient: the interaction of nanoparticles with the biological environment (target) is strictly related to the particle properties (particle size, shape, and surface charge and chemistry) and the biological milieu (through the formation of a protein corona around the material) (Bobo et al., 2016; Kharazian et al., 2016; Lorenz et al., 2006; Murugan et al., 2015). Nanoparticles are able to pass through the cell membrane by different mechanisms including phagocytosis, pinocytosis, caveolae and clathrin mediated endocytosis (Beddoes et al., 2015). The intracellular uptake of silk nanoparticles has been previously demonstrated on different cell lines, such as breast cancer cells (Gupta et al., 2009; Seib et al., 2013), gastric cancer cells (Wu et al., 2013) and carcinoma cells (Kundu et al., 2010). In all these applications cells represent the target of the pharmaceutical product. To the best of our knowledge, for the first time in this paper, the uptake of silk nanoparticles has been investigated on MSCs and cells were used as drug carrier: the nanoparticle uptake depends on time of incubation (Figure 6) and nanoparticles have been found in the cytoplasm, without cytotoxic effects (Figure 7). The final goal of our study was to demonstrate the ability of MSCs to secrete extracellular vesicles loaded of silk/curcumin nanoparticles. Drugs, such as small RNA therapeutics and small molecules (e.g. anti-inflammatory and anti-cancer drugs (Kim et al., 2016)), are usually encapsulated in EVs using endogenous or exogenous methods: in the endogenous method, cells are loaded with a drug, which is then released in EVs; in the exogenous method, EVs are first isolated and subsequently loaded with the drug (Batrakova and Kim, 2015). Pascucci and colleagues had already shown the MSC ability to deliver paclitaxel through their membranous-vesicular systems, suggesting the possibility of using stem cells as a drug store and exploiting their innate properties (Pascucci et al., 2014). The encapsulation of curcumin in exosomes has been performed by Sun et al. (Sun et al., 2010), demonstrating higher solubility, stability in blood

and higher bioavailability in vivo than free curcumin. We investigated a novel carrier-in-carrier system, composed by MSC-EVs loaded of nanoparticles (Figure 8), exploiting the endogenous loading technique: the first carrier is represented by silk nanoparticles, able to encapsulate high curcumin content, while the second carrier is represented by MSC-EVs, able to retain peculiar properties of their parental cells (Ohno et al., 2016). The cell culture in serum free medium induces the secretion of a heterogeneous milieu of EVs, including exosomes and microvesicles characterized by different size (from 40 to 1000 nm). Qualitative analyses on released product highlighted a higher MSC ability to release nanoparticles within microvesicular systems than exosomes, probably due to nanosystem size (Figure 9).

This combined biological-technological approach represents a novel class of nanosystems, combining beneficial effects of both regenerative cell therapies and pharmaceutical nanomedicine, avoiding the use of viable replicating stem cells. The carrier-in-carrier system, based on stem cell-extracellular vesicles and silk/curcumin nanoparticles, could hold new promises for clinical application, avoiding regulatory affairs related to Advanced Therapy Medicinal Products.

Acknowledges

This work was partially funded by MIUR Pavia-Boston project (call 2015), and the authors thank Prof David Kaplan (Department of Biomedical Engineering, Tufts University, USA) for him fundamental support.

The authors thank Nembri Industrie Tessili S.r.l. (Capriolo (BG), Italy) for certified *Bombyx mori* cocoons, Alfatest Srl (Cinisello Balsamo, Milan, Italy) for nanoparticle tracking analysis, Prof. Sergio Schinelli and Dott. Mayra Paolillo (Drug Sciences Dept., Pavia University, Italy) for willingness on the use of Synergy HT (BioTek) and Dott. Patrizia Vaghi (Centro Grandi Strumenti, Pavia University, Italy) for confocal microscopy analysis.

References

Abel Lozano-Perez, A., Rodriguez-Nogales, A., Ortiz-Cullera, V., Algieri, F., Garrido-Mesa, J., Zorrilla, P., Elena Rodriguez-Cabezas, M., Garrido-Mesa, N., Utrilla, M.P., De Matteis, L., Martinez de la Fuente, J., Luis Cenis, J., Galvez, J., 2014. Silk fibroin nanoparticles constitute a vector for controlled release of resveratrol in an experimental model of inflammatory bowel disease in rats. *International Journal of Nanomedicine* 9, 4507-4520.

Aggarwal, B.B., Harikumar, K.B., 2009. Potential therapeutic effects of curcumin, the anti-inflammatory agent, against neurodegenerative, cardiovascular, pulmonary, metabolic, autoimmune and neoplastic diseases. *International Journal of Biochemistry & Cell Biology* 41, 40-59.

Altman, G.H., Horan, R.L., Lu, H.H., Moreau, J., Martin, I., Richmond, J.C., Kaplan, D.L., 2002. Silk matrix for tissue engineered anterior cruciate ligaments. *Biomaterials* 23, 4131-4141.

Azarmi, S., Huang, Y., Chen, H., McQuarrie, S., Abrams, D., Roa, W., Finlay, W., Miller, G., Löbenberg, R., 2006. Optimization of a two-step desolvation method for preparing gelatin nanoparticles and cell uptake studies in 143B osteosarcoma cancer cells. *J Pharm Pharm Sci.*, pp. 124-132.

Batrakova, E.V., Kim, M.S., 2015. Using exosomes, naturally-equipped nanocarriers, for drug delivery. *Journal of Controlled Release* 219, 396-405.

Beddoes, C.M., Case, C.P., Briscoe, W.H., 2015. Understanding nanoparticle cellular entry: A physicochemical perspective. *Advances in Colloid and Interface Science* 218, 48-68.

Bobo, D., Robinson, K., Islam, J., Thurecht, K., Corrie, S., 2016. Nanoparticle-based medicines: a review of FDA-approved materials and clinical trials to date. *Pharm Res.*

Camussi, G., Quesenberry, P., 2013. Perspectives on the potential therapeutic uses of vesicles. *Exosomes and Microvesicles.*

Caplan, A.I., 2010. What's in a Name? *Tissue Engineering Part A* 16, 2415-2417.

Chlapanidas, T., Farago, S., Mingotto, F., Crovato, F., Tosca, M.C., Antonioli, B., Bucco, M., Lucconi, G., Scalise, A., Vigo, D., Faustini, M., Marazzi, M., Torre, M.L., 2011. Regenerated Silk Fibroin Scaffold and Infrapatellar Adipose Stromal Vascular Fraction as Feeder-Layer: A New Product for Cartilage Advanced Therapy. *Tissue Engineering Part A* 17, 1725-1733.

Chlapanidas, T., Perteghella, S., Farago, S., Boschi, A., Tripodo, G., Vigani, B., Crivelli, B., Renzi, S., Dotti, S., Preda, S., Marazzi, M., Torre, M.L., Ferrari, M., 2016. Platelet lysate and adipose mesenchymal stromal cells on silk fibroin nonwoven mats for wound healing (vol 133, 42942, 2016). *Journal of Applied Polymer Science* 133.

Chlapanidas, T., Tosca, M.C., Farago, S., Perteghella, S., Galuzzi, M., Lucconi, G., Antonioli, B., Ciancio, F., Rapisarda, V., Vigo, D., Marazzi, M., Faustini, M., Torre, M.L., 2013. Formulation and characterization of silk fibroin films as a scaffold for adipose-derived stem cells in skin tissue engineering. *International journal of immunopathology and pharmacology* 26, 43-49.

de Girolamo, L., Lucarelli, E., Alessandri, G., Avanzini, M.A., Bernardo, M.E., Biagi, E., Brini, A.T., D'Amico, G., Fagioli, F., Ferrero, I., Locatelli, F., Maccario, R., Marazzi, M., Parolini, O., Pessina, A., Torre, M.L., Italian Mesenchymal Stem Cell, G., 2013. Mesenchymal Stem/Stromal Cells: A New "Cells as Drugs" Paradigm. Efficacy and Critical Aspects in Cell Therapy. *Current Pharmaceutical Design* 19, 2459-2473.

Faisant, N., Siepmann, J., Benoit, J.P., 2002. PLGA-based microparticles: elucidation of mechanisms and a new, simple mathematical model quantifying drug release. *European Journal of Pharmaceutical Sciences* 15, 355-366.

Farago, S., Lucconi, G., Perteghella, S., Vigani, B., Tripodo, G., Sorrenti, M., Catenacci, L., Boschi, A., Faustini, M., Vigo, D., Chlapanidas, T., Marazzi, M., Torre, M.L., 2016. A dry powder formulation from silk fibroin microspheres as a topical auto-gelling device. *Pharmaceutical Development and Technology* 21, 453-462.

Faustini, M., Bucco, M., Chlapanidas, T., Lucconi, G., Marazzi, M., Tosca, M.C., Gaetani, P., Klinger, M., Villani, S., Ferretti, V.V., Vigo, D., Torre, M.L., 2010. Nonexpanded Mesenchymal Stem Cells for Regenerative Medicine: Yield in Stromal Vascular Fraction from Adipose Tissues. *Tissue Engineering Part C-Methods* 16, 1515-1521.

Gaetani, P., Torre, M.L., Klinger, M., Faustini, M., Crovato, F., Bucco, M., Marazzi, M., Chlapanidas, T., Levi, D., Tancioni, F., Vigo, D., Rodriguez Y Baena, R., 2008. Adipose-derived stem cell therapy for intervertebral disc regeneration: An in vitro reconstructed tissue in alginate capsules. *Tissue Engineering Part A* 14, 1415-1423.

Gupta, V., Aseh, A., Rios, C.N., Aggarwal, B.B., Mathur, A.B., 2009. Fabrication and characterization of silk fibroin-derived curcumin nanoparticles for cancer therapy. *International Journal of Nanomedicine* 4, 115-122.

Hu, X., Kaplan, D., Cebe, P., 2006. Determining beta-sheet crystallinity in fibrous proteins by thermal analysis and infrared spectroscopy. *Macromolecules* 39, 6161-6170.

Kharazian, B., Hadipour, N.L., Ejtehadi, M.R., 2016. Understanding the nanoparticle-protein corona complexes using computational and experimental methods. *International Journal of Biochemistry & Cell Biology* 75, 162-174.

Kim, M.S., Haney, M.J., Zhao, Y., Mahajan, V., Deygen, I., Klyachko, N.L., Inskoe, E., Piroyan, A., Sokolsky, M., Okolie, O., Hingtgen, S.D., Kabanov, A.V., Batrakova, E.V., 2016. Development of exosome-encapsulated paclitaxel to overcome MDR in cancer cells. *Nanomedicine-Nanotechnology Biology and Medicine* 12, 655-664.

- Kumari, A., Yadav, S.K., Yadav, S.C., 2010. Biodegradable polymeric nanoparticles based drug delivery systems. *Colloids and Surfaces B-Biointerfaces* 75, 1-18.
- Kundu, B., Rajkhowa, R., Kundu, S.C., Wang, X., 2013. Silk fibroin biomaterials for tissue regenerations. *Advanced Drug Delivery Reviews* 65, 457-470.
- Kundu, J., Chung, Y.-I., Kim, Y.H., Taeb, G., Kundu, S.C., 2010. Silk fibroin nanoparticles for cellular uptake and control release. *International Journal of Pharmaceutics* 388, 242-250.
- L Ramos, T., Sanchez-Abarca, L.I., Muntion, S., Preciado, S., Puig, N., Lopez-Ruano, G., Hernandez-Hernandez, A., Redondo, A., Ortega, R., Rodriguez, C., Sanchez-Guijo, F., del Canizo, C., 2016. MSC surface markers (CD44, CD73, and CD90) can identify human MSC-derived extracellular vesicles by conventional flow cytometry. *Cell communication and signaling : CCS* 14, 2-2.
- Lammel, A.S., Hu, X., Park, S.-H., Kaplan, D.L., Scheibel, T.R., 2010. Controlling silk fibroin particle features for drug delivery. *Biomaterials* 31, 4583-4591.
- Lorenz, M.R., Holzapfel, V., Musyanovych, A., Nothelfer, K., Walther, P., Frank, H., Landfester, K., Schrezenmeier, H., Mailander, V., 2006. Uptake of functionalized, fluorescent-labeled polymeric particles in different cell lines and stem cells. *Biomaterials* 27, 2820-2828.
- Mishra, D., Hubenak, J.R., Mathur, A.B., 2013. Nanoparticle systems as tools to improve drug delivery and therapeutic efficacy. *Journal of Biomedical Materials Research Part A* 101, 3646-3660.
- Mottaghitalab, F., Farokhi, M., Shokrgozar, M.A., Atyabi, F., Hosseinkhani, H., 2015. Silk fibroin nanoparticle as a novel drug delivery system. *Journal of Controlled Release* 206, 161-176.
- Murugan, K., Choonara, Y.E., Kumar, P., Bijukumar, D., du Toit, L.C., Pillay, V., 2015. Parameters and characteristics governing cellular internalization and trans-barrier trafficking of nanostructures. *International Journal of Nanomedicine* 10, 2191-2206.
- Myung, S.J., Kim, H.-S., Kim, Y., Chen, P., Jin, H.-J., 2008. Fluorescent Silk Fibroin Nanoparticles Prepared Using a Reverse Microemulsion. *Macromolecular Research* 16, 604-608.
- Ohno, S.-i., Drummen, G.P.C., Kuroda, M., 2016. Focus on Extracellular Vesicles: Development of Extracellular Vesicle-Based Therapeutic Systems. *International Journal of Molecular Sciences* 17.
- Parveen, S., Misra, R., Sahoo, S.K., 2012. Nanoparticles: a boon to drug delivery, therapeutics, diagnostics and imaging. *Nanomedicine-Nanotechnology Biology and Medicine* 8, 147-166.

- Pascucci, L., Cocce, V., Bonomi, A., Ami, D., Ceccarelli, P., Ciusani, E., Vigano, L., Locatelli, A., Sisto, F., Doglia, S.M., Parati, E., Bernardo, M.E., Muraca, M., Alessandri, G., Bondiolotti, G., Pessina, A., 2014. Paclitaxel is incorporated by mesenchymal stromal cells and released in exosomes that inhibit in vitro tumor growth: A new approach for drug delivery. *Journal of Controlled Release* 192, 262-270.
- Qu, J., Liu, Y., Yu, Y., Li, J., Luo, J., Li, M., 2014. Silk fibroin nanoparticles prepared by electrospray as controlled release carriers of cisplatin. *Materials Science & Engineering C-Materials for Biological Applications* 44, 166-174.
- Seib, F.P., Jones, G.T., Rnjak-Kovacina, J., Lin, Y., Kaplan, D.L., 2013. pH-Dependent Anticancer Drug Release from Silk Nanoparticles. *Advanced Healthcare Materials* 2, 1606-1611.
- Shaikh, J., Ankola, D.D., Beniwal, V., Singh, D., Kumar, M.N.V.R., 2009. Nanoparticle encapsulation improves oral bioavailability of curcumin by at least 9-fold when compared to curcumin administered with piperine as absorption enhancer. *European Journal of Pharmaceutical Sciences* 37, 223-230.
- Sharma, S., Bano, S., Ghosh, A.S., Mandal, M., Kim, H.-W., Dey, T., Kundu, S.C., 2016. Silk fibroin nanoparticles support in vitro sustained antibiotic release and osteogenesis on titanium surface. *Nanomedicine-Nanotechnology Biology and Medicine* 12, 1193-1204.
- Soppimath, K.S., Aminabhavi, T.M., Kulkarni, A.R., Rudzinski, W.E., 2001. Biodegradable polymeric nanoparticles as drug delivery devices. *Journal of Controlled Release* 70, 1-20.
- Sun, D., Zhuang, X., Xiang, X., Liu, Y., Zhang, S., Liu, C., Barnes, S., Grizzle, W., Miller, D., Zhang, H.-G., 2010. A Novel Nanoparticle Drug Delivery System: The Anti-inflammatory Activity of Curcumin Is Enhanced When Encapsulated in Exosomes. *Molecular Therapy* 18, 1606-1614.
- Tompkins, A.J., Chatterjee, D., Maddox, M., Wang, J., Arciero, E., Camussi, G., Quesenberry, P.J., Renzulli, J.F., 2015. The emergence of extracellular vesicles in urology: fertility, cancer, biomarkers and targeted pharmacotherapy. *Journal of Extracellular Vesicles* 4.
- Torre, M.L., Lucarelli, E., Guidi, S., Ferrari, M., Alessandri, G., De Girolamo, L., Pessina, A., Ferrero, I., Gism, 2015. Ex Vivo Expanded Mesenchymal Stromal Cell Minimal Quality Requirements for Clinical Application. *Stem Cells and Development* 24, 677-685.
- Tripodo, G., Chlapanidas, T., Perteghella, S., Vigani, B., Mandracchia, D., Trapani, A., Galuzzi, M., Tosca, M.C., Antonioli, B., Gaetani, P., Marazzi, M., Torre, M.L., 2015a.

Mesenchymal stromal cells loading curcumin-INVITE-micelles: A drug delivery system for neurodegenerative diseases. *Colloids and Surfaces B-Biointerfaces* 125, 300-308.

Tripodo, G., Pasut, G., Trapani, A., Mero, A., Lasorsa, F.M., Chlapanidas, T., Trapani, G., Mandracchia, D., 2015b. Inulin-D-alpha-Tocopherol Succinate (INVITE) Nanomicelles as a Platform for Effective Intravenous Administration of Curcumin. *Biomacromolecules* 16, 550-557.

Tsai, Y.-M., Chien, C.-F., Lin, L.-C., Tsai, T.-H., 2011. Curcumin and its nano-formulation: The kinetics of tissue distribution and blood-brain barrier penetration. *International Journal of Pharmaceutics* 416, 331-338.

Um, I.C., Kweon, H.Y., Park, Y.H., Hudson, S., 2001. Structural characteristics and properties of the regenerated silk fibroin prepared from formic acid. *International Journal of Biological Macromolecules* 29, 91-97.

van der Meel, R., Fens, M.H.A.M., Vader, P., van Solinge, W.W., Eniola-Adefeso, O., Schiffelers, R.M., 2014. Extracellular vesicles as drug delivery systems: Lessons from the liposome field. *Journal of Controlled Release* 195, 72-85.

Vepari, C., Kaplan, D.L., 2007. Silk as a biomaterial. *Progress in Polymer Science* 32, 991-1007.

Vigani, B., Mastracci, L., Grillo, F., Perteghella, S., Preda, S., Crivelli, B., Antonioli, B., Galuzzi, M., Tosca, M.C., Marazzi, M., Torre, M.L., Chlapanidas, T., 2016. Local biological effects of adipose stromal vascular fraction delivery systems after subcutaneous implantation in a murine model. *Journal of Bioactive and Compatible Polymers* 31, 600-612.

Wang, H.-Y., Zhang, Q., 2015. Processing Silk Hydrogel and Its Applications in Biomedical Materials. *Biotechnology Progress* 31, 630-640.

Weber, C., Coester, C., Kreuter, J., Langer, K., 2000. Desolvation process and surface characterisation of protein nanoparticles. *International Journal of Pharmaceutics* 194, 91-102.

Wu, P., Liu, Q., Li, R., Wang, J., Zhen, X., Yue, G., Wang, H., Cui, F., Wu, F., Yang, M., Qian, X., Yu, L., Jiang, X., Liu, B., 2013. Facile Preparation of Paclitaxel Loaded Silk Fibroin Nanoparticles for Enhanced Antitumor Efficacy by Locoregional Drug Delivery. *Acs Applied Materials & Interfaces* 5, 12638-12645.

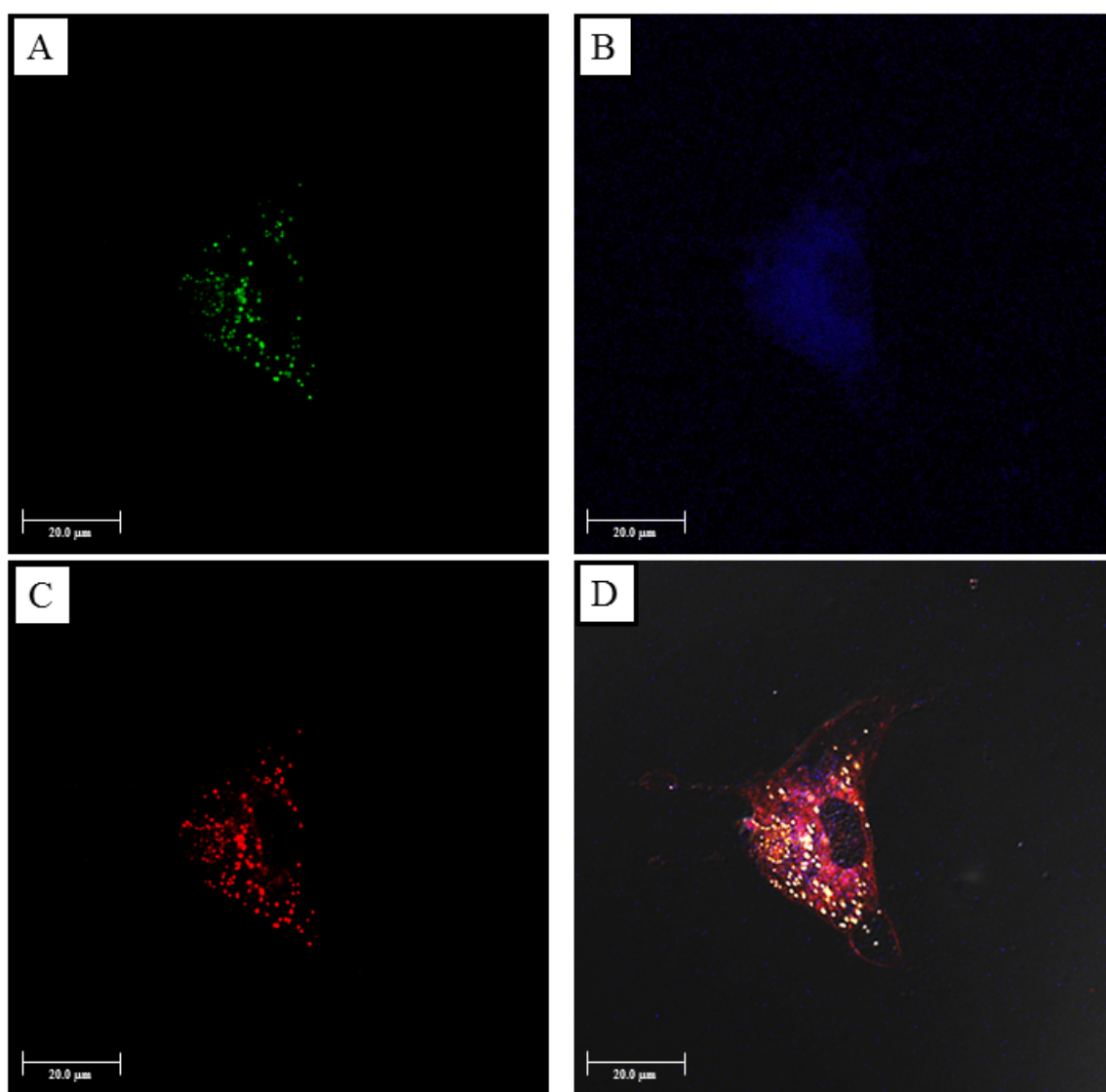
Zhang, Y.-Q., Shen, W.-D., Xiang, R.-L., Zhuge, L.-J., Gao, W.-J., Wang, W.-B., 2007. Formation of silk fibroin nanoparticles in water-miscible organic solvent and their characterization. *Journal of Nanoparticle Research* 9, 885-900.

Zhao, Z., Chen, A., Li, Y., Hu, J., Liu, X., Li, J., Zhang, Y., Li, G., Zheng, Z., 2012. Fabrication of silk fibroin nanoparticles for controlled drug delivery. *Journal of Nanoparticle Research* 14.

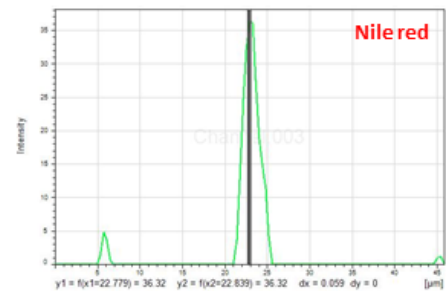
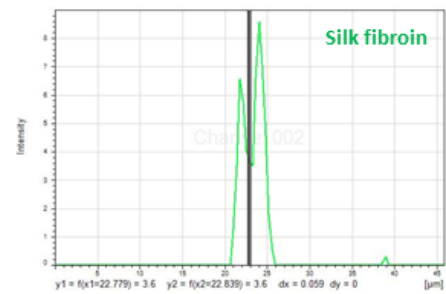
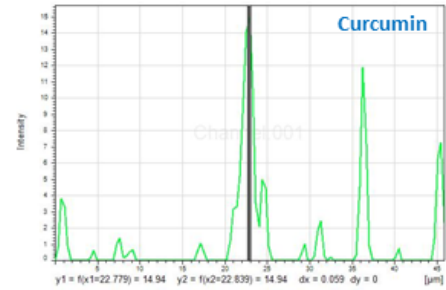
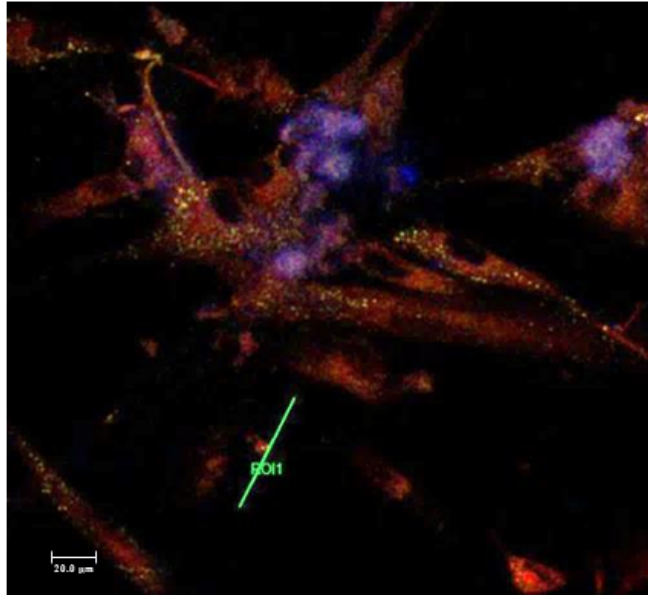
Zhao, Z., Li, Y., Xie, M.-B., 2015. Silk Fibroin-Based Nanoparticles for Drug Delivery. *International Journal of Molecular Sciences* 16, 4880-4903.

Supplementary informations

Focus on nanoparticle uptake by mesenchymal stem cells captured during confocal microscopy analysis. Three different excitation/emission filters employed: green for silk fibroin – Ex 488, Em 500-550 (Fig. 1A), blue for curcumin - Ex 405, Em 430-500 (Fig. 1B) and Nile red for phospholipid detection - Ex 543, Em 580-660 (Fig. 1C). notably, the green spots, showing the presence of silk fibroin nanoparticles, are perfectly overlapped to the blue spots of curcumin, suggesting that the curcumin is mainly loaded in silk fibroin nanoparticles and it is not free in the cytoplasmic environment. In figure 1D is shown the merged resulting from the overlapping of the three different filters employed. This qualitative analysis allowed to verify the nanoparticle localization within the cellular environment.



Photograph of the carrier in carrier took in the supernatants captured during confocal microscopy analysis with respective stack profile charts. Three different filters were considered: green for silk fibroin, blue for curcumin and Nile red for phospholipid detection.



Conclusions

Advanced drug delivery systems have been developed to satisfy the need to improve the technological and biological features of conventional drugs and thus their kinetic release, bioavailability, biodistribution and pharmacokinetics for patient benefits. When considering a drug delivery system, the main issue is the specific targeting, thus showing selectivity and avoiding toxic phenomena, while preserving a high dosage, in order to guarantee the drug efficacy and the therapeutic effect. The advent of nanotechnology 30 years ago opened new frontiers in drug delivery field, overcoming the issues of conventional drug delivery system: a nanotechnological approach would provide the equilibrium between targeting, efficacy and toxicity, which are the three minimum criteria to define a drug. Owing to their biocompatibility, controllable bio-degradability by tuning the protein's degree of crystallinity, molecular weight or adopting crosslinking approaches, mechanical features and non-toxicity, silk fibroin based-nanoparticles have been widely investigated as smart and promising nano drug delivery systems of several drugs, including small molecules, proteins and gene drugs. As demonstrated in this PhD thesis, silk fibroin nanoparticles were obtained via desolvation technique employing acetone as the coacervating agent, which succeeded in triggering the silk fibroin nanoprecipitation. Curcumin and celecoxib were successfully loaded in silk nanosystems, achieving different loadings in relation to the drug solubilized amount in the starting acetone bath. *In vitro* biological studies confirmed that the applied nanotechnological approach avoided the severe cytotoxic and hemotoxic phenomena observed when considering the free drugs, acting as an invisibility cloak, but at the same time allowing the manifestation of their anti-oxidant and anti-inflammatory properties. Silk fibroin nanoparticles, independently from the considered encapsulated active, showed a strong anti-inflammatory activity, highlighted by the reduction of the secretion of the three pro-inflammatory mediators involved in the osteoarthritic pathway. For this reason, silk fibroin can be elevated to an effective anti-inflammatory active and no longer be considered as just an inert polymer support for drug delivery system manufacture. Despite the excellent properties and results obtained using silk fibroin nanoparticles, it is still necessary to address some critical challenges related to the manufacture process; in fact, silk fibroin is a natural polymer whose features are very hard to standardize and each preparation technique shows pros and cons. For these reasons, it is important to continue developing and testing novel nanoparticles fabrication techniques to match different demands, to ameliorate the production parameters and to fulfill the existing gaps.

Among the bio-inspired nano-drug delivery systems, extracellular vesicles have been recently proposed since they retain similarities with already employed nano drug delivery systems, such as liposomes, offering even better features that can not be found in other carriers: they are expected to be less toxic since they are composed of the same phospholipid bilayer of cellular membrane and less immunogenic since they are composed of the same constituents of the organism to which they are going to be administered showing the innate tropism to diseased tissues and the ability to overcome physiological barriers of our body. Cells can be considered as natural “cargo maker” able to release in the extracellular milieu extracellular vesicles as small bilayer-enclosed membranous nanosystems, both in physiological and pathological conditions. Extracellular vesicles act as shuttles by carrying lipids, proteins, mRNAs and miRNAs, thus allowing cell-to-cell communication. Thanks to their cargo, they are able to preserve and mimic their parent cell properties: for this reason, depending on their origin, they retain intrinsic immune regulatory activities. In particular, those derived from mesenchymal stem cells retain intrinsic immunomodulatory, regenerative, tissue reprogramming and homing properties. This PhD thesis aimed to combine a nanotechnological approach with a nanobiological one throughout the development of an innovative carrier-in-carrier system. Exploiting the silk fibroin-based nanoparticles previously obtained, loaded with two drug molecules and *in vitro* tested, and coupling them with the extracellular vesicles secreted by mesenchymal stem/stromal cells, it was possible to harness both features of the two considered carriers. The nanosystems were effectively and completely uptaken within 60 minutes by the cells, showing a cytoplasmic localization, and they were released in the extracellular milieu as “extracellular vesicles enriched systems” as demonstrated by both confocal and transmission microscopies. After nanoparticle internalization, cells were able to release extracellular vesicles loaded with silk fibroin nanosystems thus creating a “Next Generation Drug Delivery Systems”, which would boost the therapeutic efficacy of many small molecules, drugs and nanosystems while allowing specific targeting to injured tissues and avoiding unspecific dissemination.

Future Outlooks

This PhD research does not end with the obtained results: conversely, they are the starting points for further investigations that will complete the project. The carrier-in-carrier system, based on stem cell-extracellular vesicles and silk/curcumin nanoparticles, proposed in this PhD thesis, could hold new promises for several clinical applications. Future steps will provide the delivery of other hydrophobic drugs but also of hydrophilic molecules into silk fibroin nanosystems, the characterization of the nanoparticle internalization mechanism and the full both qualitative and quantitative characterization profile of the developed carrier-in-carrier system. Moreover, the investigation of the anti-inflammatory potential of the carrier-in-carrier will be carried out for the treatment of musculoskeletal diseases and *in vitro* efficacy studies will be done by comparing the nanoparticles, the EVs and the carrier-in-carrier products to find the optimal formulation. Finally, we want to verify in an *in vivo* model the effective innate homing of our “next generation drug delivery system” towards pathological tissues. All of these purposes need to be addressed in order to achieve the final goal of this project that is to obtain an innovative and effective product suitable for scale-up GMP production and exploitable for the treatment of musculoskeletal diseases.

Appendix



Sericin is a bioactive silk-protein, considered for centuries as a waste product of textile industry, showing intrinsic biological activities such as anti-oxidant, anti-elastase, anti-tyrosinase, immunomodulatory and regenerative. As described in the introduction of this PhD thesis, silk sericin represents a suitable “active” polymer for the creation of drug delivery systems. Today, microalgae are at the cutting edge in several fields including nutraceutical, food, cosmetics, biofuels and pollution prevention: they are prokaryotic or eukaryotic photosynthetic microorganisms, able to live in harsh conditions. They are enriched in proteins, sterols, polyunsaturated fatty acids (PUFAs), vitamins, anti-oxidants (polyphenols), pigments (carotenoids) making them suitable for the treatment of different diseases. With this research we wanted to investigate a possible synergism between silk sericin and microalgae extracts for the wound regeneration.

Paper 5



Article

In Vitro Effectiveness of Microspheres Based on Silk Sericin and *Chlorella vulgaris* or *Arthrospira platensis* for Wound Healing Applications

Elia Bari ¹ , Carla Renata Arciola ^{2,3}, Barbara Vigani ¹, Barbara Crivelli ¹, Paola Moro ¹, Giorgio Marrubini ¹, Milena Sorrenti ¹, Laura Catenacci ¹, Giovanna Bruni ⁴, Theodora Chlapanidas ¹, Enrico Lucarelli ⁵, Sara Perteghella ^{1,*} and Maria Luisa Torre ¹ 

¹ Department of Drug Sciences, University of Pavia, Viale Taramelli 12, 27100 Pavia, Italy; elia.bari@unipv.it (E.B.); barbara.vigani@unipv.it (B.V.); barbara.crivelli@unipv.it (B.C.); paola.moro@unipv.it (P.M.); giorgio.marrubini@unipv.it (G.M.); milena.sorrenti@unipv.it (M.S.); laura.catenacci@unipv.it (L.C.); theodora.chlapanidas@unipv.it (T.C.); marina.torre@unipv.it (M.L.T.)

² Research Unit on Implant Infections, Rizzoli Orthopaedic Institute of Bologna, Via di Barbiano 1/10, 40136 Bologna, Italy; carlarena.arciola@ior.it

³ Department of Experimental, University of Bologna, Diagnostic and Specialty Medicine (DIMES), Via San Giacomo 14, 40126 Bologna, Italy

⁴ Department of Chemistry, University of Pavia, Viale Taramelli 16, 27100 Pavia, Italy; giovanna.bruni@unipv.it

⁵ Osteoarticular Regeneration Laboratory, Rizzoli Orthopaedic Institute of Bologna, Via Giulio Cesare Pupilli 1, 40136 Bologna, Italy; enrico.lucarelli@ior.it

* Correspondence: sara.perteghella@unipv.it; Tel.: +39-0382-987359

Received: 5 July 2017; Accepted: 21 August 2017; Published: 23 August 2017

Abstract: Some natural compounds have recently been widely employed in wound healing applications due to their biological properties. One such compound is sericin, which is produced by *Bombix mori*, while active polyphenols, polysaccharides and proteins are synthesized by *Chlorella vulgaris* and *Arthrospira platensis* microalgae. Our hypothesis was that sericin, as an optimal bioactive polymeric carrier for microencapsulation process, could also improve the regenerative effect of the microalgae. A solvent-free extraction method and spray drying technique were combined to obtain five formulations, based on algal extracts (*C. vulgaris* and *A. platensis*, Chl and Art, respectively) or silk sericin (Ser) or their mixtures (Chl-Ser and Art-Ser). The spray drying was a suitable method to produce microspheres with similar dimensions, characterized by collapsed morphology with a rough surface. Art and Art-Ser showed higher antioxidant properties than other formulations. All microspheres resulted in cytocompatibility on fibroblasts until 1.25 mg/mL and promoted cell migration and the complete wound closure; this positive effect was further highlighted after treatment with Art and Art-Ser. To our surprise the combination of sericin to Art did not improve the microalgae extract efficacy, at least in our experimental conditions.

Keywords: silk sericin; *Chlorella vulgaris*; *Arthrospira platensis*; spray drying; microspheres; wound healing

1. Introduction

Bioactive compounds from natural matrices are valuable and attractive products for the pharmaceutical and cosmetic industry [1,2]. Microalgae are unicellular microorganisms, which react to the harsh conditions of their habitats (temperature, salinity, light intensity) with adaptive mechanisms, such as the synthesis of a wide range of biologically active secondary metabolites [3]. The different metabolic pathways activated as defense strategies by each species of microalgae explain their immense diversity in terms of structural and chemical composition [4]. Several studies demonstrated the antioxidant [5], anti-inflammatory [6] and antimicrobial [7] properties of microalgae due to their content in polyunsaturated acids, vitamins, pigments, polyphenols, polysaccharides and proteins [8].

Arthrospira platensis and *Chlorella vulgaris*, approved by the Food and Drug Administration (FDA) as GRAS (Generally Recognized As Safe), are two of the most interesting and abundant species of microalgae, with an annual industrial production of 3000 and 4000 tons, respectively

[9]. These photosynthetic organisms, generally cultivated in open ponds, rapidly grow under extreme environmental conditions: the simple and low-cost cultivation systems make *A. platensis* and *C. vulgaris* suitable for industrial-scale production [10]. Over the years, several studies have been performed on both microalgae species to optimize the extraction and purification of bioactive compounds, potentially useful for different medicinal applications [11].

A. platensis, also called Spirulina due to its helical filamentous morphology, is a Cyanobacterium rich in proteins (60–70% w/w), vitamins (4% w/w, particularly pro-vitamin A, B₁, B₂, B₆, B₁₂, E and D), polysaccharides, carotenoids, minerals and essential fatty acids [12]. Due to its chemical composition, *A. platensis* has been extensively used as a nutritional supplement [13] and, nowadays, it is also considered a potential pharmaceutical source due to its antioxidant, immunomodulatory and anti-inflammatory properties, as demonstrated both in vitro and in vivo [14]. Multiple health and nutritional needs have also been met by *Chlorella vulgaris* extracts, for which its essential amino acid, vitamin, fatty acid and mineral contents is known for and has been reported [15]. Moreover, *C. vulgaris* contains several polysaccharides, including β -1,3-glucan, an active immunostimulator and a free-radical scavenger, [16] and a significant amount of antioxidant pigments, such as β -carotene, lutein and chlorophylls [17].

In cosmetics and in wound healing dressings, sericin has been appreciated as an additive due to its biological activities [18–20]. Silk sericin has long been known to be a potent natural antioxidant due to the high content of hydroxyl amino acids [21]. It has been reported that silk sericin exhibits ROS (Reactive Oxygen Species)-scavenging, anti-tyrosinase, anti-elastase, immunomodulatory activities [22] and promotes wound healing and collagen deposition by fibroblasts and keratinocytes [23].

Silk sericin for wound healing has been investigated in two clinical trials (www.clinicaltrials.gov): a wound dressing composed of silk sericin/PVA was shown to accelerate the healing of split-thickness skin graft donor sites as compared to the commercially available Bactigras[®] (ID. NCT02091076, study completed). In another study (NCT01539980, study completed), the application of a silver zinc sulfadiazine cream, with or without silk sericin powder, confirmed the efficacy of sericin in promoting the re-epithelialization of a second degree burn in 5–7 days less than in the control group.

In a previous paper, we demonstrated that the biological effect of a natural flavanone, such as naringenin, was surprisingly increased when associated with sericin [24]. Based on this evidence, we hypothesized that sericin could improve the regenerative effect of the microalgae

extracts. To the best of our knowledge, the association of silk sericin and microalgae aqueous extracts has never been tested in wound healing fields: in the present work, these natural bioactive compounds have been selected to assess their synergic effects on cell proliferation and migration. The aqueous extracts of both *C. vulgaris* and *A. platensis* were combined with silk sericin to manufacture microspheres intended for the topical treatment of skin wounds, and a set of characterization analyses has been carried out to verify the final product performances.

2. Methods

2.1. Materials

Bovine serum albumin (BSA), phenol, glucose monohydrate, sulfuric acid 99.999%, 2,2-diphenyl-2-picrylhydrazyl hydrate (DPPH), 3-(4,5-dimethylthiazol-2-yl)-2,5-diphenyltetrazolium bromide (MTT) and dimethyl sulfoxide (DMSO) were purchased from Sigma-Aldrich (Milan, Italy). Human fibroblast cells were obtained from the European Collection of Authenticated Cell Cultures Cell Bank (ECACC, Salisbury, UK), while all reagents used for cell cultures were purchased from Euroclone (Milan, Italy).

2.2. Preparation of Microalgae Extracts

Chlorella vulgaris and *Arthrospira platensis* were purchased from Archimede Ricerche S.r.l (Camporosso, Imola, Italy). Microalgae were added to distilled water (2.5% w/v) and heated at 105 °C for 15 min in autoclave (Auclave 760, Asal Srl, Milan, Italy). After cooling, microalgae suspensions were centrifuged at 3000× g for 10 min and the algal aqueous extracts [25] were collected. Known volumes of both extracts were dried in a stove to calculate the final concentrations.

2.3. Extraction of Silk Sericin

The sericin extraction was performed as previously reported [22]: briefly, *Bombyx mori* cocoons were cut, soaked in distilled water (40 mL/g of cocoons) and autoclaved for 1 h at 120 °C. Sericin solution was separated from degummed fibroin fibers and the concentration was calculated by drying of known volumes.

2.4. Microsphere Preparation by Spray Drying

Five different microsphere formulations, based on algal extracts (*Chlorella vulgaris* and *Arthrospira platensis*) or silk sericin or their combination (Chl, Art, Ser, Chl-Ser, Art-Ser) were prepared. The concentration of both algal extracts and silk sericin solution was 0.8% w/v. Samples were spray dried using a Büchi Mini Spray Dryer (Flawil, Switzerland). The following process parameters were set: pump, 7 mL/min; inlet temperature, 110 °C; outlet temperature, 60 °C; air pressure, 3 bar; fluid flow, 500–600 mL/h [26,27]. Table 1 reported the relative amounts of each component. For each considered formulation, at least three batches were produced. At the end of the spray drying process, the percentage yield was determined as follows: $(w_{mic}/w_{comp}) \times 100$, where w_{mic} was the weight of the spray dried microspheres and w_{comp} was the total weight of the components dissolved in the spray dried solution.

Table 1. Theoretical composition of microspheres reported as % w/w of *A. platensis* extract, *C. vulgaris* extract and silk sericin in each formulation (Chl, Art, Ser, Chl-Ser and Art-Ser).

Formulation	<i>A. platensis</i> Extract	<i>C. vulgaris</i> Extract	Silk Sericin
Chl	0	100	0
Art	100	0	0
Ser	0	0	100
Chl-Ser	0	50	50
Art-Ser	50	0	50

2.5. Microsphere Characterization

Microsphere characterization has been carried out following the current pharmaceutical requirements to qualify products and processes in an application context: particle size distribution, physicochemical characterization of solid state (morphology, Fourier transform infrared spectroscopy, Thermogravimetric Analysis), chemical composition, and, for this specific antioxidant product, ROS-scavenging activity (quality requirement). Therefore, the product cytotoxicity was assessed in an in vitro cellular model (safety requirement), and finally the wound healing potential was evaluated by a standard scratch test (efficacy requirement).

2.5.1. Granulometric Analysis

Granulometric analysis of microspheres was performed by a laser light scattering granulometer (Beckman Coulter LS230, Miami, Florida), equipped with a small volume cell (120 mL volume; obscuration 5%); the refractive index was set at 1.359 for ethanol. A sample for each microsphere formulation was suspended in ethanol and maintained, under magnetic stirring, for 5 min; ethanol suspensions were then put into the measurement cell and ran in five replicates

of 90 s each. Results were expressed as the average of at least five replicates for each microsphere formulation. The analysis of the data included the computation of the mean, standard deviation (S.D.), 10th, 50th, and 90th percentile of the volume-weighted diameter $d_{4,3}$ (d_{10} , d_{50} and d_{90} , respectively) and the mean and S.D. of the surface-weighted diameter ($d_{3,2}$). The width of the particle size distribution was described by the relative span value that was calculated as follows: $(d_{90} - d_{10})/d_{50}$.

2.5.2. Scanning Electron Microscopy (SEM)

A Zeiss EVO MA10 (Carl Zeiss, Oberkochen, Germany) was used to analyze the morphology of microparticles. The samples were gold-sputter coated under argon to render them electrically conductive prior to microscopy.

2.5.3. Fourier Transform Infrared Spectroscopy (FTIR)

FT-IR spectra were obtained using a Spectrum One Perkin-Elmer spectrophotometer (Perkin Elmer, Wellesley, MA, USA) equipped with a MIRacle™ ATR device (Pike Technologies, Madison, WI, USA). The IR spectra in transmittance mode were obtained in the spectral region of $650\text{--}4000\text{ cm}^{-1}$ with a resolution of 4 cm^{-1} .

2.5.4. Simultaneous Thermogravimetric Analysis (TGA/DSC 1)

Thermogravimetric Analysis is a typical analytical technique applied in the physicochemical characterization of the solid state. In this context, it was used to quantify the water content of the products and, above all, their thermal stability, comparing the microalgae as is, and after their extraction by solvent free method and formulation in microspheres by spray-drying technique. The TGA was carried out with a Mettler STARe system (Mettler Toledo, Milan, Italy) TGA on 3–4 mg samples in 70 μL alumina crucibles ($30\text{--}600\text{ }^\circ\text{C}$ temperature range; heating rate 10 K min^{-1} ; nitrogen air atmosphere flux 50 mL min^{-1}). The instrument was previously calibrated with Indium as standard reference, and measurements were carried out at least in triplicate.

2.5.5. Determination of Protein Content

The protein content of each microsphere formulation was estimated by using a Micro BCA™ Protein Assay Kit (ThermoFisher Scientific, Rockford, IL, USA), according to the manufacturer's instructions. Bicinchoninic acid (BCA) was used as detection reagent for

cuprous ion (Cu^{1+}) that is produced when a protein reduces Cu^{2+} in an alkaline environment. The chelation of two BCA molecules with one Cu^{+} produces a water-soluble purple complex, which exhibits a strong absorbance at 562 nm that is directly proportional to the protein content [28]. Microsphere samples were suspended in distilled water, combined with the reagents (provided with Micro BCA™ Protein Assay Kit) in a 1:1 ratio and incubated at 37 °C for 2 h. Bovine Serum Albumin (BSA), chosen as protein standard, was diluted in deionized water at different concentrations (10–75 $\mu\text{g}/\text{mL}$) and processed as reported for the samples in order to prepare a standard curve from which the protein concentration of each microsphere formulation was extrapolated. The optical density was measured at 562 nm with multi-plate reader (Synergy HT, BioTek, Swindon, UK); analyses were performed in three replicates and results were reported as μg proteins/mg sample.

2.5.6. Determination of Carbohydrate Content

The carbohydrate content of each microsphere formulation was determined by using the phenol-sulfuric acid method, as reported by DuBois and colleagues [29]. Briefly, 2 mL of microspheres suspended in distilled water (0.1 mg/mL) were mixed with 1 mL of phenol aqueous solution (5% w/v) and 5 mL of sulphuric acid in test tubes. After 10 min at room temperature in dark conditions, the test tubes were placed in ice for 20 min and then centrifuged at $3000\times g$ for 10 min. Glucose monohydrate, selected as carbohydrate standard, was diluted in deionized water at different concentrations (0–0.1 mg/mL) and processed in an identical manner as above in order to prepare a standard curve from which the carbohydrate concentration of each microsphere formulation was extrapolated. The absorbance was measured at 490 nm with a UV-vis spectrophotometer Uvikon 930 (Kontron Instruments, Everett, MA, USA). Analyses were performed in three replicates and results were reported as μg carbohydrates/mg sample.

2.5.7. ROS-Scavenging Activity Assay

The ROS-scavenging activity was evaluated by the DPPH (2,2-diphenyl-2-picrylhydrazyl hydrate) method, according to Chaudhuri et al., with slight modifications [30]. In detail, each microsphere formulation was tested at different concentrations (1.25, 2.5, 5.0, 10, 25 and 50 mg/mL) after dissolution in distilled water under magnetic stirring. Fifty μL of each dilution were mixed with 1950 μL of DPPH solution (1 mM) in 70% v/v methanol and kept in the dark for 20 min at room temperature. All reaction mixtures were centrifuged at $3000\times g$ for 10 min

and then the optical density was measured at 517 nm with a UV-vis spectrophotometer. Ascorbic acid, chosen as the positive control, was tested at the same concentrations of microsphere samples, while a reaction mixture composed by 50 μL of 70% v/v methanol and 1950 μL of DPPH solution was prepared as a negative control. The percentage of ROS-scavenging activity was calculated according to the following equation: % activity = $(A - B)/A \times 100$, where A was the optical density of negative control and B was the optical density of the samples. Analyses were performed in three replicates, and results were reported as the mean \pm standard deviation of the ROS-scavenging activity percentage.

2.6. In Vitro Assays

2.6.1. Cytotoxicity Assay

Human fibroblast cells were seeded at a density of 10,000 cells/cm² in a 96-well plate and cultured for 24 h in DMEM/F12 culture medium with the addition of 10% FBS, 1% penicillin/streptomycin and 1% amphotericin B (37 °C, 5% CO₂). Each microsphere formulation was solubilized in the aforementioned culture medium and then filtered using 0.22 μm membranes (Merck Millipore, Tullagreen Carrigtwohill, Ireland). Different concentrations were tested: 0.05, 0.1, 0.25, 0.5, 1.25, 2.5, 5.0 and 10 mg/mL for Chl, Art and Ser formulations, while 0.1, 0.2, 0.5, 1.0, 2.5, 5.0, 10 and 20 mg/mL for Chl-Ser and Art-Ser formulations were used in order to test the cytotoxic effect of the same amount (mg/well) of algal aqueous extract and sericin. After culture medium removal, human fibroblast cells were incubated with 100 μL of each sample for 24 h and thus cell metabolic activity was evaluated by performing an MTT assay. Specifically, supernatants were discarded from each well and 100 μL of MTT solution (0.5 mg/mL) were added. After 3 h, MTT solution was substituted with 100 μL of DMSO. The optical density (OD) was measured at 570 and 670 nm (reference wavelength) with a multi-plate reader; analyses were performed in three replicates for each sample. Cell metabolic activity (%) was calculated as follows: $100 \times (\text{ODs}/\text{ODc})$, where ODs is the mean value of the measured optical density of each tested sample and ODc is the mean value of the measured optical density of cells incubated without microspheres (control). The study was performed in three replicates, using primary human fibroblasts obtained from 3 donors (4th passage), with viability $\geq 95\%$, (Trypan blue staining, $n = 150$), and showing no variability in term of cellular doubling time (data not shown).

2.6.2. Scratch Assay

Microspheres were solubilized in the aforementioned culture medium and sterilized by filtration; different concentrations were tested: 0.05, 0.1, 0.25 and 0.5 mg/mL for Chl, Art and Ser formulations, while 0.1, 0.2, 0.5 and 1.0 mg/mL for Chl-Ser and Art-Ser formulations.

The same three human fibroblast cell lines used in the previous experiment, seeded at a density of 40,000 cells/cm² in a 24-well plate, were scraped with a sterile p200 pipet tip, creating a linear “scratch” [31]. “Scatched” cells were incubated with 1 mL of each sample. After 24, 48 and 72 h, images of treated cells were acquired using a digital camera (Lumenera Infinity 1-3C, Nepean, Canada) connected to a phase-contrast microscope (Nikon Eclipse E400, Melville, New York, NY, USA) in order to evaluate the cell migration. Using scratch wounded cells and closed wound as standards, images were observed by five independent expert operators and a score between 0 (no cell migration) and 10 (completed cell migration) was given for each formulation at each considered time endpoint [27,32].

2.6.3. Statistical Analysis

Raw data were processed using STATGRAPHICS XVII (Statpoint Technologies, Inc., Warrenton, VA, USA), Microsoft[®] Excel 2013, and R, R Core Team (2014). R: A language and environment for statistical computing. R Foundation for Statistical Computing, Vienna, Austria (<http://www.R-project.org>). The libraries outliers by Lukasz Komsta (2011), (<http://CRAN.R-project.org/package=outliersoutliers>), and apl-pack by Hans Peter Wolf and Uni Bielefeld (2014), (<http://CRAN.R-project.org/package=aplpack>), were used to test the granulometric analysis data for the presence of univariate and bivariate outliers. A linear generalized Analysis of Variance model (ANOVA) was used to study the data.

The amount of proteins and carbohydrates contained in each microsphere formulation was analyzed taking into account the µg proteins/mg microspheres and µg carbohydrates/mg microspheres as response variables and the microsphere formulation (Chl, Art, Ser, Chl-Ser and Art-Ser) as a fixed factor. The ROS-scavenging activity (%) was evaluated considering the effect of both microsphere formulation and concentration (1.25, 2.5, 5.0, 10, 25, 50 mg/mL). Moreover, the cytotoxicity of each formulation was analyzed, fixing microsphere formulation and concentration. The scores given by the five independent operators at each time were compared using a t-test for paired means; finally, results of scratch assay were processed, considering microsphere formulation and time (0, 24, 48 and 72 h) as fixed factors in a two-way ANOVA.

The differences between groups were analyzed with the post hoc LSD's (Least Significant Difference) test for multiple comparisons. Statistical significance was set at $p \leq 0.05$.

3. Results

3.1. Microsphere Characterization

The microalgae aqueous extracts and the sericin solution were spray dried, alone or combined, to obtain microspheres (Chl, Art, Ser, Chl-Ser and Art-Ser): the composition of the starting solutions did not influence the spray drying process, obtaining a satisfactory process yield ($35 \pm 8\%$), considering the lab-scale production.

All formulations showed a unimodal distribution of the volume-weight ($d_{4,3}$) and surface-weight ($d_{3,2}$) diameters. Results evidenced that the spray drying was a suitable method to produce microspheres with similar dimensions. The 95% confidence interval ($\alpha = 0.05$) of the volume-weight diameters ($d_{4,3}$) were $4.7 \pm 0.2 \mu\text{m}$ for Chl ($n = 9$), $3.5 \pm 0.2 \mu\text{m}$ for Art ($n = 10$), $3.4 \pm 0.1 \mu\text{m}$ for Ser ($n = 10$), $6.5 \pm 0.1 \mu\text{m}$ for Chl-Ser ($n = 5$) and $4.1 \pm 0.1 \mu\text{m}$ for Art-Ser ($n = 6$). The 95% confidence interval ($\alpha = 0.05$) of the surface-weight diameters ($d_{3,2}$) were $3.09 \pm 0.08 \mu\text{m}$ for Chl, $2.58 \pm 0.05 \mu\text{m}$ for Art, $2.1 \pm 0.2 \mu\text{m}$ for Ser, $2.56 \pm 0.05 \mu\text{m}$ for Chl-Ser and $2.02 \pm 0.02 \mu\text{m}$ for Art-Ser. The presence of sericin elicited a slight increase of the $d_{4,3}$ and a decrease of the $d_{3,2}$ for Chl-Ser formulation compared with Chl and for Art-Ser compared to the Art one. The Art microspheres presented the narrowest size distribution as confirmed by the span: 1.74 for Chl, 1.37 for Art, 1.52 for Ser, 1.89 for Chl-Ser and 1.51 for Art-Ser (the values which tend to indicate a narrow distribution). Moreover, all microspheres showed typical ellipsoid or bi-concave shapes, as evidenced by the observation that the mean volume-weight diameter ($d_{4,3}$) was always higher than the mean surface-weight diameter ($d_{3,2}$) with high statistical significance ($p < 0.001$). These results were confirmed by the scanning electron microscopy analysis: all formulations were characterized by collapsed microspheres with a rough surface, even if some scattered smooth and round elements were appreciated in Chl-Ser and Art-Ser (Figure 1).

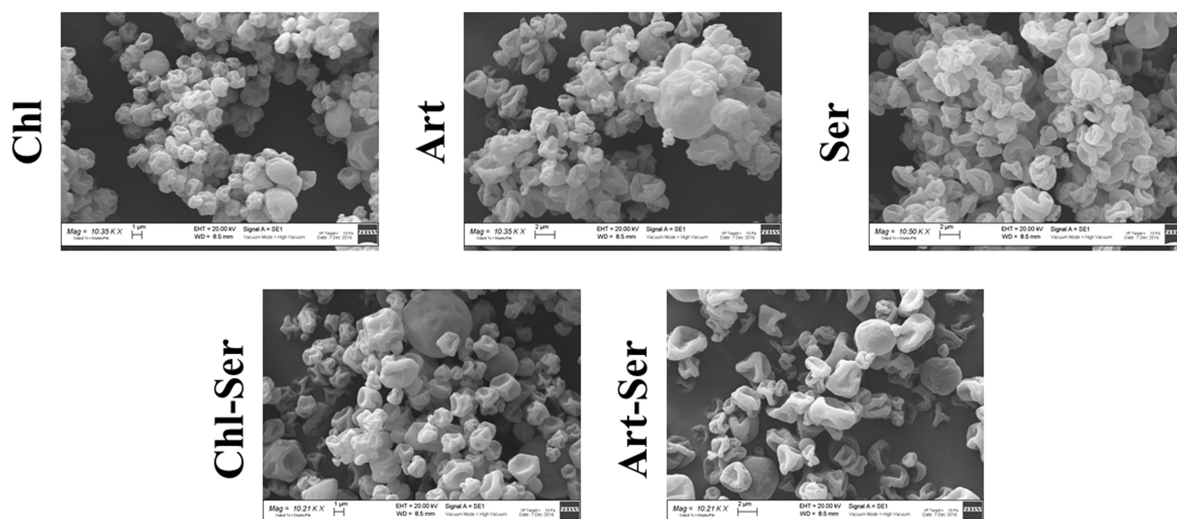


Figure 1. SEM images of Chl, Art, Ser, Chl-Ser and Art-Ser microspheres formulations; scale bar: 2 µm.

The thermogravimetric analysis revealed a first mass loss of about 10% due to the absorbed water evaporation in the temperature range 30–200 °C. Furthermore, a rapid loss of weight was recorded at 220 °C indicating the decomposition of the microparticles (curves not reported). The absence of differences in the decomposition temperatures indicated that the solvent-free extraction method and spray-drying technique allowed the production of stable microspheres. In Figure 2a FT-IR spectra of Chl and Art formulations are reported: Art microspheres exhibited more intensive absorption bands, especially in the -OH phenolic region (3580–3650 cm^{-1}), indicating higher antioxidant properties. The FT-IR spectra of formulations containing sericin, alone or in association with microalgae extracts, are reported in Figure 2b: Ser showed typical bands at 1638 and 1520 cm^{-1} due to amide I and II, respectively; the shift of these bands to higher wavenumbers in Chl-Ser and Art-Ser formulations is attributable to the interaction between Ser and microalgae extracts. Moreover, the band at 1399 cm^{-1} is due to symmetric deformation of -CH₂ and -CH₃ of proteins/carboxylic groups; finally, two typical bands, related to the stretching vibration of polysaccharides, were evidenced in the region at 1250–900 cm^{-1} (Figure 2b).

Microsphere protein and carbohydrate contents are reported in Table 2. ANOVA analyses indicated that the formulation had a significant effect on both protein and carbohydrate content ($p < 0.001$). In particular, the protein content of Ser was significantly higher than the other formulations and the simultaneous presence of silk sericin and microalgae extracts (Chl-Ser and Art-Ser) increased proteins when compared to Chl and Art (Table 2). No significant differences

were observed between Chl and Art in terms of carbohydrate concentration, which showed higher content than Ser, Chl-Ser and Art-Ser (Table 2).

Table 2. Protein and carbohydrate contents in the resulting microspheres. Results are reported as mean values \pm S.D. ($n = 3$). Different letters (a, b, c, d and e) indicate significant differences between formulations ($p < 0.0001$).

Formulation	Protein Content ($\mu\text{g Proteins/mg Microspheres}$)	Carbohydrate Content ($\mu\text{g Carbohydrates/mg Microspheres}$)
Chl	162.74 \pm 2.11 ^a	97.45 \pm 3.29 ^a
Art	217.41 \pm 21.26 ^b	100.50 \pm 6.67 ^a
caSer	1104.89 \pm 46.07 ^c	17.14 \pm 0.05 ^b
Chl-Ser	640.94 \pm 8.02 ^d	46.48 \pm 0.10 ^c
Art-Ser	714.35 \pm 21.95 ^e	36.53 \pm 3.45 ^d

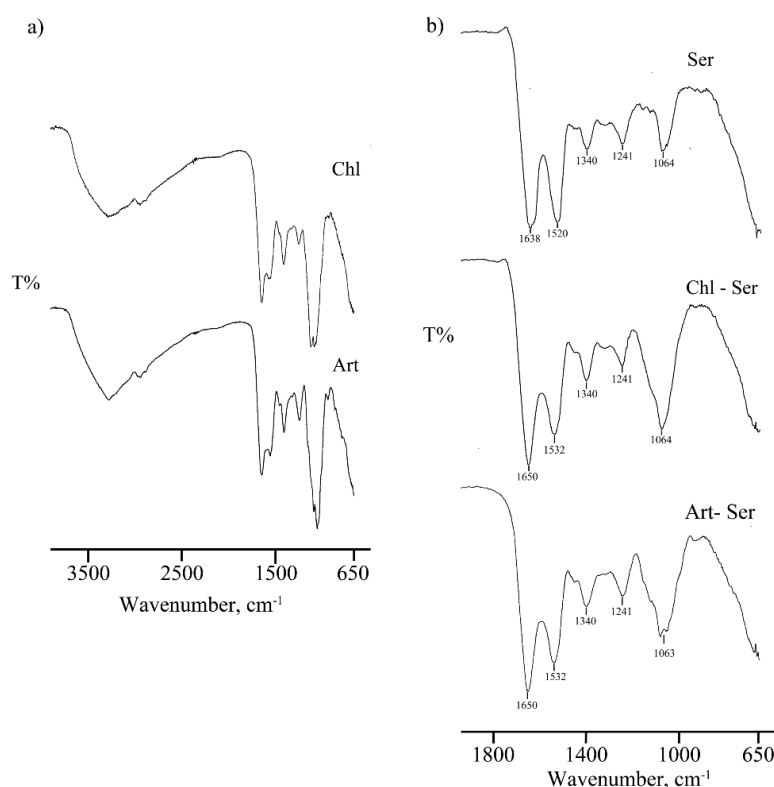


Figure 2. Fourier Transform Infrared Spectroscopy spectra of (a) Chl and Art formulations (spectral region 4000–650 cm^{-1}); (b) Ser, Chl-Ser and Art-Ser formulations (spectral region 2000–650 cm^{-1}).

3.2. ROS-Scavenging Activity

ANOVA analysis evidenced that both formulation and microsphere concentration had a significant effect on the ROS-scavenging activity ($p < 0.0001$).

All formulations exhibited antioxidant activity strongly correlated with the microsphere's concentration. The equations of the straight lines obtained are presented as $y = (\text{slope} \pm 95\%$

probability confidence interval) x + intercept \pm 95% probability confidence interval, together with their determination coefficient (R^2).

$$\text{Art: ROS-s.a. (\%)} = (1.1 \pm 0.1)x + 7 \pm 3, R^2 = 0.992 \quad (1)$$

$$\text{Art-Ser: ROS-s.a. (\%)} = (1.11 \pm 0.09)x + 6 \pm 2, R^2 = 0.997 \quad (2)$$

$$\text{Chl-Ser: ROS-s.a. (\%)} = (0.96 \pm 0.03)x + 6 \pm 1, R^2 > 0.999 \quad (3)$$

$$\text{Ser: ROS-s.a. (\%)} = (0.6 \pm 0.3)x + 7 \pm 8, R^2 = 0.895 \quad (4)$$

$$\text{Chl: ROS-s.a. (\%)} = (0.66 \pm 0.04)x + 8 \pm 1, R^2 = 0.998 \quad (5)$$

Art showed the highest antioxidant property, although it was not significantly different from Art-Ser. Moreover, Art and Art-Ser formulations showed ROS-scavenging activity linear functions with slopes comparable with Chl-Ser formulation. ROS-scavenging activity of Chl-Ser was significantly higher than Chl and Ser formulations in the concentration range from 10 to 50 mg/mL. The Ser formulation was significantly more effective in preventing oxidant events than Chl, but no significant differences were highlighted with Chl-Ser. At concentrations lower than 10 mg/mL, all formulations had comparable antioxidant activity (Figure 3).

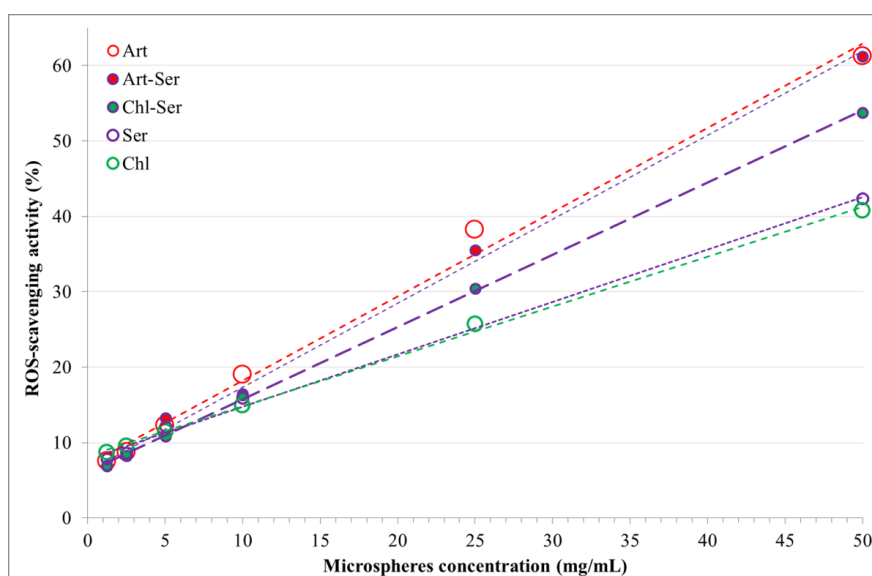


Figure 3. Reactive Oxygen Species (ROS)-scavenging activity (%) and microspheres concentrations (mg/mL) for the formulations studied.

3.3. In Vitro Results

A wide range of concentrations was investigated for each formulation in order to identify the non-toxic concentration of microspheres, which were further used to treat the “scratched” cells.

ANOVA results showed that both formulation and microsphere concentration had a significant effect on cell metabolic activity ($p < 0.05$, Figure 4a,b).

In detail, Ser did not induce any cytotoxic effects on fibroblast cells, which showed metabolic activity higher than 75% at all tested concentrations (0.05–10 mg/mL). Conversely, both Chl and Art were found to be cytotoxic for fibroblasts starting from 1.25 mg/mL: Figure 4a shows the gradual decrease of cell metabolic activity in line with the increase of Art concentrations. Figure 4b shows the metabolic activity results for Chl-Ser and Art-Ser: the negative trend observed for Art (Figure 4a) was shown also for Art-Ser, proving that silk sericin was unable to prevent the Art cytotoxic effect. The mean % metabolic activity of cells treated with Chl-Ser was significantly higher than that of the cells treated with Art-Ser ($p = 0.006$). No significant differences between Chl-Ser and Art-Ser were observed at the lowest concentrations (0.1–1 mg/mL), with a cell metabolic activity higher than 80%. Instead, the % metabolic activity of fibroblast cells was lower than roughly 70% after treatment with Chl-Ser at 2.5–20 mg/mL and lower than 50% after treatment with Art-Ser, considering the same concentration range (Figure 4b).

Considering the cell metabolic activity together with the ROS-scavenging activity in the range of microsphere concentrations between 1.25 and 10 mg/mL, the antioxidant activity resulted in lower than 20%; the formulations which provided the better ROS-scavenging activity and the higher cell metabolic activity are those at the higher concentration of microspheres (Figure 5). As expected, Ser was cytocompatible on fibroblast cells (cell metabolic activity $>70\%$), while the only formulation, based on silk sericin and algal aqueous extract, which provides an adequate cell metabolic activity was that obtained from *C. vulgaris* (Chl-Ser) at the concentration 10 mg/mL, offering the better compromise between antioxidant activity and cytocompatibility (Figure 5).

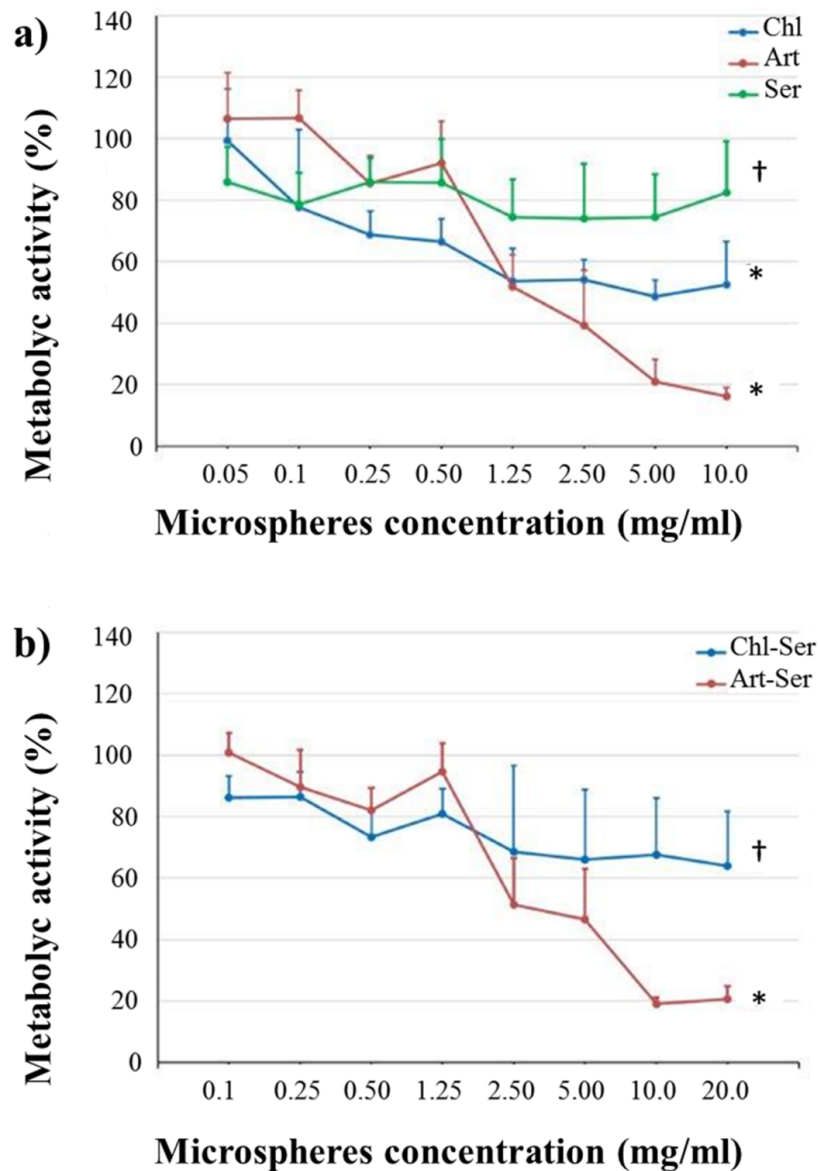


Figure 4. Mean values of cell metabolic activity (%) and standard deviations, considering (a) Chl (blue line), Art (red line) and Ser (green line) formulations and (b) Chl-Ser (blue line) and Art-Ser (red line) formulations. For each graph, different symbols († and *) indicate significant differences between formulations ($p < 0.05$).

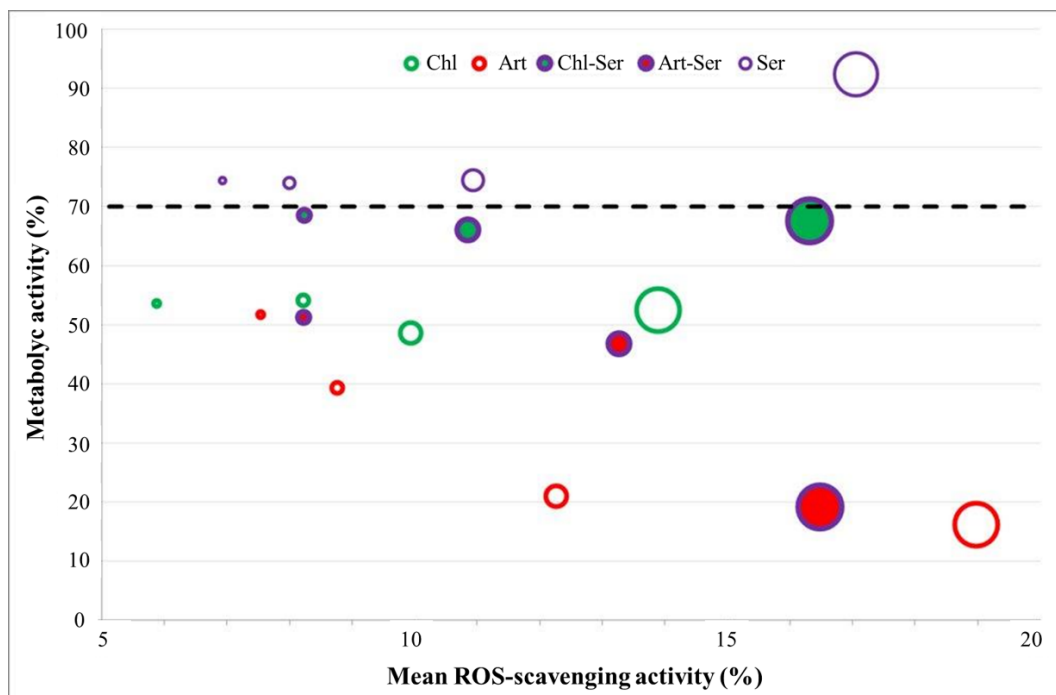


Figure 5. Mean ROS-scavenging activity (%) and cell metabolic activity % for the all tested formulations. The diameter of the circles in the plot is proportional to the microsphere concentration: the larger circles correspond to the 10 mg/mL, the intermediate and intermediate-small circles are those of the 5 and 2.5 mg/mL, while the smaller circles represent the properties of the 1.25 mg/mL concentration of microspheres.

According to these results, scratch assay was performed considering non-toxic microparticle concentrations: 0.05–0.5 mg/mL for Chl, Art and Ser and 0.1–1 mg/mL for Chl-Ser and Art-Ser. Figure 6a reports the images of cell migration after treatment with microspheres; in order to quantify the cell migration, images were observed by five independent expert operators and a score between 0 (absence of cell migration) and 10 (completed cell migration) was given for each formulation at each considered time endpoint. ANOVA results evidenced that both formulation and time significantly influenced the scores ($p < 0.0001$) (Figure 6b,c). All formulations promoted cell migration and the complete wound closure within 72 h, and this positive effect was further highlighted after treatment with Art and Art-Ser microspheres. The comparison of the mean scores obtained by the formulations of Chl, Art, and Ser showed no significant differences after 24h (2.2 ± 1.2 , 3.2 ± 1.7 , and 2.6 ± 1.3 , respectively), whereas at 48h and 72h, Chl appeared to be the worst formulation in promoting cell migration. After 48 h, the mean score \pm S.D. of cells treated with Chl was 4.4 ± 0.8 , and it resulted significantly lower than the mean scores of Ser, 6.6 ± 0.8 , and Art, 7.6 ± 1.3 ($p < 0.01$). At 72 h, the mean score of Chl was 7.8 ± 0.2 , and it resulted in scores significantly lower than the mean scores of Ser, 8.6 ± 0.3 , and Art, 9.0 ± 0.0 ($p < 0.05$) (Figure 6).

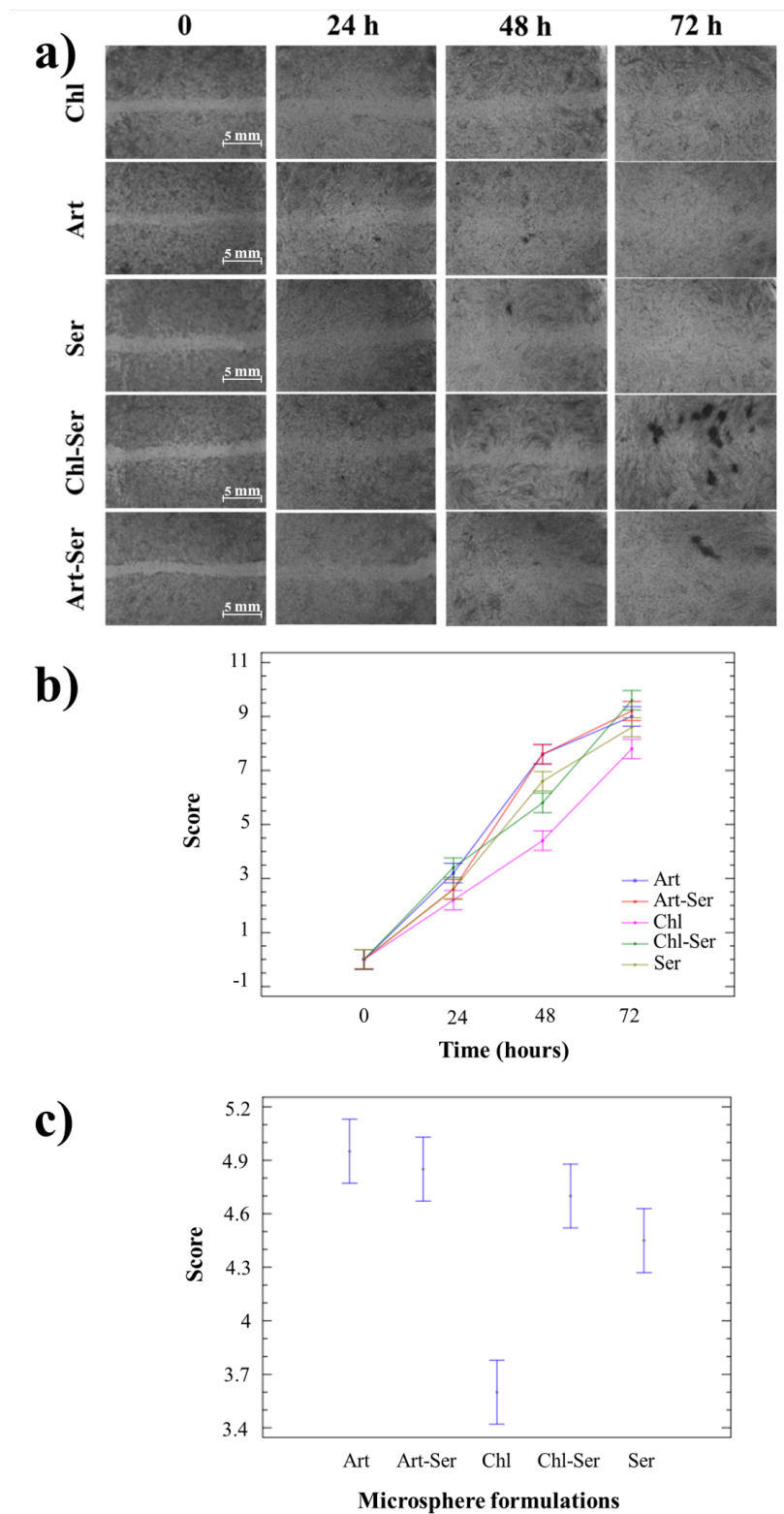


Figure 6. (a) Representative images of scratched fibroblast migration after treatment with microspheres. Mean values of wound healing scores and 95.0 percent LSD (Least Significant Difference) intervals, considering (b) time of treatment and (c) microsphere formulations.

Considering formulations based on silk sericin and algal extracts, the mean scores were not significantly different at 24h (2.6 ± 0.8 and 3.4 ± 1.8 , respectively) and 72h (9.2 ± 0.2 and 9.6 ± 0.3 , respectively), whereas at the 48h time-point the Art-Ser received a mean score significantly higher than that of the Chl-Ser (7.6 ± 1.3 and 5.8 ± 0.7 , respectively, $p = 0.012$) (Figure 6b).

4. Discussion

Microalgae represent a novel natural source of highly interesting bioactive compounds: recently, their use has been considered in tissue regeneration, developing innovative scaffolds such as nanofibers based on polyethylene oxide [33], polycaprolactone [34] and silk fibroin [35].

For the first time, in this work, *C. vulgaris* and *A. platensis* aqueous extracts have been used in combination with silk sericin, obtained from *Bombyx mori* cocoons, for the production of microspheres suitable for the topical treatment of skin wounds. Specifically, *C. vulgaris* and *A. platensis* aqueous extracts and silk sericin were spray dried, alone or combined, to obtain five microsphere formulations (Chl, Art, Ser, Chl-Ser and Art-Ser). The aqueous extraction of both microalgae was performed to obtain a pool of phytochemicals that have synergistic or additive effects as reported in literature [25], particularly against the oxidative stress. Sericin, due to its wound healing potential [18], may improve the regenerative effect of the microalgae extracts; moreover, it represents an adequate polymeric carrier [36] for the microencapsulation process of algal extracts. Sericin microspheres loaded with naringenin have previously been developed in our group for the topical treatment of middle-stage psoriasis, highlighting that the microencapsulated drug was more effective in the down regulation of TNF- α than as a free drug [24].

Even though *Arthrospira platensis* and *Chlorella vulgaris* are approved by FDA as GRAS, for safety requirements, our formulations were tested in vitro on fibroblast at different concentrations. According to our results, all the formulations showed good cytocompatibility: Ser did not induce any cytotoxic effect on fibroblast cells; while Art and Chl started to be cytotoxic at the higher concentrations. In this regard, sericin was unable to reduce the cytotoxic effect of Art.

Subsequently, wound healing potential was investigated for all the formulations at the non-toxic microparticle concentrations. The in vitro scratch assay is an easy method suitable to study the effects of cell–matrix and cell–cell interactions on cell migration and to mimic cell

migration during wound healing in vivo. The scratch assay has revealed that all the formulation tested promoted cell migration and a complete wound closure within 72 h. In particular, the wound healing potential of *A. platensis* extract seemed to be higher than *C. vulgaris*. The addition of Ser to Chl formulation improve the ability to promote wound closure, while Art-Ser formulation did not result more effective than Art. Our results are not in contrast with literature: due to its mitogenic effect, sericin was recently reported to support keratinocyte and fibroblast adhesion and proliferation, promoting collagen deposition in damaged areas and thereby accelerating wound re-epithelialization [37]. In the literature, the wound healing potential of *C. vulgaris* and *A. platensis* has been less discussed. To the best of our knowledge, there have been very few papers published investigating the use of microalgae in wound healing. Syarina et al., [38] have demonstrated that *A. platensis* was effective in promoting the wound healing process: the phytochemical profile of microalgae aqueous extract was defined, showing the presence of several therapeutic compounds useful in chronic wound treatment. *C. vulgaris* has also been shown to be a potential source of bioactive agents capable of accelerating the wound healing process with minimal scar formation, as confirmed by Zailan et al. [39].

The use of spray dried microparticulate systems has generated great attention in skin regeneration: microspheres are adequate systems for drug encapsulation and for controlling the release of active molecules, depending on physicochemical properties of polymers, even if other formulations are quite common as creams, bandages, films, sponges and ointments [40]. There may be many reasons for the formulation of antioxidant algal extract in microspheres, mainly related to their intrinsic lability: isolation of active ingredients from external environment, moisture protection, oxidation protection, light exposure protection, aroma masking, and metering of ingredients. Moreover, the algal extracts in its native liquid form have disadvantages in portability and commercial viability for use as natural antioxidant sources: microencapsulation of the algal extracts in silk sericin would circumvent these aspects, albeit it does not provide sustained/prolonged/slow release of active, since sericin is a water-soluble protein.

Biodegradable polymers are preferred in wound healing due to their surface properties and their biocompatibility [41]. The main advantage of microparticulate systems is related to their easy fabrication. Spray drying is an economically feasible technique that has already been used to produce dry biomass powders enriched with bioactive molecules without altering their physicochemical and, hence, functional properties [42]. In the last decades, some research groups have evaluated the effect of spray drying on the biological content of different algal

species. In particular, Leach et al. and Orset et al. [43,44] have investigated the β -carotene content and stereoisomer composition of spray dried *Dunaliella salina* biomass: the spray-drying process neither promoted an excessive degradation nor a change in isomer composition of β -carotene. Furthermore, Leach et al., [43] evidenced that the stability of the antioxidant compound greatly improved when *D. salina* cells were microencapsulated in a polymeric blend of maltodextrin and gum arabic, minimizing β -carotene degradation in the presence of light and oxygen.

Granulometric analysis, performed by laser light scattering, and SEM images evidenced that spray drying was a robust technique which allowed the obtainment of microspheres with dimensions and morphology suitable for the purposes of the present study.

A wrinkled texture characterized the surface of all microsphere formulations, even if some scattered smooth and round particles were appreciated in the presence of sericin. As reported by Mishara et al., [45], microsphere morphology may be influenced by irregular shrinkage forces during the spray drying process, which could be related to the formulation composition and process parameters. The solvent vapor pressure and the polymer concentration might be critical factors, able to condition particle morphology, as reported by Raula et al., [46]. Genç et al., [47] have observed that the spherical structure of sericin spray dried particles tend to collapse due to fast solvent evaporation, which is strictly correlated to the low concentration of the starting sericin solution and the lack of excipients; the same morphological results were observed by Chlapanidas et al., [22]. The rough appearance that characterized all formulations might be also explained by the collapse of microparticles during SEM analysis, performed according to the sputtering technique.

Proteolytic enzymes, proinflammatory cytokines, growth factors and ROS are secreted by cells with a crucial role during the wound healing process, albeit that high concentrations of these substances can alter the wound re-epithelialization through the degradation of extracellular matrix and the functionality of fibroblasts and keratinocytes. Antioxidant compounds are able to neutralize the deleterious effect of ROS [48]. Several publications reported in the literature have attributed the antioxidant potential of algal biomass mainly to their phenolic content, although many other compounds, such as amino acids and polysaccharides, are also known to be antioxidants [49]. The composition of *C. vulgaris* and *A. platensis* extracts was recently examined by other authors in order to identify the compounds responsible for their antioxidant potential [15]. Our results evidenced that Ser had more protein and less polysaccharides than algal aqueous extract. Art formulation was significantly richer in proteins than Chl, while both

Art and Chl microspheres were constituted by about 10% w/w of polysaccharides. Moreover, the protein content of each microsphere formulation was related to its theoretical composition: a detailed analysis demonstrated that total proteins contained in Art-Ser resulted as the half algebraic sum of proteins contained in Ser and Art. An analogous assessment was carried out for *C. vulgaris* and for the carbohydrate content. The higher protein content of Art (compared to Chl) and the higher polysaccharides content (compared to Ser) may be responsible to its more promising biological effects, especially regarding the antioxidant activity.

According to DPPH results and FTIR analyses, the *A. platensis* aqueous extract and, to a significantly lesser extent, the silk sericin were the most responsible for the microsphere ROS-scavenging activity. These results were confirmed by Wu et al. [50], who compared *A. platensis* and *C. vulgaris* aqueous extracts in terms of antioxidant and anti-proliferative properties. They highlighted a correlation between the antioxidant activity and the extract composition, particularly with the total phenolic content. *A. platensis* extract was a stronger antioxidant than *C. vulgaris*: total phenolic compounds extracted with water from *A. platensis* were almost five times more than those contained in *C. vulgaris* [50].

The ROS-scavenging activity of sericin has been extensively investigated both in vitro and in vivo; it has been explained due to the high presence of hydroxyl amino groups in its amino acid sequence, mainly from serine and threonine [21]. Moreover, silk sericin has been shown to protect human fibroblasts against oxidative damage when used in sponge-like dressings intended for the treatment of chronic skin ulcers [19].

In conclusion, *Arthrospira platensis* aqueous extract showed the highest antioxidant activity and the capability to induce a complete wound closure within 72 h. In contrast to our hypothesis, the combination of *Arthrospira platensis* aqueous extract and sericin did not prove more effective with respect to algal extract alone; this could be probably due to algal high biological activity, which conceals the silk sericin effect. The microencapsulation process may not be a confounding factor for the combination studied: sericin is a soluble polymer and thus there is no risk for a slow release of active algal. Silk sericin can be considered an optimal polymeric carrier for phytocomplex microencapsulation process, and a murine in vivo model of wound healing will consolidate the in vitro efficacy results obtained in this work.

Acknowledgments: This work was supported by Fondazione Cariplo (MICROFLOWER, Project Id. 2014-0601). The authors thank Nembri Industrie Tessili S.r.l. (Capiolo (BS), Italy) for certified *Bombyx mori* cocoons, Sergio Schinelli and Dott. Mayra Paolillo (Drug Sciences

Dept., Pavia University, Pavia, Italy) for willingness regarding the use of Synergy HT (BioTek, Swindon, UK). We are grateful to Ryan Rogers, University of Michigan, for editorial help.

Author Contributions: Elia Bari, Carla Renata Arciola, Sara Perteghella, and Maria Luisa Torre conceived of the study, participated in its design and coordination. Barbara Vigani wrote the first draft of the manuscript; Sara Perteghella, Enrico Lucarelli, and Theodora Chlapanidas wrote the final paper. Barbara Vigani, Paola Moro, and Barbara Crivelli carried out microspheres, protein and carbohydrate contents, and antioxidant activity. Sara Perteghella performed the experiments on cell cultures. Milena Sorrenti and Laura Catenacci carried out FTIR and TGA. Giovanna Bruni performed SEM analysis. Giorgio Marrubini performed the statistical analysis. All authors revised and approved the final manuscript.

Conflicts of Interest: The authors declare no conflict of interest.

Abbreviations

ANOVA	Analysis of variance
BCA	Bicinchoninic acid
BSA	Bovine serum albumin
DMSO	Dimethyl sulfoxide
DPPH	2,2-Diphenyl-2-picrylhydrazyl hydrate
FTIR	Fourier transform infrared spectroscopy
GRAS	Generally recognized as safe
MTT	3-(4,5-Dimethylthiazol-2-yl)-2,5-diphenyltetrazolium bromide
ROS	Reactive oxygen species
SEM	Scanning electron microscopy
TGA	Thermogravimetric Analysis

References

1. Gil-Chàvez, G.J.; Villa, J.A.; Ayala-Zavala, F.; Heredia, B.; Sepulveda, D.; Yahia, E.M.; González-Aguilar, G.A. Technologies for extraction and production of bioactive compounds to be used as nutraceuticals and food ingredients: An overview. *Compr. Rev. Food Sci. Food. Saf.* **2013**, *12*, 5–23, doi:10.1016/j.peptides.2011.11.013.
2. Wang, H.M.; Chen, C.C.; Huynh, P.; Chang, J.S. Exploring the potential of using algae in cosmetics. *Bioresour. Technol.* **2015**, *184*, 355–362, doi:10.1016/j.biortech.2014.12.001.

3. Markou, G.; Nerantzis, E. Microalgae for high-value compounds and biofuels production: A review with focus on cultivation under stress conditions. *Biotechnol. Adv.* **2013**, *31*, 1532–1542, doi:10.1016/j.biotechadv.2013.07.011.
4. De Morais, M.G.; Vaz Bda, S.; de Morais, E.G.; Costa, J.A. Biologically active metabolites synthesized by microalgae. *BioMed Res. Int.* **2015**, 835761, doi:10.1155/2015/835761.
5. Plaza, M.; Santoyo, S.; Jaime, L.; Reina, G.G.B.; Herrero, M.; Señoráns, F.J.; Ibáñez, E. Screening for bioactive compounds from algae. *J. Pharmac. Biomed. Anal.* **2010**, *51*, 450–455, doi:10.1016/j.jpba.2009.03.016.
6. Vázquez, A.I.F.; Sánchez, C.M.D.; Delgado, N.G.; Alfonso, A.M.S.; Ortega, Y.S.; Sanchez, H.C. Anti-inflammatory and analgesic activities of red seaweed *Dichotomaria obtusata*. *Braz. J. Pharm. Sci.* **2011**, *47*, 111–118, doi:10.1590/S1984-82502011000100014.
7. Al-Saif, S.S.A.; Abdel-Raouf, N.; El-Wazanani, H.A.; Aref, I.A. Antibacterial substances from marine algae isolated from Jeddah coast of Red sea, Saudi Arabia. *Saudi J. Biol. Sci.* **2014**, *21*, 57–64, doi:10.1016/j.sjbs.2013.06.001.
8. Michalak, I.; Chojnacka, K. Algae as production systems of bioactive compounds. *Eng. Life Sci.* **2015**, *15*, 160–176, doi:10.1002/elsc.201400191.
9. Masojìdek, J., Prášil, O. The development of microalgal biotechnology in the Czech Republic. *J. Ind. Microbiol. Biotechnol.* **2010**, *37*, 1307–1317.
10. Demir, B.S.; Tükel, S.S. Purification and characterization of lipase from *Spirulina platensis*. *J. Mol. Catal. B Enzym.* **2010**, *64*, 123–128, doi:10.1016/j.molcatb.2009.03.011.
11. Cuellar-Bermudez, S.P.; Aguilar-Hernandez, I.; Cardenas-Chavez, D.L.; Ornelas-Soto, N.; Romero-Ogawa, M.A.; Parra-Saldivar, R. Extraction and purification of high-value metabolites from microalgae: Essential lipids, astaxanthin and phycobiliproteins. *Microb. Biotechnol.* **2015**, *8*, 190–209, doi:10.1111/1751-7915.12167.
12. Kulshreshtha, A.; Zacharia, A.J.; Jarouliya, U.; Bhadauriya, P.; Prasad, G.B.; Bisen, P.S. *Spirulina* in health care management. *Curr. Pharm. Biotechnol.* **2008**, *9*, 400–405, doi:10.2174/138920108785915111.
13. Small, E. *Spirulina*-food for the universe. *Biodiversity* **2011**, *12*, 255–265, doi:10.1080/14888386.2011.642735.
14. Deng, R.; Chow, T.J. Hypolipidemic, antioxidant, and anti-inflammatory activities of microalgae *Spirulina*. *Cardiovasc. Ther.* **2010**, *28*, 33–45, doi:10.1111/j.1755-5922.2010.00200.x.

15. Safi, C.; Zebib, B.; Merah, O.; Pontalier, P.; Vaca-Garcia, C. Morphology, composition, production, processing and applications of *Chlorella vulgaris*: A review. *Renew. Sust. Energ. Rev.* **2014**, *35*, 265–278, doi:10.1016/j.rser.2014.01.007.
16. Wang, H.; Pan, J.; Chen, C.; Chiu, C.; Yang, M.; Chang, H.; Chang, J. Identification of anti-lung cancer extract from *Chlorella vulgaris* C-C by antioxidant property using supercritical carbon dioxide extraction. *Process Biochem.* **2010**, *45*, 1865–1872, doi:10.1016/j.procbio.2010.05.023.
17. Li, H.B.; Jiang, Y.; Chen, F. Isolation and purification of lutein from the microalga *Chlorella vulgaris* by extraction after saponification. *J. Agric. Food Chem.* **2002**, *50*, 1070–1072, doi:10.1021/jf010220b.
18. Cao, T.T.; Zhang, Y.Q. Processing and characterization of silk sericin from *Bombyx mori* and its application in biomaterials and biomedicine. *Mater. Sci. Eng. C Mater. Biol. Appl.* **2016**, *61*, 940–952, doi:10.1016/j.msec.2015.12.082.
19. Mori, M.; Rossi, S.; Ferrari, F.; Bonferoni, M.C.; Sandri, G.; Chlapanidas, T.; Torre, M.L.; Caramella, C. Sponge-like dressings based on the association of chitosan and sericin for the treatment of chronic skin ulcers. I. Design of experiments—Assisted development. *J. Pharm. Sci.* **2016**, *105*, 1180–1187, doi:10.1016/j.xphs.2015.11.047.
20. Mori, M.; Rossi, S.; Ferrari, F.; Bonferoni, M.C.; Sandri, G.; Riva, F.; Tenci, M.; Del Fante, C.; Nicoletti, G.; Caramella, C. Sponge-like dressings based on the association of chitosan and sericin for the treatment of chronic skin ulcers. II. Loading of the hemoderivative platelet lysate. *J. Pharm. Sci.* **2016**, *105*, 1188–1195, doi:10.1016/j.xphs.2015.11.043.
21. Fan, J.; Wu, L.; Chen, L.; Mao, X.; Ren, F. Antioxidant activities of silk sericin from silkworm *Bombyx mori*. *J. Food Biochem.* **2009**, *33*, 74–88, doi:10.1111/j.1745-4514.2008.00204.x.
22. Chlapanidas, T.; Faragò, S.; Lucconi, G.; Perteghella, S.; Galuzzi, M.; Mantelli, M.; Avanzini, M.A.; Tosca, M.C.; Marazzi, M.; Vigo, D.; et al. Sericins exhibit ROS-scavenging, anti-tyrosinase, anti-elastase, and in vitro immunomodulatory activities. *Int. J. Biol. Macromol.* **2013**, *58*, 47–56, doi:10.1016/j.ijbiomac.2013.03.054.
23. Tsubouchi, K.; Igarashi, Y.; Takasu, Y.; Yamada, H. Sericin enhances attachment of cultured human skin fibroblasts. *Biosci. Biotechnol. Biochem.* **2005**, *69*, 403–405, doi:10.1271/bbb.69.403.
24. Chlapanidas, T.; Perteghella, S.; Leoni, F.; Faragò, S.; Marazzi, M.; Rossi, D.; Martino, E.; Gaggeri, R.; Collina, S. TNF- α blocker effect of naringenin-loaded sericin microparticles

- that are potentially useful in the treatment of psoriasis. *Int. J. Mol. Sci.* **2014**, *15*, 13624–13636, doi:10.3390/ijms150813624.
25. Kuda, T.; Eda, M.; Kataoka, M.; Nemoto, M.; Kawahara, M.; Oshio, S.; Takahashi, H.; Kimura, B. Anti-glycation properties of the aqueous extract solutions of dried algae products and effect of lactic acid fermentation on the properties. *Food Chem.* **2016**, *192*, 1109–1115, doi:10.1016/j.foodchem.2015.07.073.
 26. Faragò, S.; Lucconi, G.; Perteghella, S.; Vigani, B.; Tripodo, G.; Sorrenti, M.; Catenacci, L.; Boschi, A.; Faustini, M.; Vigo, D.; et al. A dry powder formulation from silk fibroin microspheres as a topical auto-gelling device. *Pharm. Dev. Technol.* **2016**, *21*, 453–462, doi:10.3109/10837450.2015.1022784.
 27. Lucconi, G.; Chlapanidas, T.; Martino, E.; Gaggeri, R.; Perteghella, S.; Rossi, D.; Faragò, S.; Vigo, D.; Faustini, M.; Collina, S.; et al. Formulation of microspheres containing *Crataegus monogyna Jacq.* extract with free radical scavenging activity. *Pharm. Dev. Technol.* **2013**, *19*, 65–72, doi:10.3109/10837450.2012.752387.
 28. Smith, P.K.; Krohn, R.I.; Hermanson, G.T.; Mallia, A.K.; Gartner, F.H.; Provenzano, M.D.; Fujimoto, E.K.; Goetze, N.M.; Olson, B.J.; Klenk, D.C. Measurement of protein using bicinchoninic acid. *Anal. Biochem.* **1985**, *150*, 76–85, doi:10.1016/0003-2697(85)90442-7.
 29. DuBois, M.; Gilles, K.; Hamilton, J.; Rebers, P.; Smith, F. Colorimetric method for determination of sugars and related substances. *Anal. Chem.* **1956**, *28*, 350–356, doi:10.1021/ac60111a017.
 30. Chaudhuri, D.; Ghate, N.B.; Deb, S.; Panja, S.; Sarkar, R.; Rout, J.; Mandal, N. Assessment of the phytochemical constituents and antioxidant activity of a bloom forming microalgae *Euglena tuba*. *Biol. Res.* **2014**, *47*, 24, doi:10.1186/0717-6287-47-24.
 31. Liang, C.C.; Park, A.Y.; Guan, J.L. In vitro scratch assay: A convenient and inexpensive method for analysis of cell migration in vitro. *Nat. Protoc.* **2007**, *2*, 329–333, doi:10.1038/nprot.2007.30.
 32. Chlapanidas, T.; Perteghella, S.; Faragò, S.; Boschi, A.; Tripodo, G.; Vigani, B.; Crivelli, B.; Renzi, S.; Dotti, S.; Preda, S.; et al. Platelet lysate and adipose mesenchymal stromal cells on silk fibroin nonwoven mats for wound healing. *J. Appl. Polym. Sci.* **2016**, *133*, doi:10.1002/APP.42942.

33. De Morais, M.G.; Stillings, C.; Dersch, R.; Rudisile, M.; Pranke, P.; Costa, J.A.V.; Wendorff, J. Preparation of nanofibers containing the microalga *Spirulina* (*Arthrospira*). *Bioresour. Technol.* **2010**, *101*, 2872–2876, doi:10.1016/j.biortech.2009.11.059.
34. Kim, S.H.; Shin, C.; Min, S.K.; Jung, S-M.; Shim, H.S. In vitro evaluation of the effects of electrospun PCL nanofiber mats containing the microalgae *Spirulina* (*Arthrospira*) extract on primary astrocytes. *Colloids Surf. B Biointerfaces* **2012**, *90*, 113–118, doi:10.1016/j.colsurfb.2011.10.004.
35. Cha, B-G.; Kwan, H.W.; Park, A.R.; Kim, S.H.; Park, S-Y.; Kim, H-J.; Kim, I-S., Lee, K.H.; Park, Y.H. Structural characteristics and biological performance of silk fibroin nanofiber containing microalgae *Spirulina* extract. *Biopolymers* **2014**, *101*, 307–318, doi:10.1002/bip.22359.
36. Oh, H.; Kim, M.K.; Lee, K.H. Preparation of sericin microparticles by electrohydrodynamic spraying and their application in drug delivery. *Macromol. Res.* **2011**, *19*, 266–272, doi:10.1007/s13233-011-0301-6.
37. Aramwit, P.; Palapinyo, S.; Srichana, T.; Chottanapund, S.; Muangman, P. Silk sericin ameliorates wound healing and its clinical efficacy in burn wounds. *Arch. Dermatol. Res.* **2013**, *305*, 585–594, doi:10.1007/s00403-013-1371-4.
38. Syarina, P.N.; Karthivashan, G.; Abas, F.; Arulselvan, P.; Fakurazi, S. Wound healing potential of *Spirulina platensis* extracts on human dermal fibroblast cells. *EXCLI J.* **2015**, *14*, 385–393, doi:10.17179/excli2014-697.
39. Zailan, N.; Abdul Rashid, A.H.; Das, S.; Abdul Mokti, N.A.; Hassan Basri, J.; Teoh, S.L.; Wan Ngah, W.Z.; Mohd Yusof, Y.A. Comparison of *Chlorella vulgaris* dressing and sodium alginate dressing: An experimental study in rats. *Clin. Ther.* **2010**, *161*, 515–521.
40. Napavichayanun, S.; Aramwit P. Effect of animal products and extracts on wound healing promotion in topical applications: A review. *J. Biomater. Sci. Polym. Ed.* **2017**, *28*, 703–729. doi:10.1080/09205063.2017.1301772.
41. Degim, Z. Use of microparticulate systems to accelerate skin wound healing. *J. Drug. Target.* **2008**, *16*, 437–448, doi:10.1080/10611860802088572.
42. Dehnad, D.; Jafari, S.M.; Afrasiabi, M. Influence of drying on functional properties of food biopolymers: From traditional to novel dehydration techniques. *Trends Food Sci. Tech.* **2016**, *57*, 116–131, doi:10.1016/j.tifs.2016.09.002.

43. Leach, G.; Oliveira, G.; Morais, R. Spray-drying of *Dunaliella salina* to produce a β -carotene rich powder. *J. Ind. Microbiol. Biotechnol.* **1998**, *20*, 82–85, doi:10.1038/sj.jim.2900485.
44. Orset, S.; Leach, G.C.; Morais, R.; Young, A.J. Spray-drying of the microalga *Dunaliella salina*: Effects on β -carotene content and isomer composition. *J. Agric. Food Chem.* **1999**, *47*, 4782–4790, doi:10.1021/jf990571e.
45. Mishara, M.; Mishara, B. Formulation optimization and characterization of spray dried microparticles for inhalation delivery of doxycycline hyclate. *Yakugaku Zasshi* **2011**, *113*, 1813–1825, doi:10.1248/yakushi.131.1813.
46. Raula, J.; Eerikäinen, H.; Kauppinen, E.I. Influence of the solvent composition on the aerosol synthesis of pharmaceutical polymer nanoparticles. *Int. J. Pharm.* **2004**, *284*, 13–21, doi:10.1016/j.ijpharm.2004.07.003.
47. Genç, G.; Narin, G.; Bayrakcar, O. Spray drying as a method of producing silk sericin powders. *J. Achiev. Mater. Manuf. Eng.* **2009**, *37*, 78–86.
48. Dunnill, C.; Patton, T.; Brennan, J.; Barrett, J.; Dryden, M.; Cooke, J.; Leaper, D.; Georgopoulos, N.T. Reactive oxygen species (ROS) and wound healing: The functional role of ROS and emerging ROS-modulating technologies for augmentation of the healing process. *Int. J. Wound* **2017**, *14*, 89–96, doi:10.1111/iwj.12557.
49. Safafar, H.; van Wagenen, J.; Møller, P.; Jacobsen, C. Carotenoids, phenolic compounds and tocopherols contribute to the antioxidative properties of some microalgae species grown on industrial wastewater. *Mar. Drugs* **2015**, *13*, 7339–7356, doi:10.3390/md13127069.
50. Wu, L.C.; Ho, J.A.; Shieh, M.C.; Lu, I.W. Antioxidant and antiproliferative activities of *Spirulina* and *Chlorella* water extracts. *J. Agric. Food Chem.* **2005**, *53*, 4207–4212, doi:10.1021/jf0479517.



© 2017 by the authors. Submitted for possible open access publication under the terms and conditions of the Creative Commons Attribution (CC BY) license (<http://creativecommons.org/licenses/by/4.0/>).